MycoKeys 92: 1–25 (2022)
doi: 10.3897/mycokeys.92.80682
https://mycokeys.pensoft.net

RESEARCH ARTICLE

A peer-reviewed open-access journal
MycoKeys
Launched to accelerate biodiversity research

Diversity of fungi associated with *Monochamus alternatus* larval habitats in *Bursaphelenchus xylophilus*-infected *Pinus massoniana* and identification of two new ophiostomatalean species (Ascomycota, Ophiostomatales)

Guiheng Zheng[1], Minqi You[2], Xuening Li[3], Qinzheng Zhou[1], Zheng Wang[1], Huimin Wang[1], Quan Lu[1]

1 *Key Laboratory of Forest Protection, National Forestry and Grassland Administration; Ecology and Nature Conservation Institute, Chinese Academy of Forestry, Beijing 100091, China* **2** *Agriculture and Rural Affairs Bureau of Huangyan District, Taizhou City 318020, China* **3** *Research Institute of Desertification, Chinese Academy of Forestry, Beijing 100091, China*

Corresponding authors: Huimin Wang (whuimin19@126.com), Quan Lu (luquan@caf.ac.cn)

Academic editor: Danny Haelewaters | Received 18 January 2022 | Accepted 1 June 2022 | Published 1 August 2022

Citation: Zheng G, You M, Li X, Zhou Q, Wang Z, Wang H, Lu Q (2022) Diversity of fungi associated with *Monochamus alternatus* larval habitats in *Bursaphelenchus xylophilus*-infected *Pinus massoniana* and identification of two new ophiostomatalean species (Ascomycota, Ophiostomatales). MycoKeys 92: 1–25. https://doi.org/10.3897/mycokeys.92.80682

Abstract

Bursaphelenchus xylophilus, a pathogenic pine wood nematode (PWN), is responsible for pine wilt disease (PWD), which has caused significant economic and ecological damage worldwide, particularly in East Asia. Multiple biological factors, such as the beetle vector *Monochamus*, symbiotic bacteria and associated fungi, are involved in the disease infection cycle. This study isolated and identified the fungal communities of *Monochamus alternatus* larval galleries and pupal chambers from different instars through field investigation, morphological observation and multi-locus DNA sequence analyses in Zhejiang Province, China. A total of 255 and 454 fungal strains were isolated from *M. alternatus* galleries and pupal chambers infected with PWN, from the 2nd–3rd and 4th–5th instar larvae, respectively. A total of 18 species of fungi were identified, 14 species were isolated from the 2nd–3rd instar larval galleries and six species from the galleries and pupal chambers of the 4th–5th instar larvae. Amongst them were six species belonging to four genera of ophiostomatalean fungi, including two novel species, *Graphilbum xianjuensis* **sp. nov.** and *Ophiostoma taizhouense* **sp. nov.** and four known species,

Ceratocystiopsis weihaiensis, *Ophiostoma ips*, *Sporothrix zhejiangensis* and *S. macroconidia*. The findings revealed that the fungal diversity and abundance of the 2nd–3rd instar larvae differed markedly from those of the 4th–5th instar larvae. This difference could be the result of fungal succession. This study provides a thorough understanding of the fungi associated with PWD and lays the groundwork for future research.

Keywords
Ceratocystiopsis, fungal succession, *Graphilbum*, *Ophiostoma*, pine wilt disease, *Sporothrix*, two new species

Introduction

The pine wood nematode (PWN), *Bursaphelenchus xylophilus* (Steiner & Buhrer) Nickle, is a pathogenic nematode that is responsible for the devastating epidemic of pine wilt disease (PWD) worldwide (Mota and Vieira 2008; Robertson et al. 2011), particularly throughout Japan, Korea and China (Togashi and Jikumaru 2007; Jung et al. 2010; Abelleira et al. 2011; Foit et al. 2019). Since the first report in Nanjing, China, in 1982, PWD has spread through more than 700 counties in 19 provinces (State Forestry Administration of the People's Republic of China 2021), killing over one billion pine trees (Zhu et al. 2021). Economic and ecological losses have totalled thousands of billions of Chinese Yuan. PWN has diverse carriers and hosts. Carriers include more than eight beetle species and at least 25 hosts are susceptible under natural conditions (Zheng et al. 2021). In China, the primary PWN vector is the sawyer beetle *Monochamus alternatus* Hope (Coleoptera, Cerambycidae), while *Pinus massoniana* is one of the earliest and most susceptible hosts (Linit et al. 1983; Kobayashi et al. 1984; Ye 2019; Ji et al. 2021).

The PWN is the predominant pathogen in this complex ecosystem (Zhao et al. 2014). The symbiotic interaction between the PWN-vector and fungi is a key biological factor that promotes PWN pathogenicity and invasiveness (Zhao et al. 2014; Zhao and Sun 2017). Molecular analysis has repeatedly demonstrated that the fungus and the PWN have a close symbiotic relationship, as evidenced by the draft genome sequence of a PWN inbred line which revealed that all PWN cellulases were most likely acquired independently from fungi (Kikuchi et al. 2011). Metagenomic analysis of the PWN microbiome indicates that the PWN and its microbiome have established a potentially mutualistic symbiotic relationship with complementary pathways in detoxification metabolism (Kikuchi et al. 2011; Cheng et al. 2013).

Current research has shown that PWN has an important mycetophagous phase in its life history (Ryss et al. 2005; Espada et al. 2016). Many airborne fungi, including endophytes (*Botrytis cinerea* and *Cladosporium herbarum*) and pathogens (*Sirococcus conigenus* and *Sphaeropsis sapinea*), are positively correlated with the growth of the nematode population (Pimentel et al. 2021), with ophiostomatalean fungi (Ascomycota: Sordariomycetes: Ophiostomatales) particularly important in terms of

their association with PWN-*M. alternatus* symbionts. The Ophiostomatales order includes one family (Ophiostomataceae) and twenty genera (*Afroraffaelea*, *Aureovirgo*, *Ceratocystiopsis*, *Chrysosphaeria*, *Dryadomyces*, *Esteya*, *Fragosphaeria*, *Graphilbum*, *Grosmannia*, *Hawksworthiomyces*, *Harringtonia*, *Heinzbutinia*, *Intubia*, *Jamesreidia*, *Leptographium*, *Masuyamyces*, *Ophiostoma*, *Paleoambrosia*, *Raffaelea* and *Sporothrix*) (de Beer et al. 2014, 2016, 2022; Hyde et al. 2020; Wijayawardene et al. 2022). *Sporothrix* sp.1, for example, induces the xylem tissue of the pine tree to produce diacetone alcohol, which may increase PWN propagation and beetle larvae growth (Zhao et al. 2013). PWN produces ascarosides that promote fungal (*Leptographium pini-densiflora* and *Sporothrix* sp.1) growth and sporulation (Zhao et al. 2018). In addition, some fungi are detrimental to PWN. *Esteya vermicola* is an example of direct antagonism (Wang et al. 2011). The lunate conidia of *E. vermicola* are highly infectious to PWN (Liou et al. 1999).

The invasion of beetles altered the internal habitat and mycoflora of pine trees (Zhang et al. 2021). Fungal invasion patterns in beetle-infested hosts may have been successional. *Ips typographus*, for example, attacked Norway spruce with the virulent *Ceratocystis polonica*, followed by other beetle-diffused *Graphium* and *Ophiostoma* fungi (Solheim 1992a, 1992b); *Tomicus minor* invaded *Pinus sylvestris* with *Hormonema dematioides* first, followed by *Ophiostoma tingens* and *O. canum* (Jankowiak 2008). *Ophiostoma ips* was not isolated from the 2nd–3rd instar larvae galleries of *M. alternatus*, but the isolation rate from the 4th–5th instar larvae galleries was 92.5% (Lun et al. 2019). The diversity and abundance of fungi associated with *M. alternatus* larvae of different instars in PWN-infected pines, as well as the successional pattern of fungi in PWN-*M. alteratus* symbionts are unknown. To date, 14 ophiostomatalean fungi have been obtained from *M. alternatus* galleries and pupal chambers along with PWN (Zhao et al. 2013, 2014, 2018; Wang et al. 2018; Lun et al. 2019). However, these studies are sporadic reports and no systematic studies have been conducted.

This research aimed to compare the diversity of fungi in different instars of the PWN-infected *M. alternatus* larval galleries and pupal chambers in south-eastern China. Field surveys were used in conjunction with integrated morphological observation and multi-locus DNA sequence analysis to describe the diversity of fungi associated with PWN and *M. alternatus*. This study provides a scientifically reliable and theoretical foundation for effective PWD control from the fungal perspective.

Materials and methods

Collection of samples and fungal isolations

From October to November 2020, fungi were isolated from 380 and 510 samples of different instars from *M. alternatus* larvae galleries and pupal chambers in *Pinus massoniana*, respectively, in the Huangyan District (28°56'90"N, 121°17'56"E), Xianju County (28°75'28"N, 120°59'97"E), Zhejiang Province. All the trees used

in this study showed signs of death and sap stains and PWNs were simultaneously isolated from galleries and pupal chambers by Behrman funnel. The samples were collected by hand saw, individually placed in sterile envelopes, stored at 4 °C and separated within a week. The surfaces of galleries and pupal chambers were disinfected with 1.5% sodium hypochlorite for 1 min, rinsed with sterile water three times and then cut into approximately 3 × 3 mm^2 tissue blocks. They were then inoculated on to a 2% (w/v) water agar medium (20 g agar powder in 1 l of deionised water) and cultured in the dark at 25 °C (Seifert et al. 1993; Wang et al. 2019; Wang et al. 2020). Subsequently, all strains were purified by hyphal tip isolation (Eckhardt 2002) and transferred on to 2% (w/v) malt extract agar (MEA: 20 g malt extract powder and 20 g agar powder in 1 l of deionised water) for growth in the dark at 25 °C. All strains were deposited at the Chinese Academy of Forestry (Table 1). Representative cultures were deposited at the China Forestry Culture Collection Center (CFCC) (Table 2).

Culture and morphological studies

The growth of representative strains was monitored daily and the culture characteristics of the colonies were recorded. Microscopic features were observed using a BX51

Table 1. Species of the fungi isolated from *Pinus massoniana* infected by *Monochamus alternates* and *Bursaphelenchus xylophilus* in the current study.

Taxon	Species	2nd–3rd instar larvae		4th~5th instar larvae	
		number	isolation rate	number	isolation rate
1	*Ceratocystiopsis weihaiensis*	3	1.18%	N/A	N/A
	Chaetomium globosum	1	0.39%	N/A	N/A
	Colletotrichum gloeosporioides	8	3.14%	N/A	N/A
	Cytospora sp.	11	4.31%	N/A	N/A
	Diplodia sapinea	27	10.59%	76	16.74%
	Fusarium sp.	10	3.92%	N/A	N/A
2	*Graphilbum* sp.	N/A	N/A	12	2.64%
3	*Ophiostoma ips*	N/A	N/A	231	50.88%
4	*Ophiostoma* sp.	62	24.31%	N/A	N/A
	Penicillium sp.	2	0.78%	5	1.10%
	Pestalotiopsis sp.	N/A	N/A	2	0.44%
	Phialocephala sp.	45	17.65%	N/A	N/A
	Pseudocosmospora sp.	14	5.49%	N/A	N/A
	Schizophyllum sp.	8	3.14%	N/A	N/A
5	*Sporothrix macroconidia*	4	1.57%	N/A	N/A
6	*S. zhejiangensis*	8	3.14%	N/A	N/A
	Trichoderma atroviride	N/A	N/A	107	23.57%
	Xenoacremonium sp.	37	14.51%	N/A	N/A
	Unidentified	15	5.88%	21	4.63%
	The total number of strains	255	100%	454	100%

Unseparated data is represented by [N/A].

Table 2. Strains of ophiostomatalean fungi isolated from *Pinus massoniana* infested by *Monochamus alternatus* and *Bursaphelenchus xylophilus* in the current study.

Taxon	Species	Strain no	Location	GenBank no		
				ITS	TUB2	TEF1-α
1	*Ceratocystiopsis weihaiensis*	CFCC 55742 CXY4012	Huangyan	OK104016	OM103280	N/A
		CFCC 55743 CXY4013	Huangyan	OK104017	OM103281	N/A
		CXY4019	Huangyan	N/A	N/A	N/A
2	***Graphilbum xianjuensis* sp. nov.**	**CFCC 55738^{T} CXY4010**	Xianju	OK104014	OM103285	ON033177
		CFCC 55739 CXY4011	Xianju	OK104015	OM103286	ON033178
		CXY4018	Xianju	N/A	N/A	N/A
3	*Ophiostoma ips*	CFCC 55735 CXY4005	Xianju	OK104009	OM056673	N/A
		CFCC 55736 CXY4006	Xianju	OK104010	OM056674	N/A
		CFCC 55732 CXY4007	Xianju	OK104011	OM056675	N/A
4	***Ophiostoma taizhouense* sp. nov.**	**CFCC 55740^{T} CXC4001**	Huangyan	OK104005	OM103276	N/A
		CFCC 55731 CXY4002	Huangyan	OK104006	OM103277	N/A
		CFCC 55733 CXY4003	Huangyan	OK104007	OM103278	N/A
		CFCC 55734 CXY4004	Huangyan	OK104008	OM103279	N/A
5	*Sporothrix macroconidia*	CFCC 55741 CXY4009	Huangyan	OK104013	OL352730	N/A
		CXY4016	Huangyan	N/A	N/A	N/A
		CXY4017	Huangyan	N/A	N/A	N/A
6	*S. zhejiangensis*	CFCC 55737 CXY4008	Huangyan	OK104012	OM103282	N/A
		CXY4014	Huangyan	N/A	OM103283	N/A
		CXY4015	Huangyan	N/A	OM103284	N/A

Species names in bold are novel species described in this study. "T" indicates ex-type strains.
CFCC: China Forestry Culture Collection Center, Beijing, China.
CXY (Culture Xingyao): Culture collection of the Research Institute of Forest Ecology and Nature Conservation, Chinese Academy of Forestry.
Sequences missing data are indicated by [N/A]

Olympus microscope (Tokyo, Japan) with differential interference contrast. Fifty measurements were made for each microscopic taxonomical structure. The formula (min–) (mean–SD)–(mean+SD) (–max) was used to calculate averages, ranges, standard deviation (SD), minimum (min) and maximum (max) measurements, respectively. All relevant data pertaining to type specimens were deposited in MycoBank (www.MycoBank.org).

A 7 mm diameter mycelium plug was taken from a flourishing fungal colony using a sterile puncher and placed at the centre of 90 mm diameter 2% MEA plates, with one side of mycelium in contact with the media. Five replicate plates for each strain were incubated in a dark incubator at 5–35 °C with a temperature interval of 5 °C. The diameter of the colonies on each dish was measured every day by the orthogonal method until the fastest-growing mycelium reached the edge of the dish. The colony colour was then described using the Rayner (1970) colour chart.

DNA extraction, amplification and sequencing

Mycelia of representative strains were scraped with a sterile blade from the edge of the medium and transferred to 2 ml Eppendorf tubes for DNA extraction. DNA extraction and purification were carried out using the Invisorb Spin Plant Mini Kit (Tiangen, Beijing, China) according to the manufacturer's instructions. The primer pairs ITS1/ITS4 (White et al. 1990), BT2a/BT2b (Glass and Donaldson 1995) and EF1/EF2 (Jacobs et al. 2004) were used for the internal transcribed spacer (ITS) region of the nuclear ribosomal DNA operon, including spacers 1 and 2 and the 5.8S gene, the β-tubulin (BT) gene region and transcription elongation factor-1α (TEF-1α), respectively.

Polymerase chain reaction (PCR) amplification was performed using a Veriti 96-Well Fast Thermal Cycler (Applied Biosystems Veriti96, Foster City, CA, USA). PCR was carried out in a final volume of 25 μl (2.5 mM $MgCl_2$, 1× PCR buffer, 0.2 mM dNTP, 0.2 mM of each primer and 2.5 U Taq-polymerase enzyme). The cycling conditions were the same as those described for primer design (White et al. 1990; Glass and Donaldson 1995; Jacobs et al. 2004). The PCR products were purified using the MSB Spin PCR Apace Kit (250) (Invitek, Berlin, Germany) in accordance with the manufacturer's instructions.

Sequencing reactions were performed using a CEQ DTCS Quick Start Kit (Beckman Coulter, Brea, CA, USA) according to the manufacturer's instructions, with the same PCR primers as above. Nucleotide sequences were determined using a CEQ 2000 XL capillary automated sequencer (Beckman Coulter). Complementary and overlapping DNA electropherograms were checked and assembled using BioEdit v. 7.2.0. (Hall 1999).

Sequence alignment and phylogenetic analysis

Preliminary identification of the strains was conducted using the standard basic local alignment search tool (BLAST) searches in NCBI GenBank (http://blast.ncbi.nlm.nih.gov/Blast.cgi) and sequences with the highest similarity were downloaded from GenBank. Alignment of the genes was performed using MAFFT 7.0 (https://mafft.cbrc.jp/alignment/server/) (Katoh and Standley 2013), with the E-INS-I option with a gap-opening penalty of 1.53 and an offset value of 0.00 and edited manually using Molecular Evolutionary Genetic Analyses (MEGA) 7.0 software (Kumar et al. 2016).

Maximum Parsimony (MP), Maximum Likelihood (ML) and Bayesian Inference (BI) were used to infer the phylogenetic trees from each dataset. Two concatenated matrices of ITS and BT sequences were generated for *Ceratocystiopsis* and the *O. ips* complex.

MP analyses were implemented using PAUP* version 4.0b10 (Swofford 2003). The gaps were treated as the fifth base. Bootstrap analysis (1000 bootstrap repetitions) was used to determine the confidence level for inferring the nodes in the tree topology. Tree bisection and reconnection were selected as the branch swapping option. For each dataset of the 5000 most-parsimonious trees, the best tree that was automatically output by PAUP* v. 4.0b10 was selected for use in the figure.

ML analyses were carried out using RAxML-HPC (version 8.2.3; Stamatakis 2014) and the selected GTR-GAMMA model of site substitution included the estimation of gamma-distributed rate heterogeneity and a proportion of invariant sites. ML analysis included 1000 bootstrap analyses to evaluate the overall reliability of the node support value and tree topology.

BI analyses using Markov Chain Monte Carlo (MCMC) methods were implemented in MrBayes version 3.1.2 (Ronquist et al. 2012), from a random starting tree for 5,000,000 generations, to calculate posterior probability values for the nodes. When we run to 5,000,000 generations, the split frequencies of all datasets were less than 0.01. Chain convergence for all datasets was determined using Tracer 1.7 (Rambaut et al. 2018). No lack of convergence was detected. Trees were sampled every 100 generations and the first 25% of trees sampled were discarded as burn-in, while the remaining trees were used to calculate Bayesian posterior probabilities of the clades. Phylogenetic trees were edited in Figtree version 1.4.3 (http://tree.bio.ed.ac.uk/sosftware/figtree/) and Adobe Illustrator CS6.

Results

Fungal isolation and sequence comparison

A total of 709 strains of fungi were isolated from the *M. alternatus* larval galleries and pupal chambers (2^{nd}–5^{th} instars). The strains were divided into 18 taxa, based on colony morphology and multi-locus DNA sequence alignment (ITS and BT) analysis. A total of 255 fungal strains, representing 14 taxa, were isolated from the galleries of 2^{nd}–3^{rd} instar larvae. Taxon 4 was the dominant taxon accounting for 62 of the 255 strains. A total of 454 fungal strains were isolated from the galleries and pupal chambers of the 4^{th}–5^{th} instar larvae and divided into six taxa. The dominant taxon was *O. ips*, accounting for 231 out of the 454 strains (Table 1). Only two fungi (*Diplodia sapinea* and *Penicillium* sp.) could be isolated from both 2^{nd}–3^{rd} instar larval galleries and 4^{th}–5^{th} instar larval galleries and pupal chambers, except for unidentified species. In this study, 320 ophiostomatalean fungi strains (320 strains out of 709 fungal strains) were isolated, including six tentative species. Four

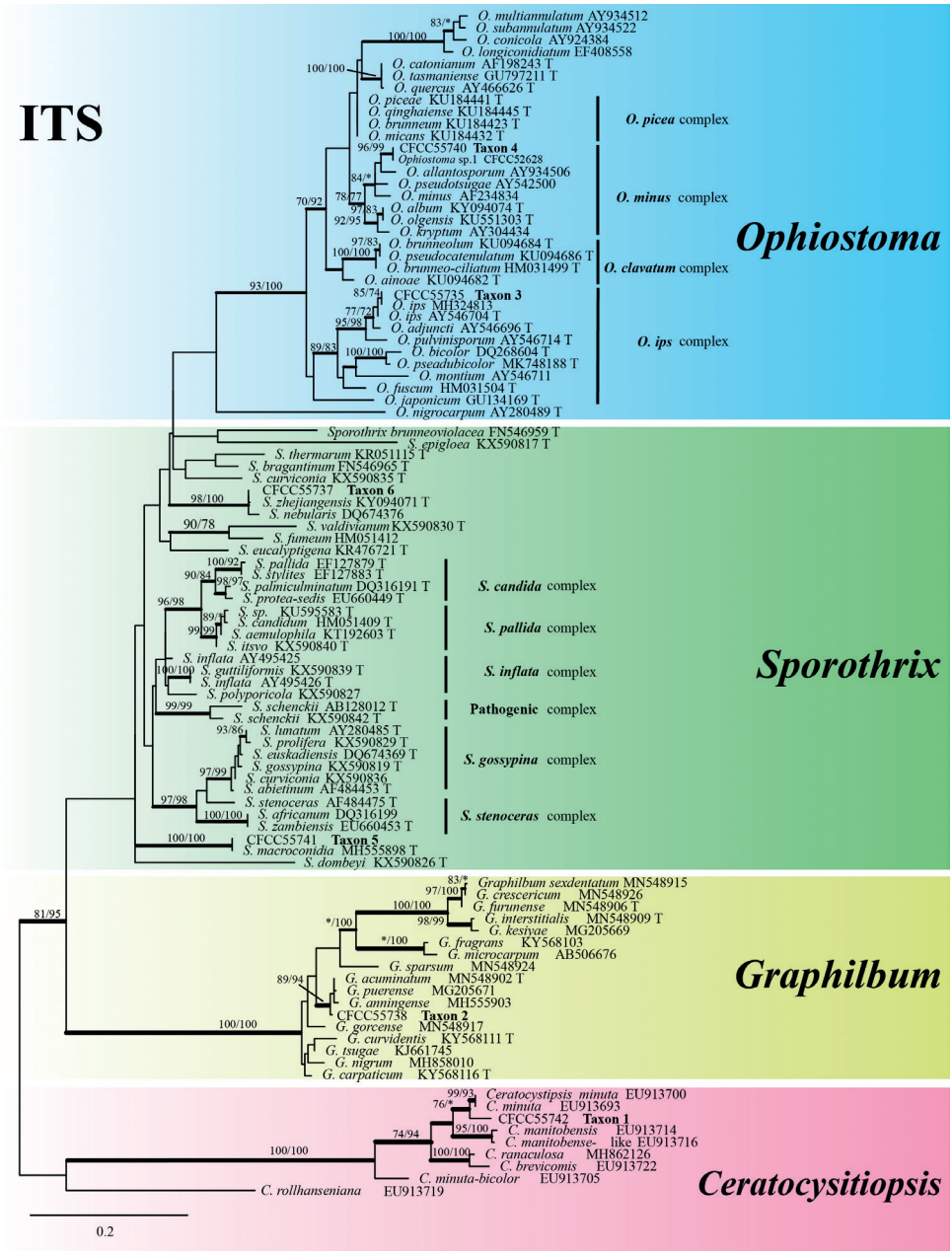

Figure 1. ML tree of the ITS region of *Ophiostoma*, *Sporothrix*, *Graphilbum*, *Ceratocystiopsis*. Bootstrap values of ML/MP ≥ 70% are recorded at nodes as ML/MP and bold branches indicate posterior probability values ≥ 0.9. ML and MP, Bootstrap values < 70% are indicated by the symbol *. The tree is drawn to scale (see bar) with branch length measured in the number of substitutions per site. Strains representing ex-type sequences are marked with "T." ML, Maximum Likelihood; MP, Maximum Parsimony; BI, Bayesian Inference and the final alignment of 734 positions, including gaps.

of these six species were obtained from the galleries of the 2nd–3rd instar larvae and two species were isolated from the galleries and pupal chambers of the 4th–5th instar larvae (Table 1).

Phylogenetic analyses

There were 709 strains obtained in this study, but some strains have a small number of strains. In this study, we selected 2–4 representative strains from each Taxon and nineteen representative strains of Ophiostomatales belonging to six tentative species (Taxa 1–6) were selected for phylogenetic analyses (Table 2). All the sequences used for the phylogenetic trees were submitted to GenBank. The three phylogenetic approaches yielded similar topologies, with statistical support varying slightly for each sequence dataset. Phylograms derived from ML analysis were presented

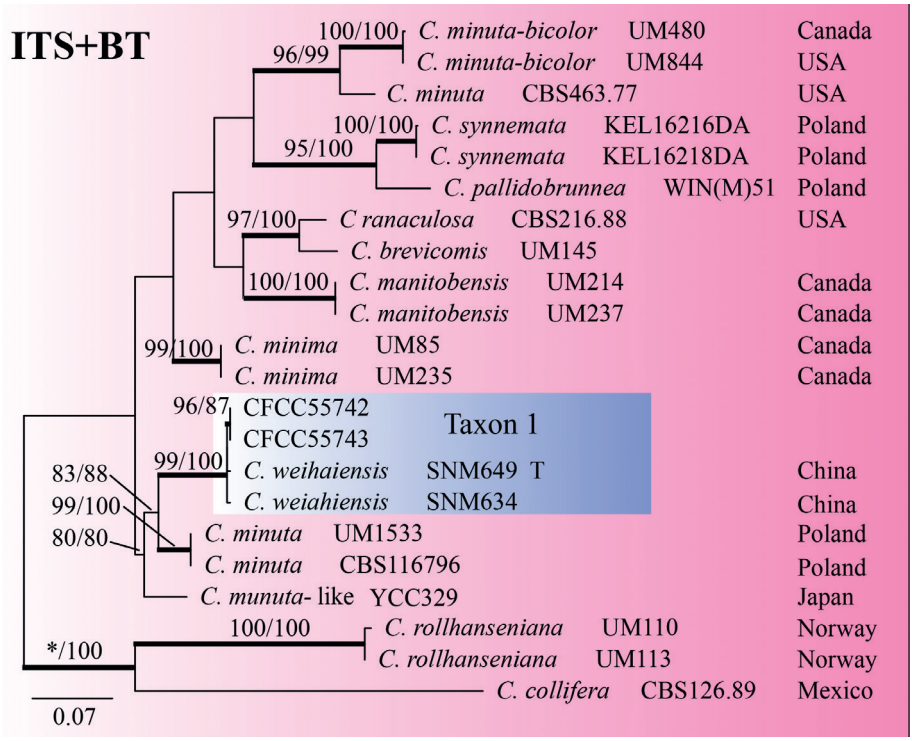

Figure 2. ML tree of *Ceratocystiopsis* generated from the combined (ITS+BT) sequence data. Bootstrap values of ML/MP ≥ 70% are recorded at nodes as ML/MP and bold branches indicate posterior probability values ≥ 0.9. ML and MP, Bootstrap values < 70% are indicated by the symbol *. The tree is drawn to scale (see bar) with branch length measured in the number of substitutions per site. Strains representing ex-type sequences are marked with "T." Abbreviations: ML, Maximum Likelihood; MP, Maximum Parsimony; BI, Bayesian Inference and the final alignment of 1040 positions, including gaps.

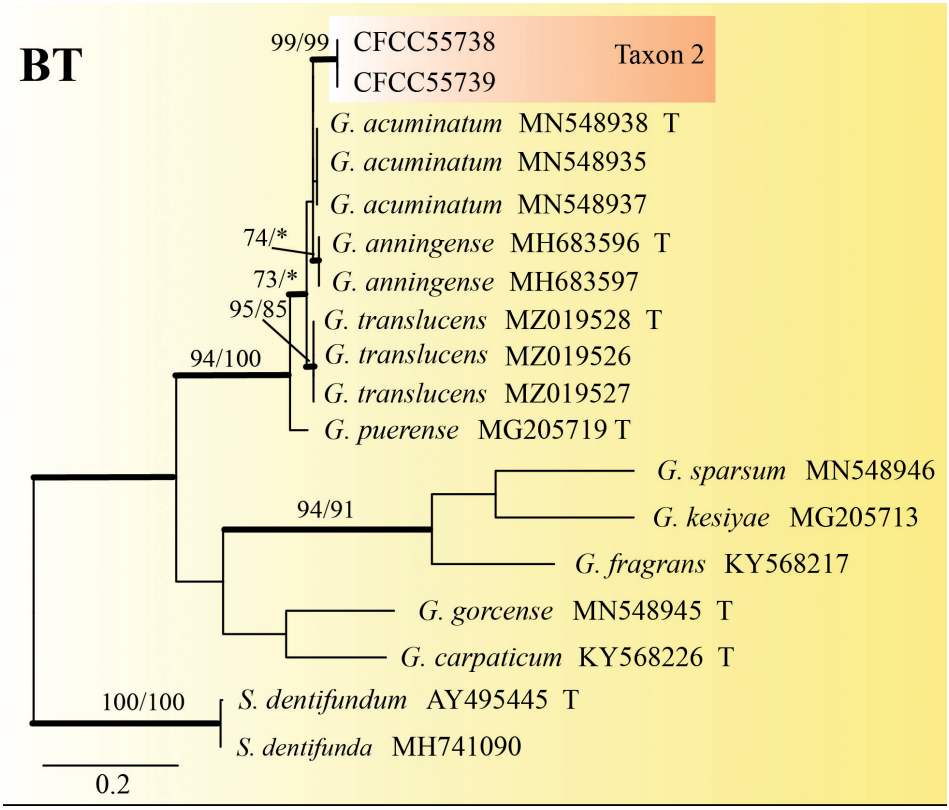

Figure 3. ML tree of the BT region of *Graphilbum*. Bootstrap values of ML/MP ≥ 70% are recorded at nodes as ML/MP and bold branches indicate posterior probability values ≥ 0.9. ML and MP, Bootstrap values < 70% are indicated by the symbol *. The tree is drawn to scale (see bar) with branch length measured in the number of substitutions per site. Strains representing ex-type sequences are marked with "T." Abbreviations: ML, Maximum Likelihood; MP, Maximum Parsimony; BI, Bayesian Inference and the final alignment of 548 positions, including gaps.

for each individual dataset, along with nodal supports derived from the MP and BI analyses.

The ITS phylogenetic tree showed that six representative taxa (Table 2) belonged to six phylogenetic clades (Fig. 1). Taxa 1–2 nested within the *Ceratocystiopsis* and *Graphilbum* lineages, respectively; Taxa 3–4 nested within the *Ophiostoma* lineage, Taxon 3 belonging to the *Ophiostoma minus* complex and Taxon 4 belonging to the *O. ips* complex (de Beer and Wingfield 2013); Taxa 5–6 belonged to the *Sporothrix* and were not placed in any complex defined by de Beer et al. (2016) (Fig. 1).

Taxon 1 included three isolates, all of which were included in the analyses (Tables 1, 2). Based on the phylogenetic analysis of the combined dataset (ITS+BT), this taxon forms a well-supported clade with *Ceratocystiopsis weihaiensis* (Fig. 2). Hence, the strains in Taxon 1 should be identified as *C. weihaiensis*.

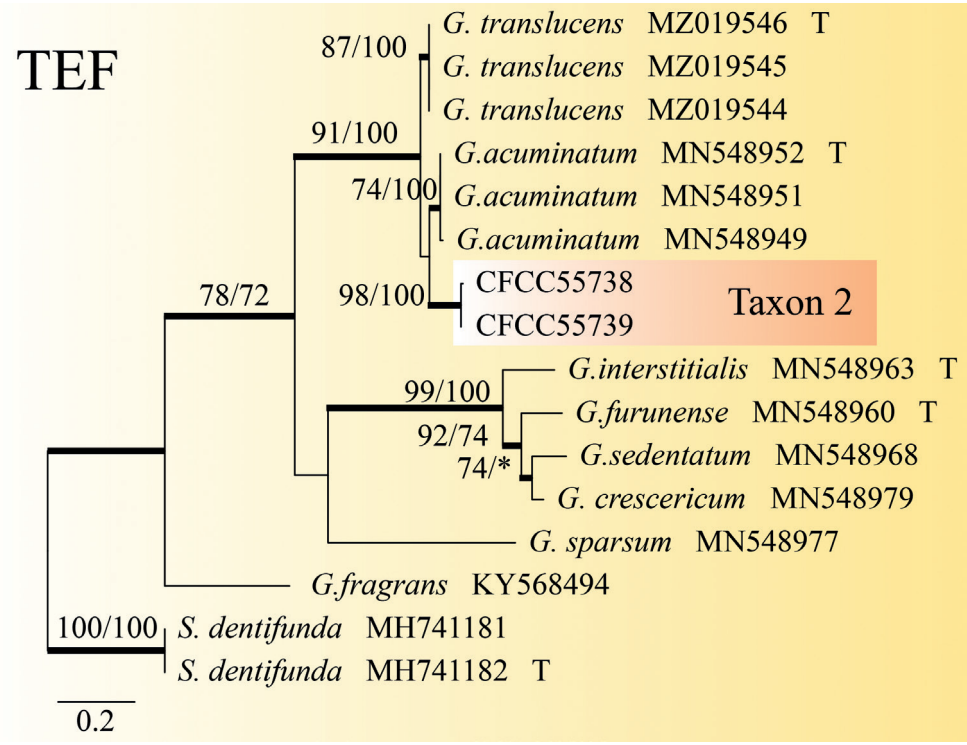

Figure 4. ML tree of the TEF region of *Graphilbum*. Bootstrap values of ML/MP ≥ 70% are recorded at nodes as ML/MP and bold branches indicate posterior probability values ≥ 0.9. ML and MP, Bootstrap values < 70% are indicated by the symbol *. The tree is drawn to scale (see bar) with branch length measured in the number of substitutions per site. Strains representing ex-type sequences are marked with "T." Abbreviations: ML, Maximum Likelihood; MP, Maximum Parsimony; BI, Bayesian Inference and the final alignment of 725 positions, including gaps.

Taxon 2 consisted of 12 isolates, three of which were used for phylogenetic analyses (Tables 1, 2). The phylograms of ITS, BT and TEF-1α datasets revealed that Taxon 2 was an independent clade closely related to *Graphilbum acuminatum*, *G. anningense* and *G. translucens* (Figs 1, 3, 4). As a result, Taxon 2 should be interpreted as belonging to a distinct, undescribed *Graphilbum* species.

Taxon 3 was represented by three sequences that formed a well-supported clade with *O. ips*, based on the ITS tree (Fig. 1). Further phylogenetic analysis, based on combined datasets (ITS+BT) yielded similar results (Fig. 5). Based on ITS and BT phylogenetic analysis, Taxon 4, represented by three sequences, has a well-supported independent clade with *Ophiostoma* sp.1 (CFCC52628) (Wang et al. 2019), which is closely related to *O. allantosporum*, *O. pseudotsugae* and *O. wuyingensis* (Figs 6, 7). Thus, Taxon 3 should be identified as a known species of *O. ips*, whereas Taxon 4 should be interpreted as a distinct, undescribed *Ophiostoma* species.

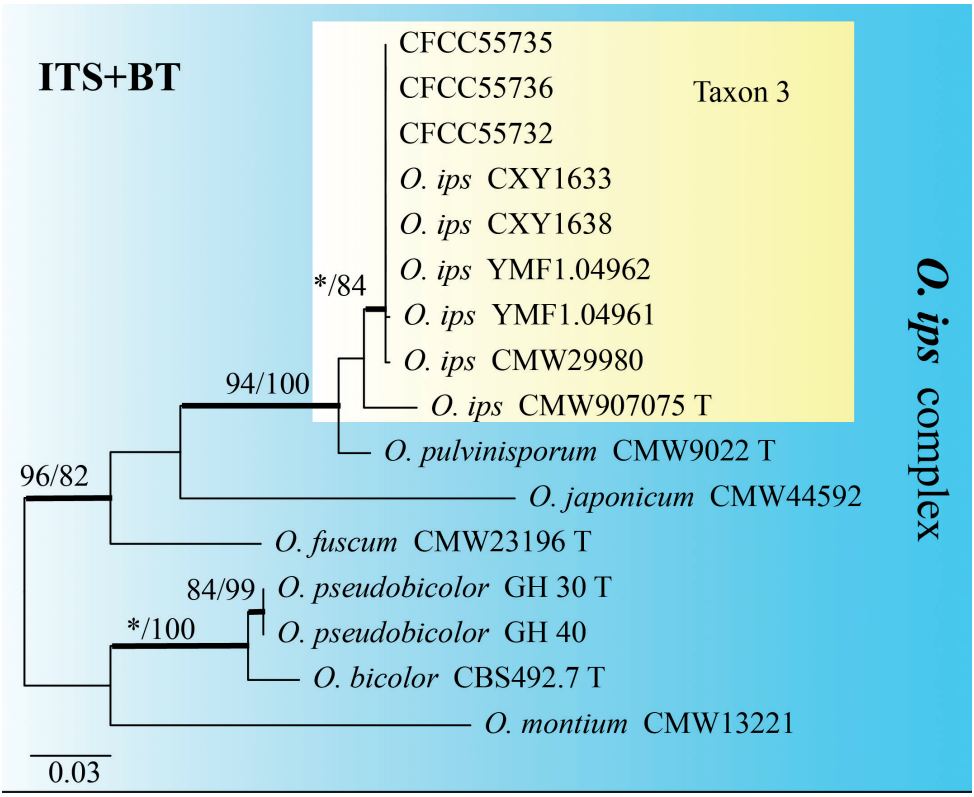

Figure 5. ML tree of the *O. ips* complex generated from the combined (ITS+BT) sequence data. Bootstrap values of ML/MP ≥ 70% are recorded at nodes as ML/MP and bold branches indicate posterior probability values ≥ 0.9. ML and MP, Bootstrap values < 70% are indicated by the symbol *. The tree is drawn to scale (see bar) with branch length measured in the number of substitutions per site. Strains representing ex-type sequences are marked with "T." Abbreviations: ML, Maximum Likelihood; MP, Maximum Parsimony; BI, Bayesian Inference and the final alignment of 953 positions, including gaps.

Taxon 5 consisted of four isolates, three of which were used for the phylogenetic analyses. Based on the ITS and BT phylogenetic trees, Taxon 5 grouped with *Sporothrix zhejiangensis* (Figs 1, 8). Thus, it should be identified as *S. zhejiangensis.*

Taxon 6 consisted of eight isolates, three of which were selected for analysis. Taxon 6 grouped with *Sporothrix macroconidia*, based on the ITS and BT phylogenetic trees (Figs 1, 8). As a result, Taxon 6 was designated as *S. macroconidia*.

Taxonomy

According to the ITS and BT phylogenetic analyses, six different taxa (Taxon 1–6) were identified in this study. They represent four known species, *Ceratocystiopsis weihaiensis*, *O. ips*, *S. macroconidia* and *S. zhejiangensis* (Lun et al. 2019; Wang et al. 2019; Chang et al. 2021), in addition to two novel species. They are described as follows:

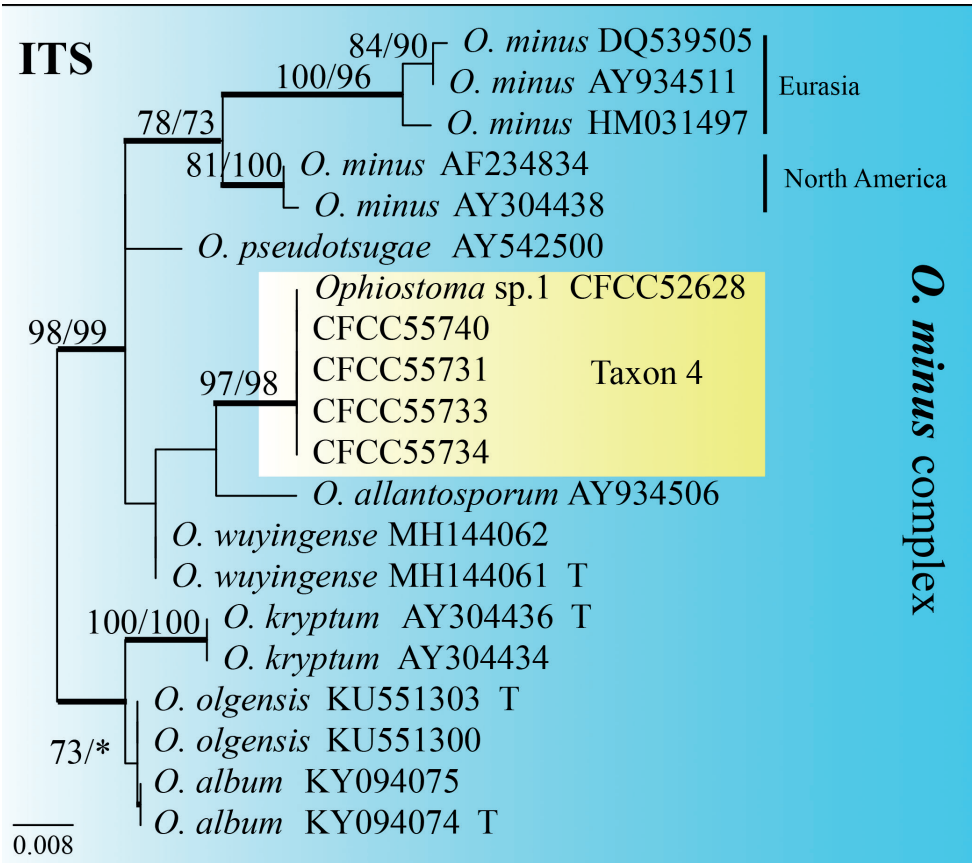

Figure 6. ML tree of the ITS region of *O. minus* complex. Bootstrap values of ML/MP ≥ 70% are recorded at nodes as ML/MP and bold branches indicate posterior probability values ≥ 0.9. ML and MP, Bootstrap values < 70% are indicated by the symbol *. The tree is drawn to scale (see bar) with branch length measured in the number of substitutions per site. Strains representing ex-type sequences are marked with "T." Abbreviations: ML, Maximum Likelihood; MP, Maximum Parsimony; BI, Bayesian Inference and the final alignment of 537 positions, including gaps.

***Graphilbum xianjuensis* G. H. Zheng & Q. Lu, sp. nov.**
MycoBank No: 842387
Fig. 9

Etymology. The epithet *xianju* (Latin) refers to the type locality.

Type. China, Zhejiang, Xianju County, from *Monochamus alternatus* galleries and pupal chambers of *Pinus massoniana* infested by *Bursaphelenchus xylophilus*, December 2020, collected by G. H. Zheng, culture ex-holotype CFCC55738 = CXY4010.

Description. Sexual morph: not observed.

Asexual form: *Hyalorhincladiella*-like. Conidiogenous cells were simple or loosely branched, (9.12–) (15.44) – (48.64) (–62.49) × (1.25–) (1.53) – (2.21) (–2.45) μm. Co-

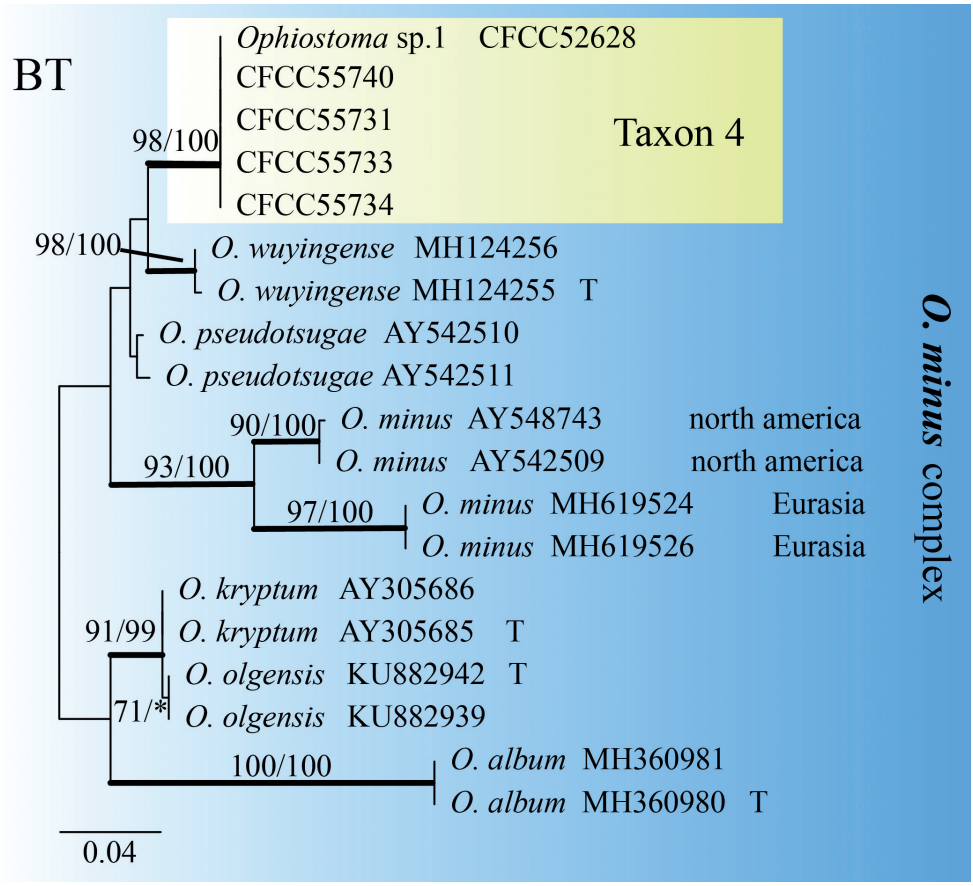

Figure 7. ML tree of the BT region of *O. minus* complex. Bootstrap values of ML/MP ≥ 70% are recorded at nodes as ML/MP and bold branches indicate posterior probability values ≥ 0.9. ML and MP, Bootstrap values < 70% are indicated by the symbol *. The tree is drawn to scale (see bar) with branch length measured in the number of substitutions per site. Strains representing ex-type sequences are marked with "T." Abbreviations: ML, Maximum Likelihood; MP, Maximum Parsimony; BI, Bayesian Inference and the final alignment of 495 positions, including gaps.

nidia hyaline, smooth, cylindrical, aseptate, (4.76–) (6.07) – (9.87) (–13.41) × (0.99 –) (1.32) – (2.1) (–2.65) μm.

Culture characteristics. Colonies on 2% MEA reaching 44.9 mm diameter, after incubation in the dark at 25 °C for 3 d, growth rate up to 14.98 mm/d at the fastest and colony margin irregular. Mycelium superficial to flocculose or floccose, hyaline, reverse grey-white. The optimal temperature for growth at 30 °C; no growth was observed at 5 °C.

Habitat and distribution. Larval galleries and pupal chambers of *Monochamus alternatus* in *Pinus massoniana*, infested by *Bursaphelenchus xylophilus*, in Zhejiang Province, China.

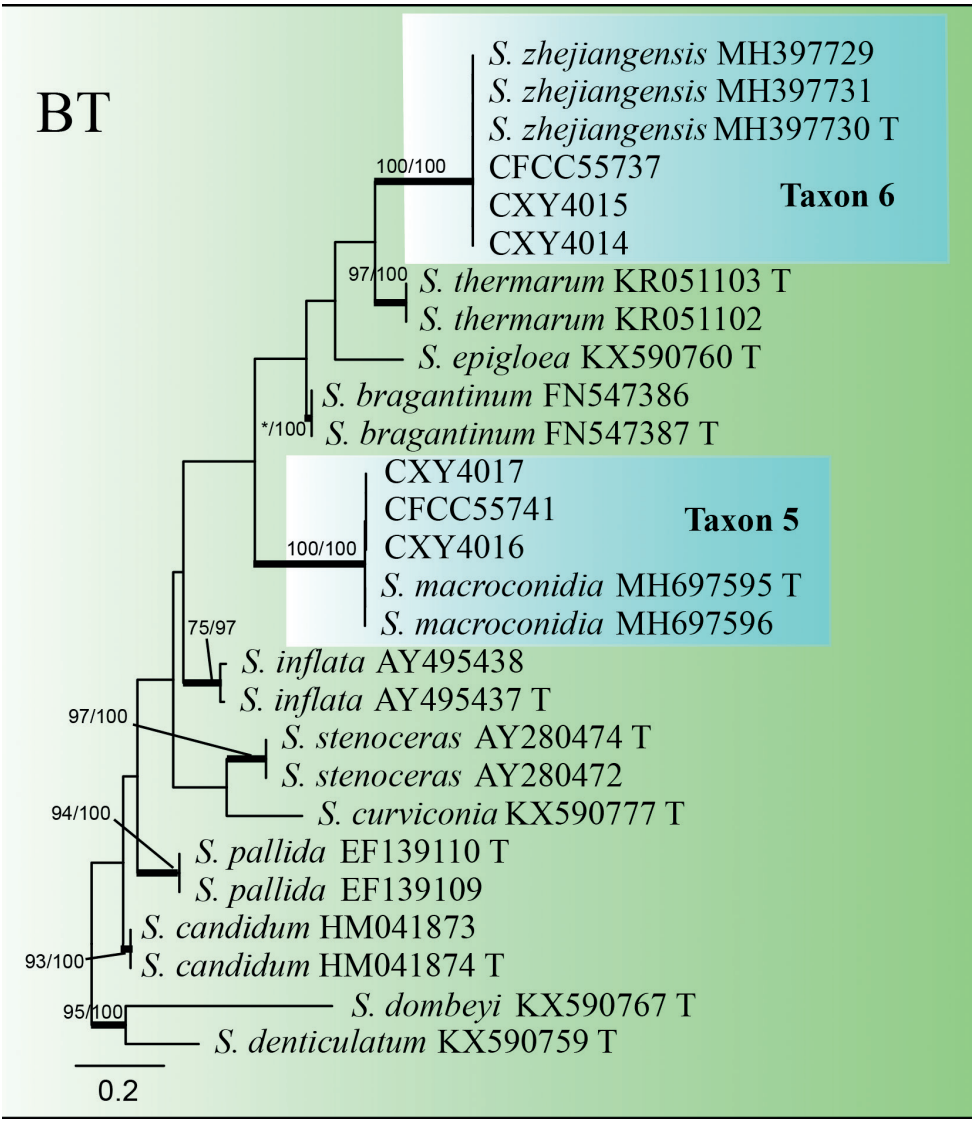

Figure 8. ML tree of *Sporothrix* generated from the BT sequence data. Bootstrap values of ML/MP ≥ 70% are recorded at nodes as ML/MP and bold branches indicate posterior probability values ≥ 0.9. ML and MP, Bootstrap values < 70% are indicated by the symbol *. The tree is drawn to scale (see bar) with branch length measured in the number of substitutions per site. Strains representing ex-type sequences are marked with "T." Abbreviations: ML, Maximum Likelihood; MP, Maximum Parsimony; BI, Bayesian Inference and the final alignment of 313 positions, including gaps.

Additional specimens examined. China, Zhejiang, from *Monochamus alternatus* galleries and pupal chambers of *Pinus massoniana* infested by *Bursaphelenchus xylophilus*, December 2020, collected by G. H. Zheng, CFCC55739 = CXY4011, CXY4018.

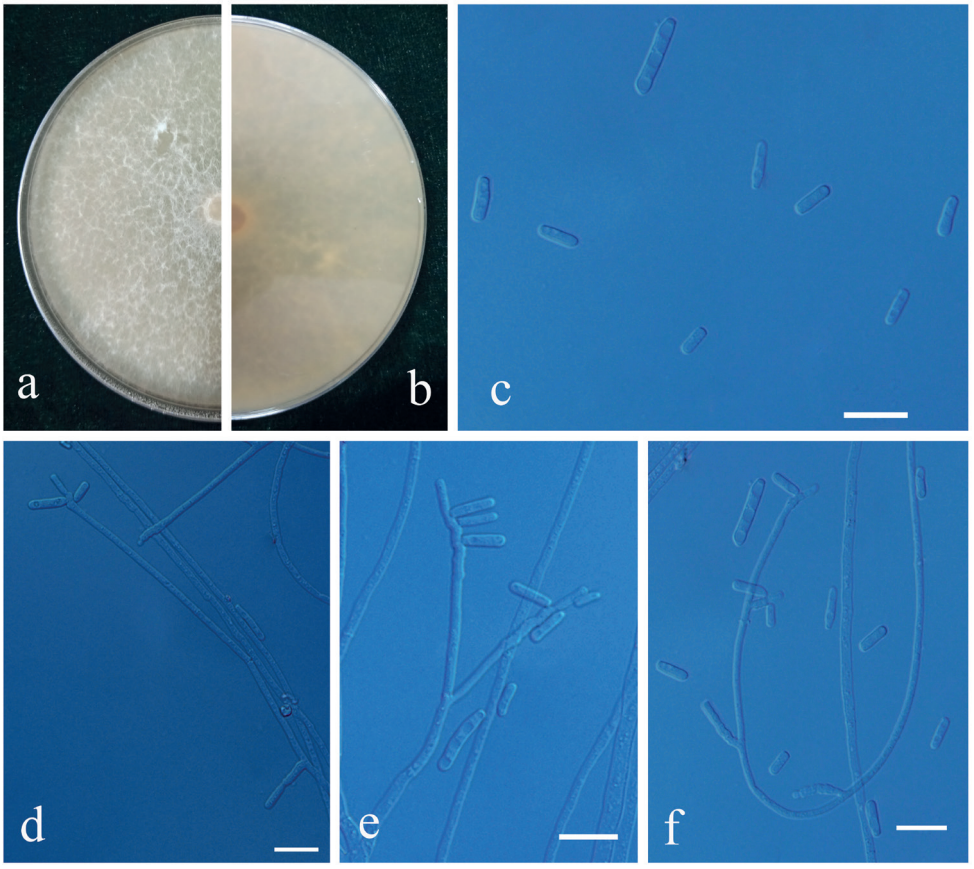

Figure 9. Morphological characteristics of *Graphilbun xianjuensis* sp. nov. (CFCC = 55738, Taxon 2). **a, b** thirty-day-old cultures on 2% MEA **c–f** *Hyalorhincladiella*-like asexual morph: conidiogenous cells and conidia. Scale bars: 10 μm (**c–f**).

Note. Only the *Hyalorhincladiella*-like asexual form was observed in *Graphilbum xianjuensis*. This is closely related to *the G. acuminatum*, *G. anningense* and *G. translucens*, based on the ITS, BT and TEF1-α phylogenetic trees (Figs 1, 3, 4). Four species differed according to the size of their conidia. The conidia of *G. xianjuensis* (6.07–9.87 μm) are longer than those of *G. anningense* (4.5–6.4 μm), *G. acuminatum* (3.5–6 μm) and *G. translucens* (2.4–3.5 μm) (Wang et al. 2019; Jankowiak et al. 2020). Besides, *G. xianjuensis* was found to be associated with *M. alternatus* and PWN-infested *P. massoniana*, whereas *G. anningense* was reported in galleries of *T. yunnanensis* and *T. minor* associated with *P. yunnanensis* in southwest China (Wang et al. 2019), *G. acuminatum* has been reported in galleries of *Ips acuminatus* and *Pityogenes bidentatus* associated with *P. sylvestris* in Europe (Jankowiak et al. 2020) and *G. translucens* was first reported in *Cryphalus piceae* associated with *P. densiflora*. In conclusion, four species of *Graphilbum* differ not only in geographical distribution, but also in hosts and vectors. The optimum

growth temperature of *G. xianjuensis*, *G. anningense* and *G. translucens* is 30 °C and only *G. acuminatum* had an optimum growth temperature of 25 °C (Wang et al. 2019; Jankowiak et al. 2020).

***Ophiostoma taizhouense* G. H. Zheng & Q. Lu, sp. nov.**
MycoBank No: 842388
Fig. 10

Etymology. '*taizhou*' (Latin) refers to the type locality.

Type. China, Zhejiang Province, Taizhou City, from *Monochamus alternatus* galleries of *Pinus massoniana* infested by *Bursaphelenchus xylophilus*, October 2020, collected by G. H. Zheng and Q. Lu, culture ex-holotype CFCC55740 = CXY4001.

Description. Sexual morph: not observed.

Asexual form: *Hyalorhincladiella*-like. Conidiophores abundant, conidiogenous cells single, disposed in a dense rachis (3.08–) (6.6) – (15.63) (–23.07) × (1.11–) (1.44) – (2.23) (–2.9) µm. Conidia hyaline, smooth, lunate, ellipsoid

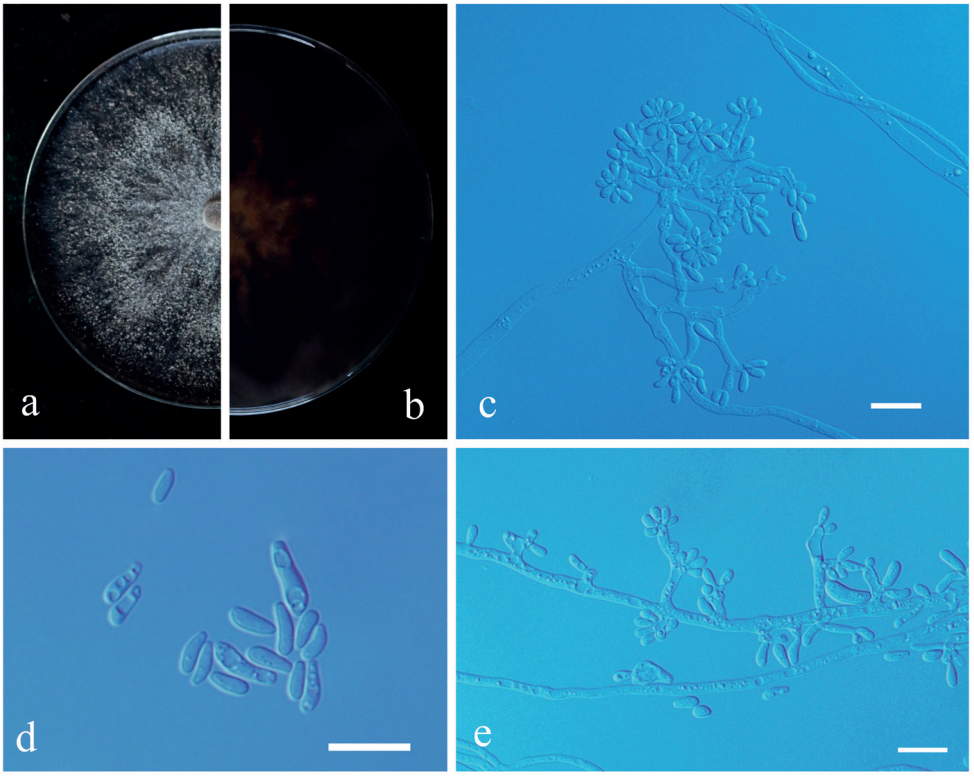

Figure 10. Morphological characteristics of *Ophiostoma taizhouense* sp. nov. (CFCC = 55740, Taxon 4). **a, b** twenty-day-old cultures on 2% MEA **c–e** *Hyalorhincladiella*-like asexual morph: conidiogenous cells and conidia. Scale bars: 10 µm (**c–e**).

to ovoid, curvulate, aseptate, (3.24–) (4.27) – (7.42) (–10.08) × (1.17–) (1.6) – (2.39) (–2.86) μm.

Culture characteristics. Colonies on 2% MEA reaching 62.5 mm diameter, after incubation in the dark at 25 °C for 3 d, growth rate up to 22.83 mm/d at the fastest, colony margin smooth, hyphae are superficial on agar. Some white mycelium was produced early during growth and became black after 8–15 d, transitioning from brown to dark brown. The optimal temperature for growth at 30 °C; no growth was observed at 5 °C.

Habitat and distribution. Larval galleries of *Monochamus alternatus* in *Pinus massoniana*, infested by *Bursaphelenchus xylophilus*, in Zhejiang Province, China.

Additional specimen examined. China, Zhejiang, Taizhou City, from *Monochamus alternatus* galleries of *Pinus massoniana* infested by *Bursaphelenchus xylophilus*, October 2020, collected by G. H. Zheng and Q. Lu, CFCC55731 = CXY4002, CFCC55733 = CXY4003, CFCC55734 = CXY4004.

Note. Only the *Hyalorhincladiella*-like asexual form was observed in *Ophiostoma taizhouense*. According to ITS and BT phylogenetic analysis, it has a well-supported independent clade with *Ophiostoma* sp.1 (CFCC52628) and is closely related to *O. allantosporum*, *O. pseudotsugae* and *O. wuyingensis* (Figs 1, 5, 6). Only one strain of *Ophiostoma* sp.1 was isolated in our laboratory from *P. yunnanensis* infested with *T. yunnanensis* in Yunnan Province, so this strain was not officially named before this study. Although the geographical location and host of *O. taizhouense* and *Ophiostoma* sp.1 are different, their culture characteristics and gene sequences (ITS and BT) are identical (Figs 1, 5, 6) (Wang et al. 2019). In general, the conidia of *O. taizhouense* (4.27–7.42 μm) are longer than those of *O. minus* (2.5–6 μm) (Upadhyay 1981) and *O. pseudotsugae* (2.7–5 μm) (Rumbold 1936). The optimal growth temperature of *O. allantosporum* and *O. pseudotsugae* was 25 °C, that of *O. wuyingensis* was 25–30 °C and that of *O. taizhouense* was 30 °C (Gorton and Webber 2000, Chang et al. 2019). Both *O. wuyingensis* and *O. taizhouense* showed pigmentation on 2% MEA medium, whereas *O. allantosporum* has mid-brown hyphae, *O. pseudotsugae* has white-grey to snuff-brown, both showed no agar pigmentation (Rumbold 1936; Villarreal et al. 2005). *Ophiostoma wuyingensis* was first isolated from the gallery of *Ips typographus* on *P. koraiensis* in Heilongjiang Province (Chang et al. 2019). *Ophiostoma allantosporum* and *O. pseudotsugae* were isolated from *P. resinosa* in the USA and *P. menziesii* were infected with *Dendroctonus frontalis* in North America (Gorton and Webber 2000). Strains of *O. taizhouense* in this study were isolated from *P. massoniana* infected with PWN and *M. alternatus*.

Discussion

In the current study, 255 (containing 14 species) and 454 (containing six species) strains were obtained from *M. alternatus* larval galleries and pupal chambers of 2nd–3rd and 4th–5th instar, respectively, in *P. massoniana* infested with PWN in the Zhejiang Province, south-eastern China (Table 1). A total of 320 ophiostomatalean fungal strains out of overall 709 strains were obtained. The fungal diversity of 2nd–3rd

instar larvae was higher than that of 4th–5th instar larvae (Table 1; Fig. 11). *Ophiostoma taizhouense* is the dominant species in the 2nd–3rd instar and *O. ips* is the primary species at the 4th–5th instar. This is both similar and distinct from the previous research. Some studies found *Trichoderma* sp. or *Sporothrix* sp.1 to be the most common fungus associated with PWD (Zeng et al. 2006; Zhao et al. 2013), while others found the same to be *O. ips* (Lun et al. 2019), as was found here. The phenomenon could be caused by fungal succession, which occurs when PWN and *M. alternatus* select fungal companions that are more conducive to their own growth and reproduction at different life cycle stages. Therefore, future research on fungal diversity and abundance will necessitate a more comprehensive sampling analysis.

Only two common fungal species were obtained from both 2nd–3rd instar larval galleries, 4th–5th instar larval galleries and pupal chambers. The abundance of *D. sapinea* (103 out of 709) was higher than that of *Penicillium* sp. (7 out of 709). *Diplodia sapinea* is commonly isolated from *P. nigra* tip blight, *P. halepensis* and *P. pinaster* branch cankers worldwide (Luchi et al. 2014). It is an important pathogen of the *Pinus* spp. In addition, research has shown that *D. sapinea* can promote PWN reproduction and settlement (Kobayashi et al. 1974; Sriwati et al. 2007). *Penicillium* sp. is a common fungus in nature that also serves as an important biocontrol fungus (Sartaj et al. 2011; Win et al. 2021). However, there are no reports of *Penicillium* sp. affecting PWN, either negatively or positively.

Ophiostoma ips was first reported in pine trees associated with bark beetles in the south-eastern United States (Rumbold 1936) and it has since been confirmed, using

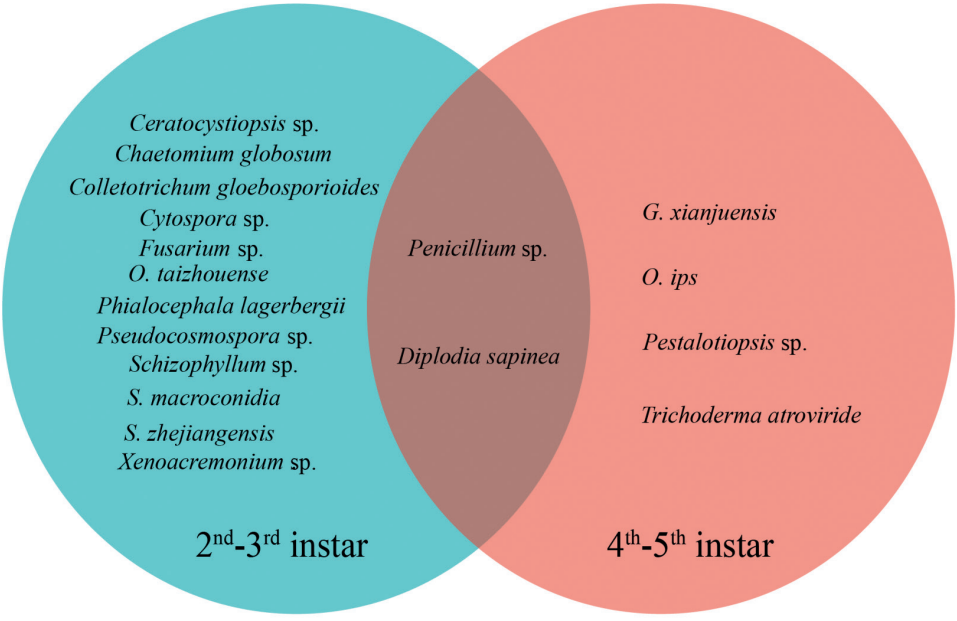

Figure 11. Diagram showing the species of fungi were isolated from the galleries and pupae chambers of different instar larvae of *Monochamus alternates*.

microsatellite markers, to be distributed worldwide (Zhou et al. 2007). Unfortunately, the study did not include Chinese strains. However, *O. ips* is regarded as one of the most stable natural associates of PWN in the wild of China (Zhao et al. 2013; Lun et al. 2019). According to Lun et al. (2019), *O. ips* was the dominant strain associated with PWN and was frequently isolated at the late stage of PWD. In a study by Zhao et al. (2013), *O. ips* was one of the three dominant ophiostomatoid fungi associated with PWN, with an isolation rate of 36%. Although *O. ips* was not found in the galleries of *M. alternatus* 2nd–3rd instar larvae in this study, it was the primary species at the 4th–5th instar, with an isolation rate of 50.88% and fungal abundance was much higher than that of other fungi during this period. Experiments with nematode propagation revealed that *O. ips* could breed nematodes, but not as effectively as *Botrytis cinerea* (Pimentel et al. 2021). In addition, biochemical analysis results revealed that *O. ips* could produce a wide range of volatile chemical substances (Cale et al. 2019). The 4th–5th instar larvae of *M. alternatus* are closely related to pinewood nematode dispersal stage J_{IV} (the fourth-stage dispersal juvenile). However, the mechanism underlying the interaction between *O. ips* and dispersal nematode juveniles is still lacking.

Ophiostoma taizhouense was the second most frequently isolated species of ophiostomatalean fungi in our study (62 out of the 255 strains); nevertheless, it was only associated with 2nd–3rd instar larvae. The association between *O. taizhouense* and PWD needs further experimental verification as a new species. Although the isolation rate of *Phialocephala* sp. and *Xenoacremonium* sp. is relatively high in 2nd–3rd instar larvae, these two fungi are both endophytes and there are no reports relating them to PWD.

In addition, three known ophiostomatalean fungi (*C. weihaiensis*, *S. macroconidia* and *S. zhejiangensis*) and one new species (*G. xianjuensis*) were revealed with low isolation rates during the survey. Simultaneously, some common endophytic and saprophytic fungi were isolated from the galleries and pupal chambers of *M. alternatus* larvae. The relationship between these fungi and PWN has not yet been reported.

In this study, a relatively large diversity of fungal species was obtained and identified as associated with PWN and *M. alternatus* in south-eastern China. The results showed that the fungal diversity and abundance of the 2nd–3rd instar larvae differed from those of the 4th–5th instar larvae. Fungi play an important role during the successful survival, reproduction and spread of PWN (Zhao et al. 2014; Zhao and Sun 2017). Hence, it is vital to explore the relationship between fungi and PWDs. This study provides a research basis for the fungi-PWN-*M. alternatus* symbiosis.

Acknowledgements

This work was supported by Zhejiang Science and Technology Program (2020C02007) and the National Natural Science Foundation of China (Project Nos. 32071769, 31770682). We thank Prof. Jiafu Hu of the Zhejiang A&F University for sampling in the fieldwork. We thank Editage (www.editage.cn) for its linguistic assistance during the preparation of this manuscript.

References

Abelleira A, Picoaga A, Mansilla JP, Aguin O (2011) Detection of *Bursaphelenchus xylophilus*, causal agent of pine wilt disease on *Pinus pinaster* in Northwestern Spain. Plant Disease 95(6): 776–776. https://doi.org/10.1094/PDIS-12-10-0902

Cale JA, Ding R, Wang F, Rajabzadeh R, Erbilgin N (2019) Ophiostomatoid fungi can emit the bark beetle pheromone verbenone and other semiochemicals in media amended with various pine chemicals and beetle-released compounds. Fungal Ecology 39: 285–295. https://doi.org/10.1016/j.funeco.2019.01.003

Chang R, Duong TA, Taerum SJ, Wingfield MJ, Zhou X, Yin M, de Beer ZW (2019) Ophiostomatoid fungi associated with the spruce bark beetle *Ips typographus*, including 11 new species from China. Persoonia. Molecular Phylogeny and Evolution of Fungi 42(1): 50–74. https://doi.org/10.3767/persoonia.2019.42.03

Chang RL, Zhang XY, Si HL, Zhao GY, Yuan XW, Liu TT, Bose T, Dai MX (2021) Ophiostomatoid species associated with pine trees (*Pinus* spp.) infested by *Cryphalus piceae* from eastern China, including five new species. MycoKeys 83: 181–208. https://doi.org/10.3897/mycokeys.83.70925

Cheng XY, Tian XL, Wang YS, Lin RM, Mao ZC, Chen NS, Xie BY (2013) Metagenomic analysis of the pinewood nematode microbiome reveals a symbiotic relationship critical for xenobiotics degradation. Scientific Reports 3(1): e1869. https://doi.org/10.1038/srep01869

de Beer ZW, Wingfield MJ (2013) Emerging lineages in the Ophiostomatales. In: Seifert KA, de Beer ZW, Wingfield MJ (Eds) The Ophiostomatoid Fungi: Expanding Frontiers. CBS-KNAW Fungal Biodiversity Centre, Utrecht, The Netherlands 21–46.

de Beer ZW, Duong TA, Barnes I, Wingfield BD, Wingfield MJ (2014) Redefining Ceratocystis and allied genera. Studies in Mycology 79(1): 187–219. https://doi.org/10.1016/j.simyco.2014.10.001

de Beer ZW, Duong TA, Wingfield MJ (2016) The divorce of *Sporothrix* and *Ophiostoma*: Solution to a problematic relationship. Studies in Mycology 83(1): 165–191. https://doi.org/10.1016/j.simyco.2016.07.001

de Beer ZW, Procter M, Wingfield MJ, Marincowitz S, Duong TA (2022) Generic boundaries in the Ophiostomatales reconsidered and revised. Studies in Mycology 101: 57–120. https://doi.org/10.3114/sim.2022.101.02

Eckhardt LG (2002, November) *Leptographium* Species: Tree Pathogens, Insect Associates, and Agents of Blue-Stain. Forest Science 48(4): e791. https://doi.org/10.1093/forestscience/48.4.791

Espada M, Silva AC, van den Akker SE, Peter JA, Cock, Mota M, Jones JT (2016) Identification and characterization of parasitism genes from the pinewood nematode *Bursaphelenchus xylophilus* reveals a multilayered detoxification strategy. Molecular Plant Pathology 17(2): 286–295. https://doi.org/10.1111/mpp.12280

Foit J, Čermák V, Gaar V, Hradil K, Nový V, Rolincová P (2019) New insights into the life history of *Monochamus galloprovincialis* can enhance surveillance strategies for the pinewood nematode. Journal of Pest Science 92(3): 1203–1215. https://doi.org/10.1007/s10340-019-01110-y

Glass NL, Donaldson GC (1995) Development of primer sets designed for use with the PCR to amplify conserved genes from filamentous ascomycetes. Applied and Environmental Microbiology 61(4): 1323–1330. https://doi.org/10.1128/aem.61.4.1323-1330.1995

Gorton C, Webber JF (2000) Reevaluation of the status of the bluestain fungus and bark beetle associate *Ophiostoma minus.* Mycologia 92(6): 1071–1079. https://doi.org/10.1080/00275514.2000.12061254

Hall TA (1999) BIOEDIT: A user-friendly biological sequence alignment editor and analysis program for Windows 95/98/NT. Nucleic Acids Symposium Series 41: 95–98.

Hyde KD, Norphanphoun C, Maharachchikumbura SSN, Bhat DJ, Jones EBG, Bundhun D (2020) Refined families of Sordariomycetes. Mycosphere : Journal of Fungal Biology 11(1): 305–1059. https://doi.org/10.5943/mycosphere/11/1/7

Jacobs K, Bergdahl DR, Wingfield MJ, Halik S, Seifert KA, Bright DE, Wingfield BD (2004) *Leptographium wingfieldii* introduced into North America and found associated with exotic *Tomicus piniperda* and native bark beetles. Mycological Research 108(4): 411–418. https://doi.org/10.1017/S0953756204009748

Jankowiak R (2008) Fungi associated with *Tomicus minor* on *Pinus sylvestris* in Poland and their succession into the sapwood of beetle-infested windblown trees. Canadian Journal of Forest Research 38(10): 2579–2588. https://doi.org/10.1139/X08-101

Jankowiak R, Solheim H, Bilański P, Marincowitz S, Wingfield MJ (2020) Seven new species of *Graphilbum* from conifers in Norway, Poland and Russia. Mycologia 112(6): 1240–1262. https://doi.org/10.1080/00275514.2020.1778375

Ji YC, Zhang QM, Zhou CG, Liu ZY (2021) Risk Analysis of Pine Wilt Disease in Shandong Province. Journal of Shandong Agricultural University 52(02): 219–223. [Natural Science]

Jung J, Han H, Ryu SH, Kim W (2010) Microsatellite variation in the pinewood nematode, *Bursaphelenchus xylophilus* (Steiner and Buhrer) Nickle in South Korea. Genes & Genomics 32(2): 151–158. https://doi.org/10.1007/s13258-009-0842-7

Katoh K, Standley DM (2013) MAFFT multiple sequence alignment software version 7: Improvements in performance and usability. Molecular Biology and Evolution 30(4): 772–780. https://doi.org/10.1093/molbev/mst010

Kikuchi T, Cotton JA, Dalzell JJ, Hasegawa K, Kanzaki N, McVeigh P, Takanashi T, Tsai IJ, Assefa SA, Cock PJA, Otto TD, Hunt M, Reid AJ, Sanchez-Flores A, Tsuchihara K, Yokoi T, Larsson MC, Miwa J, Maule AG, Sahashi N, Jones JT, Berriman M (2011) Genomic Insights into the Origin of Parasitism in the Emerging Plant Pathogen *Bursaphelenchus xylophilus.* PLoS Pathogens 7(9): e1002219. https://doi.org/10.1371/journal.ppat.1002219

Kobayashi T, Sasaki K, Mamiya Y (1974) Fungi Associated with *Bursaphelenchus lignicolus*, the Pine Wood Nematode. Nihon Shinrin Gakkaishi 56(4): 136–145. https://doi.org/10.11519/jjfs1953.56.4_136

Kobayashi F, Yamane A, Ikeda T (1984) The Japanese pine sawyer beetle as the vector of pine wilts disease. Annual Review of Entomology 29(1): 115–135. https://doi.org/10.1146/annurev.en.29.010184.000555

Kumar S, Stecher G, Tamura K (2016) MEGA7: Molecular evolutionary genetics analysis version 7.0 for bigger datasets. Molecular Biology and Evolution 33(7): 1870–1874. https://doi.org/10.1093/molbev/msw054

Linit MJ, Kondo E, Smith MT (1983) Insects associated with the pinewood nematode, *Bursaphelenchus xylophilus* (Nematoda: Aphelenchoididae), in Missouri. Environmental Entomology 12(2): 457–470. https://doi.org/10.1093/ee/12.2.467

Liou J, Shih J, Tzean S (1999) *Esteya*, a new nematophagous genus from Taiwan, attacking the pinewood nematode (*Bursaphelenchus xylophilus*). Mycological Research 103(2): 242–248. https://doi.org/10.1017/S0953756298006984

Luchi N, Oliveira Longa CM, Danti R, Capretti R, Maresi G (2014) *Diplodia sapinea*: The main fungal species involved in the colonization of pine shoots in Italy. Forest Pathology 44(5): 372–381. https://doi.org/10.1111/efp.12109

Lun YY, Wang HM, Lu Q, Liu HX, Yao XH, Jiang WZ, Zhang XY (2019) Dominantly Ophiostomatoid fungus inhabiting tunnels and pupal chambers of *Monochamus alternatus* in pines infected by *Bursaphelenchus xylophilus.* Journal of Beijing Forestry University 41(06): 102–110.

Mota MM, Vieira PC (2008) Pine wilt disease: a worldwide threat to forest ecosystems. Springer, Dordrecht, 1–10. http://www.springerlink.com/index/10.1007/978-1-4020-8455-3

Pimentel CS, Firmino PN, Ayres MP (2021) Interactions between pinewood nematodes and the fungal community of pine trees. Fungal Ecology 51: e101046. https://doi.org/10.1016/j.funeco.2021.101046

Rambaut A, Drummond AJ, Xie D, Baele G, Suchard MA (2018) Posterior summarization in Bayesian phylogenetics using Tracer 1.7. Systematic Biology 67(5): 901–904. https://doi.org/10.1093/sysbio/syy032

Rayner RW (1970) A mycological colour chart. Commonwealth Mycological Institute and British Mycological Society.

Robertson L, Arcos SC, Escuer M, Santiago MR, Esparrago G, Abelleira A, Navas A (2011) Incidence of the pinewood nematode *Bursaphelenchus xylophlius* Steiner & Buhrer, 1934 (Nickle, 1970) in Spain. Nematology 13(6): 755–757. https://doi.org/10.1163/138855411X578888

Ronquist F, Teslenko M, van der Mark P, Ayres DL, Darling A, Höhna S, Larget B, Liu L, Suchard MA, Huelsenbeck JP (2012) MrBayes 3.2: Efficient Bayesian phylogenetic inference and model choice across a large model space. Systematic Biology 61(3): 539–542. https://doi.org/10.1093/sysbio/sys029

Rumbold CT (1936) Three blue-staining fungi, including two new species, associated with bark beetles. US Government Printing Office.

Ryss A, Vieira P, Mota M, Kulinich O (2005) A synopsis of the genus *Bursaphelenchus Fuchs*, 1937 (Aphelenchida: Parasitaphelenchidae) with keys to species. Nematology 7(3): 393–458. https://doi.org/10.1163/156854105774355581

Sartaj AS, Kazunori S, Kazuyuki I (2011) Effect of *Penicillium* sp. EU0013 inoculation on tomato growth and *Fusarium* wilt. Horticulture Research 65: 69–73.

Seifert KA, Webber JF, Wingfield MJ (1993) Methods for studying species of *Ophiostoma* and *Ceratocystis*. In: Wingfield MJ, Seifert KA, Webber JF (Eds) *Ceratocystis* and *Ophiostoma*: taxonomy, ecology and pathogenicity. The American Phytopathological Society Press, Minnesota, USA, 255–259.

Solheim H (1992a) Fungal succession in the sapwood of Norway spruce infested by the bark beetle *Ips typographus.* European Journal of Forest Pathology 22(3): 136–148. https://doi.org/10.1111/j.1439-0329.1992.tb01440.x

Solheim H (1992b) The early stages of fungal invasion in Norway spruce infested by the bark beetle *Ips typographus*. Canadian Journal of Botany 70(1): 1–5. https://doi.org/10.1139/b92-001

Sriwati R, Takemoto S, Futai K (2007) Cohabitation of the pine wood nematode, *Bursaphelenchus xylophilus*, and fungal species in pine trees inoculated with *B. xylophilus*. Nematology 9(1): 77–86. https://doi.org/10.1163/156854107779969655

Stamatakis A (2014) RaxML version 8: A tool phylogenetic analysis and postanalysis of large phylogenies. Bioinformatics (Oxford, England) 30(9): 1312–1313. https://doi.org/10.1093/bioinformatics/btu033

State Forestry Administration of the People's Republic of China (2021) Announcement of State Forestry Administration of the People's Republic of China No. 5. https://www.forestry.gov.cn/main/3457/20210329/151957233445926.html

Swofford DL (2003) PAUP*: phylogenetic analysis using parsimony, version 4.0 b10.

Togashi K, Jikumaru S (2007) Evolutionary change in a pine wilt system following the invasion of Japan by the pinewood nematode, *Bursaphelenchus xylophilus*. Ecological Research 22(6): 862–868. https://doi.org/10.1007/s11284-007-0339-2

Upadhyay HP (1981) A monograph of *Ceratocystis* and *Ceratocystiopsis.* University of Georgia Press, Athens 36(2): 175. https://doi.org/10.1007/BF02858713

Villarreal M, Ruelo V, De Tov AMT, Arenal E (2005) A new *Ophiostoma* species isolated from. Mycotaxon 92: 259–268.

Wang CY, Fang ZM, Wang Z, Zhang DL, Gu LJ, Lee MR, Liu L, Sung CK (2011) Biological control of the pinewood nematode *Bursaphelenchus xylophilus* by application of the endoparasitic fungus *Esteya vermicola*. BioControl 56(1): 91–100. https://doi.org/10.1007/s10526-010-9302-1

Wang HM, Lun YY, Lu Q, Liu HX, Decock C, Zhang XY (2018) Ophiostomatoid fungi associated with pines infected by *Bursaphelenchus xylophilus* and *Monochamus alternatus* in China, including three new species. MycoKeys 1(39): 1–27. https://doi.org/10.3897/mycokeys.39.27014

Wang HM, Wang Z, Liu F, Wu CX, Zhang SF, Kong XB, Decock C, Lu Q, Zhang Z (2019) Differential patterns of ophiostomatoid fungal communities associated with three sympatric *Tomicus* species infesting pines in south-western China, with a description of four new species. MycoKeys 50: 93–133. https://doi.org/10.3897/mycokeys.50.32653

Wang Z, Liu Y, Wang HM, Meng XJ, Liu XW, Decock C, Zhang XY, Lu Q (2020) Ophiostomatoid fungi associated with *Ips subelongatus*, including eight new species from northeastern China. IMA Fungus 11(1): e3. https://doi.org/10.1186/s43008-019-0025-3

White TJ, Bruns T, Lee SJWT, Taylor JL (1990) Amplification and direct sequencing of fungal ribosomal RNA genes for phylogenetics. PCR protocols: a guide to methods and applications 18(1): 315–322. https://doi.org/10.1016/B978-0-12-372180-8.50042-1

Wijayawardene NN, Hyde KD, Dai DQ, Sánchez-García M, Goto BT, Saxena RK, Erdoğdu M, Selçuk F, Rajeshkumar KC, Aptroot A, Błaszkowski J, Boonyuen N, da Silva GA, de Souza FA, Dong W, Ertz D, Haelewaters D, Jones EBG, Karunarathna SC, Kirk PM, Kukwa M, Kumla J, Leontyev DV, Lumbsch HT, Maharachchikumbura SSN, Marguno F, Martínez-Rodríguez P, Mešić A, Monteiro JS, Oehl F, Pawłowska J, Pem D, Pfliegler

WP, Phillips AJL, Pošta A, He MQ, Li JX, Raza M, Sruthi OP, Suetrong S, Suwannarach N, Tedersoo L, Thiyagaraja V, Tibpromma S, Tkalčec Z, Tokarev YS, Wanasinghe DN, Wijesundara DSA, Wimalaseana SDMK, Madrid H, Zhang GQ, Gao Y, Sánchez-Castro I, Tang LZ, Stadler M, Yurkov A, Thines M (2022) Outline of Fungi and fungus-like taxa – 2021. Mycosphere: Journal of Fungal Biology 13(1): 53–453. https://doi.org/10.5943/mycosphere/13/1/2

Win TT, Bo B, Malec P, Fu P (2021) The effect of a consortium of *Penicillium* sp. and *Bacillus* spp. in suppressing banana fungal diseases caused by *Fusarium* sp. and *Alternaria* sp. Journal of Applied Microbiology 131(4): 1890–1908. https://doi.org/10.1111/jam.15067

Ye JR (2019) Epidemic status of pine wilt disease in China and its prevention and control techniques and counter measures. Linye Kexue 55(9): 1–10.

Zeng FY, Luo YQ, Lu Q, Liang J, Zhang XY (2006) Studies on the mycoflora of *Pinus thunbergii* infected by *Bursaphelenchus xylophilus*. Forest Research 19(4): 537–540.

Zhang W, Wang X, Li YX, Liu ZK, Li DZ, Wen XJ, Feng YQ, Zhang XY (2021) Pinewood Nematode Alters the Endophytic and Rhizospheric Microbial Communities of *Pinus massoniana*. Microbial Ecology 81(3): 807–817. https://doi.org/10.1007/s00248-020-01619-1

Zhao LL, Sun JH (2017) Pinewood Nematode *Bursaphelenchus xylophilus* (Steiner and Buhrer) Nickle. In: Wan F, Jiang M, Zhan A (Eds) Biological Invasions and Its Management in China. Invading Nature - Springer Series in Invasion Ecology vol 13. Springer, Singapore. https://doi.org/10.1007/978-981-10-3427-5_1

Zhao LL, Lu M, Niu H, Zhang S, Sun J (2013) A native fungal symbiont facilitates the prevalence and development of an invasive pathogen-native vector symbiosis. Ecology 94(12): 2817–2826. https://doi.org/10.1890/12-2229.1

Zhao LL, Mota M, Vieira P, Butcher RA, Sun J (2014) Interspecific communication between pinewood nematode, its insect vector, and associated microbes. Trends in Parasitology 30: 299–308. https://doi.org/10.1016/j.pt.2014.04.007

Zhao LL, Ahmad F, Lu M, Zhang W, Wickham JD, Sun J (2018) Ascarosides Promote the Prevalence of Ophiostomatoid Fungi and an Invasive Pathogenic Nematode, *Bursaphelenchus xylophilus.* Journal of Chemical Ecology 44(7–8): 701–710. https://doi.org/10.1007/s10886-018-0996-3

Zheng YN, Liu PX, Shi Y, Wu H, Yu HY, Jiang SW (2021) Difference analysis on pine wilt disease between Liaoning Province of northeastern China and other epidemic areas in China. Journal of Beijing Forestry University 43(5): 155–160. https://doi.org/10.12171/j.1000-1522.20200108

Zhou X, Burgess TI, De Beer ZW, Lieutier F, Yart A, Klepzig K, Wingfield MJ (2007) High intercontinental migration rates and population admixture in the sapstain fungus *Ophiostoma ips.* Molecular Ecology 16(1): 89–99. https://doi.org/10.1111/j.1365-294X.2006.03127.x

Zhu YQ, Huang WY, Xie WL, Ma Y, Wen XJ, Wang J (2021) Research progress on control methods of pine wilt disease. Hebei Forestry Science and Technology (02): 44–48. https://doi.org/10.16449/j.cnki.issn1002-3356.2021.02.010

MycoKeys 92: 27–43 (2022)
doi: 10.3897/mycokeys.92.86521
https://mycokeys.pensoft.net

RESEARCH ARTICLE

A peer-reviewed open-access journal
MycoKeys
Launched to accelerate biodiversity research

A new *Arthrinium*-like genus of Amphisphaeriales in China

Ning Jiang[1], Hermann Voglmayr[2], Chun-Yan Ma[3], Han Xue[1], Chun-Gen Piao[1], Yong Li[1]

1 *Key Laboratory of Biodiversity Protection of National Forestry and Grassland Administration, Ecology and Nature Conservation Institute, Chinese Academy of Forestry, Beijing 100091, China* **2** *Department of Botany and Biodiversity Research, University of Vienna, Rennweg 14, A-1030 Vienna, Austria* **3** *Natural Resources and Planning Bureau of Rizhao City, Rizhao 276827, China*

Corresponding author: Yong Li (lylx@caf.ac.cn)

Academic editor: Nattawut Boonyuen | Received 13 May 2022 | Accepted 21 July 2022 | Published 1 August 2022

Citation: Jiang N, Voglmayr H, Ma C-Y, Xue H, Piao C-G, Li Y (2022) A new *Arthrinium*-like genus of Amphisphaeriales in China. MycoKeys 92: 27–43. https://doi.org/10.3897/mycokeys.92.86521

Abstract

Species of *Arthrinium s. l.* are usually known as endophytes, pathogens or saprobes occurring on various hosts and substrates and are characterised by globose to subglobose, sometimes irregular, dark brown and smooth-walled or finely verruculose conidia, always with a truncate basal scar. Currently, *Arthrinium s. l.* contains two phylogenetically distinct clades, namely, *Apiospora* and *Arthrinium s. s.* However, *Arthrinium trachycarpi* and *Ar. urticae* have still not been properly classified. With new isolates from diseased leaves of *Lithocarpus glaber* collected in China, we propose the new *Arthrinium*-like genus *Neoarthrinium* in Amphisphaeriales. Based on the morphology and phylogeny of multiple loci, the new genus is established with the type species, *N. lithocarpicola* and three new combinations, *N. moseri* (syn. *Wardomyces moseri*), *N. trachycarpi* (syn. *Ar. trachycarpi*) and *N. urticae* (syn. *Ar. urticae*) are added to this genus.

Keywords

Apiospora, *Arthrinium*, *Neoarthrinium*, phylogeny, taxonomy

Introduction

Apiosporaceae, including *Arthrinium*-like taxa, was proposed to accommodate genera with apiosporous hyaline ascospores and a basauxic, *Arthrinium*-like conidiogenesis (Hyde et al. 1998). In a recent outline of Sordariomycetes, Hyde et al. (2020)

accepted five genera viz. *Appendicospora*, *Arthrinium*, *Dictyoarthrinium*, *Endocalyx* and *Nigrospora* in family Apiosporaceae. Soon thereafter, *Dictyoarthrinium* was transferred to Didymosphaeriaceae, based on a multigene phylogeny (Samarakoon et al. 2020). Subsequently, Pintos and Alvarado (2021) separated *Apiospora* from *Arthrinium*, based on the study of the type species of both genera and on multigene phylogeny. Recently, Konta et al. (2021) transferred *Endocalyx* to Cainiaceae, based on morphological and phylogenetic evidence and Samarakoon et al. (2022) described the new family Appendicosporaceae for *Appendicospora*. Therefore, Apiosporaceae currently contains three genera, viz. *Apiospora*, *Arthrinium* and *Nigrospora.*

Until the study of Pintos and Alvarado (2021), the genera *Apiospora* and *Arthrinium* were considered synonymous, the first being used for the sexual morph and the second for the asexual morph in dual nomenclature (Réblová et al. 2016). Following the abandonment of dual nomenclature, the older name *Arthrinium* was recommended for use in unitary nomenclature (Réblová et al. 2016). The genus *Arthrinium* was proposed by Kunze and Schmidt (1817) and validated by Fries (1832) with *Ar. caricicola* as the generic type. *Apiospora*, the type genus of Apiosporaceae, was typified with *Ap. montagnei*, a new name for *Sphaeria apiospora* (Saccardo 1875). However, the phylogenetic identity of *Ap. montagnei* has been confused because multiple names in *Arthrinium* have similar sexual morphs that have been referred to as *Apiospora montagnei* (Hudson et al. 1976; Pintos et al. 2019; Pintos and Alvarado 2021). New collections from the original region and hosts (*Arundo*, *Piptatherum*) of *Ap. montagnei* have been isolated in pure culture and sequenced (Crous and Groenewald 2013; Pintos et al. 2019). Five species, previously placed in *Arthrinium*, are classified in *Apiospora*. Two of these phylogenetically distinct species, *Ap. marii* and *Ap. phragmitis*, are morphologically similar to *Ap. montagnei* (Pintos and Alvarado 2021), but due to a lack of sequence data from the type, it cannot be determined which of these two species should become a synonym of *Ap. montagnei*. Irrespective of these taxonomic uncertainties in species concept, recent multigene phylogenies revealed that *Arthrinium* and *Apiospora* represent two well-supported, distinct lineages close to *Nigrospora* in Apiosporaceae (Pintos and Alvarado 2021; Samarakoon et al. 2022). However, two *Arthrinium* species resembling *Apiospora* in conidial morphology, viz. *Ar. trachycarpi* and *Ar. urticae*, were not considered in these studies.

Arthrinium-like species are globally distributed, inhabiting various substrates, mainly associated with plant tissues as endophytes, pathogens and saprobes (Cooke 1954; Minter 1985; Larrondo and Calvo 1992; Senanayake et al. 2020; Feng et al. 2021; Jiang and Tian 2021; Tian et al. 2021). Some species are important plant pathogens; for example, *Ap. arundinis* causes bamboo brown culm streak, chestnut leaf spot and barley kernel blight (Martínez-Cano et al. 1992; Chen et al. 2014; Jiang et al. 2021), while *Ap. sacchari* causes damping-off of durum wheat (Mavragani et al. 2007). Another species, *Ar. phaeospermum*, can cause dermatomycosis in humans (Zhao et al. 1990).

In the present study, new *Arthrinium*-like isolates were collected and morphologically examined and their phylogenetic affiliation was determined by analyses of

a combined matrix of ITS, LSU, *tef1* and *tub2* sequences. The aim of this study was to determine the phylogenetic placement of *Ar. trachycarpi*, *Ar. urticae* and our new isolates within Amphisphaeriales, which resulted in the identification of a new phylogenetic lineage with isolates belonging to neither *Arthrinium* nor *Apiospora*. As a result, a new genus is established for these isolates.

Materials and methods

Isolation and morphology

Diseased leaves of *Lithocarpus glaber* were observed and collected in Guangdong Province of China (39 m elevation; 23°8'52"N, 113°27'18"E), packed in paper bags and transferred to the laboratory for pure culture isolation. The samples were first surface-sterilised for 1 min in 75% ethanol, 3 min in 1.25% sodium hypochlorite and 1 min in 75% ethanol, rinsed for 2 min in distilled water and blotted on dry sterile filter paper. Then, the diseased areas of the leaves were cut into 0.5 × 0.5 cm pieces using an aseptic razor blade, transferred on to the surface of potato dextrose agar plates (PDA; 200 g potatoes, 20 g dextrose, 20 g agar per litre) and incubated at 25 °C to obtain pure cultures. The cultures were deposited in the China Forestry Culture Collection Center (CFCC; http://cfcc.caf.ac.cn/) and the specimen was deposited in the Herbarium of the Chinese Academy of Forestry (CAF; http://museum.caf.ac.cn/).

The morphology of the isolates was studied, based on sporulating axenic cultures grown on PDA in the dark at 25 °C. The conidiomata were observed and photographed under a dissecting microscope (M205 C, Leica, Wetzlar, Germany). The conidiogenous cells and conidia were immersed in tap water and then the microscopic photographs were captured with an Axio Imager 2 microscope (Zeiss, Oberkochen, Germany), equipped with an Axiocam 506 colour camera using differential interference contrast (DIC) illumination. For measurements, 50 conidiogenous cells and conidia were randomly selected. Culture characteristics were recorded from PDA after 10 d of incubation at 25 °C in the dark.

DNA extraction, PCR amplification and phylogenetic analyses

Genomic DNA was extracted from colonies grown on cellophane-covered PDA using a cetyltrimethylammonium bromide (CTAB) method (Doyle and Doyle 1990). DNA was checked by electrophoresis in a 1% agarose gel and the quality and quantity were measured using a NanoDrop 2000 (Thermo Scientific, Waltham, MA, USA). The following primer pairs were used for amplification of the gene regions sequenced in the present study: ITS1/ITS4 for the ITS1-5.8S-ITS2 nrDNA region (ITS) (White et al. 1990); LR0R/LR5 for the 28S nrDNA region (LSU) (Vilgalys and Hester 1990); EF1-728F/EF2 for the translation elongation factor 1-α (*tef1*) gene (O'Donnell and Cigelnik 1997; Carbone and Kohn 1999); Bt2a/Bt2b for the beta-tubulin (*tub2*) gene

(Glass and Donaldson 1995). The PCR conditions were set as follows: an initial denaturation step of 5 min at 94 °C, followed by 35 cycles of 30 s at 94 °C, 50 s at 52 °C (ITS and LSU) or 54 °C (*tef1* and *tub2*) and 1 min at 72 °C and a final elongation step of 7 min at 72 °C. The PCR products were assayed via electrophoresis in 2% agarose gels. DNA sequencing was performed using an ABI PRISM 3730XL DNA Analyser with a BigDye Terminator Kit v.3.1 (Invitrogen, USA) at the Shanghai Invitrogen Biological Technology Company Limited (Beijing, China).

The quality of the chromatograms obtained was checked and the nucleotide sequences were assembled using SeqMan v.7.1.0, the DNASTAR lasergene core suite software (DNASTAR Inc, Madison, WI, USA). Reference sequences were retrieved from the National Center for Biotechnology Information (NCBI; https://www.ncbi.nlm.nih.gov), based on related publications (Crous and Groenewald 2013; Wang et al. 2018; Liu et al. 2019; Pintos and Alvarado 2021; Samarakoon et al. 2022). Sequences were aligned using MAFFT v. 6 (Katoh and Toh 2010) and corrected manually using MEGA 7.0.21 (Kumar et al. 2016).

The phylogenetic analyses of the combined loci were performed using Maximum Likelihood (ML) and Bayesian Inference (BI) methods. The ML was implemented on the CIPRES Science Gateway portal (https://www.phylo.org) using RAxML-HPC BlackBox 8.2.10 (Stamatakis 2014), employing a GTRGAMMA substitution model with 1000 bootstrap replicates. The Bayesian posterior probabilities (BPP) were determined by Markov Chain Monte Carlo (MCMC) sampling in MrBayes v. 3.2.6 (Ronquist et al. 2012). The six simultaneous Markov chains were run for 1 M generations, starting from random trees and sampling trees every 100th generation and 25% of aging samples were discarded, running until the average standard deviation of the split frequencies dropped below 0.01. The phylogram was visualised in FigTree v.1.3.1 (http://tree.bio.ed.ac.uk/software) and edited in Adobe Illustrator CS5 (Adobe Systems Inc., USA). The newly-generated nucleotide sequences were deposited in GenBank (Table 1).

Results

Phylogenetic analyses

The combined sequence dataset (ITS, LSU, *tef1* and *tub2*) was analysed to infer the phylogenetic placement of our new isolates within Amphisphaeriales. The dataset consisted of 136 sequences, including two outgroup taxa, *Clypeosphaeria mamillana* (CBS 140735) and *Pseudosporidesmium knawiae* (CBS 123529). A total of 3526 characters, including gaps (793 for ITS, 859 for LSU, 762 for *tef1* and 1112 for *tub2*), were included in the phylogenetic analysis. Of these characters, 1543 were constant, 284 were variable, but parsimony-uninformative and 1699 were parsimony-informative. The best ML tree (lnL = - 72640.48) revealed by RAxML is shown in Fig. 1. The topologies resulting from ML and BI analyses of the concatenated dataset were congruent (Fig. 1). Isolates CFCC 54456 and CFCC 55883 from the present study, together with CFCC

53038, CFCC 53039, CBS 164.80 and IMI 326344, formed a clade distinct from Apiosporaceae and the other families in Amphisphaeriales. Hence, a new genus named *Neoarthrinium* is proposed herein for this clade. *Arthrinium trachycarpi*, *Ar. urticae* and *Wardomyces moseri* are transferred to *Neoarthrinium*. In addition, the two new isolates (CFCC 54456 and CFCC 55883) that form a sister clade to *N. moseri*, *N. trachycarpi* and *N. urticae* are described here as the new species *N. lithocarpicola.*

Table 1. Isolates and GenBank accession numbers used in the phylogenetic analyses.

Species	Strain	Host	Origin	GenBank accession numbers			
				ITS	LSU	*tub2*	*tef1*
Allelochaeta acuta	CPC 16629	*Eucalyptus dives*	Australia	MH554086	MH554297	MH554758	MH554519
Allelochaeta neoacuta	CBS 115131	*Eucalyptus smithii*	South Africa	JN871200	JN871209	MH704627	MH704602
Amphisphaeria micheliae	MFLUCC 20-0121	*Michelia alba*	China	MT756626	MT756620	MT774371	NA
Apiospora acutiapica	KUMCC 20-0209	*Bambusa bambos*	China	MT946342	MT946338	MT947365	MT947359
Apiospora acutiapica	KUMCC 20-0210	*Bambusa bambos*	China	MT946343	MT946339	MT947366	MT947360
Apiospora arundinis	CBS 114316	*Hordeum vulgare*	Iran	KF144884	KF144928	KF144974	KF145016
Apiospora aurea	CBS 244.83	Air	Spain	AB220251	KF144935	KF144981	KF145023
Apiospora balearica	CBS 145129	Poaceae	Spain	MK014869	MK014836	MK017975	NA
Apiospora biserialis	CGMCC 3.20135	Bamboo	China	MW481708	MW478885	MW522955	MW522938
Apiospora camelliae-sinensis	LC8181	*Brassica campestris*	China	KY494761	KY494837	KY705229	NA
Apiospora camelliae-sinensis	CGMCC 3.18333	*Camellia sinensis*	China	KY494704	KY494780	KY705173	KY705103
Apiospora cyclobalanopsidis	CGMCC 3.20136	*Cyclobalanopsis glauca*	China	MW481713	MW478892	MW522962	MW522945
Apiospora descalsii	CBS 145130	*Ampelodesmos mauritanicus*	Spain	MK014870	MK014837	MK017976	NA
Apiospora dichotomanthi	LC8175	*Dichotomanthes tristaniiaecarpa*	China	KY494755	KY494831	KY705223	KY705151
Apiospora dichotomanthi	CGMCC 3.18332	*Dichotomanthes tristaniiaecarpa*	China	KY494697	KY494773	KY705167	KY705096
Apiospora esporlensis	CBS 145136	*Phyllostachys aurea*	Spain	MK014878	MK014845	MK017983	NA
Apiospora gelatinosa	GZAAS 20-0107	Bamboo	China	MW481707	MW478889	MW522959	MW522942
Apiospora guizhouensis	LC5318	Air	China	KY494708	KY494784	KY705177	KY705107
Apiospora guizhouensis	CGMCC 3.18334	Air	China	KY494709	KY494785	KY705178	KY705108
Apiospora hydei	CBS 114990	Bamboo	China	KF144890	KF144936	KF144982	KF145024
Apiospora iberica	CBS 145137	*Arundo donax*	Portugal	MK014879	MK014846	MK017984	NA
Apiospora intestini	CBS 135835	Gut of a grasshopper	India	KR011352	MH877577	KR011350	NA
Apiospora italica	CBS 145138	*Arundo donax*	Italy	MK014880	MK014847	MK017985	NA
Apiospora jiangxiensis	CGMCC 3.18381	*Maesa* sp.	China	KY494693	KY494769	KY705163	KY705092
Apiospora kogelbergensis	CBS 113332	*Cannomois virgata*	South Africa	KF144891	KF144937	KF144983	KF145025
Apiospora kogelbergensis	CBS 113333	Restionaceae	South Africa	KF144892	KF144938	KF144984	KF145026
Apiospora malaysiana	CBS 102053	*Macaranga hullettii*	Malaysia	KF144896	KF144942	KF144988	KF145030
Apiospora marii	CBS 497.90	Air	Spain	AB220252	KF144947	KF144993	KF145035
Apiospora neobambusae	CGMCC 3.18335	Bamboo	China	KY494718	KY494794	KY705186	KY806204
Apiospora neobambusae	LC7107	Bamboo	China	KY494719	KY494795	KY705187	KY705117
Apiospora obovata	CGMCC 3.18331	*Lithocarpus* sp.	China	KY494696	KY494772	KY705166	KY705095
Apiospora obovata	LC8177	*Lithocarpus* sp.	China	KY494757	KY494833	KY705225	KY705153
Apiospora ovata	CBS 115042	*Arundinaria hindsii*	China	KF144903	KF144950	KF144995	KF145037
Apiospora phragmitis	CBS 135458	*Phragmites australis*	Italy	KF144909	KF144956	KF145001	KF145043
Apiospora phyllostachydis	MFLUCC 18-1101	*Phyllostachys heteroclada*	China	MK351842	MH368077	MK291949	MK340918
Apiospora pseudoparenchymatica	CGMCC 3.18336	Bamboo	China	KY494743	KY494819	KY705211	KY705139
Apiospora pseudospegazzinii	CBS 102052	*Macaranga hullettii*	Malaysia	KF144911	KF144958	KF145002	KF145045
Apiospora pterosperma	CBS 134000	*Machaerina sinclairii*	Australia	KF144913	KF144960	KF145004	KF145046
Apiospora saccharicola	CBS 191.73	Air	Netherlands	KF144920	KF144966	KF145009	KF145051
Apiospora septata	CGMCC 3.20134	Bamboo	China	MW481711	MW478890	MW522960	MW522943
Apiospora serenensis	IMI 326869	NA	Spain	AB220250	AB220344	AB220297	NA

Species	Strain	Host	Origin	GenBank accession numbers			
				ITS	LSU	*tub2*	*tef1*
Apiospora subrosea	LC7291	Bamboo	China	KY494751	KY494827	KY705219	KY705147
Apiospora subrosea	CGMCC 3.18337	Bamboo	China	KY494752	KY494828	KY705220	KY705148
Apiospora xenocordella	CBS 595.66	Soil	Austria	KF144926	KF144971	KF145013	KF145055
Arthrinium caricicola	CBS 145127	*Carex ericetorum*	Germany	MK014871	MK014838	MK017977	NA
Arthrinium crenatum	CBS 146353	Grass	France	MW208931	MW208861	MW221923	MW221917
Arthrinium curvatum	CBS 145131	*Carex* sp.	Germany	MK014872	MK014839	MK017978	NA
Arthrinium japonicum	IFO 30500	*Carex despalata*	Japan	AB220262	AB220356	AB220309	NA
Arthrinium japonicum	IFO 31098	*Carex despalata*	Japan	AB220264	AB220358	AB220311	NA
Arthrinium luzulae	AP7619-3	*Luzula sylvatica*	Spain	MW208937	MW208863	MW221925	MW221919
Arthrinium morthieri	GZU 345043	*Carex digitata*	Austria	MW208938	MW208864	MW221926	MW221920
Arthrinium puccinioides	CBS 549.86	*Lepidosperma gladiatum*	Germany	AB220253	AB220347	AB220300	NA
Arthrinium sphaerospermum	CBS 146355	Poaceae	Norway	MW208943	MW208865	NA	NA
Arthrinium sporophleum	CBS 145154	*Juncus* sp.	Spain	MK014898	MK014865	MK018001	NA
Bartalinia bella	CBS 125525	*Maytenus abbottii*	South Africa	GU291796	MH554214	MH554663	MH554421
Bartalinia pini	CBS 143891	*Pinus patula*	Uganda	MH554125	MH554330	MH554797	MH554559
Beltrania pseudorhombica	CBS 138003	*Pinus tabulaeformis*	China	MH554124	KJ869215	NA	MH554558
Beltrania rhombica	CBS 123.58	Sand near mangrove swamp	Mozambique	MH553990	MH554209	MH704631	MH704606
Beltraniopsis neolitseae	CPC 22168	*Neolitsea australiensis*	Australia	KJ869126	KJ869183	NA	NA
Broomella vitalbae	HPC 1154	NA	NA	MH554173	MH554367	MH554846	MH554608
Castanediella cagnizarii	CBS 542.96	Leaf litter	Cuba	MH862597	MH874222	NA	NA
Ciliochorella phanericola	MFLUCC 12-0310	Dead leaves	Thailand	KF827444	KF827445	KF827478	KF827477
Clypeophysalospora latitans	CBS 141463	*Eucalyptus* sp.	Portugal	NR_153929	NG_058958	NA	NA
Clypeosphaeria mamillana	CBS 140735	*Cornus alba*	France	KT949897	MH554225	MH704637	MH704610
Cylindrium elongatum	CBS 115974	*Fagus* sp.	The Netherlands	KM231853	KM231733	KM232123	KM231989
Diploceras hypericinum	CBS 109058	*Hypericum* sp.	New Zealand	MH553955	MH554178	MH554614	MH554373
Disaeta arbuti	CBS 143903	*Acacia pycnantha*	Australia	MH554148	MH554346	MH554821	MH554583
Discosia artocreas	CBS 124848	*Fagus sylvatica*	Germany	MH553994	MH554213	MH554662	MH554420
Discosia brasiliensis	MFLUCC 12-0429	Dead leaf	Thailand	KF827432	KF827436	KF827469	KF827465
Distononappendiculata banksiae	CBS 131308	*Banksia marginata*	Australia	JQ044422	JQ044442	MH554670	MH554428
Distononappendiculata casuarinae	CBS 143884	*Casuarina* sp.	Australia	MH554093	MH554303	MH554766	MH554527
Diversimediispora humicola	CBS 302.86	Soil	USA	MH554028	MH554247	MH554705	MH554463
Heterotruncatella acacigena	CBS 143880	*Acacia pedina*	Australia	MH554084	MH554295	MH554756	MH554517
Heterotruncatella aspera	CBS 144140	*Acacia glaucoptera*	Australia	MH554156	MH554352	MH554829	MH554591
Hyalotiella spartii	MFLUCC 13-0397	*Spartium junceum*	Italy	KP757756	KP757752	NA	NA
Hyalotiella transvalensis	CBS 303.65	Leaf litter and topsoil of *Acacia karroo* community	South Africa	MH554029	MH554248	MH554706	MH554464
Hymenopleella austroafricana	CBS 143886	*Gleditsia triacanthos*	South Africa	MH554115	MH554320	MH554788	MH554549
Hymenopleella hippophaëicola	CBS 113687	*Hippophaë rhamnoides*	Sweden	MH553969	MH554188	MH554628	MH554387
Immersidiscosia eucalypti	NBRC 104195	*Quercus myrsinifolia*	Japan	AB594790	AB593722	NA	NA
Lepteutypa fuckelii	CBS 140409	*Tilia cordata*	Belgium	NR_154123	KT949902	MH554677	MH554435
Lepteutypa sambuci	CBS 131707	*Sambucus nigra*	UK	NR_154124	MH554219	MH704632	MH704612
Monochaetia monochaeta	CBS 115004	*Quercus robur*	Netherlands	AY853243	MH554198	MH554639	MH554398
Monochaetia quercus	CBS 144034	*Quercus eduardi*	Mexico	MH554171	MH554365	MH554844	MH554606
Morinia acaciae	CBS 137994	*Acacia melanoxylon*	France	MH554002	MH554221	MH554673	MH554431
Morinia crini	CBS 143888	*Crinum bulbispermum*	South Africa	MH554118	MH554323	MH554791	MH554552
Neoarthrinium lithocarpicola	**CFCC 54456**	***Lithocarpus glaber***	**China**	**ON427580**	**ON427582**	**ON456914**	**NA**
Neoarthrinium lithocarpicola	**CFCC 55883**	***Lithocarpus glaber***	**China**	**ON427581**	**ON427583**	**ON456915**	**NA**
Noarthrinium moseri	CBS 164.80	Dead petiole	Colombia	LN850995	LN851049	LN851154	NA
Neoarthrinium trachycarpi	CFCC 53038	*Trachycarpus fortunei*	China	MK301098	NA	MK303394	MK303396

Species	Strain	Host	Origin	GenBank accession numbers			
				ITS	LSU	*tub2*	*tef1*
Neoarthrinium trachycarpi	CFCC 53039	*Trachycarpus fortunei*	China	MK301099	NA	MK303395	MK303397
Neoarthrinium urticae	IMI 326344	Leaf litter	India	AB220245	AB220339	NA	NA
Neopestalotiopsis cubana	CBS 600.96	Leaf litter	Cuba	KM199347	KM116253	KM199438	KM199521
Neophysalospora eucalypti	CBS 138864	*Corymbia henryi*	Mozambique	KP004462	MH878627	NA	NA
Nigrospora aurantiaca	CGMCC 3.18130	*Nelumbo* sp.	China	KX986064	KX986098	KY019465	KY019295
Nigrospora camelliae-sinensis	CGMCC 3.18125	*Camellia sinensis*	China	KX985986	KX986103	KY019460	KY019293
Nigrospora chinensis	CGMCC 3.18127	*Machilus breviflora*	China	KX986023	KX986107	KY019462	KY019422
Nigrospora gorlenkoana	CBS 480.73	*Vitis vinifera*	Kazakhstan	KX986048	KX986109	KY019456	KY019420
Nigrospora guilinensis	CGMCC 3.18124	*Camellia sinensis*	China	KX985983	KX986113	KY019459	KY019292
Nigrospora hainanensis	CGMCC 3.18129	*Musa paradisiaca*	China	KX986091	KX986112	KY019464	KY019415
Nigrospora lacticolonia	CGMCC 3.18123	*Camellia sinensis*	China	KX985978	KX986105	KY019458	KY019291
Nigrospora musae	CBS 319.34	*Musa* sp.	Australia	MH855545	KX986110	KY019455	KY019419
Nigrospora oryzae	LC2693	*Neolitsea* sp.	China	KX985944	KX986101	KY019471	KY019299
Nigrospora osmanthi	CGMCC 3.18126	*Osmanthus* sp.	China	KX986010	KX986106	KY019461	KY019421
Nigrospora pyriformis	CGMCC 3.18122	*Citrus sinensis*	China	KX985940	KX986100	KY019457	KY019290
Nigrospora rubi	LC2698	*Rubus* sp.	China	KX985948	KX986102	KY019475	KY019302
Nigrospora sphaerica	LC7298	*Nelumbo* sp.	China	KX985937	KX986097	KY019606	KY019401
Nigrospora vesicularis	CGMCC 3.18128	*Musa paradisiaca*	China	KX986088	KX986099	KY019463	KY019294
Nonappendiculata quercina	CBS 116061	*Quercus suber*	Italy	MH553982	MH554199	MH554641	MH554400
Parabartalinia lateralis	CBS 399.71	*Acacia karroo*	South Africa	MH554043	MH554256	MH554719	MH554478
Parapleurotheciopsis inaequiseptata	MUCL 41089	Rotten leaf	Brazil	EU040235	EU040235	NA	NA
Parapleurotheciopsis caespitosa	CBS 519.93	*Syzygium cordatum*	South Africa	MH862437	NG_066263	NA	NA
Pestalotiopsis adusta	CBS 263.33	*Rhododendron ponticum*	Netherlands	KM199316	KM116198	KM199414	KM199489
Pestalotiopsis australasiae	CBS 114126	*Knightia* sp.	New Zealand	KM199297	KM116218	KM199409	KM199499
Phlogicylindrium eucalypti	CBS 120080	*Eucalyptus globulus*	Australia	NR_132813	DQ923534	MH704633	MH704607
Phlogicylindrium eucalyptorum	CBS 120221	*Eucalyptus globus*	Australia	EU040223	MH554204	MH704635	MH704608
Pseudopestalotiopsis ampullacea	LC6618	*Camellia sinensis*	China	KX895025	KX895039	KX895358	KX895244
Pseudopestalotiopsis camelliae-sinensis	LC3009	*Camellia sinensis*	China	KX894935	KX895050	KX895267	KX895152
Pseudosarcostroma osyridicola	CBS 103.76	*Osyris alba*	France	MH553954	MH554177	MH554613	MH554372
Pseudosporidesmium knawiae	CBS 123529	NA	NA	MH863299	MH874823	NA	NA
Robillarda africana	CBS 122.75	NA	South Africa	KR873253	KR873281	MH554656	MH554414
Robillarda terrae	CBS 587.71	Soil	India	KJ710484	KJ710459	MH554734	MH554493
Sarcostroma africanum	CBS 143879	*Pelargonium cucullatum*	South Africa	MH554078	MH554289	MH554752	MH554513
Sarcostroma australiense	CBS 144160	*Daviesia latifolia*	Australia	MH554138	MH554340	MH554811	MH554573
Seimatosporium germanicum	CBS 437.87	NA	Germany	MH554047	MH554259	MH554723	MH554482
Seimatosporium luteosporum	CBS 142599	*Vitis vinifera*	USA	KY706284	KY706309	KY706259	KY706334
Seiridium cancrinum	CBS 226.55	*Cupressus macrocarpa*	Kenya	LT853089	MH554241	LT853236	LT853186
Seiridium cupressi	CBS 224.55	*Cupressus macrocarpa*	Kenya	LT853083	MH554240	LT853230	LT853180
Sporocadus biseptatus	CBS 110324	NA	NA	MH553956	MH554179	MH554615	MH554374
Sporocadus cornicola	CBS 143889	*Cornus sanguinea*	Germany	MH554121	MH554326	MH554794	MH554555
Sporocadus trimorphus	CBS 114203	*Rosa canina*	Sweden	MH553977	MH554196	MH554636	MH554395
Strickeria kochii	CBS 140411	*Robinia pseudoacacia*	Austria	NR_154423	KT949918	MH554679	MH554437
Subramaniomyces fusisaprophyticus	CBS 418.95	Leaf litter	Cuba	EU040241	EU040241	NA	NA
Synnemapestaloides juniperi	CBS 477.77	*Juniperus phoenicea*	France	MH554053	MH554266	MH554729	MH554488
Truncatella angustata	CBS 113.11	*Picea abies*	Germany	MH553966	MH554185	MH554625	MH554384
Xenoseimatosporium quercinum	CBS 129171	*Rhododendron* sp.	Latvia	MH553997	MH554216	MH554666	MH554424
Xyladictyochaeta lusitanica	CBS 143502	*Eucalyptus* sp.	Australia	MH107926	MH107972	MH108053	MH108033

Note: NA, not applicable. Strains in this study are marked in bold.

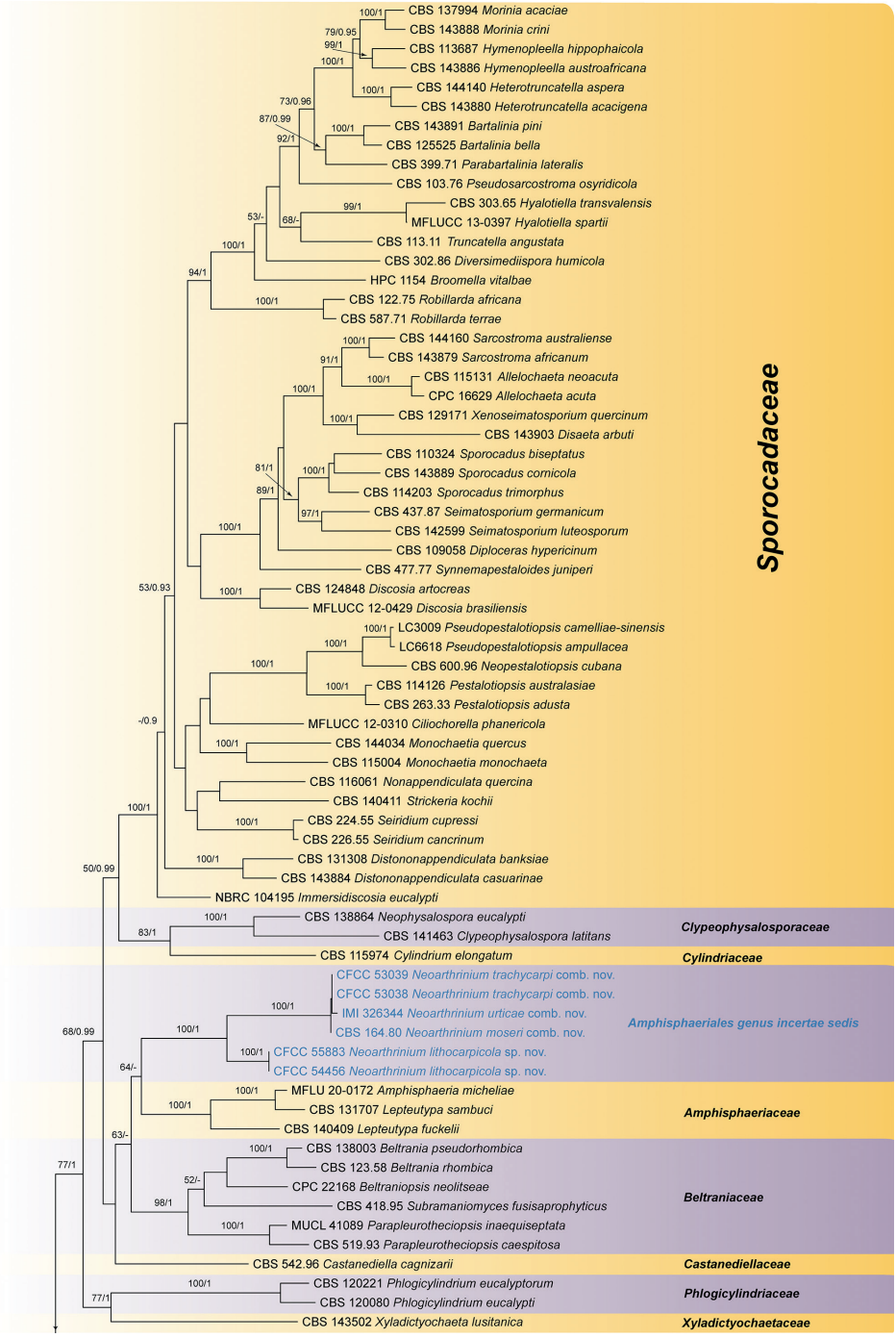

Figure 1. Phylogram of Amphisphaeriales resulting from a Maximum Likelihood analysis, based on a combined matrix of ITS, LSU, *tef1* and *tub2*. Numbers above the branches indicate ML bootstraps (left, ML BS ≥ 50%) and Bayesian Posterior Probabilities (right, BPP ≥ 0.90). The tree is rooted with *Clypeosphaeria mamillana* (CBS 140735) and *Pseudosporidesmium knawiae* (CBS 123529). New species and combinations proposed in the present study are marked in blue.

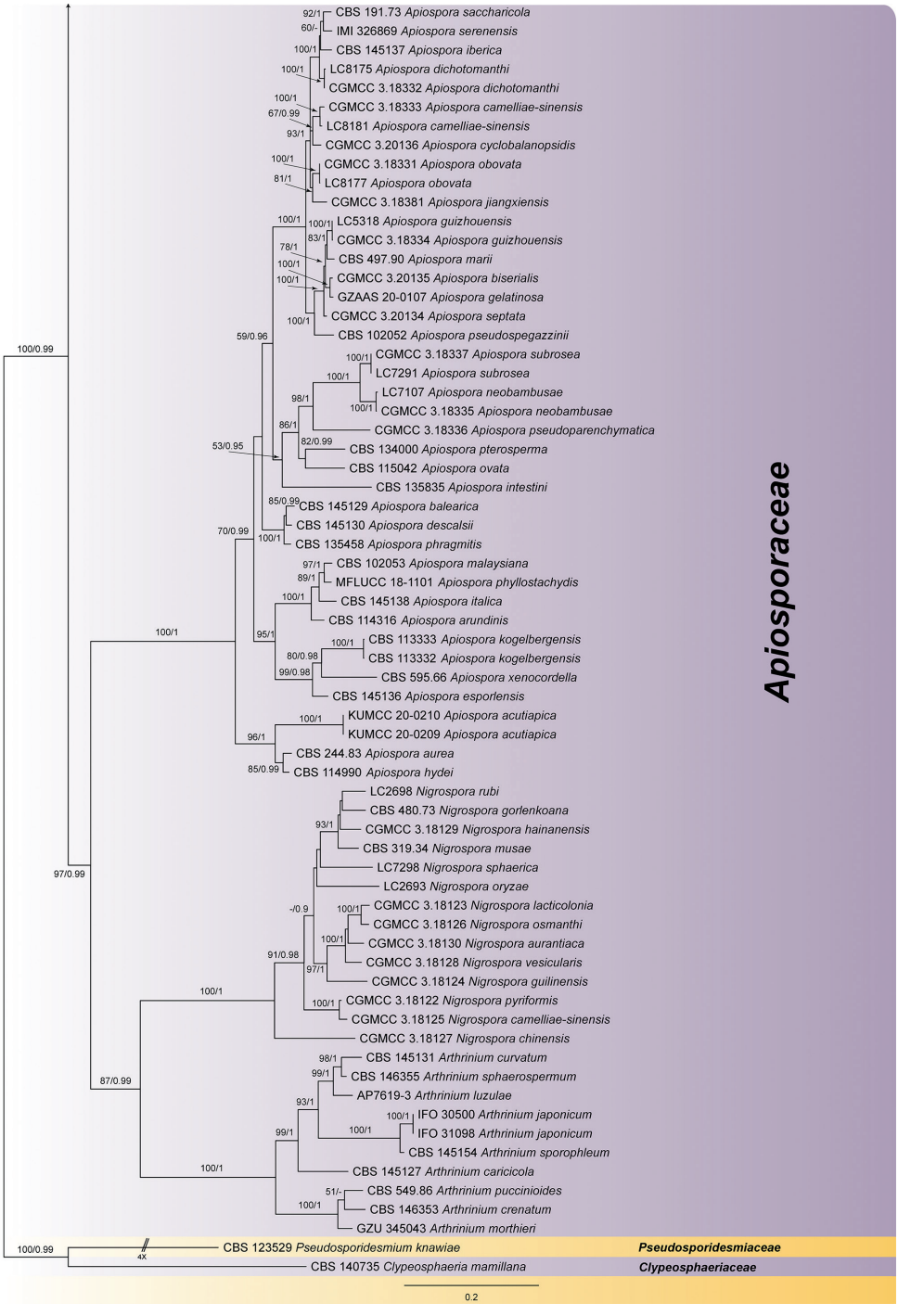

Figure 1. Continued.

Taxonomy

***Neoarthrinium* Ning Jiang, gen. nov.**
MycoBank No: 843845

Etymology. Named after its morphological similarity to *Arthrinium*.

Type species. *Neoarthrinium lithocarpicola* Ning Jiang

Description. ***Hyphae*** formed on PDA hyaline, branched, septate. Asexual morph: ***Conidiophores*** cylindrical, septate, verrucose, flexuous, sometimes reduced to conidiogenous cells. ***Conidiogenous cells*** erect, blastic, aggregated in clusters on hyphae, hyaline to pale brown, smooth, doliiform, subglobose to lageniform, branched. ***Conidia*** brown to dark brown, smooth to finely roughened, subglobose, ellipsoid to lenticular, with a longitudinal germ slit, occasionally elongated to ellipsoidal. Sexual morph: Undetermined.

***Neoarthrinium lithocarpicola* Ning Jiang, sp. nov.**
MycoBank No: 843846
Fig. 2

Etymology. Named for its host genus "*Lithocarpus*" and "*-cola*" = inhabiting.

Description. ***Hyphae*** 1.5–4.5 µm diam., hyaline, branched, septate. Asexual morph: ***Conidiophores*** cylindrical, septate, verrucose, flexuous, sometimes reduced to conidiogenous cells. ***Conidiogenous cells*** erect, blastic, aggregated in clusters on hyphae, hyaline to pale brown, smooth, globose to subglobose, branched, (4–)5.5–8 × 2.5–3.5(–4) µm, mean ± SD = 6.6 ± 1.3 × 3.1 ± 0.4 µm, n = 50. ***Conidia*** brown to dark brown, smooth to finely roughened, subglobose to lenticular, with a longitudinal germ slit, occasionally elongated to ellipsoidal, (5–)6–8(–8.5) × (4.5–)5–5.5(–6) µm, mean ± SD = 7 ± 0.8 × 5.3 ± 0.5 µm, L/W = 1.1–1.8, n = 50. Sexual morph: Undetermined.

Culture characters. ***Colonies*** on PDA flat, spreading, with flocculent aerial mycelium forming concentric rings, edge entire, mouse grey to greyish-green, reaching 60 mm diam. after 10 d at 25 °C, forming abundant conidiomata.

Specimens examined. China. Guangdong Province, Guangzhou City, on leaf spots of *Lithocarpus glaber* (Thunb.) Nakai, *Shang Sun* (holotype CAF800050 = JNH0046; ex-type living culture: CFCC 54456; other living culture: CFCC 55883).

Notes. Two isolates of *Neoarthrinium lithocarpicola* from *Lithocarpus glaber* (Thunb.) Nakai formed a well-supported monophyletic clade, distinct from *N. moseri*, *N. trachycarpi* and *N. urticae* (Fig. 1). Morphologically, *N. lithocarpicola* is distinguished from *N. moseri* in smaller conidia (5–8.5 × 4.5–6 µm in *N. lithocarpicola* vs. 10–14 × 3–4.5 µm in *N. moseri*; Gams 1995). *Neoarthrinium lithocarpicola* is different from *N. urticae* by lacking thick blackish septa in conidiophores (Ellis 1965). *Neoarthrinium lithocarpicola* is similar to *N. trachycarpi* in the size of its conidiogenous cells and conidia, but it can be distinguished by its globose to subglobose conidiogenous cells (Yan et al. 2019).

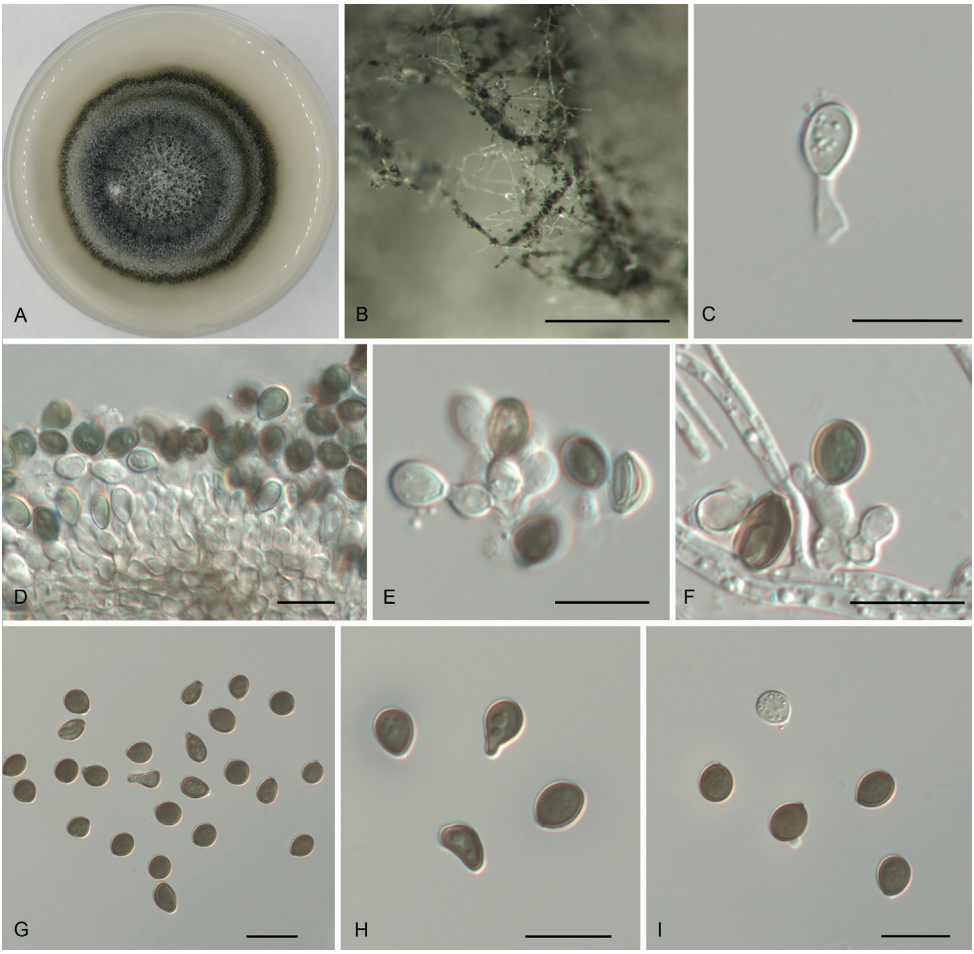

Figure 2. *Neoarthrinium lithocarpicola* **A** colony on PDA **B** conidiomata formed in culture **C–F** conidiogenous cells giving rise to conidia **G–I** conidia. Scale bars: 500 µm (**B**), 10 µm (**C–I**).

***Neoarthrinium moseri* (W. Gams) Voglmayr, comb. nov.**
MycoBank No: 844772

Basionym. *Wardomyces moseri* W. Gams, Beih. Sydowia 10: 67 (1995)

Notes. Based on a placement within Xylariales in phylogenetic analyses, Sandoval-Denis et al. (2016) excluded this species from the genus (Microascales); however, they did not suggest an alternative generic classification. The blastic hyaline, smooth, lageniform conidiogenous cells aggregated in clusters and the subglobose to ellipsoid dark brown conidia with a longitudinal germ slit (Gams 1995) fully matched the genus *Neoarthrinum*. The ITS, LSU and *tub2* sequences of the ex-holotype strain of *N. moseri* (CBS 164.80) are almost identical to those of *N. trachycarpi*, indicating that they may be synonymous. Both species were isolated from petioles of palms: *N. moseri* from *Mauritia minor* Burret in Colombia and *N. trachycarpi* from *Trachycarpus fortunei*

(Hook.) H.Wendl. in China. However, the two species were reported to differ in conidial size (10–14 × 3–4.5 μm in *N. moseri* vs. 6.1–8.5 × 4.2–5.8 μm in *N. trachycarpi*; Gams 1995; Yan et al. 2019) and for the time being, we therefore kept them separate.

***Neoarthrinium trachycarpi* (C.M. Tian & H. Yan) Ning Jiang, comb. nov.**
MycoBank No: 843847

Basionym. *Arthrinium trachycarpi* C.M. Tian & H. Yan [as '*trachycarpum*'], Phytotaxa 400(3): 208 (2019)

***Neoarthrinium urticae* (M.B. Ellis) Ning Jiang, comb. nov.**
MycoBank No: 843848

Basionym. *Arthrinium urticae* M.B. Ellis, Mycol. Pap. 103: 16 (1965)

Notes. The possibility that *Apiosporella urticae* (Rehm) Höhn. is the sexual morph of *Arthrinium urticae* is raised by the fact that both share the same host (*Urtica*) and are classified as members of the Apiosporaceae (Index Fungorum, accessed 4 July 2022). This evidence would have far reaching nomenclatural consequences not only for species, but also for generic classification, as *Apiosporella* (Höhnel 1909) may then qualify for an older genus name to be used for *Neoarthrinium*. However, according to L. Holm, the holotype specimen of its basionym, *Apiospora urticae* (S-F12119), represents a very different fungus, *Didymella eupyrena* (Didymellaceae, Pleosporales, Dothideomycetes; https://herbarium.nrm.se/specimens/F12119, accessed 4 July 2022). The status of the genus *Apiosporella* is still unclear because Höhnel (1909) did not choose a type from the six different species included in the genus. However, none of the original species is a close relative of Apiosporaceae or *Neoarthrinium*; therefore, *Apiosporella* should be excluded from Apiosporaceae.

No sequence data are available for isolates from the type host *Urtica dioica* L. (Urticaceae). The single culture sequenced (IMI 326344) was isolated from unidentified leaf litter collected in India. Additional molecular studies on verified isolates from *Urtica* collected in Europe are necessary to reveal whether IMI 326344 represents true *N. urticae*. However, *N. urticae* appears to be very rare and we are unaware of any additional collections with the exception of the type.

Discussion

Arthrinium and related genera are important fungal taxa whose concepts and classification have undergone many changes and additions (e.g. Cooke 1954; Samuels et al. 1981; Larrondo and Calvo 1990; Hyde et al. 1998; Jaklitsch and

Voglmayr 2012; Crous and Groenewald 2013; Singh et al. 2013; Sharma et al. 2014; Dai et al. 2016, 2017; Hyde et al. 2016; Jiang et al. 2018, 2020; Wang et al. 2018; Pintos et al. 2019; Pintos and Alvarado 2021). In recent years, substantial changes in classification were implemented in the course of unitary nomenclature. A large number of newly-discovered species have been described as a result of extensive sampling of new isolates, based on multigene phylogenies (e.g. Crous and Groenewald 2013; Wang et al. 2018; Pintos and Alvarado 2021). Currently, *Arthrinium*-like asexual morphs are shared by three distinct lineages within Amphisphaeriales, viz. *Apiospora*, *Arthrinium s. s.* and *Neoarthrinium* as shown in Fig. 1. *Arthrinium s. s.* is the sister genus to *Nigrospora*, which morphologically differs from *Apiospora*, *Arthrinium* and *Neoarthrinium* in conidial ontogeny (Wang et al. 2017). The phylogram shown in Fig. 1 is consistent with that shown in Tian et al. (2021) in placing *Apiospora*, *Arthrinium* and *Nigrospora* within a clade that is distinct from the new genus *Neoarthrinium*, although *Apiospora* and *Arthrinium* share conidial morphology similar to that of *Neoarthrinium.*

Morphologically, *Apiospora*, *Arthrinium* and *Neoarthrinium* are similar in having basauxic conidiogenesis. Conidia of *Apiospora* and *Neoarthrinium* are generally more or less rounded in face view and lenticular in side view, while those of *Arthrinium* are variously shaped, viz. globose, angular, polygonal, curved, fusiform or navicular (Yan et al. 2019; Pintos and Alvarado 2021). However, the conidiophores of several *Arthrinium* and *Neoarthrinium* species have thick blackish septa, which are rarely observed in *Apiospora* (Ellis 1965; Wang et al. 2018; Pintos and Alvarado 2021). Hence, these three genera are difficult to distinguish by only asexual morphology.

Regarding their hosts, there are some tendencies in host preferences, while *Arthrinium* species are predominantly found in Cyperaceae and Juncaceae (Pintos and Alvarado 2021) and species of *Apiospora* primarily occur on Poaceae (but also on many other hosts; Wang et al. 2018). Four *Neoarthrinium* species were discovered on four hosts from three distantly-related host families (i.e. *N. lithocarpicola* from *Lithocarpus glaber* (Thunb.) Nakai, Fagaceae; *N. moseri* from *Mauritia minor* Burret, Arecaceae; *N. trachycarpi* from *Trachycarpus fortune* (Hook.) H.Wendl., Arecaceae; and *N. urticae* from *Urtica dioica* L., Urticaceae; Ellis 1965; Yan et al. 2019). Hence, host association is not a fully reliable feature to distinguish *Apiospora*, *Arthrinium* and *Neoarthrinium.*

Compared to species, generic delimitation is much more subjective. However, there is a broad agreement that genera, along with all taxonomic classification units at all ranks, should be monophyletic. As morphology is frequently insufficient for phylogenetic classification, molecular evidence is regarded as significant data or even an essential characteristic in the classification and identification of fungal taxa. In the present study, *Neoarthrinium* is proposed as a new genus for a group of species phylogenetically distinct from *Apiospora*, *Arthrinium* and *Nigrospora* to maintain monophyletic *Arthrinium*-like genera. Using morphological and phylogenetic data, however, we need more samples to improve our understanding of *Arthrinium*-like taxa and genera in the Amphisphaeriales.

Acknowledgements

This research was funded by the National Microbial Resource Center of the Ministry of Science and Technology of the People's Republic of China (NMRC-2021-7). The three anonymous reviewers are also acknowledged for their useful comments.

References

Carbone I, Kohn LM (1999) A method for designing primer sets for speciation studies in filamentous ascomycetes. Mycologia 3(3): 553–556. https://doi.org/10.1080/00275514.1999.12061051

Chen K, Wu XQ, Huang MX, Han YY (2014) First report of brown culm streak of *Phyllostachys praecox* caused by *Arthrinium arundinis* in Nanjing, China. Plant Disease 98(9): 1274. https://doi.org/10.1094/PDIS-02-14-0165-PDN

Cooke WB (1954) The genus *Arthrinium.* Mycologia 46(6): 815–822. https://doi.org/10.1080/00275514.1954.12024418

Crous PW, Groenewald JZ (2013) A phylogenetic re-evaluation of *Arthrinium.* IMA Fungus 4(1): 133–154. https://doi.org/10.5598/imafungus.2013.04.01.13

Dai DQ, Jiang HB, Tang LZ, Bhat DJ (2016) Two new species of *Arthrinium* (Apiosporaceae, Xylariales) associated with bamboo from Yunnan, China. Mycosphere: Journal of Fungal Biology 7(9): 1332–1345. https://doi.org/10.5943/mycosphere/7/9/7

Dai DQ, Phookamsak R, Wijayawardene NN, Li WJ, Bhat DJ, Xu JC, Taylor JE, Hyde KD, Chukeatirote E (2017) Bambusicolous fungi. Fungal Diversity 82(1): 1–105. https://doi.org/10.1007/s13225-016-0367-8

Doyle JJ, Doyle JL (1990) Isolation of plant DNA from fresh tissue. Focus (San Francisco, Calif.) 12: 13–15.

Ellis MB (1965) Dematiaceous Hyphomycetes. VI. Mycological Papers 103: 1–46.

Feng Y, Liu JK, Lin CG, Chen YY, Xiang MM, Liu ZY (2021) Additions to the genus *Arthrinium* (Apiosporaceae) from bamboos in China. Frontiers in Microbiology 12: 661281. https://doi.org/10.3389/fmicb.2021.661281

Fries EM (1832) Systema Mycologicum vol. 3(2). Sumptibus Ernesti Mauritii, Greifswald.

Gams W (1995) An unusual species of *Wardomyces* (Hyphomycetes). Beihefte zur Sydowia 10: 67–72.

Glass NL, Donaldson GC (1995) Development of primer sets designed for use with the PCR to amplify conserved genes from filamentous ascomycetes. Applied and Environmental Microbiology 61(4): 1323–1330. https://doi.org/10.1128/aem.61.4.1323-1330.1995

Höhnel FXR (1909) Fragmente zur Mykologie (VIII. Mitteilung, Nr. 354 bis 406). Sitzungsberichte der Kaiserlichen Akademie der Wissenschaften in Wien Mathematisch-Naturwissenschaftliche Klasse, Abt. 1(118): 1157–1246.

Hudson HJ, McKenzie EHC, Tommerup IC (1976) Conidial states of *Apiospora* Sacc. Transactions of the British Mycological Society 66(2): 359–362. https://doi.org/10.1016/S0007-1536(76)80075-7

Hyde KD, Fröhlich J, Taylor JE (1998) Fungi from palms. XXXVI. Reflections on unitunicate ascomycetes with apiospores. Sydowia 50: 21–80.

Hyde KD, Hongsanan S, Jeewon R, Bhat DJ, McKenzie EHC, Jones EBG, Phookamsak R, Ariyawansa HA, Boonmee S, Zhao Q, Abdel-Aziz FA, Abdel-Wahab MA, Banmai S, Chomnunti P, Cui B-K, Daranagama DA, Das K, Dayarathne MC, de Silva NI, Dissanayake AJ, Doilom M, Ekanayaka AH, Gibertoni TB, Góes-Neto A, Huang S-K, Jayasiri SC, Jayawardena RS, Konta S, Lee HB, Li W-J, Lin C-G, Liu J-K, Lu Y-Z, Luo Z-L, Manawasinghe IS, Manimohan P, Mapook A, Niskanen T, Norphanphoun C, Papizadeh M, Perera RH, Phukhamsakda C, Richter C, de A. Santiago ALCM, Drechsler-Santos ER, Senanayake IC, Tanaka K, Tennakoon TMDS, Thambugala KM, Tian Q, Tibpromma S, Thongbai B, Vizzini A, Wanasinghe DN, Wijayawardene NN, Wu H-X, Yang J, Zeng X-Y, Zhang H, Zhang J-F, Bulgakov TS, Camporesi E, Bahkali AH, Amoozegar MA, Araujo-Neta LS, Ammirati JF, Baghela A, Bhatt RP, Bojantchev D, Buyck B, da Silva GA, de Lima CLF, de Oliveira RJV, de Souza CAF, Dai Y-C, Dima B, Duong TT, Ercole E, Mafalda-Freire F, Ghosh A, Hashimoto A, Kamolhan S, Kang J-C, Karunarathna SC, Kirk PM, Kytövuori I, Lantieri A, Liimatainen K, Liu Z-Y, Liu X-Z, Lücking R, Medardi G, Mortimer PE, Nguyen TTT, Promputtha I, Raj KNA, Reck MA, Lumyong S, Shahzadeh-Fazeli SA, Stadler M, Soudi MR, Su H-Y, Takahashi T, Tangthirasunun N, Uniyal R, Wang Y, Wen T_C, Xu J-C, Zhang Z-K, Zhao Y-C, Zhou J-L, Zhu L (2016) Fungal diversity notes 367–490: Taxonomic and phylogenetic contributions to fungal taxa. Fungal Diversity 80: 1–270. https://doi.org/10.1007/s13225-016-0373-x

Hyde KD, Norphanphoun C, Maharachchikumbura SSN, et al. (2020) Refined families of Sordariomycetes. Mycosphere: Journal of Fungal Biology 11(1): 305–1059. https://doi.org/10.5943/mycosphere/11/1/7

Jaklitsch WM, Voglmayr H (2012) Phylogenetic relationships of five genera of Xylariales and *Rosasphaeria* gen. nov. (Hypocreales). Fungal Diversity 52(1): 75–98. https://doi.org/10.1007/s13225-011-0104-2

Jiang N, Tian CM (2021) The holomorph of *Arthrinium setariae* sp. nov. (Apiosporaceae, Xylariales) from China. Phytotaxa 483(2): 149–159. https://doi.org/10.11646/phytotaxa.483.2.7

Jiang N, Li J, Tian CM (2018) *Arthrinium* species associated with bamboo and reed plants in China. Fungal Systematics and Evolution 2: 1–9. https://doi.org/10.3114/fuse.2018.02.01

Jiang N, Liang YM, Tian CM (2020) A novel bambusicolous fungus from China, *Arthrinium chinense* (Xylariales). Sydowia 72: 77–83. https://doi.org/10.12905/0380.sydowia72-2020-0077

Jiang N, Fan XL, Tian CM (2021) Identification and characterization of leaf-inhabiting fungi from *Castanea* plantations in China. Journal of Fungi 7(1): 64. https://doi.org/10.3390/jof7010064

Katoh K, Toh H (2010) Parallelization of the MAFFT multiple sequence alignment program. Bioinformatics 26(15): 1899–1900. https://doi.org/10.1093/bioinformatics/btq224

Konta S, Hyde KD, Eungwanichayapant PD, Karunarathna SC, Samarakoon MC, Xu J, Dauner LAP, Aluthwattha ST, Lumyong S, Tibpromma S (2021) Multigene phylogeny reveals *Haploanthostomella elaeidis* gen. et sp. nov. and familial replacement of *Endocalyx* (Xylariales, Sordariomycetes, Ascomycota). Life 11(6): 486. https://doi.org/10.3390/life11060486

Kumar S, Stecher G, Tamura K (2016) MEGA7: Molecular evolutionary genetics analysis version 7.0 for bigger datasets. Molecular Biology and Evolution 33(7): 1870–1874. https://doi.org/10.1093/molbev/msw054

Kunze G, Schmidt JC (1817) Mykologische 1: 1–109.

Larrondo JV, Calvo MA (1990) Two new species of *Arthrinium* from Spain. Mycologia 82(3): 396–398. https://doi.org/10.1080/00275514.1990.12025899

Larrondo JV, Calvo MA (1992) New contributions to the study of the genus *Arthrinium.* Mycologia 84(3): 475–478. https://doi.org/10.1080/00275514.1992.12026164

Liu F, Bonthond G, Groenewald JZ, Cai L, Crous PW (2019) Sporocadaceae, a family of coelomycetous fungi with appendage-bearing conidia. Studies in Mycology 92(1): 287–415. https://doi.org/10.1016/j.simyco.2018.11.001

Martínez-Cano C, Grey WE, Sands DC (1992) First report of *Arthrinium arundinis* causing kernel blight on barley. Plant Disease 76(10): 1077. https://doi.org/10.1094/PD-76-1077B

Mavragani DC, Abdellatif L, McConkey B, Hamel C, Vujanovic V (2007) First report of damping-off of durum wheat caused by *Arthrinium sacchari* in the semi-arid Saskatchewan fields. Plant Disease 91(4): 469. https://doi.org/10.1094/PDIS-91-4-0469A

Minter DW (1985) A re-appraisal of the relationships between *Arthrinium* and other hyphomycetes. Proceedings of the Indiana Academy of Sciences 94(2–3): 281–308. https://doi.org/10.1007/BF03053145

O'Donnell K, Cigelnik E (1997) Two divergent intragenomic rDNA ITS2 types within a monophyletic lineage of the fungus *Fusarium* are nonorthologous. Molecular Phylogenetics and Evolution 7(1): 103–116. https://doi.org/10.1006/mpev.1996.0376

Pintos A, Alvarado P (2021) Phylogenetic delimitation of *Apiospora* and *Arthrinium.* Fungal Systematics and Evolution 7(1): 197–221. https://doi.org/10.3114/fuse.2021.07.10

Pintos A, Alvarado P, Planas J, Jarling R (2019) Six new species of *Arthrinium* from Europe and notes about *A. caricicola* and other species found in *Carex* spp. hosts. MycoKeys 49: 15–48. https://doi.org/10.3897/mycokeys.49.32115

Réblová M, Miller AN, Rossman AY, Seifert KA, Crous PW, Hawksworth DL, Abdel-Wahab MA, Cannon PF, Daranagama DA, De Beer ZW, Huang S-K, Hyde KD, Jayawardena R, Jaklitsch W, Jones EBG, Ju Y-M, Judith C, Maharachchikumbura SSN, Pang K-L, Petrini LE, Raja HA, Romero AI, Shearer C, Senanayake IC, Voglmayr H, Weir BS, Wijayawarden NN (2016) Recommendations for competing sexual-asexually typified generic names in Sordariomycetes (except Diaporthales, Hypocreales, and Magnaporthales). IMA Fungus 7(1): 131–153. https://doi.org/10.5598/imafungus.2016.07.01.08

Ronquist F, Teslenko M, Van Der Mark P, Ayres DL, Darling A, Höhna S, Larget B, Liu L, Suchard MA, Huelsenbeck JP (2012) MrBayes 3.2: Efficient Bayesian phylogenetic inference and model choice across a large model space. Systematic Biology 61(3): 539–542. https://doi.org/10.1093/sysbio/sys029

Saccardo PA (1875) Fungi veneti novi vel critici. Series II. Nuovo Giornale Botanico Italiano 7: 299–329.

Samarakoon BC, Wanasinghe DN, Samarakoon MC, Phookamsak R, McKenzie EHC, Chomnunti P, Hyde KD, Lumyong S, Karunarathna SC (2020) Multi-gene phylogenetic evidence suggests *Dictyoarthrinium* belongs in Didymosphaeriaceae (Pleosporales,

Dothideomycetes) and *Dictyoarthrinium musae* sp. nov. on *Musa* from Thailand. MycoKeys 71: 101–118. https://doi.org/10.3897/mycokeys.71.55493

Samarakoon MC, Hyde KD, Maharachchikumbura SSN, Stadler M, Gareth Jones EB, Promputtha I, Suwannarach N, Camporesi E, Bulgakov TS, Liu J-K (2022) Taxonomy, phylogeny, molecular dating and ancestral state reconstruction of Xylariomycetidae (Sordariomycetes). Fungal Diversity 112(1): 1–88. https://doi.org/10.1007/s13225-021-00495-5

Samuels GJ, McKenzie EHC, Buchanan DE (1981) Ascomycetes of New Zealand. 3. Two new species of *Apiospora* and their *Arthrinium* anamorphs on bamboo. New Zealand Journal of Botany 19(2): 137–149. https://doi.org/10.1080/0028825X.1981.10425113

Sandoval-Denis M, Guarro J, Cano-Lira JF, Sutton DA, Wiederhold NP, de Hoog GS, Abbott SP, Decock C, Sigler L, Gené J (2016) Phylogeny and taxonomic revision of Microascaceae with emphasis on synnematous fungi. Studies in Mycology 83(1): 193–233. https://doi.org/10.1016/j.simyco.2016.07.002

Senanayake IC, Bhat JD, Cheewangkoon R, Xie N (2020) Bambusicolous *Arthrinium* species in Guangdong Province, China. Frontiers in Microbiology 11: 602773. https://doi.org/10.3389/fmicb.2020.602773

Sharma R, Kulkarni G, Sonawane MS, Shouche YS (2014) A new endophytic species of *Arthrinium* (Apiosporaceae) from *Jatropha podagrica*. Mycoscience 55(2): 118–123. https://doi.org/10.1016/j.myc.2013.06.004

Singh SM, Yadav LS, Singh PN, Hepat R, Sharma R, Singh SK (2013) *Arthrinium rasikravindrii* sp. nov. from Svalbard, Norway. Mycotaxon 122(1): 449–460. https://doi.org/10.5248/122.449

Stamatakis A (2014) RAxML version 8: A tool for phylogenetic analysis and post-analysis of large phylogenies. Bioinformatics 30(9): 1312–1313. https://doi.org/10.1093/bioinformatics/btu033

Tian X, Karunarathna SC, Mapook A, Promputtha I, Xu J, Bao D, Tibpromma S (2021) One new species and two new host records of *Apiospora* from bamboo and maize in northern Thailand with thirteen new combinations. Life 11(10): 1071. https://doi.org/10.3390/life11101071

Vilgalys R, Hester M (1990) Rapid genetic identification and mapping of enzymatically amplified ribosomal DNA from several *Cryptococcus* species. Journal of Bacteriology 172(8): 4238–4246. https://doi.org/1 0.1128/jb.172.8.4238-4246.1990

Wang M, Liu F, Crous PW, Cai L (2017) Phylogenetic reassessment of *Nigrospora*: Ubiquitous endophytes, plant and human pathogens. Persoonia 39(1): 118–142. https://doi.org/10.3767/persoonia.2017.39.06

Wang M, Tan X-M, Liu F, Cai L (2018) Eight new *Arthrinium* species from China. MycoKeys 34: 1–24. https://doi.org/10.3897/mycokeys.34.24221

White TJ, Bruns T, Lee S, Taylor J (1990) Amplification and direct sequencing of fungal ribosomal RNA genes for phylogenetics. PCR Protocols: A Guide to Methods and Applications 18: 315–322.

Yan H, Jiang N, Liang LY, Yang Q, Tian CM (2019) *Arthrinium trachycarpum* sp. nov. from *Trachycarpus fortuneii* in China. Phytotaxa 400(3): 203–210. https://doi.org/10.11646/phytotaxa.400.3.7

Zhao YM, Deng CR, Chen X (1990) *Arthrinium phaeospermum* causing dermatomycosis, a new record of China. Acta Mycologica Sinica 9: 232–235.

MycoKeys 92: 45–62 (2022)
doi: 10.3897/mycokeys.92.83939
https://mycokeys.pensoft.net

RESEARCH ARTICLE

A peer-reviewed open-access journal
MycoKeys
Launched to accelerate biodiversity research

Taxonomy of *Buellia epigaea*-group (Caliciales, Caliciaceae), revealing a new species and two new records from China

Min Ai[1,2], Li Juan Li[3], Fiona Ruth Worthy[1,2], An Cheng Yin[1,2], Qiu Yi Zhong[1,2], Shi Qiong Wang[4], Li Song Wang[1,2], Xin Yu Wang[1,2]

1 *Key Laboratory for Plant Diversity and Biogeography of East Asia, Kunming Institute of Botany, CAS, Kunming, Yunnan 650201, China* **2** *Yunnan Key Laboratory for Fungal Diversity and Green Development, Kunming Institute of Botany, CAS, Kunming, Yunnan 650201, China* **3** *Department of Botany and Molecular Evolution, Senckenberg Research Institute, 60325 Frankfurt am Main, Germany* **4** *Kunming Botanical Garden, Kunming Institute of Botany, CAS, Kunming, Yunnan 650201, China*

Corresponding author: Xin Yu Wang (wangxinyu@mail.kib.ac.cn)

Academic editor: Thorsten Lumbsch | Received 17 March 2022 | Accepted 16 July 2022 | Published 5 August 2022

Citation: Ai M, Li LJ, Worthy FR, Yin AC, Zhong QY, Wang SQ, Wang LS, Wang XY (2022) Taxonomy of *Buellia epigaea*-group (Caliciales, Caliciaceae), revealing a new species and two new records from China. MycoKeys 92: 45–62. https://doi.org/10.3897/mycokeys.92.83939

Abstract

During the Second Tibetan Plateau Scientific Expedition and Research Program, we discovered that white terricolous lichenized fungal species of *Buellia* De Not. were widely distributed across the Tibetan Plateau. After examining their morphology, chemistry and phylogeny, we describe *Buellia alpina* Xin Y. Wang & Li S. Wang, **sp. nov.** as new to science. It is present in alpine meadows, and is characterized by its effigurate thallus, distinct linear marginal lobes, cover of thick white pruina and four-spored asci. This is also the first report of *Buellia elegans* Poelt and *Buellia epigaea* (Pers.) Tuck from China. The *Buellia epigaea*-group has previously been characterized by white and often effigurate thalli that occur mainly on soil. However, our results show that species in this group actually belong to two distinct clades. This conclusion is based on analyses of the nuITS region and the combined regions dataset (nuITS-nuLSU-mtSSU-β-tubulin). We discuss differences in morphology, anatomy, chemistry and ecology among the putative *Buellia epigaea*-group. Detailed descriptions and figures for the three species from China and a key for species of *Buellia epigaea*-group are provided.

Keywords

Lichenized fungi, nuITS-nuLSU-mtSSU-β-tubulin, phylogenetic analysis, terricolous, Tibetan Plateau

Introduction

The lichen genus *Buellia* De Not. (Caliciales, Caliciaceae) comprises approximately 400 species worldwide (Bungartz et al. 2007). *Buellia* s.l. is characterized by a crustose thallus, black lecideine apothecia, *Bacidia*-type asci, brown ascospores with one or more septate and reddish-brown or rarely hyaline hypothecia. Several other genera, which were previously included in *Buellia* s.l. (such as *Amandinea* M. Choisy, *Diplotomma* Flot. and *Tetramelas* Norman), have since been segregated based on their morphology, anatomy, chemistry and ecological environment (Scheidegger 1993; Marbach 2000; Nordin 2000). However, there remain other *Buellia* s.l. species with distinct morphological characters currently placed in groups instead of defined genera. Two examples are the species related to *Buellia aethalea* (Ach.) Th. Fr. or *B. epigaea* (Pers.) Tuck, which are currently treated as *aethalea*-group or *epigaea*-group, respectively (Poelt and Sulzer 1974; Scheidegger 1993). Their current classification is based solely on external morphology, without the support of molecular data, therefore strict phylogenetic relationships between *Buellia* s.l. species remain unclear.

More than 64 species of the genus *Buellia* s.l. were previously reported from China, mostly located in the Tibetan Plateau region (Wei 2020; Wang et al. 2020). During the Second Tibetan Plateau Scientific Expedition and Research Program (STEP), a large number of additional lichen specimens were collected, including *Buellia epigaea*-group species.

The *Buellia epigaea*-group contains seven species; these are characterized by white and often effigurate thalli that occur mainly on soil. *Buellia epigaea*, which was reported from Europe, is the core species of this group. *Buellia asterella* Poelt & Sulzer and *B. elegans* were reported from Europe, and *B. zoharyi* Galun was reported from Asia and Europe by Poelt and Sulzer (1974). Trinkaus and Mayrhofer (2000) published a revision of the four species above. A further three new species were described from Australia: *Buellia dijiana* Trinkaus, *B. georgei* Trinkaus, Mayrhofer & Elix, and *B. lobata* Trinkaus & Elix (Trinkaus et al. 2001). *B. epigaea*, *B. dijiana* and *B. georgei* formed a monophyletic clade, but data is still lacking for the remaining species (Grube and Arup 2001).

The aim of this study is to determine which *Buellia epigaea*-group species are distributed in China and whether they form a monophyletic clade. For this purpose, we carried out a phylogenetic study of the *Buellia epigaea*-group based on four loci.

Materials and methods

Morphological and chemical analyses

During STEP, 92 specimens of the *Buellia epigaea*-group were collected from the Qinghai-Tibetan Plateau and deposited in the Lichen Herbarium, Kunming Institute of Botany, China (KUN). Morphological characteristics of thalli and apothecia were examined under a dissecting microscope (Nikon SMZ 745T). Anatomical characteristics

of apothecia were examined under an optical microscope (Nikon Eclipse Ci-S). Photographs were taken using a digital camera (Nikon DS-Fi2). Descriptions of the range of anatomical characteristics for each species were determined by the smallest and largest single values measured for all specimens. Thin-layer chromatography (TLC) was performed in order to identify secondary metabolites using solvent systems C (toluene: acetic acid = 85:15), according to Orange et al. (2001).

DNA extraction, amplification and sequencing

DNA was extracted from fresh apothecia or thallus pieces with a DNA secure Plant Kit (TIANGEN) according to the manufacturer's instructions. Amplified gene markers and their corresponding primers are shown in Table 1. PCR amplifications were achieved using 1.1 × T3 Super PCR Mix (TSINGKE) in a 25 μL total volume, containing 1 μL of genomic DNA, 1 μL of a 10 mM solution for each primer and 22 μL of 1.1 × T3 Super PCR Mix. The PCR program was: initial denaturation at 98 °C for 3 min, followed by 35 cycles of 98 °C for 10 s, 54–56 °C for 10 s, 72 °C for 15 s, followed by a final extension at 72 °C for 2 min. The PCR products were sequenced with the same amplification primers using Sanger technology by Tsingke Biotechnology Co., Ltd. (Kunming).

Table 1. Gene markers and primer pairs used in this study.

Gene markers	Primers	Sequences of Primers 5'-3'	References
nuITS	ITS1F	CTTGGTCATTTAGAGGAAGTAA	Gardes and Bruns 1993
	ITS4	TCCTCCGCTTATTGATATGC	White et al. 1990
nuLSU	LR0R	GTACCCGCTGAACTTAAGC	Rehner and Samuels 1994
	LR5	ATCCTGAGGGAAACTTC	Vilgalys and Hester 1990
mtSSU	SSU1	AGCAGTGAGGAATATTGGTC	Zoller et al. 1999
	SSU3R	ATGTGGCACGTCTATAGCCC	
β-tubulin	Bt3-LM	GAACGTCTACTTCAACGAG	Myllys et al. 2001
	Bt10-LM	TCGGAAGCAGCCATCATGTTCTT	

Phylogenetic analyses

All newly obtained original sequences were edited manually using GENEIOUS v8.0.2. Their taxon name, voucher and GenBank accession number are shown in Table 2. All sequences, including those downloaded from GenBank, were aligned using MAFFT v7 with the option of E-INS-I (Katoh et al. 2005). Ambiguous regions were excluded using GBLOCKS (Talavera and Castresana 2007) with the default settings. Congruence between different gene regions was analyzed before combining. Bayesian inference (BI) and maximum likelihood (ML) were employed to determine the phylogenetic relationships. The best-fit partition substitution models were selected based on the lowest Bayesian information criterion (BIC) using PARTITION FINDER 2

(Guindon et al. 2010; Lanfear et al. 2012, 2017): nuITS dataset (TIM2e+G4) and the combined regions dataset (GTR+G for ITS1, ITS2 and mtSSU; GTR+I+G for 5.8S, nuLSU and β-tubulin), respectively.

ML analyses were performed with RAxML v8.2.12 (Stamatakis 2006). Bootstrap support values (MLBS) were estimated from the 70% majority rule tree of all saved trees obtained from 2000 non-parametric bootstrapping pseudo-replicates. BI analyses were performed with MrBayes v3.2.7 (Ronquist et al. 2012) running for 2 million generations. The trees were sampled every 100 generations and the first 25% of the trees were discarded as burn-in, since the average SD of split frequencies had converged at the step of 20% of the total. Bayesian posterior probabilities (BPP) were obtained from the 95% majority rule consensus tree of all saved trees. The final trees were visualized in FigTree v1.4.0 (Rambaut 2012). The final matrices were submitted to TreeBASE: TB2: 29562 for nuITS and TB2: 29563 for the combined regions dataset.

Results

The nuITS matrix (478bp) comprised 55 sequences including 15 newly generated sequences for new species and new records. The combined regions dataset (478bp for 43 nuITS sequences; 740bp for 27 mtSSU sequences; 899bp for 33 nuLSU sequences; 755bp for 23 β-tubulin sequences) comprised 126 terminals, including 31 newly generated sequences (Table 2). In the two phylogenetic analyses, eight representative monophyletic genera (*Acolium* (Ach.) Gray, *Amandinea*, *Buellia* s.str., *Calicium* Pers., *Diplotomma*, *Pyxine* Fr., *Tetramelas*, *Thelomma* A. Massal.) were selected from Caliciaceae Chevall. and six Physciaceae Zahlbr. species were selected as the outgroup. The results of the phylogenetic analyses showed that the species in the *Buellia epigaea*-group formed two clades (Figs 1, 2).

In clade 1: *B. dijiana*, *B. georgei* and *B. epigaea* formed an independent clade with strong support (100% BS and 1.00 PP in Figs 1, 2). The specimens designated as *B. epigaea* (including one sequence from GenBank) clustered as a single lineage with high support (96% BS and 1.00 PP in Fig. 1). These specimens had identical morphological and chemical characters to those described for *B. epigaea*, and thus have been confirmed as a new record for China.

In clade 2: specimens here described as *B. alpina* formed a well-supported sister clade to *B. zoharyi* (100% BS and 1.00 PP in Figs 1, 2). These two species are distinctively different in their anatomical and chemical characteristics. We therefore recognize *B. alpina* as a new species within *Buellia epigaea*-group. The collections designated as *B. elegans* also formed a highly supported monophyletic lineage, clustering with sequences downloaded from GenBank (96% BS and 1.00 PP in Fig. 1). This constitutes the first record of *B. elegans* from China. These three species (*B. zoharyi*, *B. alpina* and *B. elegans*) formed a monophyletic clade with strong support (100% BS and 1.00 PP in Figs 1, 2). Clade 2 was sister to the genus *Tetramelas* (previously included in *Buellia* s.l.), which also contains alpine terricolous species.

Table 2. Specimens used in this study, with taxon name, voucher and GenBank accession number. Newly obtained sequences are in bold font. "*" indicates that the sample was not included in the combined regions' dataset analysis. "NA" indicates that there is no sequence available.

Taxon	Voucher	Accession number			
		nuITS	**mtSSU**	**nuLSU**	**β-tubulin**
Acolium inquinans	Wedin 6352 (UPS)	AY450583	AY143404	AY453639	KX529023
Ac. karelicum	Hermansson 16472 (UPS)	KX512897	NA	KX512879	NA
Amandinea punctata 1	18-60759 (KUN)	OL467351	NA	NA	NA
Am. punctata 2	AFTOL 1306	HQ650627.1	NA	DQ986756.1	NA
Buellia alpina	**16-53720 (KUN)**	**OM914626**	NA	NA	NA
B. alpina	**16-53737 (KUN)**	**OM914627**	NA	**OP060154**	**OM925561**
B. dijiana	-	AF250788	NA	NA	NA
B. disciformis 1	EDNA09-01524	FR799139	NA	NA	NA
B. disciformis 2	EDNA09-02095	FR799136	NA	NA	NA
B. disciformis 3	EDNA09-02116	FR799138	NA	NA	NA
B. elegans	**18-60340 (KUN)**	**OM914622**	NA	**OM935566**	**OM925559**
B. elegans	**20-68266 (KUN)**	**OM914634**	NA	**OM935569**	**OM925562**
B. elegans	**XY19-272 (KUN)**	**OM914624**	NA	**OM935567**	**OM925560**
B. elegans	**18-59513 (KUN)**	**OM914623**	NA	NA	NA
**B. elegans*	**18-62336 (KUN)**	**OM914630**	/	/	/
**B. elegans*	**XY19-1907 (KUN)**	**OM914632**	/	/	/
**B. elegans*	**XY19-1372 (KUN)**	**OM914631**	/	/	/
**B. elegans*	**XY19-2308 (KUN)**	**OM914633**	/	/	/
**B. elegans*	**12-34754 (KUN)**	**OM914625**	/	/	/
**B. elegans*	**10-0089 (KUN)**	**OM914636**	/	/	/
**B. elegans*	16-0084 (NXAC)	MN103116	/	/	/
**B. elegans*	Beck 242 (GZU)	AY143411	/	/	/
**B. elegans*	Leavitt 19085	MZ922074	/	/	/
B. epigaea	**XY19-1218 (KUN)**	**OM914628**	**OM913210**	**OM935568**	NA
B. epigaea	**XY19-2294 (KUN)**	**OM914629**	**OM913211**	NA	NA
**B. epigaea*	-	AF250785	/	/	/
**B. epigaea*	**18-59162 (KUN)**	**OM914635**	/	/	/
B. georgei	Trinkaus 356a (GZU)	AJ421416	NA	NA	NA
B. zoharyi 1	SA2	MG592314	MG592321	MG592328	MG592346
B. zoharyi 2	MT30	MG592315	MG592322	MG592329	MG592347
B. zoharyi 3	SA6	MG592316	MG592323	MG592330	MG592348
B. zoharyi 4	TE13	MG592317	MG592324	MG592331	MG592349
Calicium nobile 1	Tibell 21968 (UPS)	KX512913	KX512988	KX529070	NA
C. nobile 2	Tibell 23396 (UPS)	KX512914	KX512987	KX529071	NA
Diplotomma alboatrum 1	**18-60034 (KUN)**	MN615696	OL467286	OL444781	**OM925557**
Di. alboatrum 2	**18-60448 (KUN)**	MZ224658	OL467287	OL444782	**OM925558**
Di. venustum 1	**18-58557 (KUN)**	OL467349	OL467284	OL444779	**OM925555**
Di. venustum 2	**18-58102 (KUN)**	OL467350	OL467285	OL444780	**OM925556**
* *Di. venustum* 3	XY19-252 (KUN)	OL467353	/	/	/
Heterodermia speciosa	Wetmore (S)	KX512927	KX512975	KX512868	KX529000
He. vulgaris	Frisch 11/Ug1226 (UPS)	KX512928	KX512989	KX512857	NA
Phaeophyscia ciliata	Prieto (S)	KX512929	KX512958	KX512886	KX529012
Ph. orbicularis	Prieto 3012 (S)	KX512930	KX512967	KX512876	NA
Physcia aipolia	Wedin 6145 (UPS)	KX512931	AY143406	AY300857	KX529021
P. tenella	Odelvik and Hellström 0827 (S)	KX512932	KX512974	KX512869	NA
Pyxine coccoes	Prieto (S)	KX512936	KX512964	NA	KX529010
Py. subcinerea	-	HQ650705	NA	DQ883802	NA
Py. sorediata	Wetmore 91254 (S)	KX512937	KX512973	KX512870	KX529001
Tetramelas chloroleucus	Westberg 10–001 (S)	KX512938	NA	KX512875	KX529006

Taxon	Voucher	Accession number			
		nuITS	mtSSU	nuLSU	β-tubulin
Te. geophilus	**20-67496 (KUN)**	OL467354	OL467291	OL444785	**OM925563**
Te. pulverulentus	Nordin 6368 (UPS)	KX512940	KX512983	KX512860	KX528990
Thelomma mammosum 1	Tibell 23775 (UPS)	KX512942	KX512954	KX512888	KX529016
Th. mammosum 2	Hernández et al. 2002 (UPS)	KX512943	KX512953	KX512851	KX529017
Th. santessonii 1	Nordin 4011 (UPS)	KX512944	KX512951	KX512889	NA
Th. santessonii 2	Nash 38262 (UPS)	KX512945	KX512950	KX512890	NA

Discussion

Although species in *Buellia epigaea*-group share common characters, there are still additional diagnostic traits which could be used to distinguish between species within this group. The monophyletic clade 1 is formed by *B. dijiana* and *B. georgei*, together with *B. epigaea*. These three species share the characters of having no distinct marginal lobes and lacking atranorin. Within clade 1, only *B. georgei* has effigurate thalli; it also has short marginal lobes which often form rosettes. Both *B. georgei* and *B. dijiana* contain arthothelin acid and were described from Australia. However, their habitat differs: *B. georgei* occurs primarily on soft limestone or calcareous outcrops but never directly on calcareous soil, whereas *B. dijiana* is present on soil in open mallee vegetation (Trinkaus et al. 2001). In contrast, *B. epigaea* lacks secondary metabolites and could be reliably recognized by its crusty thallus, which is often uneven to wrinkled.

We propose a new species: *Buellia alpina*. It was clustered with *B. zoharyi* and *B. elegans* within clade 2. The common features of clade 2 are: having slim effigurate thalli covered with granulose pruina, obvious marginal lobes and always containing atranorin. The most distinctive features of the new species *B. alpina* are: heavily white pruinose apothecia and four-spored asci. *B. elegans* is similar to *B. zoharyi* in its external morphology. However, *B. elegans* can still be reliably distinguished from *B. zoharyi*, based on the ornamentation of ascospores. *B. elegans* has a loosely regulate surface (Fig. 3B and Fig. 4B), whereas the surface of *B. zoharyi* is microfoveate (Fig. 3G). In addition, the two species differ in their secondary metabolites: *B. zoharyi* contains atranorin, stictic acid and norstictic acid, while *B. elegans* has four chemotypes (Trinkaus and Mayrhofer 2000). One of these chemotypes (atranorin and 2'-O-methylperlatolic acid) is widely distributed in Asia, and was detected in most of the specimens from Yunnan, Qinghai and Xizang Provinces, China.

In addition to the species discussed above, *Buellia epigaea*-group also contains the species *B. asterella* and *B. lobata*. These have not been included in this phylogenetic study due to the lack of available sequences. Morphologically, *B. asterella* and *B. lobata* are similar to *B. alpina* in their possession of four mature ascospores within each ascus (Trinkaus and Mayrhofer 2000; Trinkaus et al. 2001). *B. alpina* differs from these two species by its heavily white pruinose apothecia, granular pruina on the thallus surface and atranorin content. Furthermore, *B. alpina* has *Callispora*-type ascospores (with lateral (subapical) thickening, always with tapering ends). However, *B. asterella* and *B. lobata* both have fine pruina on their thallus surface and *Buellia*-type ascospores

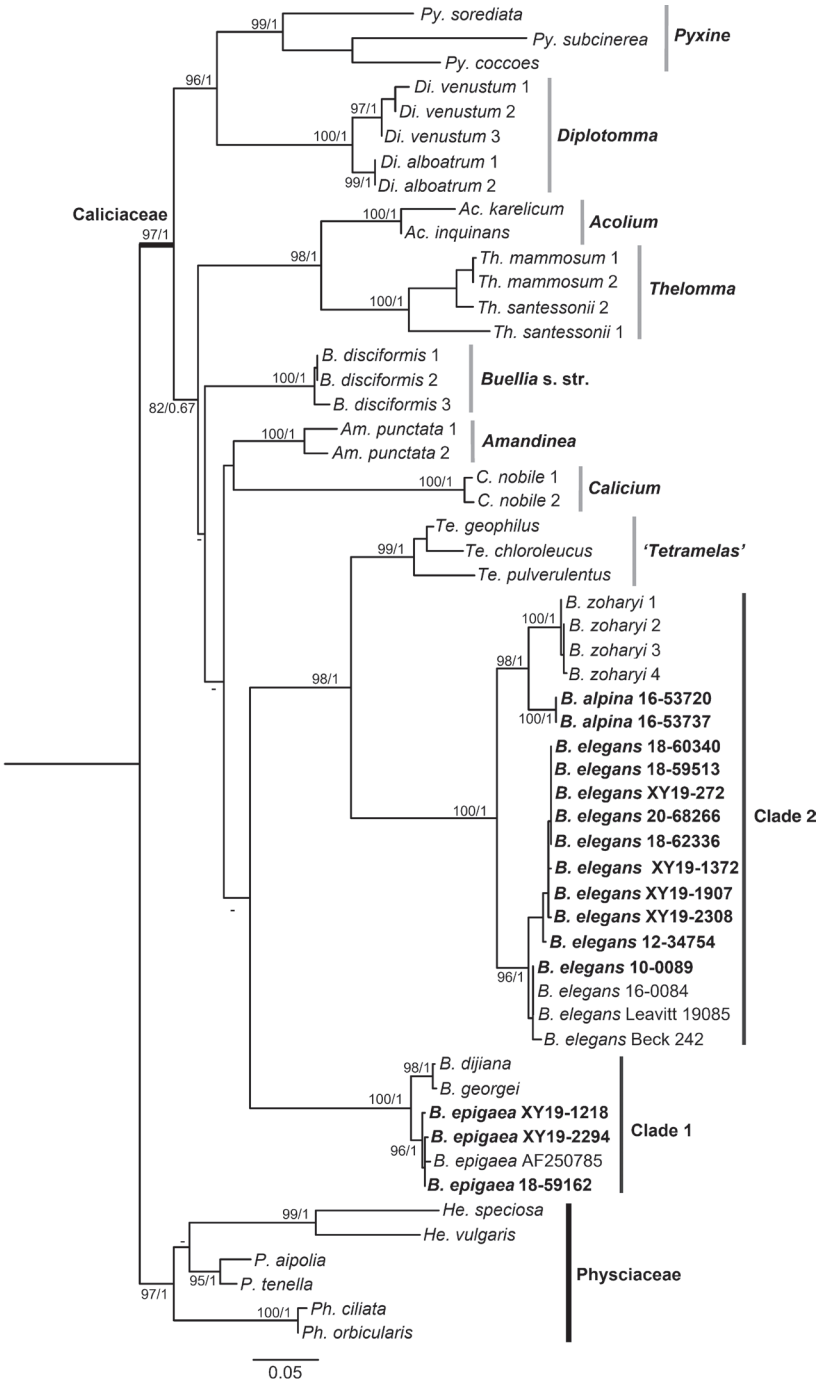

Figure 1. Phylogenetic relationships of Caliciaceae based on a Maximum Likelihood analysis of the nuITS matrix. Species positioned in clade 1 and clade 2 belong to the *Buellia epigaea*-group. Maximum Likelihood bootstrap values and posterior probabilities are shown near the nodes. New species and records are shown in bold.

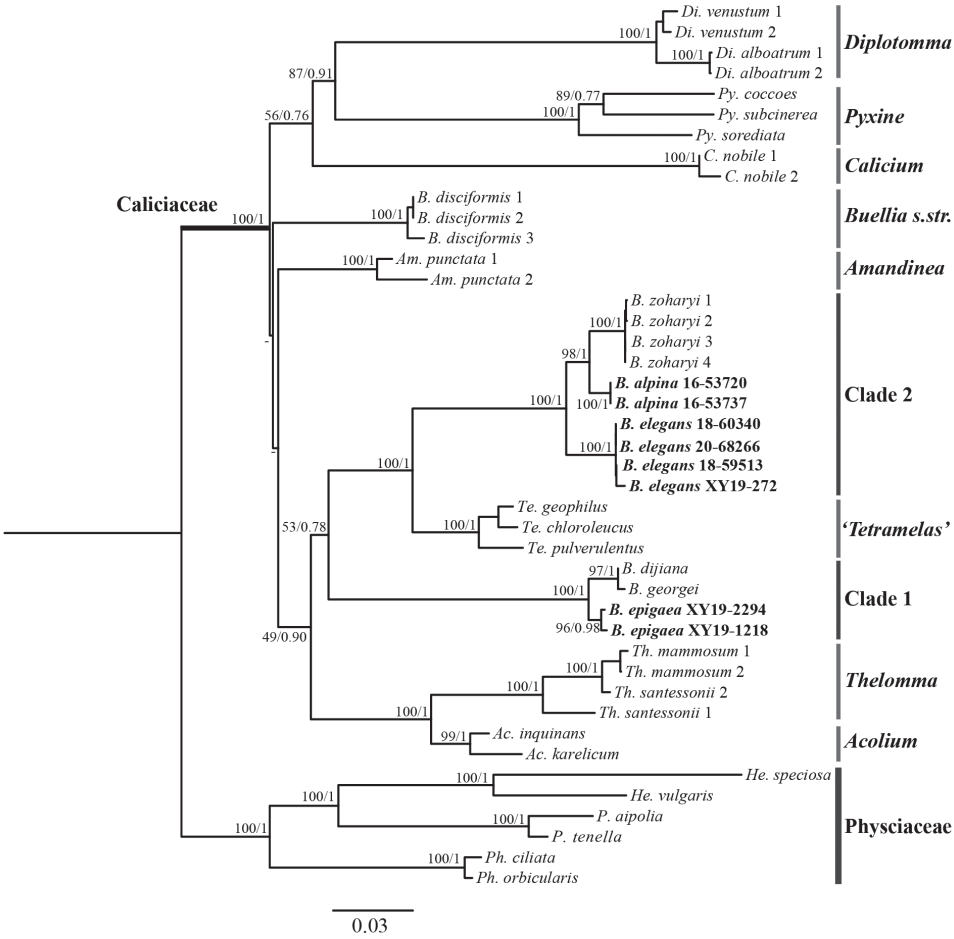

Figure 2. Phylogenetic relationships within Caliciaceae, based on a Maximum Likelihood analysis of a combined regions dataset (nuITS-nuLSU-mtSSU-β-tubulin). Species positioned in clade 1 and clade 2 belong to the *Buellia epigaea*-group. Maximum Likelihood bootstrap values and posterior probabilities are shown near the nodes. New species and records are shown in bold.

(lacking distinct wall thickening). *B. asterella* contains atranorin, norstictic acid and trace quantities of stictic acid, whereas *B. lobata* contains atranorin and thuringione.

The *Buellia* species in this study have all been classified as belonging to the *Buellia epigaea*-group, based on their terricolous habitat and distinct morphological characters of white and effigurate thalli. However, the phylogenetic trees in this study suggest that this group is not monophyletic. Thus, the previous definition of *Buellia epigaea*-group may be artificial, without support from molecular data. Phylogenetic study of both a single region (nuITS) and combined regions (nuITS-nuLSU-mtSSU-β-tubulin) showed that both clades do not group together. Therefore, the fundamental concept of the *Buellia epigaea*-group requires further research, including additional samples from across its global distribution.

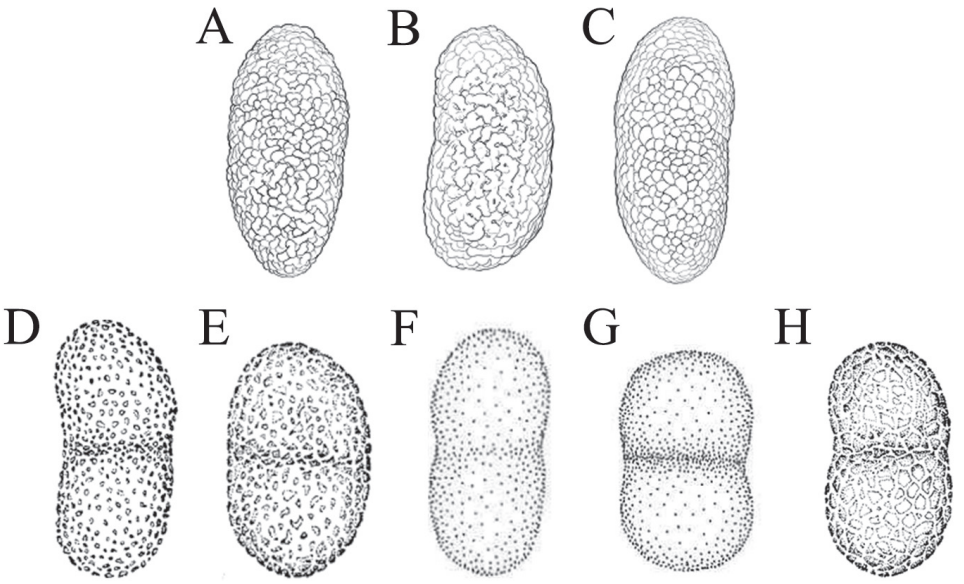

Figure 3. Ornamentation of ascospores **A** *Buellia alpina* **B** *Buellia elegans* **C** *Buellia epigaea* **D** *Buellia lobata* **E** *Buellia dijiana* **F** *Buellia asterella* **G** *Buellia zoharyi* **H** *Buellia georgei* (**A–C** were drawn by Qiu Yi Zhong **D–H** are from Trinkaus and Mayrhofer 2000; Trinkaus et al. 2001).

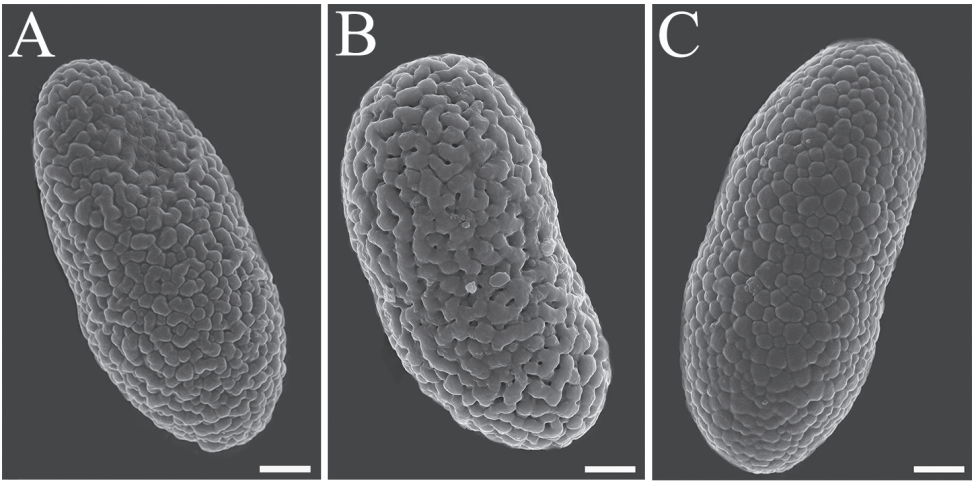

Figure 4. Ornamentation of ascospores (6000× magnification photograph under scanning electron microscope) **A** *Buellia alpina* **B** *Buellia elegans* **C** *Buellia epigaea* Scale bars: 2 μm (**A–C**).

In conclusion, species of *Buellia epigaea*-group share common characters which can be reliably recognized. There are distinct morphological and chemical differences which could be used to distinguish between different species in this group. Ornamentation of ascospores is a useful character by which to distinguish species in *Buellia epigaea*-group (Figs 3, 4; Table 3).

Table 3. Key characteristics of the *Buellia epigaea*-group.

Species	Thallus	Apothecia	Exciple	Spores	Ornamentation of spores	Major chemistry	Pycnidia	Parasitic fungi
B. alpina	effigurate, lobes linear, closely aggregate; covered with granulose pruina	flat, margin wavy and irregular	*dispersa*-type	*Callispora*-type; four-spored	densely rugulate, resulting in rough surface	atranorin	not seen	not seen
B. asterella	effigurate, lobes short and connected; surface with fine pruina	convex	*aethalea*-type	*Buellia*-type; often four well developed spores	microfoveate	atranorin, stictic acid, norstictic acid	rare	not seen
B. dijiana	not effigurate, crustose to granulose-squamulose; surface with fine pruina; dispersive	soon irregularly convex	*aethalea*-type	*Buellia*-type	warty, microrugulate	arthothelin	filiform conidia	rare
B. elegans	effigurate, lobes short to slender, multi-forked; covered with granulose pruina	flat to convex	*dispersa*-type	*Buellia*-type	Loosely rugulate, resulting in rough surface	a) atranorin; b) atranorin and 2'-O-methylperlatoric (in Asia)	not seen	common
B. epigaea	not effigurate, crusty, uneven to wrinkled; surface with fine pruina	flat	*aethalea*-type	*Callispora*-type	surface densely areolate and rough	no secondary metabolite	rare	rare
B. georgei	effigurate, marginal lobes short and often forming rosettes; surface with white granulose pruina	flat or sometimes slightly convex	*aethalea*-type	*Buellia*-type	surface densely areolate and rough	arthothelin	filiform conidia	common
B. lobata	effigurate, marginal lobes distinct but short, the tips of lobes dark; surface with lightly fine pruina	apothecia disc below margin	*aethalea*-type	*Buellia*-type; often four well developed spores	warty, microrugulate	arthothelin, thuringione	filiform conidia	common
B. zoharyi	effigurate, lobes obvious; covered with granulose pruina	flat to convex	*dispersa*-type	*Buellia*-type	microfoveate	atranorin, norstictic acid, stictic acid	common	rare

Taxonomy

Buellia alpina **Xin Y. Wang & Li S. Wang, sp. nov.**
MycoBank No: 843376
Fig. 5

Diagnosis. The species is distinguished from its closest relatives *B. elegans* and *B. zoharyi* by its linear lobate thallus, heavily pruinose apothecia and lobes, *Callispora*-type ascospores and four-spored asci.

Type. China. Xizang Prov.: Lasa Ci., Namucuo Nature Reserve, on soil beside a lake, 30°46'46"N, 90°52'24"E, alt. 4730 m, 28 Sep. 2016, L.S. Wang et al. 16-53720 (KUN-Holotype; SDNU-Isotype).

Description. Thallus effigurate, lobate and linear, lobes tightly aggregated, 0.5–1.5 mm wide, prothallus absent; upper surface white to grayish white, dull, covered with granulose pruina; medulla white, non-amyloid (I–). Apothecia sparse to dense, sometimes aggregate, adnate to the thallus, lecideine, margin covered with white pruina

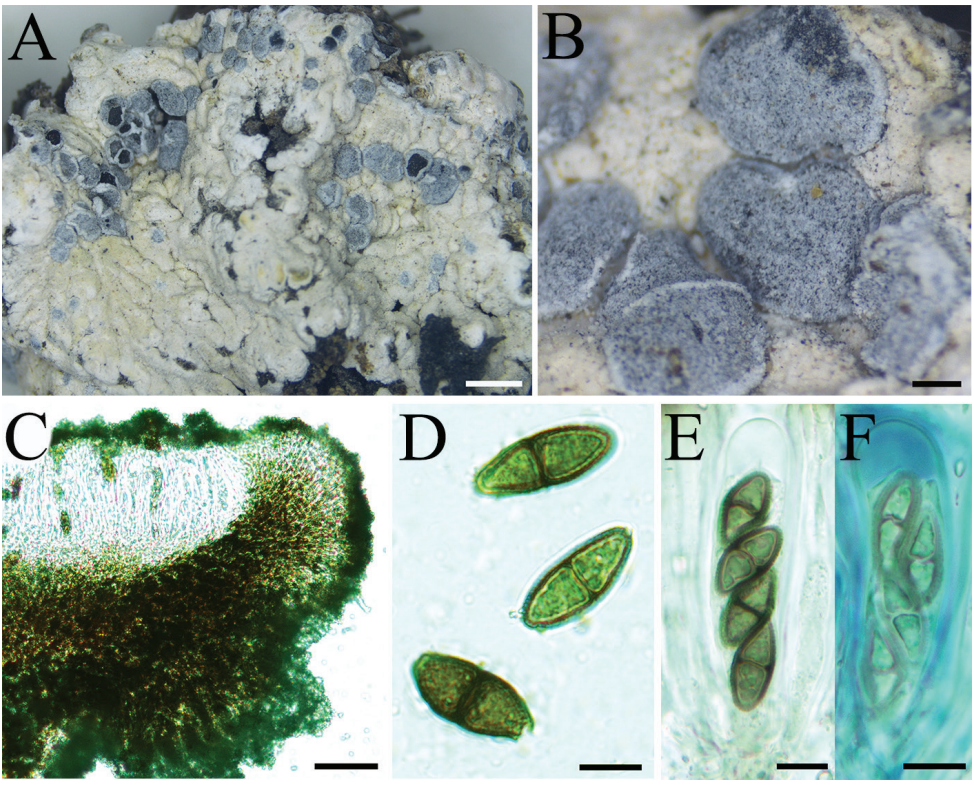

Figure 5. Morphology of *Buellia alpina* (16-53720 KUN) **A** thallus on soil within meadow **B** black lecideine apothecia covered with white pruina **C** the section of apothecium, exciple *dispersa*-type **D** ascospores with 1-septate, *Callispora*-type, with tapered ends **E** mature ascus containing four spores, *Bacidia*-type **F** young ascus containing four spores. Scale bars: 2 mm (**A**); 0.5 mm (**B**); 50 µm (**C**); 10 µm (**D–F**).

which resemble lecanorine apothecia; disc black, roundish, (0.3–)0.5–1.4(–1.6) mm in diam., heavily pruinose, roundish when immature, marginal part becoming wavy and irregular when mature; margin persistent; exciple *dispersa*-type (Bungartz et al. 2007), dark brown, without aeruginose pigments (HNO_3–); epihymenium brown to dark brown; hymenium hyaline, 80–100 µm tall, without oil droplets, paraphyses simple to moderately branched, apically swollen, with a brown pigment cap; hypothecium dark brown; asci oval-clavate, *Bacidia*-type, four-spored; spores 1-septate, hyaline when young, turning brown when mature, *Callispora*-type (Bungartz et al. 2007), ellipsoid, with tapering ends, proper septum narrow, not thickening during spore ontogeny, (13–)15–20(–22) × (6–)7–9(–10) µm. Pycnidia not seen.

Chemistry. Thallus K+ yellow, C–, PD–, UV–, medulla I–; containing atranorin.

Distribution and ecology. This species is mainly distributed in alpine meadows of the Tibetan Plateau, growing on soil within meadows, between elevations of 4700–5000 m.

Etymology. The epithet "*alpina*" refers to the alpine distribution of this species.

Note. This new species could be distinguished from all other *Buellia* species by its linear lobate thallus, covered with granulose pruina, black lecideine apothecia

with heavy whitish pruina, four-spored asci and its alpine distribution. It might be misidentified as subsquamulose or subfoliose species of *Squamarina* Poelt, but could be distinguished by the white thickened edges and hyaline simple ascospores.

Specimens examined. China. **Xizang Prov.**: Lasa Ci., Namucuo Nature Reserve, on soil beside a lake, 30°46'46"N, 90°52'24"E, alt. 4730 m, 28 Sep. 2016, L.S. Wang et al.16-53737.

Buellia elegans Poelt, Nova Hedwigia 25(1–2): 184–186 (1974)

Fig. 6

Type. Italy. Ad terram calcaream supra Clavennam (Madèsimo), Anzi M. (M! -Holotype).

Description. Thallus effigurate with distinct marginal lobes slim, 0.5–1 mm wide, the edge usually separated from the substrate and clearly foliaceous, thallus radiate, 1–2 cm in diam., prothallus absent; upper surface white, dull, usually covered with granular pruina; the upper cortex about 20 μm thick, with granular crystals, and the lower surface light

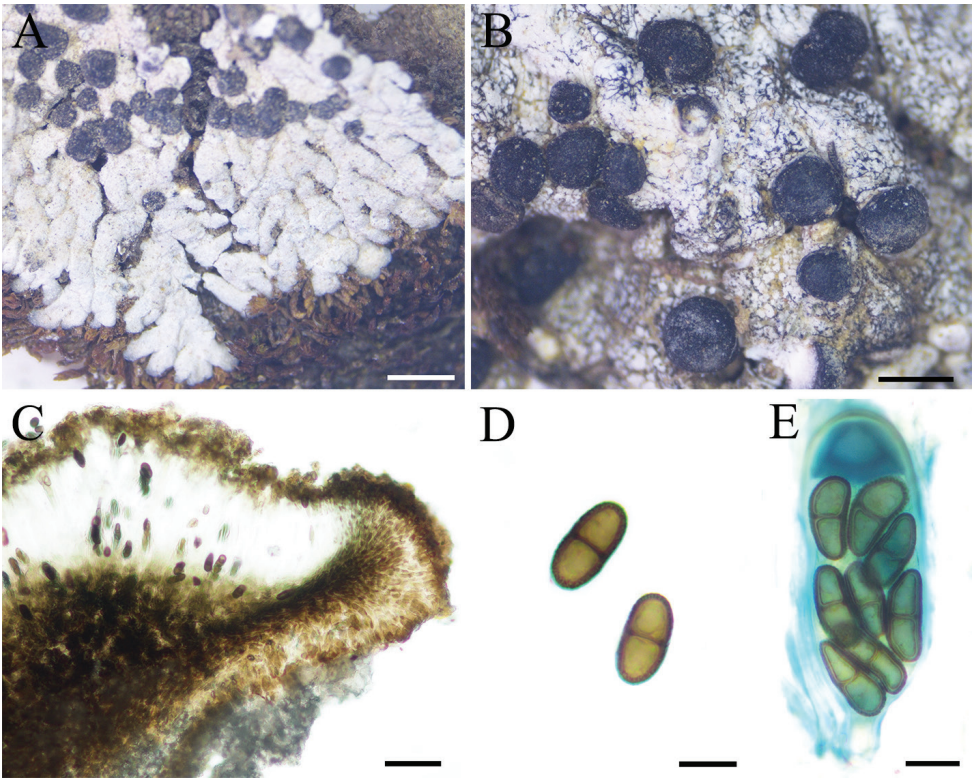

Figure 6. Morphology of *Buellia elegans* (16-51770 KUN) **A** thallus on soil within meadow **B** lecideine apothecia **C** the section of apothecium, exciple *dispersa*-type **D** ascospores with 1-septate, *Buellia*-type **E** mature ascus containing eight spores, *Bacidia*-type. Scale bars: 2 mm (**A**); 1 mm (**B**); 50 μm (**C**); 10 μm (**D, E**).

brown to white, without cortex; medulla white, without calcium oxalate crystals. Apothecia sparse, lecideine; disc and margin black, sometimes lightly pruinose, roundish, 0.3–1.0 mm in diam., immersed and smooth when young but adnate and convex when mature; margin persistent; exciple thick, *dispersa*-type, without aeruginose pigments (HNO_3–); epihymenium brown to dark brown; hymenium hyaline, 70–90 μm tall, without oil droplets, paraphyses simple to moderately branched, apically swollen, with a brown pigment cap; hypothecium dark brown; asci oval-clavate, *Bacidia*-type, eight-spored; spores 1-septate, hyaline when young, turning brown when mature, *Buellia*-type, ellipsoid, not thickening during spore ontogeny, 15–22 × 7–10 μm. Pycnidia not seen.

Chemistry. Thallus K+ yellow, C–, KC–, PD–, UV+ yellow, medulla I–; containing atranorin and norstictic acid (trace) or atranorin and 2'-O-methylperlatolic acid.

Distribution and ecology. This species is mainly distributed in open and dry soil or soil over rock or within meadows between elevations of 1400–4730 m. This species has been recorded in Asia, Afghanistan, Europe and North America (Thomson, 1997). In China, it is mainly distributed in Gansu, Ningxia, Qinghai, Xizang and Yunnan Provinces.

Note. This is a new record for China, and is unique among species of *Buellia* due to its effigurate thallus, marginal lobes linear and slim, branched near the tips. It resembles folicolous species of *Physconia* Poelt, but could be differentiated by its slim lobes and lack of lower surface. It has a wide distribution across the Tibetan Plateau, especially in arid deserts and meadows. Four chemotypes of the species were previously reported (Trinkaus and Mayrhofer 2000). Only two chemotypes have been detected in Chinese materials: atranorin and 2'-O-methylperlatolic acid account for the majority, atranorin and norstictic acid (trace) constitute only a small proportion.

Selected specimens examined. China. **Gansu Prov.:** Jiayuguan Ci., Xigou, mineral, on soil, 39°39'34"N, 97°56'15"E, alt. 2198 m, 28 May 2018, L.S. Wang et al. 18-59611; Yumen Ci., meadow along the route from Yumen to Yuerhong, on soil, 39°57'45"N, 96°39'23"E, alt. 2395 m, 27 May 2018, L.S. Wang et al. 18-59513. **Ningxia Prov.:** Zhongwei Ci., Shanpotou, Mengjiawan, on soil, 37°36'12"N, 104°55'06"E, alt. 1403 m, 18 Sep. 2010, D.L. Niu et al. 10-0089. **Qinghai Prov.:** Wulan Co., desert along the route from Wulan to Delingha, on soil, 37°02'08"N, 98°12'29"E, alt. 3072 m, 20 May 2018, L.S. Wang et al. 18-58303; Dulan Co., Xiangjia Vil., on sandy rock, 36°00'53"N, 97°44'36"E, alt. 3056 m, 15 Sep. 2020, L.S. Wang et al. 20-68266. **Xizang Prov.:** Dazi Dis., Bangdui Vil., on soil, 29°44'06"N, 91°24'55"E, alt. 3709 m, 16 Jul. 2019, L.S. Wang et al. 19-64615; Basu Co., beside Ranwu Lake, on soil over rock, 29°23'34"N, 96°50'20"E, alt. 3901 m, 15 Jul. 2019, X.Y. Wang et al. (XY19-278; XY19-272); Geji Co., beside S301 road, on soil, 32°14'47"N, 82°10'27"E, alt. 4514 m, 21 Jul. 2019, L.S. Wang et al. 19-63808; Bomi Co., along the route to Basu Co., on soil, 29°40'31"N,96°12'38"E, alt. 2920 m, 10 Nov. 2018, L.S. Wang et al. 18-62336; Langkazi Co., Simila Mt., on soil over rock, 28°50'37"N, 89°51'54"E, alt. 4343 m, 24 Jul. 2019, X.Y. Wang et al. XY19-1372; Sangri Co., Sangri Town, on soil over rock, 29°17'29"N, 92°05'30"E, alt. 3595 m, 30 Jul. 2019, X.Y. Wang et al. (XY19-1899; XY19-1907); Jangzi Co., Simila Mt., on soil over rock, 28°50'30"N, 89°51'48"E, alt. 4223 m, 24 Jul. 2019, X.Y. Wang et al. XY19-2308; Jiangda Co., Kakong Vil., on soil over rock, 31°20'22"N, 98°08'01"E, alt. 3785 m, 23 Sep. 2020, L.S. Wang et al.

20-68931. **Yunnan Prov.:** Deqin Co., Benzilan Vil., on soil over rock, 28°10'27"N, 99°22'53"E, alt. 2007 m, 26 Sep. 2020, L.S. Wang et al. 20-69241; Deqin Co., Benzilan Vil., beside JinSha river, on soil, 28°11'36"N, 99°21'08"E, alt. 2108 m, 19 Aug. 2018, L.S. Wang et al. 18-60340; Deqin Co., Benzilan Vil., on soil, 28°13'38"N, 99°19'20"E, alt. 2110 m, 3 Jul. 2012, L.S. Wang et al. 12-34754.

***Buellia epigaea* (Pers.) Tuck. Gen. lich.: 185 (1872)**
Fig. 7

Type. Germany. Hesse, ad terram inter muscos non procul a Monte Meissner, 1794, Persoon (H-Ach-Isotype, not seen).

Description. Thallus terricolous, tightly attached to the substrate, upper surface white or greyish white, usually with white fine pruina, thallus crusty, uneven to wrinkled, 0.2–1 mm thick, prothallus absent; the upper cortex 60–150 μm thick, with granular crystals, pith completely interspersed with Ca oxalate crystals; medulla white. Apothecia sparse to dense, lecideine, but usually surrounded by a thalline collar (pseudolecanorine); disc black, always with finely white pruina, roundish, 0.5–1.0 mm in diam., mostly flat, rarely slightly convex; young apothecia immersed and margin with finely white pruina breaking out broadly, mature apothecia adnate and margin absent or not obvious; exciple *aethalea*-type, up to 50 μm thick, without aeruginose pigments (HNO_3–); epihymenium brown to dark brown; hymenium hyaline, 60–80 μm tall, without oil droplets, paraphyses simple to moderately branched, apically swollen, with a brown pigment cap; hypothecium hyaline to light brown, up to 100 μm high; asci oval-clavate, *Bacidia*-type, eight-spored; spores 1-septate, hyaline when young, turning brown when mature, with tapering ends, *Callispora*-type, often curved, not thickening during spore ontogeny, 12–20 × 6–10 μm. Pycnidia not seen.

Chemistry. Thallus K–, C–, KC–, PD–, UV–; without secondary metabolites.

Distribution and ecology. This species mainly occurs on open and dry soil, soil within meadows or on soil over rock, between elevations of 2300–4700 m. This species has been recorded in Asia, Europe and North America (Trinkaus and Mayrhofer 2000). In China, it is mainly distributed in Gansu, Qinghai and Xizang Provinces.

Note. The species is a new record for China; it could be distinguished from all the other terricolous *Buellia* species reported in China by the combination of the following characteristics: thallus white crustose, uneven to wrinkled, always covered by finely white pruina, apothecia pseudolecanorine, the ornamentation of the ascospore surface densely areolate and rough, pycnidia rare, *Callispora*-type ascospores and absence of secondary metabolites. This species is close to *Tetramelas* species in phylogeny and similar in morphology, but could be distinguished by absence of the secondary metabolites 6-O-methylarthothelin or related xanthones, and pseudolecanorine apothecia covered with white pruina.

Selected specimens examined. China. **Gansu Prov.:** Sunan Co., along the route from Linze to Sunan, on soil over rock, 38°52'26"N, 99°44'21"E, alt. 2294 m, 29 May 2018, L.S. Wang et al. 18-58766; Sunan Co., along the route from Linze to Sunan, on soil over rock, 38°52'47"N, 99°43'57"E, alt. 2296 m, 29 May 2018, L.S. Wang et al. 18-59699. **Qinghai Prov.:** Gonghe Co., meadow beside Qinghai Lake, on soil within

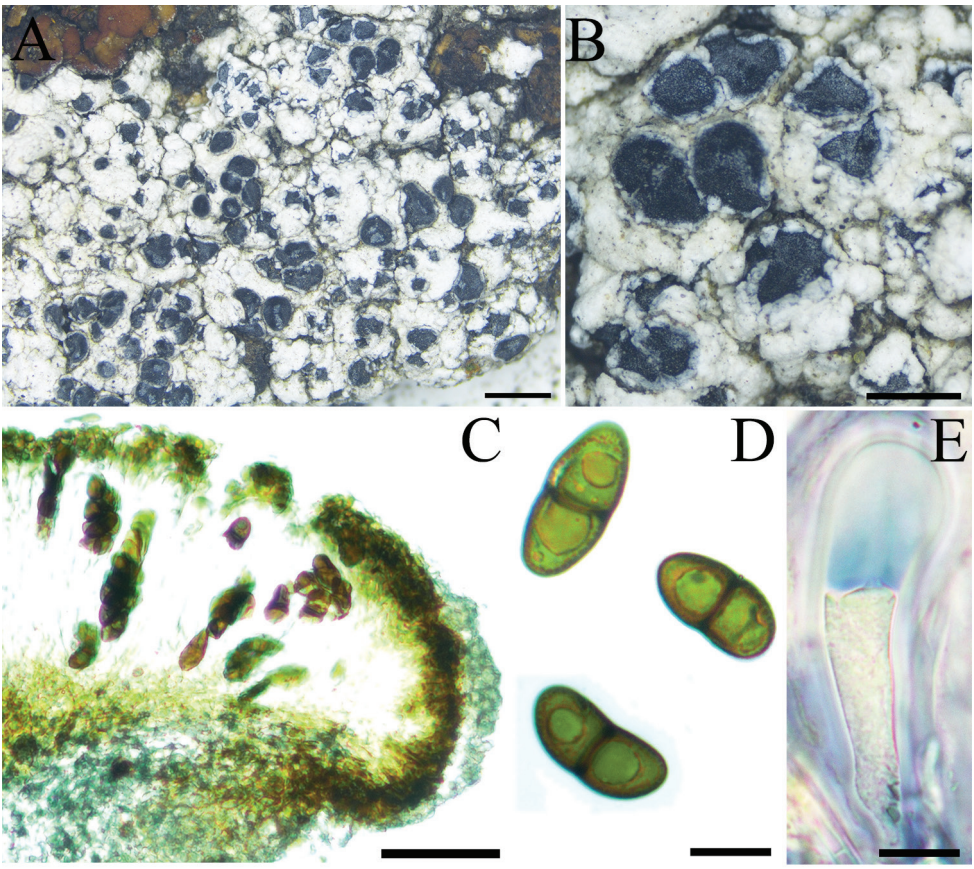

Figure 7. Morphology of *Buellia epigaea* (XY19-2294 KUN) **A** thallus growing on the soil **B** lecideine apothecia with white pruina, surrounded by a thalline collar (pseudolecanorine) **C** the section of apothecium, exciple *aethalea*-type **D** ascospores with 1-septate, *Callispora*-type **E** ascus *Bacidia*-type. Scale bars: 2 mm (**A**); 1 mm (**B**); 50 μm (**C**); 10 μm (**D, E**).

meadow, 36°33'26"N, 100°28'45"E, alt. 3431 m, 18 May 2018, L.S. Wang et al. 18-59162. **Xizang Prov.:** Qushui Co., Niedang Vil., on soil, 29°30'24"N, 90°56'17"E, alt. 3527 m, 22 Jul. 2019, X.Y. Wang et al. XY19-1234; Qushui Co., Niedang Vil., on soil over rock, 29°30'22"N, 90°56'15"E, alt. 3624 m, 22 Jul. 2019, X.Y. Wang et al. XY19-1218; Langkazi Co., entrance to Karuola Glacier, on soil over rock, 28°53'54"N, 90°13'32"E, alt. 4774 m, 24 Jul. 2019, X.Y. Wang et al. XY19-2294.

Key to species of *Buellia epigaea*-group

1 Thallus effigurate and marginal lobes long and obvious; containing atranorin **2**

– Thallus either not effigurate or effigurate but with marginal lobes short and closely aggregate; lacking atranorin **4**

2 Ascus four-spored ..... ***Buellia alpina***
– Ascus eight-spored **3**
3 Spores large, up to 23 μm long, ornamentation of spores rugulate ..... ***Buellia elegans***
– Spores smaller, less than 17 μm long, ornamentation of spores microfoveate. ..... ***Buellia zoharyi***
4 Thallus not effigurate **5**
– Thallus effigurate, usually with short lobes **6**
5 Thallus crustose to granulose-squamulose; containing arthothelin..... ***Buellia dijiana***
– Thallus crusty, uneven to wrinkled; lacking secondary metabolites..... ***Buellia epigaea***
6 On rock; ascus eight-spored; marginal lobes forming rosettes..... ***Buellia georgei***
– On soil; usually four mature spores in each ascus 7
7 Containing atranorin and thuringione; ornamentation of spores warty, microrugulate..... ***Buellia lobata***
– Containing atranorin, norstictic acid and stictic acid (trace); ornamentation of spores microfoveate..... ***Buellia asterella***

Acknowledgements

We express our sincere thanks to the M herbarium for providing type specimens and digital images. This study was supported by grants from the Flora Lichenum Sinicorum (31750001), the Second Tibetan Plateau Scientific Expedition and Research Program (STEP) (2019QZKK0503), Youth Innovation Promotion Association CAS (2020388), Yunnan Young & Elite Talents Project, National Natural Science Foundation of China (31970022) and State Key Laboratory of Phytochemistry and Plant Resources in West China (P2020-KF08).

References

Bungartz F, Nordin A, Grube M (2007) *Buellia*. In: Nash TH III, Gries C, Bungartz F (Eds) Lichen Flora of the Greater Sonoran Desert Region. Volume 3. Lichens Unlimited, Arizona State University, Tempe, 113–179.

Gardes M, Bruns TD (1993) ITS primers with enhanced specificity for basidiomycetes. Application for the identification of mycorrhizae and rusts. Molecular Ecology 2(2): 113–118. https://doi.org/10.1111/j.1365-294X.1993.tb00005.x

Grube M, Arup U (2001) Molecular and morphological evolution in the Physciaceae (Lecanorales, lichenized Ascomycotina), with special emphasis on the genus *Rinodina*. Lichenologist 33(1): 63–72. https://doi.org/10.1006/lich.2000.0297

Guindon S, Dufayard JF, Lefort V, Anisimova M, Hordijk W, Gascuel O (2010) New algorithms and methods to estimate maximum-likelihood phylogenies: Assessing the performance of PhyML 3.0. Systematic Biology 59(3): 307–321. https://doi.org/10.1093/sysbio/syq010

Katoh K, Kuma K, Toh H, Miyata T (2005) MAFFT version 7, improvement in accuracy of multiple sequence alignment. Nucleic Acids Research 33(2): 511–518. https://doi.org/10.1093/nar/gki198

Lanfear R, Calcott B, Ho SY, Guindon S (2012) PartitionFinder: Combined selection of partitioning schemes and substitution models for phylogenetic analyses. Molecular Biology and Evolution 29(6): 1695–1701. https://doi.org/10.1093/molbev/mss020

Lanfear R, Frandsen PB, Wright AM, Senfeld T, Calcott B (2017) PartitionFinder 2: New methods for selecting partitioned models of evolution for molecular and morphological phylogenetic analyses. Molecular Biology and Evolution 34: 772–773. https://doi.org/10.1093/molbev/msw260

Marbach B (2000) Corticole und lignicole Arten der Flechtengattung *Buellia* sensu lato in den Subtropen und Tropen. Bibliotheca Lichenologica, 74, Cramer J, Berlin, Stuttgart, 384 pp.

Myllys L, Lohtander K, Tehler A (2001) Beta-tubulin, ITS and group I intron sequences challenge the species pair concept in *Physcia aipolia* and *P. caesia*. Mycologia 93: 335–343.

Orange A, James PW, White FJ (2001) Microchemical methods for the identification of lichens. British Lichen Society, London, 101 pp.

Nordin A (2000) Taxonomy and phylogeny of *Buellia* species with pluriseptate spores (Lecanorales, Ascomycotina). Symbolae Botanicae Upsalienses 33(1): 1–117.

Poelt J, Sulzer M (1974) Die Erdflechte *Buellia epigaea*, eine Sammelart. Nova Hedwigia 25: 173–194.

Rambaut A (2012) FigTree, version 1.4.0, Institute of Evolutionary Biology, University of Edinburgh. http://tree.bio.ed.ac.uk/software/figtree/

Rehner SA, Samuels GJ (1994) Taxonomy and phylogeny of *Gliocladium* analysed from nuclear large subunit ribosomal DNA sequences. Mycological Research 98(6): 625–634. https://doi.org/10.1016/S0953-7562(09)80409-7

Ronquist F, Teslenko M, van der Mark P, Ayres D, Darling A, Höhna S, Larget B, Liu L, Suchard MA, Huelsenbeck JP (2012) MrBayes 3.2: Efficient Bayesian phylogenetic inference and model choice across a large model space. Systematic Biology 61(3): 539–542. https://doi.org/10.1093/sysbio/sys029

Scheidegger C (1993) A revision of European saxicolous species of the genus *Buellia* De Not. and formerly included genera. Lichenologist 25(4): 315–364. https://doi.org/10.1006/lich.1993.1001

Stamatakis A (2006) RAxML-VI-HPC, Maximum likelihood-based phylogenetic analyses with thousands of taxa and mixed models. Bioinformatics 22(21): 2688–2690. https://doi.org/10.1093/bioinformatics/btl446

Talavera G, Castresana J (2007) Improvement of phylogenies after removing divergent and ambiguously aligned blocks from protein sequence alignments. Systematic Biology 56(4): 564–577. https://doi.org/10.1080/10635150701472164

Thomson JW (1997) American Arctic Lichens. 2. The Microlichens. The University of Wisconsin Press, Madison, Wisconsin.

Trinkaus U, Mayrhofer H (2000) Revision der *Buellia epigaea*-gruppe (lichenisierte Ascomyceten, Physciaceae). I Die Arten der Nordhemisphare. Nova Hedwigia 71(3–4): 271–314. https://doi.org/10.1127/nova/71/2000/271

Trinkaus U, Mayrhofer H, Elix JA (2001) Revision of the *Buellia epigaea*-group (lichenized ascomycetes, Physciaceae) 2. The species in Australia. Lichenologist 33(1): 47–62. https://doi.org/10.1006/lich.2000.0286

Vilgalys R, Hester M (1990) Rapid genetic identification and mapping of enzymatically amplified ribosomal DNA from several *Cryptococcus* species. Journal of Bacteriology 172(8): 4238–4246. https://doi.org/10.1128/jb.172.8.4238-4246.1990

Wang XY, Li LJ, Liu D, Zhang YY, Yin AC, Zhong QY, Wang SQ, Wang LS (2020) Two new species and six new records of *Buellia* s.l. (lichenized Ascomycota, Caliciaceae) from China. The Bryologist 123(3): 431–443. https://doi.org/10.1639/0007-2745-123.3.430

Wei JC (2020) The enumeration of lichenized fungi in China. China Forestry Press, Beijing.

White TJ, Bruns TD, Lee S, Taylor J (1990) Amplification and direct sequencing of fungal ribosomal DNA genes for phylogenetics. In: Innis MA, Gelfand DH, Sninsky JJ, White TJ (Eds) PCR protocols: a guide to methods and applications. Academic Press, San Diego, 315–321. https://doi.org/10.1016/B978-0-12-372180-8.50042-1

Zoller S, Scheidegger C, Sperisen C (1999) PCR primers for the amplification of mitochondrial small subunit ribosomal DNA of lichen-forming ascomycetes. Lichenologist 31(5): 511–516. https://doi.org/10.1006/lich.1999.0220

Supplementary material 1

Ornamentation of ascospores

Authors: Min Ai, Li Juan Li, Fiona Ruth Worthy, An Cheng Yin, Qiu Yi Zhong, Shi Qiong Wang, Li Song Wang, Xin Yu Wang

Data type: Images

Explanation note: **Figure S1**. Ornamentation of ascospores (6000× magnification photograph under scanning electron microscope). A–D *Buellia alpina*. Scale bars: 2 μm. **Figure S2**. Ornamentation of ascospores (6000× magnification photograph under scanning electron microscope). A–D *Buellia elegans*. Scale bars: 2 μm. **Figure S3**. Ornamentation of ascospores (6000× magnification photograph under scanning electron microscope). A–D *Buellia epigaea*. Scale bars: 2 μm.

Link: https://doi.org/10.3897/mycokeys.92.83939.suppl1

MycoKeys 92: 63–78 (2022)
doi: 10.3897/mycokeys.92.87593
https://mycokeys.pensoft.net

RESEARCH ARTICLE

A peer-reviewed open-access journal
MycoKeys
Launched to accelerate biodiversity research

New studies on *Apiospora* (Amphisphaeriales, Apiosporaceae): epitypification of *Sphaeria apiospora*, proposal of *Ap. marianiae* sp. nov. and description of the asexual morph of *Ap. sichuanensis*

Ángel Pintos[1*], Pablo Alvarado[2*]

1 *Interdisciplinary Ecology Group, Universitat de les Illes Balears, Ctra. Valldemossa Km 7,5, 07122 Palma de Mallorca, Spain* **2** *ALVALAB, Dr. Fernando Bongera st., Severo Ochoa bldg. S1.04, 33006 Oviedo, Spain*

Corresponding author: Pablo Alvarado (pablo.alvarado@gmail.com)

Academic editor: S. Maharachchikumbura | Received 9 June 2022 | Accepted 27 July 2022 | Published 23 August 2022

Citation: Pintos Á, Alvarado P (2022) New studies on *Apiospora* (Amphisphaeriales, Apiosporaceae): epitypification of *Sphaeria apiospora*, proposal of *Ap. marianiae* sp. nov. and description of the asexual morph of *Ap. sichuanensis*. MycoKeys 92: 63–78. https://doi.org/10.3897/mycokeys.92.87593

Abstract

In the present work, an epitype for *Sphaeria apiospora*, the basionym of the type species of the genus *Apiospora*, *Apiospora montagnei*, is selected among collections growing in the host plant species reported in the original protologue, *Arundo micrantha*. Most samples obtained from localities near that of the lectotype (Perpignan, France) belong to the same species, which is not significantly different from the clade previously named *Ap. phragmitis*, suggesting that this name is a later synonym of *Ap. montagnei*. In addition, the name *Ap. marianiae* is here proposed to accommodate a newly discovered species found in the Balearic Islands (Spain), and the asexual state of *Ap. sichuanensis* is described for the first time from samples growing in the same islands.

Keywords

Apiosporaceae, *Ascomycota*, *Sordariomycetes*

* These authors contributed equally.

Introduction

Apiospora Sacc. is the type genus of family *Apiosporaceae* K.D. Hyde, J. Fröhl., Joanne E. Taylor & M.E. Barr. It occurs worldwide, and includes important pathogens and saprophytes of animals, plants and seaweeds (Heo et al. 2018, Park et al. 2018, Wang et al. 2018, Kwon et al. 2021). Genus *Apiospora* was built around *Apiospora montagnei* Sacc. (Saccardo 1875), a replacement name for *Sphaeria apiospora* Durieu & Mont. (Bory de Saint-Vincent and Durieu de Maisonneuve 1849). For a long time, *Apiospora* was considered a sexual state of genus *Arthrinium* Kunze, and both were even formally synonymyzed by Crous and Groenewald (2013), but recently shown to represent independent clades and separated again by Pintos and Alvarado (2021). These authors concluded that although the morphology of the original collections of *S. apiospora* (≡ *Ap. montagnei*) does not allow to link them with a unique phylogenetic clade, they should nest inside the clade containing most other species with basauxically-generated rounded/lenticular conidia that occur mainly on Poaceae (but also many other plant families, seaweeds and animals) worldwide (including tropical and subtropical regions), and differ from species in the clade of *Arthrinium*, which have variously shaped conidia, a narrower host range (mainly, but not exclusively, Cyperaceae and Juncaceae), and occur in temperate, cold or alpine (but not tropical or subtropical) regions. This way, Pintos and Alvarado (2021) selected a lectotype for *S. apiospora* (≡ *Ap. montagnei*), and fixed the phylogenetic limits of *Apiospora*, proposing the necessary combinations at species rank. Later authors followed this approach (Crous et al. 2021; Tian et al. 2021), and genomic analyses seem to confirm their taxonomic decision (Sørensen et al. 2022). A third group of species formerly placed within *Arthrinium*, including *Ar. urticae* M.B. Ellis (Ellis 1965) and *Ar. trachycarpi* C.M. Tian & H. Yan (Yan et al. 2019), are probably unrelated to *Arthrinium* or *Apiospora* (Tang et al. 2021), and therefore deserve to be classified in a different genus.

Despite these important taxonomic changes, the exact identity of the type species of *Apiospora*, *Ap. montagnei*, still remains uncertain. Pintos and Alvarado (2021) discussed the host plants mentioned by Bory de Saint-Vincent and Durieu de Maisonneuve (1849), concluding that the lectotype (collected near Perpignan, France) was found on *Arundo micrantha* or *Aru. donaciformis*. Only four species of *Apiospora*, *Ap. iberica* (Pintos & P. Alvarado) Pintos & P. Alvarado, *Ap. italica* (Pintos & P. Alvarado) Pintos & P. Alvarado, *Ap. marii* (Larrondo & Calvo) Pintos & P. Alvarado and *Ap. phragmitis* (Crous) Pintos & P. Alvarado had been recorded in *Arundo* spp. (Pintos et al. 2019, Pintos and Alvarado 2021), but since *Ap. iberica* and *Ap. italica* are relatively rare, *Ap. marii* and *Ap. phragmitis* were considered the most probable synonyms of *Ap. montagnei* (Pintos and Alvarado 2021).

In the present work, several collections of *Apiospora* growing on *Arundo* aff. *micrantha* in northeastern Spain and the Balearic Islands were analyzed, and an epitype of *Ap. montagnei* selected among them to fix the identity of this species. In addition,

a newly discovered species found in the same region is described and given a new name, and the asexual state of *Ap. sichuanensis* Samarak., Jian K. Liu & K.D. Hyde is described for the first time.

Materials and methods

Isolates

Methods employed to isolate the sexual and asexual states are described in Pintos and Alvarado (2021). The samples were deposited in the fungarium of the Muséum National d´Histoire Naturelle (**PC**; Paris, France) and the Fungarium of the University of Vienna (**WU**; Vienna, Austria). Living cultures were deposited in Fungal collection at the Westerdijk Fungal Biodiversity Institute (**CBS**; Utrecht, The Netherlands).

Morphology

Samples were studied with a Zeiss Axioscope compound microscope operating with differential interference contrast (DIC). Images were obtained with a FLIR camera using open source software Microscopia Oberta (A. Coloma). Measurements were taken with FIJI win64 ImajeJ software, and reported as follows: maximum value in parentheses, range between the mean plus and minus the standard deviation, minimum value in parentheses, and the number of elements measured in parentheses. For some images of conidiophores, the image stacking software Zerene Stacker v. 1.04 (Zerene Systems LLC, Richland, WA, USA) was employed. Morphological descriptions were based on fertile cultures growing on 2% MEA (20 g/L malt extract, 20 g/L soy peptone, 15 g/L agar, pH 7) at room temperature.

Phylogenetic analysis

Total DNA was extracted from cultured isolates and dried fungarium specimens employing a modified protocol based on Murray and Thompson (1980). Amplification reactions (Mullis and Faloona 1987) included 35 cycles with an annealing temperature of 54 °C. Primers ITS1F and ITS4 (White et al. 1990, Gardes and Bruns 1993) were employed to amplify the ITS1-5.8S-ITS2 nrDNA region (ITS), while LR0R and LR5 (Vilgalys and Hester 1990, Cubeta et al. 1991) were used for the 28S nrDNA region (LSU), EF1-728F, EF1-983F and EF1-1567R (Carbone and Kohn 1999, Rehner and Buckley 2005) for the translation elongation factor 1 alpha (tef1) gene, and T1, Bt2a, and Bt2b (Glass and Donaldson 1995; O'Donnell and Cigelnik 1997) for the β-tubulin gene (tub2). PCR products were checked in 1% agarose gels, and positive reactions were sequenced with one or both PCR primers. Chromatograms were checked searching for putative reading errors in MEGA v. 5.0 (Tamura et al. 2011), and these were corrected.

A single alignment was made using: 1) ITS1-5.8S-ITS2 nrDNA, 2) 28S nrDNA, 3) tef1 region between 3' extreme of intron 1 and the 5' extreme of the exon between introns 2 and 3, and 4) tub2 region between intron 3 and the 5' extreme of the exon between introns 5 and 6. Homologous sequences of selected samples of *Apiospora* available in public databases (International Nucleotide Sequence Database Collaboration, INSDC, Arita et al. 2021) were included, adding also sequences of *Arthrinium* as outgroup. The sequences employed (Suppl. material 1) were mainly retrieved from Smith et al. (2003), Singh et al. (2012), Crous and Groenewald (2013), Crous et al. (2015, 2020), Senanayake et al. (2015), Dai et al. (2016, 2017), Wang et al. (2017, 2018), Jiang et al. (2018, 2019, 2020), Liu et al. (2019), Pintos et al. (2019), Yan et al. (2019), Yang et al. (2019), Senanayake et al. (2020), Pintos and Alvarado (2021), Kwon et al. (2021), Phukhamsakda et al. (2022) and Samarakoon et al. (2022). Sequences first were aligned in MEGA software with its Clustal W application and then corrected manually. Gblocks (Castresana 2000) was employed to remove 191 ambiguously aligned positions from ITS rDNA, resulting in a final alignment with 188/463/82 (ITS rDNA), 126/786/64 (28S rDNA), 358/847/52 (tef1) and 576/807/47 (tub2) variable sites/ total sites/ sequences.

Results

The phylogenetic analysis of sequenced species of *Apiospora* including ITS1-5.8S-ITS2 and LSU rDNA, as well as exon and intron regions from tef1 and tub2 genes (Fig. 1) resulted in six significantly supported major clades: 1) /sorghi (apparently containing a single species, *Ap. sorghi* (J.D.P. Bezerra, C.M. Gonçalves & C.M. Souza-Motta) X.G. Tian & Tibpromma = *Ar. taeanense* S.L. Kwon, S. Jang & J.J. Kim), 2) /jatrophae, 3) /hysterina, 4) /arundinis, 5) /montagnei, and 6) /phaeospermum. These clades, identified in the present work for the first time, maybe represent monophyletic lineages that could be interpreted as sections or subgenera inside *Apiospora*. However, this hypothesis should be further tested with additional data from less variable DNA regions, since ITS1 rDNA and introns can be easily misaligned.

Among the samples analyzed in the present study (Suppl. material 2), five collections of *Apiospora* were found growing on *Arundo* aff. *micrantha* (the supposed host plant of the lectotype of *Sphaeria apiospora*) in Girona (northeastern Spain) and Mallorca (Balearic Islands, Spain). Four of them were not genetically different from *Ap. phragmitis*, and one matched *Ap. sichuanensis*. Another seven samples found growing on *Arundo donax* in Mallorca matched *Ap. phragmitis*, and one *Ap. sichuanensis*. Due to these results and the data available from Mediterranean species of *Apiospora*, *Ap. phragmitis* is here considered the most probable synonym of *Ap. montagnei*, and an epitype for this species selected among the samples analyzed in the present work. Finally, two samples found on *Phleum pratense* in Mallorca turned out to represent a previously unknown phylogenetic lineage, which is given a new name below.

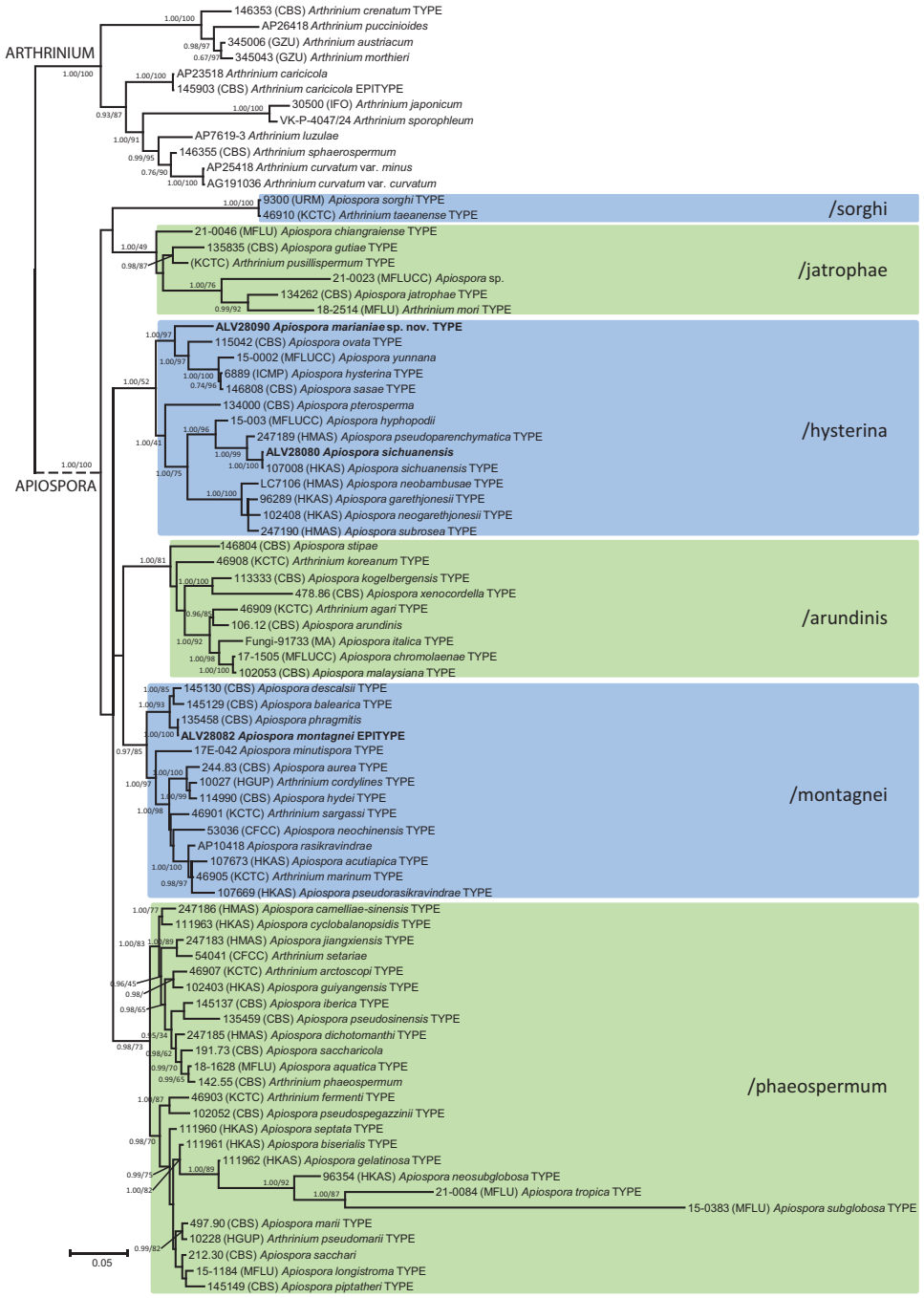

Figure 1. Majority rule consensus (50%) ITS rDNA- 28S rDNA- tef1- tub2 phylogram of the Apiosporaceae obtained in MrBayes from 4 875 sampled trees. Nodes were annotated if supported by > 0.95 Bayesian PP (left) or > 70% ML BP (right).

Taxonomy

***Apiospora montagnei* Sacc., Atti Soc. Veneto-Trent. Sci. Nat. 4: 85. 1875.**
Fig. 2C–2N

Sphaeria apiospora Durieu & Mont., Expl. Sci. Alg., Fl. Algér. 1, livr. 13: 492. 1849. [replaced name]
Hypopteris apiospora (Durieu & Mont.) Berk., Hooker's J. Bot. Kew Gard. Misc. 6: 227. 1854.
Arthrinium phragmitis Crous, IMA Fungus 4: 147. 2013.
Apiospora phragmitis (Crous) Pintos & P. Alvarado, Fungal Systematics and Evolution 7: 206. 2021.

Sexual morph. Stromata solitary to gregarious, immersed to erumpent, fusiform, with the long axis broken at the top by one or two cracks, (0.5–)2.1–2.9(–4) × (0.2–)0.25–0.35(–0.5) mm (n = 20). Ascomata uniseriate or irregularly arranged beneath stromata, pseudothecial, black, globose to subglobose with a flattened base, (150–)159–183(–200) µm high × (200–)247–278(–300) µm wide (n = 35), with a conspicuous periphysate ostiole. Peridium composed of 5 or 6 layers of brown to hyaline cells arranged in textura angularis. Hamathecium paraphyses hyphae-like, up to 4 µm wide. Asci broadly cylindrical, clavate, with an indistinct pedicel, rounded at the apex, lacking apical apparatus, (72–)99–111(–115) × (14–)15.5–16.5(–18) µm (n = 25). Ascospores uniseriate or biseriate, clavate to fusiform, straight or slightly curved, with narrowly rounded ends, composed of a large upper cell and a small lower cell, hyaline, smooth-walled, measuring (21–)23–24.5(–25) × (6–)6.3–7.1(–8) µm (n = 30).

Asexual morph. Mycelium consisting of hyaline, smooth, branched, septate hyphae 1–4 µm in diam. (n = 20). Conidiophore mother cell from hyaline to brown, solitary or aggregated in groups on hyphae, subsphaerical to lageniform or ampuliform, measuring (4–)6.6–8(–10) × (3–)4.5–5.1(–6) µm (n = 10). Conidiophores cylindrical, straight to flexuous, some of them branched, hyaline, measuring (10–)18–34(–45) × (1.5–)1.6–1.8(–2) µm (n = 20). Conidiogenous cells doliiform to lageniform or ampuliform, hyaline, measuring (10–)11.5–13.1(–15) × (2–)4.3–5.1(–6) µm (n = 20). Conidia ellipsoidal to ovoid, smooth to finely roughened, with an equatorial germ slit of paler pigment, measuring (9–)10.3–11.3(–12) µm in surface view, (5–)6.2–7.2(–8) µm in side view (n = 25). Sterile cells ellipsoidal to clavate, measuring 13–16 µm (n = 25).

Culture characteristics. Colonies flat, spreading, with moderate aerial mycelium. On MEA, surface dirty white with pale rose patches, reverse luteous. Occupying an entire 90 mm Petri dish in 14 days at room temperature, sporulating four weeks after culture.

Epitype. Spain: Catalonia, Girona, L´Escala, on *Arundo micrantha*, 30 November 2020, leg. Marc Grañem, AP301120 (epitype selected here PC:0125164, ex-type culture CBS 148707; iso-epitype WU-MYC0044524, ex-type culture CBS 148708).

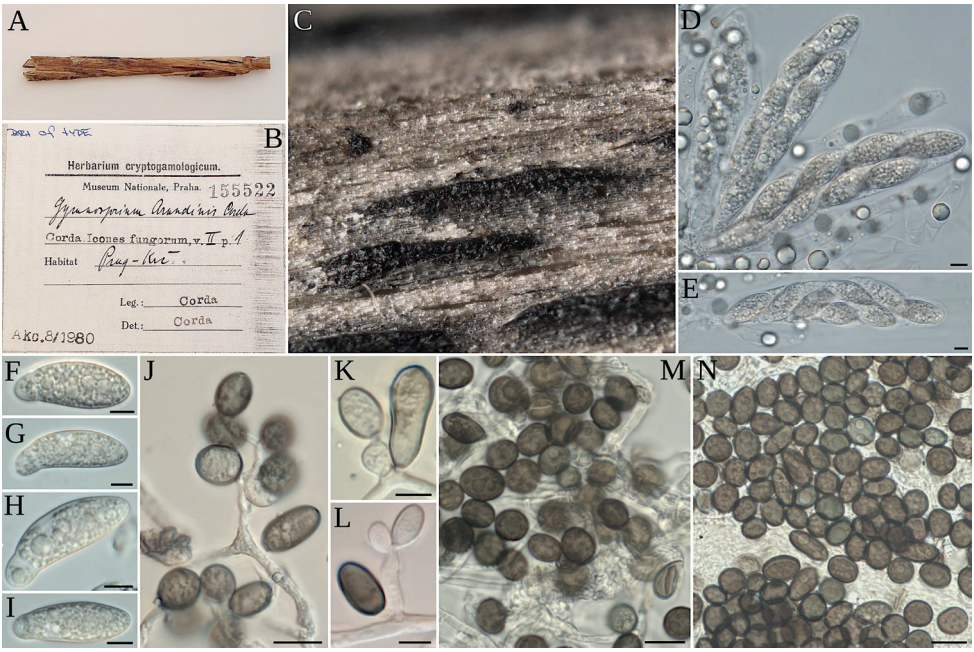

Figure 2. A, B *Gymnosporium arundinis* (original material from PRM) **A** substrate of the type **B** label of the original collection of *Gymnosporium arundinis* **C–N** *Apiospora montagnei* (AP301120) **C** stromata on host **D, E** asci and periphyses **F–I** ascospores **J–L** conidiogenous cell with conidia **M–N** conidia in face and side view. Scale bars: 100 µm (**C**); 5 µm (**D–I**); 10 µm (**J–N**).

Other specimens examined. Spain: Balearic Islands, Mallorca, Esporlas, on *Arundo donax*, 14 December 2020, leg. Ángel Pintos, AP141220 (WU-MYC0044527). Balearic Islands, Mallorca, Palma de Mallorca, Torrente de Establiments, on *Arundo micrantha*, 19 April 2021, leg Ángel Pintos, AP19421 (WU-MYC0044523). Balearic Islands, Mallorca, Puerto de Alcudia, on *Arundo donax*, 2 April 2021, leg. Ángel Pintos, AP2421 (WU-MYC0044522). Balearic Islands, Mallorca, Puerto de Andratx, on *Arundo donax*, 5 April 2021, leg. Ángel Pintos, AP5421 (WU-MYC0044529). Balearic Islands, Mallorca, Puerto de Soller, on *Arundo donax*, 3 April 2021, leg. Ángel Pintos, AP3421 (WU-MYC0044528). Balearic Islands, Mallorca, Puigpunyent, on *Arundo micrantha*, 11 December 2020, leg. Ángel Pintos, AP111220A. Balearic Islands, Mallorca, Soller, on *Arundo donax*, 4 April 2021, leg. Ángel Pintos, AP4421 (WU-MYC0044530). Balearic Islands, Mallorca, Universitat de les Illes Balears (UIB), on *Arundo donax*, 28 December 2020, leg. Ángel Pintos, AP281220 (WU-MYC0044521). Catalonia, Barcelona, Premia de Dalt, on *Arundo donax*, 10 October 2020, leg Miguel Mir, AP101020. Catalonia, Girona, Bescanó, on *Arundo micrantha*, 29 November 2020, leg. Marc Grañem, AP291120 (WU-MYC0044526).

Notes. The phylogenetic boundaries of *Apiospora* were recently discussed by Pintos and Alvarado (2021), who selected a lectotype (PC:0125160) for *S. apiospora*,

the basionym of the type species *Ap. montagnei*. In the present study, an epitype (PC:0125164) of *Ap. montagnei* is selected among modern collections growing on the same host in Girona, Spain (about 100 km south of the type locality, Perpignan, France). All samples growing on the same host collected in Girona or the Balearic Islands (Spain) are genetically identical to the epitype, and match the phylogenetic clade formerly known as *Ap. phragmitis*, excepting one that matches *Ap. sichuanensis*, but the ascospores of this species (29–48 × 7–10.5 µm, Samarakoon et al. 2022) clearly exceed those of *Ap. montagnei* (21–25 µm, Pintos and Alvarado 2021). Therefore, on the basis of these results, it is here hypothesized that *Ap. montagnei* is a prioritary synonym of *Ap. phragmitis*.

Apiospora marianiae **sp. nov. Pintos & P. Alvarado**
MycoBank No: 843732
Fig. 3

Etymology. The epithet refers to Marian Mateu, the person who found the holotype collection and beloved wife of the first author.

Holotype. Spain: Balearic Islands, Palma de Mallorca, on *Phleum pratense*, 18 February 2019, leg. Marian Mateu AP18219 (holotype CBS 148710).

Asexual morph. Mycelium branched, septate, brown to dark brown. Conidiomata sporodochial, punctiform, scattered or confluent, black, (150–)169–203(–220) µm long × (70–)76–88(–100) µm wide (n = 30). Conidiophore mother cells on the surface of the stroma lageniform to ellipsoidal or doliiform, hyaline to brown, measuring (12–)13.4–14.2(–15) × (4–)6–7.2(–8) µm (n = 10). Conidiophores arising from conidiogenous mother cells, basauxic, cylindrical, straight to flexuous, hyaline except the thin transverse septa, smooth, measuring (19–)28–44(–55) × 3–3.6(–4) µm (n = 25). Conidiogenous cells monoblastic, integrated, terminal and intercalary, cylindrical. Conidia brown, solitary; face view: globose to ovate or ellipsoidal, with pale germ slit, (11–)12.1–13.5(–18) µm in diam. (n = 70); side view: lenticular, (8–)8.4–9.2(–10) µm in diam. (n = 30). Sterile cells only seen in culture, brown, granulate, irregularly lobed, (19–)25–31(–35) × (6–)8.15–8.45(–12) µm diam. (n = 40).

Culture characteristics. colonies in MEA white and cottony, with gray patches, reverse gray. Reaching 80–90 mm in diam, in 14 days at room temperature, sporulating after 5 weeks.

Other specimens examined. Spain: Balearic Islands, Palma de Mallorca, Establiments, on *Phleum pratense*, 30 November 2019, leg. Angel Pintos, AP301119.

Notes. According to phylogenetic inference, *Ap. ovata* is the species most closely related to *Ap. marianiae*, but their ITS rDNA sequences are only 94% similar (including gaps). Their conidia are both oval to broadly ellipsoid, but those of *Ap. marianiae* measure 11–15 µm in diam., while those of *Ap. ovata* are longer, measuring about 18–20 µm in diam. in surface view.

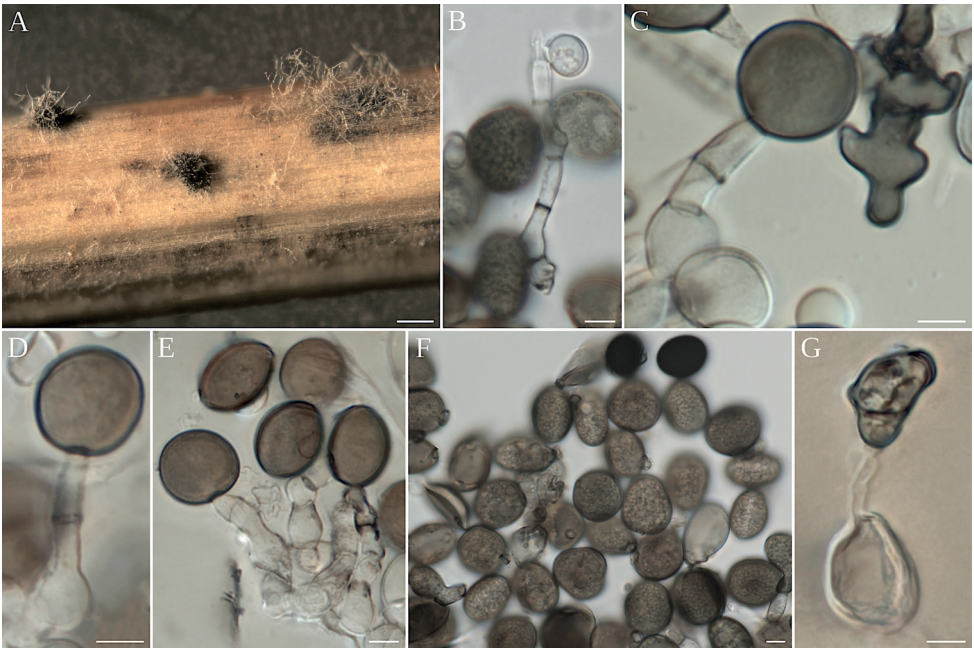

Figure 3. *Apiospora marianiae* (AP18219) **A** colony on culture **B–E** conidiophore mother cell with septate conidiophore giving rise to conidia, in C irregularly lobate sterile cell **F** conidia in face and side view **G** conidiophore mother cell with irregular conidia from agar. Scale bars: 100 μm (**A**); 5 μm (**B–G**).

Apiospora sichuanensis **Samarak., Jian K. Liu & K.D. Hyde, in Samarakoon, Hyde, Maharachchikumbura, Stadler, Gareth Jones, Promputtha, Suwannarach, Camporesi, Bulgakov & Liu, Fungal Diversity 112: 21. 2022.**
Fig. 4

Asexual morph. Mycelium branched, septate, brown. Conidiomata on host parallel to the longitudinal axis of the stem, subepidermal, opening after the dehiscence of the host epidermis, containing a black conidial mass, measuring (400–)600–950(–1000) × (275–)300–550(–600) μm (n = 40). Conidiophore mother cells arising from the stroma, lageniform to ampuliform, pale brown, with superficial granular depositions, (5–)6–10(–16) × (3–)5–7(–8) μm (n = 30). Conidiophores basauxic, cylindrical, straight or flexuous, sometimes with a thin septum, hyaline to brown, smooth, with granular pigments, (20–)43–67(–80) μm in length × (2–)2.2–3.4(–4) μm wide (n = 50). Conidia globose, subcylindrical to ovate, polygonal or obpyriform, with a lateral germ slit over the entire length, brown, smooth, irregularly lobed, measuring (10–)23–31(–35) × (5–)9–13(–14) μm (n = 30).

Culture characteristics. colonies on MEA 70–90 mm in diam. after 14 days at room temperature, flat, spreading, first white and cottony, later becoming gray, reverse

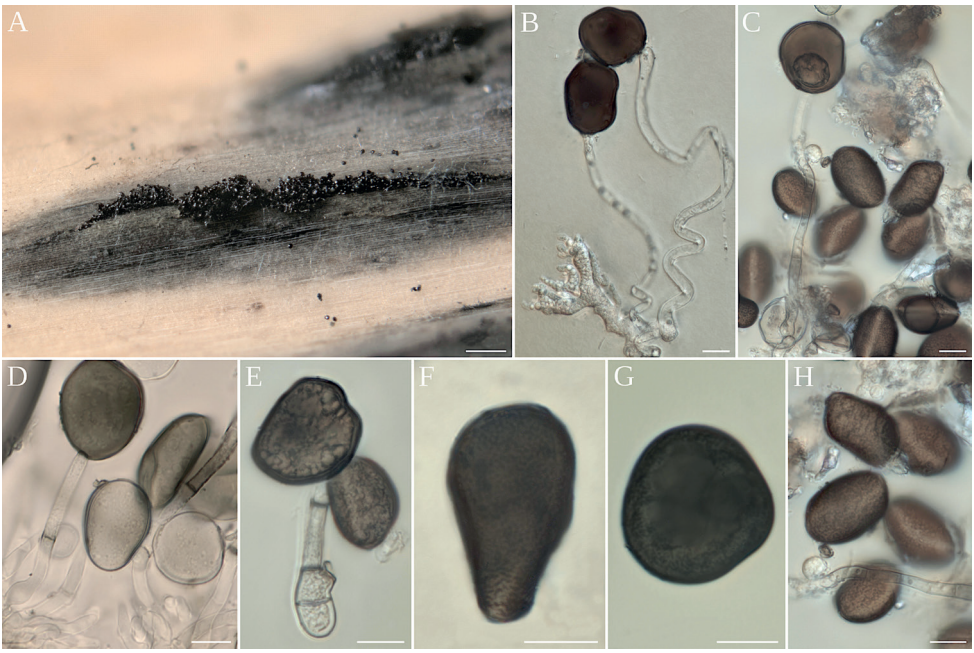

Figure 4. *Apiospora sichuanensis* (AP121220) **A** conidiomata on host **B** germinated conidia **C–E** conidiophore mother cell giving rise to septate conidiophore with conidia **F–H** conidia. Scale bars 100 μm (**A**); 10 μm (**B–H**).

dark gray. On PDA (200 g/L potato, 20 g/L dextrose, 20 g/L agar, pH 7.0), 80–90 mm in diam, after 14 days at room temperature, sporulating after 4–5 weeks, white cottony at first, then becoming gray with luteous patches, reverse dark gray.

Specimens examined. Spain: Balearic Islands, Mallorca, Palma de Mallorca, Torrente de Soller, on *Arundo donax*, 12 December 2020, leg. Ángel Pintos, AP121220 (WU-MYC0044525). Catalonia, Girona, Bescanó, on *Arundo micrantha*, 15 November 2020, leg. Marc Grañem. AP151120.

Notes. *Ap. sichuanensis* is genetically close to *Ap. pseudoparenchymatica* (M. Wang & L. Cai) Pintos & P. Alvarado, but the fruiting body of the former is an acervulus and that of the latter a sporodochium. In addition, the conidia of *Ap. sichuanensis* are 10–35 × 5–14 μm, longer and narrower than those of *Ap. pseudoparenchymatica*, which measure 13.5–27.0 × 12.0–23.5.

Discussion

In the present work, several samples of *Apiospora* growing on *Arundo* aff. *micrantha* (the most probable host plant of the lectotype collection of *S. apiospora*, PC:0125160, Pintos and Alvarado 2021) were analyzed in order to clarify the identity of the type species of *Apiospora*, *Ap. montagnei* (≡ *Sphaeria apiospora*). In previous works (Crous and Groenewald 2013, Pintos et al. 2019), four species of *Apiospora* were found on

Arundo spp.: *Ap. iberica*, *Ap. italica*, *Ap. marii*, and *Ap. phragmitis*. In the present work, the first record of *Ap. sichuanensis* in Europe was found growing also on *Arundo* spp. However, the ascospore dimensions reported in the protologues of *Ap. iberica* (29–34 × 6–8 µm, Pintos et al. 2019) and *Ap. sichuanensis* (29–48 × 7–10.5 µm, Samarakoon et al. 2022), clearly exceed those measured on the lectotype of *S. apiospora* (PC 0125160, 21–25 µm, Pintos and Alvarado 2021), and other original material of this species (23–28 µm, Hyde et al. 1998). On the contrary, ascospores of *Ap. italica*, *Ap. marii* and *Ap. phragmitis* are not significantly different from those of the lectotype of *S. apiospora*.

All samples of *Apiospora* found on *Arundo* aff. *micrantha* with an ascospore size matching that of *Ap. montagnei* are genetically identical to *Ap. phragmitis*. A single collection of *Ap. italica* (MA-Fungi 91733, Pintos et al. 2019), and another one of *Ap. marii* (MA-Fungi 91735, Pintos et al. 2019) were previously found on *Arundo donax*, a host plant were *Ap. phragmitis* and *Ap. sichuanensis* can occur too. Despite the lack of collections confirming it, it is certainly possible that *Ap. italica* and *Ap. marii* grow also on *Arundo* aff. *micrantha*, as these species have been found also on other host plants, especially *Phragmites*, but also *Ampelodesmos* and many others (*Arundinaria*, *Beta*, oats, seaweeds). *Apiospora marii* has been found in southern, central and northern Europe (Spain, Italy, Austria, The Netherlands, Sweden) and Asia (China, Korea), being most probably a widespread species. By way of contrast, *Ap. italica* and *Ap. phragmitis* have been found only in the Mediterranean region.

Given the wide host plant range observed in *Apiospora*, other species which have not been found yet on *Arundo* could be collected on this host plant genus in the future, reducing the reliability of this character for diagnosis. Of those species occurring in the Mediterranean region, some present ascosopores differing in size from *Ap. montagnei* (i.e., *Ap. balearica* (Pintos & P. Alvarado) Pintos & P. Alvarado, *Ap. hysterina* (Sacc.) Pintos & P. Alvarado). Others, such as *Ap. descalsii* (Pintos & P. Alvarado) Pintos & P. Alvarado, are apparently rare, and the probability of a synonymy with *Ap. montagnei* is therefore low. The sexual state of *Ap. rasikravindrae* (Shiv M. Singh, L.S. Yadav, P.N. Singh, Rah. Sharma & S.K. Singh) Pintos & P. Alvarado produces ascospores measuring 21.5–24.5 × 7–9.5 µm (Dai et al. 2017), therefore fitting the size range observed in *S. apiospora* lectotype, but the synonymy is here rejected because this species has never been found yet on *Arundo* sp. (only known to grow on ornamental *Phyllostachys* and bamboo plants in Mallorca). Unfortunately, the sexual state of multiple species occurring in the Mediterranean region (i.e., *Ap. aurea* (Calvo & Guarro) Pintos & P. Alvarado, *Ap. esporlensis* (Pintos & P. Alvarado) Pintos & P. Alvarado, *Ap. hispanica* (Larrondo & Calvo) Pintos & P. Alvarado, *Ap. mediterranea* (Larrondo & Calvo) Pintos & P. Alvarado, *Ap. piptatheri* (Pintos & P. Alvarado) Pintos & P. Alvarado, *Ap. serenensis* (Larrondo & Calvo) Pintos & P. Alvarado, as well as the new species introduced in the present work, *Ap. marianiae*) is still unknown, and therefore they cannot be compared yet with the lectotype of *S. apiospora* (≡ *Ap. montagnei*). However, these seem to be rare species, and they have never been found on *Arundo* yet, so the synonymy is here considered much less probable.

A classical candidate synonym of *Ap. montagnei*, *Ap. arundinis* (Corda) Pintos & P. Alvarado (Crous and Groenewald 2013), has not been found yet in the western

Mediterranean region (Pintos et al. 2019, Pintos and Alvarado 2021), but it seems to be widespread elsewhere, occurring in temperate, cold and also subtropical countries (Crous and Groenewald 2013). In Spain, it has been found in ornamental *Bambusa* plants in Galicia (north-western Spain), but not in the Mediterranean border with France (closer and ecologically more similar to Perpignan, the type locality of *Ap. montagnei*). Sequenced samples of *Ap. arundinis* found growing in *Arundo* are currently lacking, but the type collection of its basionym, *Gymnosporium arundinis* Corda was reported to grow on reeds and grasses near Prague by Corda (1838). An original sample kindly loaned by the Prague herbarium (PRM 155522) was found to present globose conidia 5–7 µm in diam., a size compatible with that observed in the clade identified as *Ar. arundinis* by Crous and Groenewald (2013), but also others, such as *Ap. descalsii*, *Ap. italicum*, *Ap. jiangxiensis* (M. Wang & L. Cai) Pintos & P. Alvarado, *Ap. malaysiana* (Crous) Pintos & P. Alvarado, *Ap. pseudospegazzinii* (Crous) Pintos & Alvarado or *Ap. sacchari* (Speg.) Pintos & P. Alvarado. Interestingly, the host plant of this original collection of *G. arundinis* loaned by PRM was not *Arundo*, but very probably *Phalaris arundinacea*. The identity of *Ap. arundinis* needs to be further investigated, and an epitype from Prague selected, to ascertain if the name is being correctly applied.

Therefore, on the basis of the data currently available (host plants, ascospore sizes, abundances, distributions), it is here hypothesized that the lectotype of *S. apiospora* (≡ *Ap. montagnei*) is not genetically different from the clade of *Ap. phragmitis*. An epitype of *S. apiospora* (≡ *Ap. montagnei*) from Girona (Spain, about 100 km south of Perpignan, the locality where the lectotype was found) is here chosen, and a synonymy between *Ap. montagnei* and *Ap. phragmitis* is suggested.

Acknowledgements

The authors wish to thank Juan Planas for assembling the image plates, as well as Jan Holec, curator of PRM herbarium for kindly allowing the authors to study original collections of *Gymnosporium arundinis*. Finally, Marc Grañem, Marian Mateu and Miguel Mir are thanked also for collaborating in finding samples of *Apiospora*.

References

Arita M, Karsch-Mizrachi I, Cochrane G (2021) The international nucleotide sequence database collaboration. Nucleic Acids Research 49: D121–D124. https://doi.org/10.1093/nar/gkaa967

Bory de Saint-Vincent JBGM, Durieu de Maisonneuve MC (1849) Exploration scientifique de l'Algérie pendant les années 1840, 1841, 1842. Sciences Physiques, Botanique. Flore d'Algérie. Imprimerie Royale, Paris.

Carbone I, Kohn L (1999) A method for designing primer sets for speciation studies in filamentous ascomycetes. Mycologia 91(3): 553–556. https://doi.org/10.1080/00275514.1999.12061051

Castresana J (2000) Selection of conserved blocks from multiple alignments for their use in phylogenetic analysis. Molecular Biology and Evolution 17(4): 540–552. https://doi.org/10.1093/oxfordjournals.molbev.a026334

Corda ACJ (1838) Icones Fungorum hucusque cognitorum. Tomus II. Apud J. G. Calve, Prague.

Crous PW, Groenewald JZ (2013) A phylogenetic re-evaluation of *Arthrinium*. IMA Fungus 4(1): 133–154. https://doi.org/10.5598/imafungus.2013.04.01.13

Crous PW, Wingfield MJ, Le Roux JJ, Richardson DM, Strasberg D, et al. (2015) Fungal Planet description sheets: 371–399. Persoonia 35(1): 264–327. https://doi.org/10.3767/003158515X690269

Crous PW, Schumacher RK, Wood AR, Groenewald JZ (2020) The genera of Fungi – G5: *Arthrinium*, *Ceratosphaeria*, *Dimerosporiopsis*, *Hormodochis*, *Lecanostictopsis*, *Lembosina*, *Neomelanconium*, *Phragmotrichum*, *Pseudomelanconium*, *Rutola* and *Trullula*. Fungal Systematics and Evolution 5(1): 77–98. https://doi.org/10.3114/fuse.2020.05.04

Crous PW, Hernández-Restrepo M, Schumacher RK, Cowan DA, Maggs-Kölling G, Marais E, Wingfield MJ, Yilmaz N, Adan OCG, Akulov A, Duarte EÁ, Berraf-Tebbal A, Bulgakov TS, Carnegie AJ, de Beer ZW, Decock C, Dijksterhuis J, Duong TA, Eichmeier A, Hien LT, Houbraken JAMP, Khanh TN, Liem NV, Lombard L, Lutzoni FM, Miadlikowska JM, Nel WJ, Pascoe IG, Roets F, Roux J, Samson RA, Shen M, Spetik M, Thangavel R, Thanh HM, Thao LD, van Nieuwenhuijzen EJ, Zhang JQ, Zhang Y, Zhao LL, Groenewald JZ (2021) New and Interesting Fungi. 4. Fungal Systematics and Evolution 7(1): 255–343. https://doi.org/10.3114/fuse.2021.07.13

Cubeta MA, Echandi E, Abernethy T, Vilgalys R (1991) Characterization of anastomosis groups of binucleate *Rhizoctonia* species using restriction analysis of an amplified ribosomal RNA gene. Phytopathology 81(11): 1395–1400. https://doi.org/10.1094/Phyto-81-1395

Dai DQ, Jiang HB, Tang LZ, Bhat DJ (2016) Two new species of *Arthrinium* (Apiosporaceae, Xylariales) associated with bamboo from Yunnan, China. Mycosphere: Journal of Fungal Biology 7(9): 1332–1345. https://doi.org/10.5943/mycosphere/7/9/7

Dai DQ, Phookamsak R, Wijayawardene NN, Li WJ, Bhat DJ, Xu JC, Taylor JE, Hyde KD, Chukeatirote E (2017) Bambusicolous fungi. Fungal Diversity 82(1): 1–105. https://doi.org/10.1007/s13225-016-0367-8

Ellis MB (1965) Dematiaceous Hyphomycetes. VI. Mycological Papers 103: 1–46.

Gardes M, Bruns TD (1993) ITS primers with enhanced specificity for Basidiomycetes—Application to the identification of mycorrhizae and rusts. Molecular Ecology 2(2): 113–118. https://doi.org/10.1111/j.1365-294X.1993.tb00005.x

Glass NL, Donaldson GC (1995) Development of primer sets designed for use with the PCR to amplify conserved genes from filamentous ascomycetes. Applied and Environmental Microbiology 61(4): 1323–1330. https://doi.org/10.1128/aem.61.4.1323-1330.1995

Heo YM, Kim K, Ryu SM, Kwon SL, Park MY, Kang JE, Hong J-H, Lim YW, Kim C, Kim BS, Lee D, Kim J-J (2018) Diversity and ecology of marine Algicolous *Arthrinium* species as a source of bioactive natural products. Marine Drugs 16(12): 508. https://doi.org/10.3390/md16120508

Hyde KD, Fröhlich J, Taylor JE (1998) Fungi from palms. XXXVI. Reflections on unitunicate ascomycetes with apiospores. Sydowia 50: 21–80.

Jiang N, Li N, Tian CM (2018) *Arthrinium* species associated with bamboo and red plants in China. Fungal Systematics and Evolution 2: 1–9. https://doi.org/10.3114/fuse.2018.02.01

Jiang HB, Hyde KD, Doilom M, Karunarathna SC, Xu JC, et al. (2019) *Arthrinium setostromum* (Apiosporaceae, Xylariales), a novel species associated with dead bamboo from Yunnan, China. Asian Journal of Mycology 2(1): 254–268. https://doi.org/10.5943/ajom/2/1/16

Jiang N, Liang YM, Tian CM (2020) A novel bambusicolous fungus from China, *Arthrinium chinense* (Xylariales). Sydowia 72: 77–83. https://doi.org/10.12905/0380.sydowia72-2020-0077

Kwon SL, Park MS, Jang S, Lee YM, Heo YM, Hong J-H, Lee H, Jang Y, Park J-H, Kim C, Kim G-H, Lim YW, Kim J-J (2021) The genus *Arthrinium* (Ascomycota, Sordariomycetes, Apiosporaceae) from marine habitats from Korea, with eight new species. IMA Fungus 12(1): 13. https://doi.org/10.1186/s43008-021-00065-z

Liu F, Bonthond G, Groenewald JZ, Cai L, Crous PW (2019) Sporocadaceae, a family of coelomycetous fungi with appendage bearing conidia. Studies in Mycology 92(1): 287–415. https://doi.org/10.1016/j.simyco.2018.11.001

Mullis K, Faloona FA (1987) Specific synthesis of DNA in vitro via a polymerase-catalyzed chain reaction. Methods in Enzymology 155: 335–350. https://doi.org/10.1016/0076-6879(87)55023-6

Murray MG, Thompson WF (1980) Rapid isolation of high molecular weight plant DNA. Nucleic Acids Research 8(19): 4321–4325. https://doi.org/10.1093/nar/8.19.4321

O'Donnell K, Cigelnik E (1997) Two divergent intragenomic rDNA ITS2 types within a monophyletic lineage of the fungus *Fusarium* are nonorthologous. Molecular Phylogenetics and Evolution 7(1): 103–116. https://doi.org/10.1006/mpev.1996.0376

Park MS, Oh S-Y, Lee S, Eimes JA, Lim YW (2018) Fungal diversity and enzyme activity associated with sailfin sandfish egg masses in Korea. Fungal Ecology 34: 1–9. https://doi.org/10.1016/j.funeco.2018.03.004

Phukhamsakda C, Nilsson RH, Bhunjun CS, Gomes de Farias AR, Sun Y-R, Wijesinghe SN, Raza M, Bao D-F, Lu L, Tibpromma S, Dong W, Tennakoon DS, Tian X-G, Xiong Y-R, Karunarathna SC, Cai L, Luo Z-L, Wang Y, Manawasinghe IS, Camporesi E, Kirk PM, Promputtha I, Kuo C-H, Su H-Y, Doilom M, Li Y, Fu Y-P, Hyde KD (2022) The numbers of fungi: Contributions from traditional taxonomic studies and challenges of metabarcoding. Fungal Diversity 114(1): 327–386. https://doi.org/10.1007/s13225-022-00502-3

Pintos Á, Alvarado P (2021) Phylogenetic delimitation of *Apiospora* and *Arthrinium*. Fungal Systematics and Evolution 7(1): 197–221. https://doi.org/10.3114/fuse.2021.07.10

Pintos Á, Alvarado P, Planas J, Jarling R (2019) Six new species of *Arthrinium* from Europe and notes about *A. caricicola* and other species found in *Carex* spp. hosts. MycoKeys 49: 15–48. https://doi.org/10.3897/mycokeys.49.32115

Rehner SA, Buckley E (2005) A *Beauveria* phylogeny inferred from nuclear ITS and EF1-a sequences: Evidence for cryptic diversification and links to *Cordyceps* teleomorphs. Mycologia 97(1): 84–98. https://doi.org/10.3852/mycologia.97.1.84

Saccardo PA (1875) Conspectus generum pyrenomycetum italicorum additis speciebus fungorum Venetorum novis vel criticis, systemate carpologico dispositorum. Atti della Società Veneto-Trentina di Scienze Naturali 4: 77–100.

Samarakoon MC, Hyde KD, Maharachchikumbura SSN, Stadler M, Jones EBG, Promputtha I, Suwannarach N, Camporesi E, Bulgakov TS, Liu J-K (2022) Taxonomy, phylogeny, molecular dating and ancestral state reconstruction of Xylariomycetidae (Sordariomycetes). Fungal Diversity 112(1): 1–88. https://doi.org/10.1007/s13225-021-00495-5

Senanayake IC, Maharachchikumbura SSN, Hyde KD, Bhat JD, Jones EBG, McKenzie EHC, Dai DQ, Daranagama DA, Dayarathne MC, Goonasekara ID, Konta S, Li WJ, Shang QJ, Stadler M, Wijayawardene NN, Xiao YP, Norphanphoun C, Li Q, Liu XZ, Bahkali AH, Kang JC, Wang Y, Wen TC, Wendt L, Xu JC, Camporesi E (2015) Towards unravelling relationships in Xylariomycetidae (Sordariomycetes). Fungal Diversity 73(1): 73–144. https://doi.org/10.1007/s13225-015-0340-y

Senanayake IC, Bhat JD, Cheewangkoon R, Xie N (2020) Bambusicolous *Arthrinium* species in Guangdong province, China. Frontiers in Microbiology 11: 602773. https://doi.org/10.3389/fmicb.2020.602773

Singh SM, Yadav LS, Singh PN, Hepat R, Sharma R, Singh SK (2012) *Arthrinium rasikravindrii* sp. nov. from Svalbard, Norway. Mycotaxon 122(1): 449–460. https://doi.org/10.5248/122.449

Smith GJD, Liew ECY, Hyde KD (2003) The Xylariales: A monophyletic order containing 7 families. Fungal Diversity 13: 185–218.

Sørensen T, Petersen C, Fechete LI, Nielsen KL, Sondergaard TE (2022) A highly contiguous genome assembly of *Arthrinium puccinoides*. Genome Biology and Evolution 14(1): 1–5. https://doi.org/10.1093/gbe/evac010

Tamura K, Peterson D, Peterson N, Stecher G, Nei M, Kumar S (2011) MEGA5: Molecular evolutionary genetics analysis using maximum likelihood, evolutionary distance, and maximum parsimony methods. Molecular Biology and Evolution 28(10): 2731–2739. https://doi.org/10.1093/molbev/msr121

Tang X, Goonasekara ID, Jayawardena RS, Jiang HB, Li JF, Hyde K, Kang J (2021) *Arthrinium bambusicola* (Fungi, Sordariomycetes), a new species from *Schizostachyum brachycladum* in northern Thailand. Biodiversity Data Journal 8: e58755. https://doi.org/10.3897/BDJ.8.e58755

Tian X, Karunarathna SC, Mapook A, Promputtha I, Xu J, Bao D, Tibpromma S (2021) One new species and two new host records of *Apiospora* from bamboo and maize in Northern Thailand with thirteen new combinations. Life (Chicago, Ill.) 11(10): 1071. https://doi.org/10.3390/life11101071

Vilgalys R, Hester M (1990) Rapid genetic identification and mapping of enzymatically amplified ribosomal DNA from several *Cryptococcus* species. Journal of Bacteriology 172(8): 4238–4246. https://doi.org/10.1128/jb.172.8.4238-4246.1990

Wang M, Liu F, Crous PW, Cai L (2017) Phylogenetic reassessment of *Nigrospora*: Ubiquitous endophytes, plant and human pathogens. Persoonia 39(1): 118–142. https://doi.org/10.3767/persoonia.2017.39.06

Wang M, Tan X-M, Liu F, Cai L (2018) Eight new *Arthrinium* species from China. MycoKeys 34: 1–24. https://doi.org/10.3897/mycokeys.34.24221

White TJ, Bruns T, Lee S, Taylor JW (1990) Amplification and direct sequencing of fungal ribosomal RNA genes for phylogenetics. In: Innis MA, Gelfand DH, Sninsky JJ, et al.

(Eds) PCR protocols: a guide to methods and applications. Academic Press, San Diego, 315–332. http://dx.doi.org/10.1016/B978-0-12-372180-8.50042-1

Yan H, Jiang N, Liang L-Y, Yang Q, Tian C-M (2019) *Arthrinium trachycarpum* sp. nov. from *Trachycarpus fortuneii* in China. Phytotaxa 400(3): 203–210. https://doi.org/10.11646/phytotaxa.400.3.7

Yang C-L, Xu X-L, Dong W, Wanasinghe DN, Liu Y-G, Hyde KD (2019) Introducing *Arthrinium phyllostachium* sp. nov. (Apiosporaceae, Xylariales) on *Phyllostachys heteroclada* from Sichuan province, China. Phytotaxa 406(2): 91–110. https://doi.org/10.11646/phytotaxa.406.2.2

Supplementary material 1

Table S1

Authors: Ángel Pintos, Pablo Alvarado

Data type: Sequences.

Explanation note: Sequences produced in the present work (in bold) and retrieved from databases.

Link: https://doi.org/10.3897/mycokeys.92.87593.suppl1

Supplementary material 2

Table S2

Authors: Ángel Pintos, Pablo Alvarado

Data type: Sequences.

Explanation note: Samples analyzed in the present work.

Link: https://doi.org/10.3897/mycokeys.92.87593.suppl2

MycoKeys 92: 79–93 (2022)
doi: 10.3897/mycokeys.92.86277
https://mycokeys.pensoft.net

RESEARCH ARTICLE

A peer-reviewed open-access journal
MycoKeys
Launched to accelerate biodiversity research

Pseudosperma arenarium (Inocybaceae), a new poisonous species from Eurasia, based on morphological, ecological, molecular and biochemical evidence

Ya-Ya Yan[1*], Yi-Zhe Zhang[2*], Jukka Vauras[4], Li-Na Zhao[3], Yu-Guang Fan[3], Hai-Jiao Li[2], Fei Xu[1,5]

1 *School of Public Health and Management, Ningxia Key Laboratory of Environmental Factors and Chronic Diseases Control, Ningxia Medical University, Yinchuan, Ningxia, 750004, China* **2** *National Institute of Occupational Health and Poison Control, Chinese Centre for Disease Control and Prevention, Beijing, 100050, China* **3** *Key Laboratory of Tropical Translational Medicine of Ministry of Education, Hainan Key Laboratory for R & D of Tropical Herbs, School of Pharmacy, Hainan Medical University, Haikou, Hainan, 571199, China* **4** *Biological Collections of Åbo Akademi University, Herbarium, Biodiversity Unit, University of Turku, FI-20014 Turku, Finland* **5** *Physical and Chemical Department, Ningxia Hui Autonomous Region Center for Disease Control and Prevention, Yinchuan, Ningxia, 750004, China*

Corresponding authors: Yu-Guang Fan (mycena@qq.com), Hai-Jiao Li (lihaijiao715@126.com), Fei Xu (lengyue0524@163.com)

Academic editor: Alfredo Vizzini | Received 8 May 2022 | Accepted 22 July 2022 | Published 30 August 2022

Citation: Yan Y-Y, Zhang Y-Z, Vauras J, Zhao L-N, Fan Y-G, Li H-J, Xu F (2022) *Pseudosperma arenarium* (Inocybaceae), a new poisonous species from Eurasia, based on morphological, ecological, molecular and biochemical evidence. MycoKeys 92: 79–93. https://doi.org/10.3897/mycokeys.92.86277

Abstract

In this study, *Pseudosperma arenarium* is proposed as a new species, based on morphological, ecological, molecular and biochemical evidence. The new species grows on sandy ground under *Populus* and *Pinus sylvestris* in north-western China and northern Europe, respectively. It is characterised by the combination of the robust habit, nearly glabrous pileus, large cylindrical basidiospores, thin-walled cheilocystidia and ecological associations with *Populus alba* × *P. berolinensis* and *Pinus sylvestris* and unique phylogenetic placement. Additionally, a comprehensive toxin determination of the new species using ultra-high performance liquid chromatography-tandem mass spectrometry was conducted. Results showed that it was a muscarine-positive species. The content were approximately five times higher in the pilei [4012.2 ± 803.1–4302.3 ± 863.2 mg/kg (k = 2, p = 95%)] than in the stipes [850.4 ± 171.1–929.1 ± 184.2 mg/kg (k = 2,

* These authors contributed equally to this work.

p = 95%)], demonstrating the severity of mushroom poisoning when patients consumed different parts of the poisonous mushroom. Amatoxins, phallotoxins, ibotenic acid, muscimol, psilocybin and psilocin were not detected.

Keywords
Agaricales, muscarine, mushroom toxin, new taxon, poisonous mushroom, ultra-high performance liquid chromatography-tandem mass spectrometry

Introduction

Inocybaceae is a family of agarics that contains many poisonous species. However, Kosentka et al. (2013) found that the most recent common ancestor of the family did not contain muscarine. Recognising its species diversity and detecting its toxins are essential to control and prevent poisoning incidents (Li et al. 2020; Deng et al. 2021a). According to the latest molecular phylogeny, seven genera were treated in Inocybaceae (Matheny et al. 2020). *Pseudosperma*, referred to as *Inocybe* sect. *Rimosae sensu stricto* (Larsson et al. 2009) or Pseudosperma clade (Matheny 2009), is one of the muscarine-containing genera in the family with numerous cryptic and semi-cryptic species. It is characterised by rimulose to rimose pileus, furfuraceous to appressed furfuraceous stipe with flocculose apex, elliptic to sub-phaseoliform basidiospores, the absence of pleurocystidia and the presence of thin-walled cheilocystidia. Ninety-seven *Pseudosperma* taxa have been recorded in the IndexFungorum database (www.indexfungroum.org; retrieved 7 May 2022). Of these, more than 40 taxa have been reported or originally described in Europe (Bandini and Oertel 2020). Since the establishment of the genus in 2020, 16 new taxa have been discovered in Asia and Europe in the past 2 years alone (Bandini and Oertel 2020; Cervini et al. 2020; Jabeen and Khalid 2020; Saba et al. 2020; Yu et al. 2020; Bandini et al. 2021; Jabeen et al. 2021). However, the species diversity of *Pseudosperma* is still poorly explored in East Asia. In China, only six taxa have been verified, including three recently described species, viz., *P. yunnanense*, *P. neoumbrinellum* and *P. citrinostipes* (Bau and Fan 2018; Yu et al. 2020).

Ecologically, *Pseudosperma* species have an ectomycorrhizal symbiosis with various plants and are commonly found in north temperate forests dominated by *Betula*, *Cedrus*, *Populus*, *Pinus*, *Picea*, *Quercus*, *Salix* etc. During field surveys in north-western China, a poisonous Inocybaceae mushroom collected under *Populus* plantations caught the authors' attention because of its strikingly robust habit. This stout Inocybaceae species has led to three poisoning incidents, with a total of seven patients in north-western China during the past 2 years. Two of these occurred in September in Ningxia and Shanxi in 2020 and another occurred in Ningxia in October 2021 (Li et al. 2021a, 2022). All patients from the three poisoning incidents suffered from classic parasympathetic nervous system stimulation syndromes. After microscopic examinations and molecular analyses, mushroom specimens obtained from poisoning locales, together with a European specimen, were proven as a new *Pseudosperma* species. Discussions

on the distribution, relationships and distinction of the new species and its affinities are also provided. Additionally, to better understand the toxicity of the new species and contribute to their poisoning control and prevention, 11 major mushroom toxins, namely, two isoxazole derivatives (ibotenic acid and muscimol), two tryptamine alkaloids (psilocybin and psilocin), three amatoxins (α-, β- and γ-amanitin), three phallotoxins (phalloidin, phallacidin and phallisacin) and muscarine, were assayed.

Methods

Sampling, morphological observations and descriptions

The Chinese materials were collected in sandy poplar plantations from Ningxia Hui Autonomous Region and Shaanxi Province, where there is a temperate continental climate. The European material JV26578 was collected in a seashore forest from Estonia, in a hemiboreal zone. Macroscopic features were described, based on fresh materials and colour photographs. A small piece of the pileus, lamella or stipe tissue was mounted in 5% aqueous potassium hydroxide (KOH) on the slide and then examined using a light microscope when the tissue was completely rehydrated. Microscopic structures, including basidiospores, basidia, cheilocystidia, hymenophoral trama, caulocystidia, pileipellis and stipitipellis, were examined from rehydrated materials. The measurements of micro-structures follow Fan and Bau (2013) and Yu et al. (2020). The number of measured basidiospores is given as an abbreviation [n/m/p], which denotes n spores measured from m basidiomata of p collections. The measurements and Q values are given as (a)b–c(d), "b–c" covers a minimum of 90% of the measured values, "a" and "d" represent the extreme values; Q means the ratio of length/width in an individual basidiospore, Q_m is the average Q of all basidiospores ± sample standard deviation (Ge et al. 2021; Na et al. 2022). Colour designations follow Kornerup and Wanscher (1978). Voucher specimens were deposited in the Herbarium of Changbai Mountain Nature Reserve (ANTU) with FCAS numbers and TUR-A.

DNA extraction, polymerase chain reaction, sequence amplification and data analysis

Genomic DNA was extracted from silica-dried materials using the NuClean Plant Genomic DNA Kit (ComWin Biotech, Beijing). The internal transcribed spacer (ITS) region, the nuclear large subunit (nLSU) and the RNA polymerase II second largest subunit (RPB2) sequences were amplified and sequenced separately by using primer pairs ITS1F/ITS4 (Gardes and Bruns 1993), LR0R/LR7 (Vilgalys and Hester 1990) and RPB2-6F/RPB2-7.1R (Matheny 2005). The PCR thermocycling protocol was 95 °C for 1 min at first, then followed by 35 cycles of denaturation at 95 °C for 30 s, annealing at 52 °C for 1 min, extension at 72 °C for 1 min and a final extension at 72 °C for 8 min (Wang et al. 2021). Sequencing work was done by Sangon Biotech

(Shanghai) Co., Ltd. Sequences of related taxa in *Pseudosperma*, retrieved from previous studies, were downloaded from GenBank (https://www.ncbi.nlm.nih.gov/) for phylogenetic analysis (Suppl. material 1). *Mallocybe terrigena* (Fr.) Matheny, Vizzini & Esteve-Rav. was used for the outgroup. The sequence data matrix for each locus was aligned by Mafft online service (https://mafft.cbrc.jp/alignment/server/) (Katoh et al. 2019) and manually adjusted by BioEdit 7.0.9.0 (Hall 1999). The aligned datasets were combined with Mega 5.02 (Tamura et al. 2011). MrModeltest v.2.3 was used to determine the optimal substitution model for each locus with the Akaike Information Criterion (Nylander 2004). Bayesian Inference (BI) analyses, executed in MrBayes v.3.2.7a (Ronquist et al. 2012), were run for 1,235,000 generations using four Metropolis-Coupled Monte Carlo Markov chains to calculate posterior probabilities and the standard deviation of the split frequencies was terminated at 0.009977. Maximum Likelihood (ML) analysis was conducted in W-IQ-TREE Web Service (http://iqtree.cibiv.univie.ac.at/) with 1,000 replicates (Trifinopoulos et al. 2016).

Toxin detection

Ultra-high performance liquid chromatography-tandem mass spectrometry (UPLC-MS/MS) was performed for toxin detection. Detailed mushroom sample preparations, analysis of muscarine, amatoxins and phallotoxins (Alta Scientific Co., Ltd., Tianjin, China) referred to our previous works (Xu et al. 2020a, 2020b).

Detailed information for analysis of ibotenic acid and muscimol (Alta Scientific Co., Ltd., Tianjin, China) are as follows: chromatographic separation was conducted on an ACQUITY UPLC C8 column (2.1 × 100 mm, 1.7 μm; Waters, USA). Acetonitrile (A) and 4% formic acid aqueous solution (B) were used as mobile phase solvent flowing at 0.3 ml/min. The column was eluted by 2% A for 1.0 min, followed by 2%–70% A for 1.0 min, then by 70% A for 1.0 min and then by 70%–2% A for 0.5 min, finally by 2% A for 1.5 min. The analytical column was set at 40 °C. The injection volume was 10 μl. The positive MS/MS conditions can refer to muscarine (Xu et al. 2020b). The ion pairs were 115.1 > 68.1 (Cone at 16 V; Collision at 12 V), 159.1 > 113.1 (Cone at 16 V; Collision at 12 V) for ibotenic acid, as well as 115.1 > 98.1 (Cone at 15 V; Collision at 10 V), 115.1 > 68.1 (Cone at 15 V; Collision at 18 V) for muscimol.

For the analysis of psilocybin and psilocin (Alta Scientific Co., Ltd., Tianjin, China), the detailed descriptions are as follows. ACQUITY UPLC T3 column (2.1 × 100 mm, 1.7 μm; Waters, USA) was used as the separation column. The mobile phases were acetonitrile (A) and 10 mmol/l ammonium acetate aqueous solution (B). The flow rate was 0.3 ml/min. The column was eluted by 0% A for 0.5 min, followed by 0%–85% A for 4 min, then by 85% A for 1.5 min and then by 85%–0% A for 1.5 min, finally by 0% A for 2 min. The analytical column was set at 40 °C and the injection volume was 10 μl. The positive MS/MS conditions can refer to muscarine (Xu et al. 2020b). The ion pairs were 285.1 > 85.2 (Cone at 16 V; Collision at 18 V), 285.1 > 240.1 (Cone at 16 V; Collision at 17 V) for psilocybin and 205.1 > 58.2 (Cone at 26 V; Collision at 13 V), 205.1 > 160.1 (Cone at 26 V; Collision at 13 V) for psilocin.

Results

Phylogenetic analyses

Nine sequences (three ITS, three LSU and three *rpb2*) were newly generated and submitted to GenBank. The best-fit model selected by MrModeltest was GTR+I+G for each gene equally. The three-gene data matrix consisted of 104 taxa and 2890 sites. The final multilocus alignment used for phylogenetic reconstruction was submitted to TreeBase (ID29310). The Bayesian Inference and Maximum Likelihood trees were similar in topology; thus, only the BI tree was presented (Fig. 1). In the BI tree (Fig. 1), all *Pseudosperma* taxa grouped in a fully supported clade and three Chinese specimens

Figure 1. Phylogram generated by Bayes Inference (BI) analysis, based on a combined sequences dataset from nuclear genes (rDNA-ITS, nrLSU and *rpb2*), rooted with *Mallocybe terrigena* (Pruned). Bayesian Inference posterior probabilities (BI-PP) ≥ 0.95 and ML bootstrap proportions (ML-BP) ≥ 70 are represented as BI-PP/ML-BP.

and a European specimen (JV26578) clustered in an independent lineage with full support. The lineage clustered with the lineage composed of *I. aureocitrinum* (Esteve-Rav.) Matheny & Esteve-Rav. but with limited support.

Taxonomy

Pseudosperma arenarium **Y.G. Fan, Fei Xu, Hai J. Li & Vauras, sp. nov.**
MycoBank No: 842603
Figs 2, 3

Etymology. refers to its habitat of sandy soils.

Holotype. China, Ningxia Hui Autonomous Region, Wuzhong, Yanchi County, Yanchi Railway Station, on sandy ground under *Populus alba* × *P. berolinensis*, 5 Oct 2020, NXYC20201005-01 (FCAS3571, holotype). GenBank accession nos.: ITS-OM304278, LSU-OM304287, *rpb2*-OM421667.

Diagnosis. Basidiomata robust, pileus beige, ivory white or yellowish; basidiospores > 13 μm, cylindrical to cylindrical-ellipsoid, cheilocystidia thin-walled. Occurs under artificial plantations of *Populus alba* × *P. berolinensis* or open seashore forest of *Pinus sylvestris* Linn. Differs from *P. arenicola* by longer basidiospores and phylogenetic distance.

Basidiomata. medium-sized, robust. Pileus 35–65 mm in diameter, spherical to hemispherical when young, convex, dome-shaped to applanate when mature, not umbonate, margin inrolled at first, becoming depressed, straight, to uplifted or recurved in age; surface dry, glabrous to slightly fibrillose, occasionally rimulose to rimose at the margin, with distinct sandy remnants; yellowish (1A2) to ochraceous (1A4), paler outwards, ivory white (1B1) to greyish-white (1B2) when dried. Lamellae crowded, up to 8 mm in width, adnexed to sub-free, not equal, alternately distributed with three tiers of lamellula, initially pure white to creamy white (1A2), becoming yellowish (4A3), brownish (5B6) to cinnamon (5C8) with age, yellowish-brown (4B8) to dark brown (6C7) after drying, edge pinkish-white, fimbricate. Stipe 40–100 × 7–20 mm, solid, equal or slightly tapering downwards, sometimes swollen towards the base, but not marginate, longitudinally fibrillose with scattered squamules, white to ivory white (1B1–1B2) with pinkish tinge (11A3) when fresh, yellowish (5A4) to brownish (5B5) upon drying. Context solid, white and fleshy in pileus, 2–5 mm in thickness, fibrillose in the stipe, striate and shiny, white to somewhat pinkish (7A2). Odour fungoid or slightly spermatic.

Basidiospores. [170/6/4] (13–)14–20(–21) × (6–)7–9.2(–11) μm, median 16.4 × 7.8 μm, Q = (1.6–)1.75–2.64(–2.95), Q_m = 2.12 ± 0.27, yellow-brown, smooth, mostly cylindrical to cylindrical-ellipsoid, less often narrowly ellipsoid to nearly phaseoliform. Basidia 32–42 × 11–14 μm, clavate, usually narrower downwards, four-spored, sterigmata up to 10 μm long, translucent with oily inclusions, occasionally with yellowish pigments. Pleurocystidia absent. Lamellae edge sterile.

Figure 2. *Pseudosperma arenarium* and its habitat **a** basidiospores **b, c** cheilocystidia **d–h** basidiomata. Scale bars: 10 μm (**a–c**); 10 mm (**d–h**). Photos by Xu Fei, Li Hai-Jiao & Zhao Li-Na.

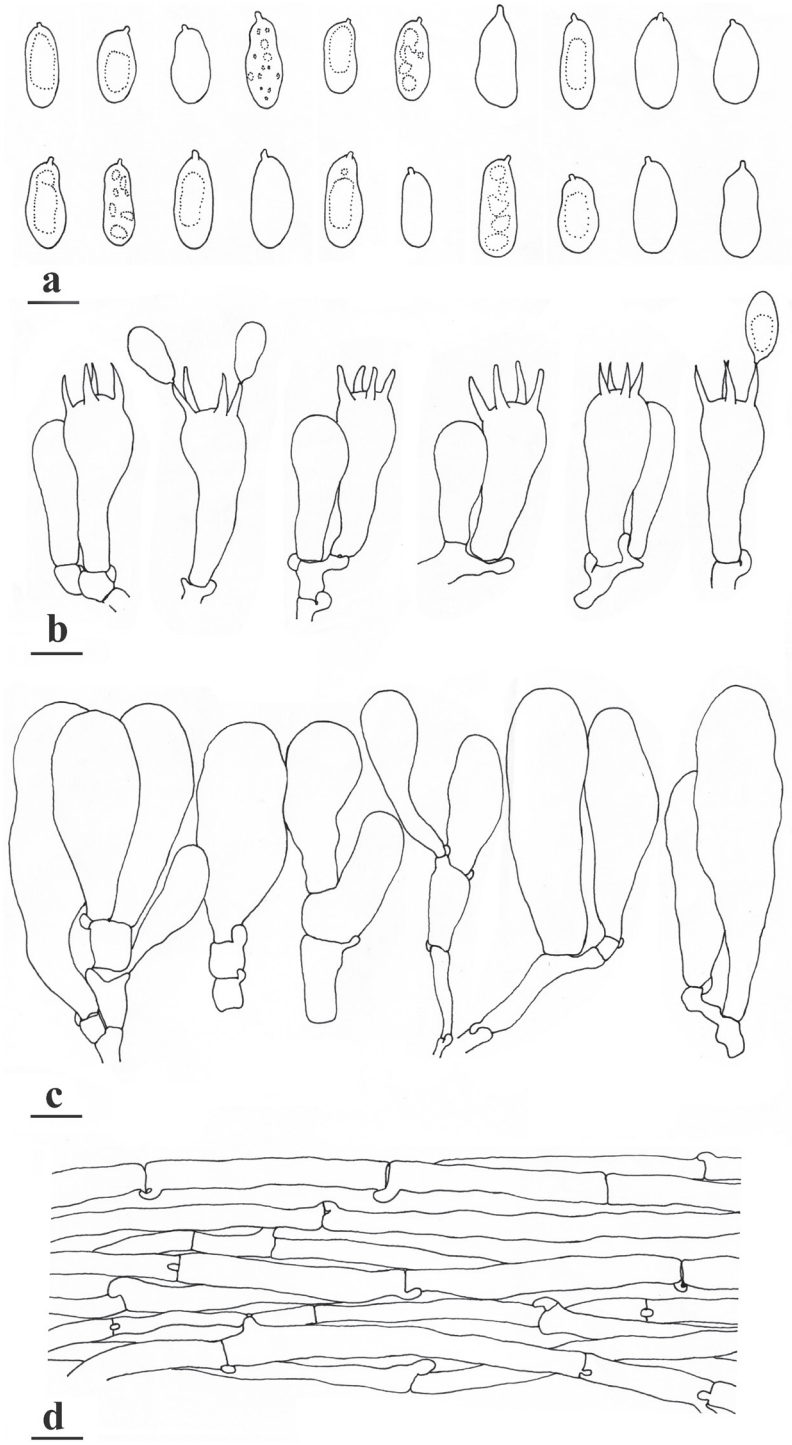

Figure 3. Microfeatures of *Pseudosperma arenarium* (holotype) **a** basidiospores **b** basidia **c** cheilocystidia **d** pileipellis. Scale bars: 10 μm (**a–d**). Line drawings by Li Hai-Jiao.

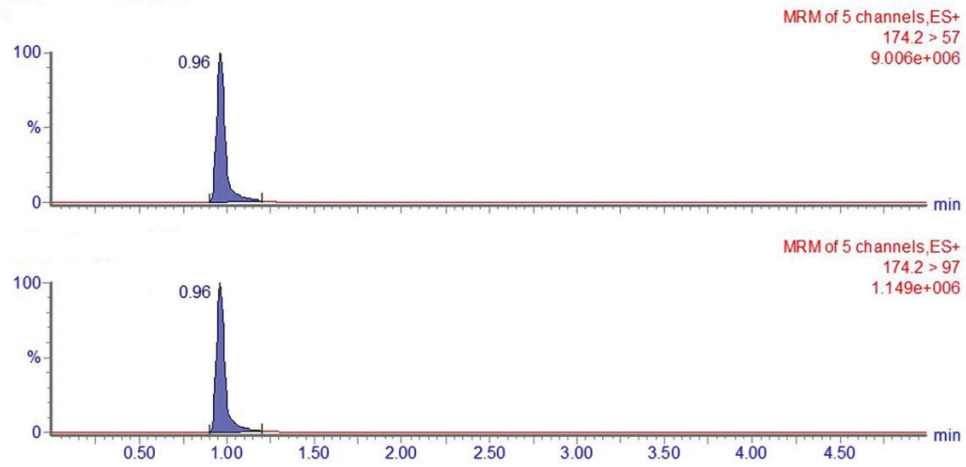

Figure 4. MRM chromatograms of muscarine from *Pseudosperma arenarium* (holotype).

Cheilocystidia 30–77 × 12–23 µm, thin-walled, colourless, broadly clavate or fusiform, rarely septate, translucent or occasionally with golden yellow inclusions, walls yellowish. Caulocystidia not observed. Hymenophoral trama nearly regularly arranged, composed of translucent and pale yellow, thin-walled hyphae up to 22 µm wide. Pileipellis a cutis, regularly arranged, orange-brown to brownish in 5% KOH, composed of cylindrical hyphae 4–15 µm in diameter; pileal trama made up of compact, parallel, hyaline hyphae, pale yellow in mass. Stipitipellis a cutis frequently disrupted by loose hyphal projections, hyphae thin-walled, colourless, 3–16 µm wide. Stipe trama regularly and densely arranged, yellowish in mass, hyphae thin-walled, colourless, 8–21 µm wide. Oleiferous hyphae 4–15 µm wide, present in pileus and stipe, bright yellow, smooth, often bent, occasionally branched or catenate. Clamp connections are common in all tissues.

Habitat. individual or scattered on sandy and saline-alkali soil under artificial plantations of *Populus alba* × *P. berolinensis* in China and open seashore forest of *Pinus sylvestris* in Estonia. Fruiting in autumn, from late September to early October.

Known distribution. China (Ningxia and Shaanxi), Estonia.

Additional materials examined. China. Ningxia Hui Autonomous Region, Wuzhong, Yanchi Country, on sandy ground under *Populus alba* × *P. berolinensis*, 22 Sep 2021, NX20210922-57 (FCAS3572), GenBank accession nos.: ITS-OM304279, LSU-OM304288, *rpb2*-OM421668; Shaanxi Province, Yulin, Dingbian Country, Yanchangbao Country, Xiliangwan Village, on sandy ground under *Populus alba* × *P. berolinensis*, 30 Sep 2021, SX20210930-65 (FCAS3573), GenBank accession nos.: ITS-OM304280, LSU-OM304289, *rpb2*-OM421669. Estonia. Saaremaa, Kaarma Municipality, Mändjala, open seashore forest with *Pinus sylvestris* Linn., on fine calcareous sand, 19 Sep 2008, Jukka Vauras 26578F (TUR-A182630), GenBank no.: ITS and LSU-FJ904154.

Muscarine detection

The new species contained only muscarine (Fig. 4), whereas amatoxins, phallotoxins, ibotenic acid, muscimol, psilocybin and psilocin were not detected. The quantitative results are expressed by (X ± U; k = 2, p = 95%; Xu et al. 2020a, 2020b). The muscarine content in the holotype (NXYC20201005-01) between different basidiomata ranged from 3981.4 ± 796.4 to 4074.2 ± 801.3 mg/kg (k = 2, p = 95%) in the pilei and from 811.2 ± 162.3 to 883.3 ± 176.5 mg/kg (k = 2, p = 95%) in the stipes (Table 1). The muscarine content from different specimens ranged from 4012.2 ± 803.1 to 4302.3 ± 863.2 mg/kg (k = 2, p = 95%) in the pilei and from 850.4 ± 171.1 to 929.1 ± 184.2 mg/kg (k = 2, p = 95%) in the stipes (Table 2).

Table 1. Muscarine content in different parts from different basidiomata of the holotype (mg/kg).

Collection number	Basidiomata 1		Basidiomata 2		Basidiomata 3		Basidiomata 4		Basidiomata 5	
	Stipe	Pileus	Stipe	Pileus	Stipe	Pileus	Stipe	Pileus	Stipe	Pileus
NXYC20201005-01	816.2 ± 163.1	3981.4 ± 796.4	816.8 ± 17.1	4004.4 ± 801.1	811.2 ± 162.3	4025.4 ± 805.3	834.3 ± 167.1	4054.3 ± 801.6	883.3 ± 176.5	4074.2 ± 801.3

Table 2. Muscarine content in different parts from different specimens collected from different locations.

Collection numbers	Muscarine (mg/kg)	
	Stipes	Pilei
NXYC20201005-01	850.4 ± 171.1	4012.2 ± 803.1
NX20210922-57	929.1 ± 184.2	4302.3 ± 863.2
SX20210930-05	863.2 ± 172.5	4085.2 ± 816.2

Discussion

The new species is known from three localities in Ningxia and Shaanxi of north-western China and is a locally common mushroom that occurs in late autumn under sandy poplar plantations (Fig. 2). As *Populus alba* × *P. berolinensis* plantations are widely distributed over north-western China, the new species may have broader distribution in adjacent areas. Moreover, the European material JV26578 collected in Estonia clustered with the new species with full support in the phylogenetic results. This collection also grew on calcareous fine sand, but under *Pinus sylvestris*. According to the file notes, the specimen also has robust basidiomata (pileus up to 38 mm broad, stipes 50–55 × 7–9 mm) with ochraceous pileus and stipes and fungoid or slightly spermatic odour. The microfeatures of JV26578 have cylindrical-ellipsoid basidiospores measuring (13.5–)13.9–16.5(–18.2) × (7.1–)7.2–8.5(–8.8) µm (average, 15.3 × 7.7 µm), Q = 1.8–2.2(–2.25) [average, 1.98 (n = 20)] and clavate cheilocystidia measuring (34–)40–62(–70) × 14–20(–22) µm [average, 50 × 18 µm (n = 20)]. Except for the ochraceous tinge in pileus and stipes, no distinct macroscopical difference was observed between the Chinese materials and the Estonian specimen. The European specimen JV26578 is now considered conspecific with the Chinese materials. Accordingly, the new species has a Eurasian distribution.

Pseudosperma arenarium is characterised by its tricholomoid habit, dirty whitish to ochraceous and glabrous pileus, crowded lamellae with fimbriate edges, large cylindrical basidiospores and thin-walled cheilocystidia. The thick and long persistent velipellis gives its pileus a nearly smooth and whitish appearance. In the field, the pileus, stipe and lamellae surfaces are usually covered with humose sands, showing a dirty yellowish or sometimes brownish colour, especially in older individuals. Its mostly large cylindrical basidiospores are microscopically impressive, but cylindrical ellipsoid to elongated ellipsoid basidiospores also exist in the same individual. With the combination of the characteristics listed above, the new species is distinctive. Without examining its microscopic features or molecular sequence analyses, a mycologist or even an Inocybaceae specialist is unlikely to be able to identify it exactly into the genus *Pseudosperma*. Unexpectedly, the three-gene phylogeny places *P. arenarium* in the *P. rimosum* complex, which clusters with the lineage that unified the type material of *P. aureocitrinum* and a sample labelled as '*P.* cf. *rimosum*.' However, *P. aureocitrinum* has a typical inocyboid habit, yellowish-tinged basidiomata and broadly ellipsoid to subovoid basidiospores and occurs in Mediterranean evergreen oak forests (Esteve-Raventós 2014).

Pseudosperma arenicola (R. Heim) Matheny & Esteve-Rav., a European species also occurring on coastal sandy soils, is similar in having a whitish appearance, long-persisting thick velipellis and long basidiospores, but it has a less robust habit, relatively short basidiospores measuring 11.5–12–18.5 × 6.0–6.4–7.5 µm (Kuyper 1986), different ecological associations and different phylogenetic positions (Heim 1931; Kuyper 1986; Stangl 1989). *Pseudosperma pseudo-orbatum* (Esteve-Rav. & García Blanco) Matheny & Esteve-Rav. is a whitish species originally described from Spain, resembling the new species in having thick velipellis, non-rimose pileus, large cylindrical basidiospores and clavate cheilocystidia. However, it is distinguished by having pinkish lamellae when young, stockier stipes and an association with *Pinus pinaster* Ait. and *P. pinea* L. (Esteve-Raventós et al. 2003). *Pseudosperma niveivelatum* (D.E. Stuntz ex Kropp, Matheny & L.J. Hutchison) Matheny & Esteve-Rav., a North American species, shares white thick velipellis, elongated large basidiospores and ecological association with *Populus tremuloides* Michx. and conifers. However, it differs by its sericeous pileus, shorter basidiospores measuring 11.5–13.9–18.5 × 6.0–6.4–7.5 µm, slender cheilocystidia (Kropp et al. 2013) and a clinically insignificant amount of muscarine (Kosentka et al. 2013).

Muscarine is a neurotoxin that causes salivation, sweating, delirium and even coma or death (Işiloğlu et al. 2009; Xu et al. 2020b). In recent years, more and more poisoning cases have been caused by eating Inocybaceae mushrooms containing toxic muscarine (Li et al. 2020, 2021a, 2022; Xu et al. 2020b). According to literature, five *Pseudosperma* species have been assayed; of these, *P. rimosum* (Bull.) Matheny & Esteve-Rav., *P. niveivelatum*, *P. sororium* (Kauffman) Matheny & Esteve-Rav. and *P. spurium* (Jacobsson & E. Larss.) Matheny & Esteve-Rav. contain muscarine; only *P. perlatum* (Cooke) Matheny & Esteve-Rav. was reported lacking muscarine (Kosentka et al. 2013). Xu et al. (2020b) reported that the muscarine content of *I. serotina* Peck in a poisoning incident was 324.0 ± 62.4 mg/kg wet weight. Li et al. (2021b) reported that the muscarine content in *I. squarrosolutea* (Corner & E. Horak) Garrido and *I. squarrosofulva* S.N. Li, Y.G. Fan & Z.H. Chen were 136.4 ± 25.4 to 1683.0 ± 313.0

and 31.2 ± 5.8 to 101.8 ± 18.9 mg/kg dry weight, respectively. Deng et al. (2021b, 2022) found that muscarine content in *Inosperma muscarium* Y.G. Fan, L.S. Deng, W.J. Yu & N.K. Zeng, *I. hainanense* Y.G. Fan, L.S. Deng, W.J. Yu & N.K. Zeng and *I. zonativeliferum* Y.G. Fan, H.J. Li, F. Xu, L.S. Deng & W.J. Yu were 16.03 ± 1.23, 11.87 ± 3.02 and [2.08 ± 0.05 (pileus) and 6.53 ± 1.88 (stipes)] g/kg dry weight, respectively. In this study, results showed that *P. arenarium* is a muscarine-positive species with middle- and upper-level muscarine content and also led to three poisoning incidents with a total of seven patients in northwest China during the past 2 years (Li et al. 2021a, 2022). Interestingly, the muscarine content in caps was approximately five times higher than in stipes. Although some studies showed that the toxin amount in the cap is higher than in the stipes (Hu et al. 2012; Garcia et al. 2015; Sun et al. 2018, 2019), the mechanism of such difference is still not clear. Li et al. (2021b) reported that the muscarine content of *Inocybe squarrosolutea* varied a lot in different specimens. However, in this study, the muscarine content in the mushroom samples collected from the same or three different places showed no significant difference. Additionally, no amatoxins, phallotoxins, ibotenic acid, muscimol, psilocybin and psilocin were detected in all samples. This study described *P. arenarium* as a new species, based on morphological, ecological, molecular and toxic evidence. The publicity and education of the new species are needed to control and prevent mushroom poisoning incidents.

Acknowledgements

This study was supported by the National Natural Science Foundation of China (Nos. 31501814, 31860009 & 31400024), the Natural Science Foundation of Ningxia (No. 2020AAC03437) and the Hainan Basic and Applied Research project for cultivating high level talents (No. 2019RC230). We also thank the anonymous reviewers for their corrections and suggestions to improve our work.

References

Bandini D, Oertel B (2020) Three new species of the genus *Pseudosperma* (Inocybaceae). Czech Mycology 72(2): 221–250. https://doi.org/10.33585/cmy.72205

Bandini D, Oertel B, Eberhardt U (2021) Even more fibre-caps (2): Thirteen new species of the family Inocybaceae. Mycologia Bavarica = Bavarian Journal of Mycology 21: 27–98.

Bau T, Fan YG (2018) Three new species of *Inocybe* sect. *Rimosae* from China. Junwu Xuebao 37(6): 693–702. https://doi.org/10.13346/j.mycosystema.180033

Cervini M, Bizio E, Alvarado P (2020) Quattro nuove specie italiane del Genere *Pseudosperma* (Inocybaceae) con odore di miele. Rivista di Micologia 63(1): 3–36.

Deng LS, Yu WJ, Zeng NK, Liu LJ, Liu LY, Fan YG (2021a) *Inosperma subsphaeorosporum*, a new species (Inocybaceae) from tropical China. Phytotaxa 502(2): 169–178. https://doi.org/10.11646/phytotaxa.502.2.5

Deng LS, Kang R, Zeng NK, Yu WJ, Chang C, Xu F, Deng WQ, Qi LL, Zhou YL, Fan YG (2021b) Two new *Inosperma* (Inocybaceae) species with unexpected muscarine contents from tropical China. MycoKeys 85: 87–108. https://doi.org/10.3897/mycokeys.85.71957

Deng LS, Yu WJ, Zeng NK, Zhang YZ, Wu XP, Li HJ, Xu F, Fan YG (2022) A new muscarine-containing *Inosperma* (Inocybaceae, Agaricales) species discovered from one poisoning incident occurring in tropical China. Frontiers in Microbiology 13: 1–12. https://doi.org/10.3389/fmicb.2022.923435

Esteve-Raventós F (2014) *Inocybe aureocitrina* (Inocybaceae), a new species of section *Rimosae* from Mediterranean evergreen oak forests. Plant Biosystems 148(2): 377–383. https://doi.org/10.1080/11263504.2013.877532

Esteve-Raventós F, Blanco AG, Carazo MS, Val JBD (2003) *Inocybe aurantiobrunnea* and *I. pseudoorbata*, two new Mediterranean species found in the Iberian peninsula. Österreichische Zeitschrift für Pilzkunde 12: 89–99.

Fan YG, Bau T (2013) Two striking *Inocybe* species from Yunnan Province, China. Mycotaxon 123(1): 169–181. https://doi.org/10.5248/123.169

Garcia J, Oliveira A, Pinho PG, Freitas V, Carvalho A, Baptista P, Pereira E, Bastos ML, Carvalho F (2015) Determination of amatoxins and phallotoxins in *Amanita phalloides* mushrooms from northeastern Portugal by HPLC-DAD-MS. Mycologia 107(4): 679–687. https://doi.org/10.3852/14-253

Gardes M, Bruns TD (1993) ITS primers with enhanced specificity for basidiomycetes – application to the identification of mycorrhizae and rusts. Molecular Ecology 2(2): 113–118. https://doi.org/10.1111/j.1365-294X.1993.tb00005.x

Ge YP, Liu Z, Zeng H, Cheng X, Na Q (2021) Updated description of *Atheniella* (Mycenaceae, Agaricales), including three new species with brightly coloured pilei from Yunnan Province, southwest China. MycoKeys 81: 139–164. https://doi.org/10.3897/mycokeys.81.67773

Hall TA (1999) BioEdit: A user-friendly biological sequence alignment editor and analysis program for Windows 95/98/NT. Nucleic Acids Symposium Series 41(41): 95–98.

Heim R (1931) Le genre *Inocybe*. Encyclopédi mycologique 1: 1–429.

Hu JS, Zhang P, Zeng J, Chen ZH (2012) Determination of amatoxins in different tissues and development stages of *Amanita exitialis*. Journal of the Science of Food and Agriculture 92(13): 2664–2667. https://doi.org/10.1002/jsfa.5685

Işiloğlu M, Helfer S, Alli H, Yilmaz F (2009) A fatal *Inocybe* (Fr.) Fr. poisoning in Mediterranean Turkey. Turkish Journal of Botany 33(1): 71–73. https://doi.org/10.3906/bot-0605-2

Jabeen S, Khalid AN (2020) *Pseudosperma flavorimosum* sp. nov. from Pakistan. Mycotaxon-Ithaca Ny 135(1): 183–193. https://doi.org/10.5248/135.183

Jabeen S, Zainab, Bashir H, Khalid AN (2021) *Pseudosperma albobrunneum* sp. nov. from coniferous forests of Pakistan. Mycotaxon-Ithaca Ny 136(2): 361–372. https://doi.org/10.5248/136.361

Katoh K, Rozewicki J, Yamada KD (2019) MAFFT online service: Multiple sequence alignment, interactive sequence choice and visualization. Briefings in Bioinformatics 20(4): 1160–1166. https://doi.org/10.1093/bib/bbx108

Kornerup A, Wanscher JH (1978) The methuen handbook of colour 3rd edn. Eyre Methuen Ltd. Reprint, London, 252 pp.

Kosentka P, Sprague S, Ryberg M, Gartz J, May A, Campagna S, Matheny PB (2013) Evolution of the toxins muscarine and psilocybin in a family of mushroom-forming fungi. PLoS ONE 8(5): e64646. https://doi.org/10.1371/journal.pone.0064646

Kropp BR, Matheny PB, Hutchison LJ (2013) *Inocybe* section *Rimosae* in Utah: Phylogenetic affinities and new species. Mycologia 105(3): 728–747. https://doi.org/10.3852/12-185

Kuyper TW (1986) A revision of the genus *Inocybe* in Europe. I. Subgenus *Inosperma* and the smooth-spored species of subgenus *Inocybe*. Persoonia (Suppl 3): 1–247.

Larsson E, Ryberg M, Moreau PA, Mathiesen AD, Jacobsson S (2009) Taxonomy and evolutionary relationships within species of section *Rimosae* (*Inocybe*) based on ITS, LSU and mtSSU sequence data. Persoonia 23(1): 86–98. https://doi.org/10.3767/003158509X475913

Li HJ, Zhang HS, Zhang YZ, Zhang KP, Zhou J, Yin Y, Jiang SF, Ma PB, He Q, Zhang YT, Wen K, Yuan Y, Lang N, Lu JJ, Sun CY (2020) Mushroom Poisoning Outbreaks – China, 2019. China CDC Weekly 2(2): 19–24. https://doi.org/10.46234/ccdcw2020.005

Li HJ, Zhang HS, Zhang YZ, Zhou J, Yin Y, He Q, Jiang SF, Ma PB, Zhang YT, Wen K, Yuan Y, Lang N, Cheng BW, Lu JJ, Sun CY (2021a) Mushroom poisoning outbreaks – China, 2020. China CDC Weekly 3(3): 41–45. https://doi.org/10.46234/ccdcw2021.014

Li SN, Xu F, Jiang M, Liu F, Wu F, Zhang P, Fan YG, Chen ZH (2021b) Two new toxic yellow *Inocybe* species from China: Morphological characteristics, phylogenetic analyses and toxin detection. MycoKeys 81: 185–204. https://doi.org/10.3897/mycokeys.81.68485

Li HJ, Zhang HS, Zhang YZ, Zhou J, Yin Y, He Q, Jiang SF, Ma PB, Zhang YT, Yuan Y, Lang N, Cheng BW, Wang M, Sun CY (2022) Mushroom Poisoning Outbreaks – China, 2021. China CDC Weekly 4(3): 35–40. https://doi.org/10.46234/ccdcw2022.010

Matheny PB (2005) Improving phylogenetic inference of mushrooms with RPB1 and RPB2 nucleotide sequences (*Inocybe*, Agaricales). Molecular Phylogenetics and Evolution 35(1): 1–20. https://doi.org/10.1016/j.ympev.2004.11.014

Matheny PB (2009) A phylogenetic classification of the Inocybaceae. McIlvainea 18(1): 11–21.

Matheny PB, Hobbs AM, Esteve-Raventós F (2020) Genera of Inocybaceae: New skin for the old ceremony. Mycologia 112(1): 83–120. https://doi.org/10.1080/00275514.2019.1668906

Na Q, Hu YP, Zeng H, Song ZZ, Ding H, Cheng XH, Ge YP (2022) Updated taxonomy on *Gerronema* (Porotheleaceae, Agaricales) with three new taxa and one new record from China. MycoKeys 89: 87–120. https://doi.org/10.3897/mycokeys.89.79864

Nylander J (2004) MrModeltest V2. program distributed by the author. Bioinformatics (Oxford, England) 24: 581–583. https://doi.org/10.1093/bioinformatics/btm388

Ronquist F, Teslenko M, van der Mark P, Ayres DL, Darling A, Höhna S, Larget B, Liu L, Suchard MA, Huelsenbeck JP (2012) MrBayes 3.2: Efficient Bayesian Phylogenetic Inference and Model Choice across a Large Model Space. Systematic Biology 61(3): 539–542. https://doi.org/10.1093/sysbio/sys029

Saba M, Haelewaters D, Pfister DH, Khalid AN (2020) New species of *Pseudosperma* (Agaricales, Inocybaceae) from Pakistan revealed by morphology and multi-locus phylogenetic reconstruction. MycoKeys 69: 1–31. https://doi.org/10.3897/mycokeys.69.33563

Stangl J (1989) Die Gattung *Inocybe* in Bayern. Hoppea 46: 1–409.

Sun J, Li HJ, Zhang HS, Zhang YZ, Xie JW, Ma PB, Guo C, Sun CY (2018) Investigating and analyzing three cohorts of mushroom poisoning caused by *Amanita exitialis* in Yunnan, China. Human and Experimental Toxicology 37(7): 665–678. https://doi.org/10.1177/0960327117721960

Sun J, Zhang HS, Li HJ, Zhang YZ, He Q, Lu JJ, Yin Y, Sun CY (2019) A case study of *Lepiota brunneoincarnata* poisoning with endoscopic nasobiliary drainage in Shandong, China. Toxicon 161: 12–16. https://doi.org/10.1016/j.toxicon.2019.02.017

Tamura K, Peterson D, Peterson N, Stecher G, Nei M, Kumar S (2011) Mega5: Molecular evolutionary genetics analysis using maximum likelihood, evolutionary distance, and maximum parsimony methods. Molecular Biology and Evolution 28(10): 2731–2739. https://doi.org/10.1093/molbev/msr121

Trifinopoulos J, Nguyen LT, von Haeseler A, Minh BQ (2016) W-IQ-TREE: A fast online phylogenetic tool for maximum likelihood analysis. Nucleic Acids Research 44(W1): 1–4. https://doi.org/10.1093/nar/gkw256

Vilgalys R, Hester M (1990) Rapid genetic identification and mapping of enzymatically amplified ribosomal DNA from several *Cryptococcus* species. Journal of Bacteriology 172(8): 4238–4246. https://doi.org/10.1128/jb.172.8.4238-4246.1990

Wang SN, Hu YP, Chen JL, Qi LL, Zeng H, Ding H, Huo GH, Zhang LP, Chen FS, Yan JQ (2021) First record of the rare genus *Typhrasa* (Psathyrellaceae, Agaricales) from China with description of two new species. MycoKeys 79: 119–128. https://doi.org/10.3897/mycokeys.79.63700

Xu F, Gong BL, Xu ZX, Wang JJ (2020a) Reverse-phase/phenylboronic-acid-type magnetic microspheres to eliminate the matrix effects in amatoxin and phallotoxin determination via ultra high performance liquid chromatography-tandem mass spectrometry. Food Chemistry 332: 49–55. https://doi.org/10.1016/j.foodchem.2020.127394

Xu F, Zhang YZ, Zhang YH, Guan GY, Zhang KP, Li HJ, Wang JJ (2020b) Mushroom poisoning from *Inocybe serotina*: A case report from Ningxia, northwest China with exact species identification and muscarine detection. Toxicon 179: 72–75. https://doi.org/10.1016/j.toxicon.2020.03.003.

Yu WJ, Chang C, Qin LW, Zeng NK, Wang SX, Fan YG (2020) *Pseudosperma citrinostipes* (Inocybaceae), a new species associated with *Keteleeria* from southwestern China. Phytotaxa 450(1): 8–16. https://doi.org/10.11646/phytotaxa.450.1.2

Supplementary material 1

Table S1

Authors: Ya-Ya Yan ,Yi-Zhe Zhang, Jukka Vauras, Li-Na Zhao, Yu-Guang Fan, Hai-Jiao Li, Fei Xu

Data type: Table (pdf file)

Explanation note: Information of taxa used in phylogenetic analysis. Newly sequenced collections are bold.

Link: https://doi.org/10.3897/mycokeys.92.86277.suppl1

MycoKeys 92: 95–108 (2022)
doi: 10.3897/mycokeys.92.83928
https://mycokeys.pensoft.net

RESEARCH ARTICLE

A peer-reviewed open-access journal
MycoKeys
Launched to accelerate biodiversity research

Two new species of *Trichoglossum* (Geoglossaceae, Ascomycota) from south Mexico

Javier Isaac de la Fuente[1], Jesús García-Jiménez[2], Tania Raymundo[3], Daniyal Gohar[4], Mohammad Bahram[5], Marcos Sánchez-Flores[2], Ricardo Valenzuela[3], Juan P. Pinzón[6]

1 *Colegio de Postgraduados, Km 36.5 Montecillo, Texcoco, 56230, Estado de México, Mexico* **2** *Tecnológico Nacional de México. Instituto Tecnológico de Ciudad Victoria. Blvd. Emilio Portes Gil #1301Pte, 87010, Ciudad Victoria, Tamaulipas, Mexico* **3** *Instituto Politécnico Nacional, Escuela Nacional de Ciencias Biológicas, Departamento de Botánica, Laboratorio de Micología, 11340, Cd. Mx., Mexicos* **4** *Institute of Ecology and Earth Sciences, University of Tartu, Lai 40, 51005, Tartu, Estonia* **5** *Department of Ecology, Swedish University of Agricultural Sciences, Ullsväg 16, 75651 Uppsala, Sweden* **6** *Departamento de Botánica, Facultad de Medicina Veterinaria y Zootecnia, Universidad Autónoma de Yucatán, carretera Mérida-Xmatkuil km 15.5, 97100, Mérida, Yucatán, Mexico*

Corresponding author: Tania Raymundo (raymundot.tr@gmail.com)

Academic editor: Chayanard Phukhamsakda | Received 17 March 2022 | Accepted 9 August 2022 | Published 30 August 2022

Citation: de la Fuente JI, García-Jiménez J, Raymundo T, Gohar D, Bahram M, Sánchez-Flores M, Valenzuela R, Pinzón JP (2022) Two new species of *Trichoglossum* (Geoglossaceae, Ascomycota) from south Mexico. MycoKeys 92: 95–108. https://doi.org/10.3897/mycokeys.92.83928

Abstract

Two new species of *Trichoglossum* are described from south Mexico based on morphological and molecular evidence. *Trichoglossum caespitosum* is characterized by the caespitose ascomata, rough and coiled paraphyses and the ascospores with 9–11 septa. *Trichoglossum tropicale* is characterized by the capitate ascomata, clavate and straight paraphyses and the ascospores with 10–12 septa. Both species grow in the tropical forests of the Yucatán peninsula. Here we provide descriptions and photographs for these species, together with a phylogenetic analyses based on the DNA sequences of nuc rDNA (ITS region and 28S gene) and a comparative table for the species known for America.

Keywords

Earth tongues, Geoglossomycetes, phylogeny, Quintana Roo, Tropical Ascomycetes

Introduction

The members of the genus *Trichoglossum* Boud. are characterized by club-like ascomata, usually with dark brown to black hues and acuminate setae covering both fertile and sterile parts of the ascomata, septate paraphyses, asci with 4 to 8 spores, and filiform, septate, brown ascospores. The genus is saprotrophic but is also present at the roots of plants as endophytic fungi (Rinaldi et al. 2008; Tedersoo et al. 2010; Wang et al. 2011; Hustad et al. 2013). They have a worldwide distribution in tropical and temperate forests (Mains 1954; Beug et al. 2014). Although the genus has been the focus of many phylogenetic studies, several species lack molecular data, which obstruct a better understanding of its phylogenetic relationships (Schoch et al. 2009; Ekanayaka et al. 2017). So far, 22 species of *Trichoglossum* are currently accepted (Ekanayaka et al. 2017; Lee et al. 2021; Chakraborty et al. 2022; Dasgupta et al. 2022; Index Fungorum, accessed May 2022).

In Mexico, five taxa of *Trichoglossum* have been recorded, mainly in temperate forest and even urban gardens: *T. hirsutum* (Pers.) Boud., *T. hirsutum* var. *hirsutum* (Pers.) Boud., *T. hirsutum* var. *heterosporum* Mains, *T. variabile* (E.J. Durand) Nanff., *T. velutipes* (Peck) E.J. Durand, and *T. walteri* (Berk.) E.J. Durand (Ramírez-López and Villegas-Ríos 2007; Raymundo et al. 2016). Most of the *Trichoglossum* collections have been made in Central Mexico, followed by a few collections from southern Mexico (Díaz-Barriga 1988; Ramírez-López and Villegas-Ríos 2007; Rodríguez-Alcántar et al. 2021; Valenzuela et al. 2021), so far, no *Trichoglossum* species has been recorded from the Yucatán Peninsula. In recent years, we have conducted several mycological explorations in southern Mexico, mainly in the state of Quintana Roo. During those explorations, several collections of *Trichoglossum* species were made, which resulted in identification of two new species. The aim of this study is to describe *Trichoglossum caespitosum* and *T. tropicale* supported by molecular and morphological characters. Further, a comparative table is provided for the species known for America.

Methods

Sampling data

Sampling of macrofungi was carried out in the Mexican state of Quintana Roo, in the Yucatán Peninsula (Fig. 1). The representative vegetation at the sampling sites was an urban garden with *Manilkara zapota* and an ecotone between a lowland forest and mangrove forest with *Yucca elephantipes*, *Metopium brownei*, *Gymnopodium floribundum*, *Conocarpus erectus*, and *Byrsonima crassifolia*. Hand cuts were made in dried specimens and mounted with KOH 5%; Melzer reagent was used to observe amyloid asci apex. At least 30 ascospores, asci, and paraphyses were measured to obtain ranges. The material was deposited at mycological collections of Instituto Politécnico Nacional (**ENCB**), Universidad Autónoma de Yucatán (**UADY**), and Instituto Tecnológico de Ciudad Victoria (**ITCV**).

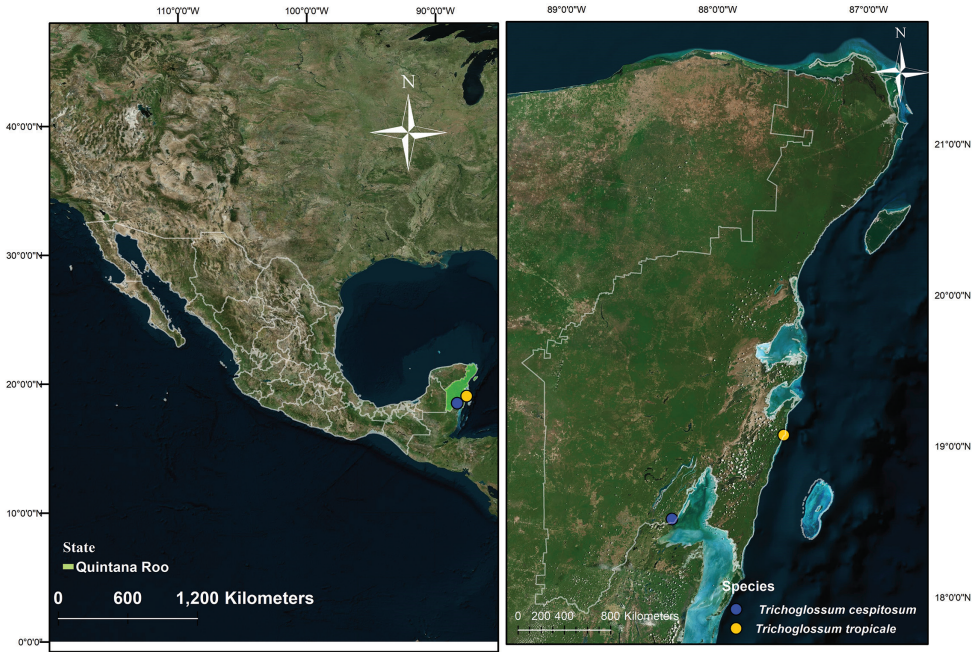

Figure 1. Map showing the collecting sites.

DNA extraction, amplification, and sequencing

Total DNA was extracted from silica-gel dried ascomata of the collected samples (specimens JF-208-ITCV and JF-526-ITCV), following a proteinase K protocol (Thermo Fisher Scientific, Waltham, MA, USA) according to Põldmaa et al. (2019). Samples were incubated in 100 µl of lysis buffer [0.8 M Tris-HCl, 0.2 M $(NH_4)_2SO_4$, 0.2% w/v Tween-20; Solis BioDyne, Tartu, Estonia] and 2.5 µl of proteinase K at 56 °C for 24 h, following by 15 min at 98 °C, and finally centrifuged for 2 min at 8000 rpm. Region nuc 28S rDNA (LSU) was amplified with the primers LR0R (Cubeta et al. 1991) and LR7 or LR5 (Vilgalys and Hester 1990), using 5× HOT FIREPol. Blend Master Mix (Solis BioDyne, Tartu, Estonia). The PCR protocol followed consisted of 35 cycles of 95 °C for 40 s, 55 °C for 1 min, and 72 °C for 1 min. ITS region nuc rDNA The Internal Transcribed Spacer (ITS) was amplified with the primer ITS5-ITS4 (White et al. 1990). The PCR protocol consisted of 35 cycles of 95 °C for 35 s, 58 °C for 1 min, and 72 °C for 2 min. The amplification program was run as follows: denaturalization at 95 °C for 4 min, 35 cycles of denaturalization at 95 °C for 1 min, annealing at 58 °C for 1 min, polymerization at 72 °C for 2 min, and final elongation at 72 °C for 10 min. Purification of the PCR products was performed with Exo-Sap enzymes (Sigma, St. Louis, Missouri) and sequenced at the Estonian Biocentre (Tartu, Estonia). Sequences were assembled in BIOEDIT 7.2.5 (Hall 1999), and compared against the sequences deposited in NCBI's database with a blastn analysis, using megablast (highly similar sequences). The sequences generated were deposited at NCBI GenBank.

Phylogenetic analyses

The taxa selection for the phylogenetic analysis was based on the available sequences of ITS and 28S of *Trichoglossum* in NCBI GenBank database considering the analysis of Geoglossomycetes by Hustad et al. (2013). All main clades within the class are represented, including all representatives of the *Trichoglossum* clade. Additionally, other specimens with ITS and 28S sequences available were included, such as *Hemileucoglossum pusillum* (GB: MF353090/NG_060706), *Leucoglossum leucosporum* (GB: KP272114/KP272115), and an uncultured Geoglossaceae (GB: D1273321/DQ273452). The molecular matrix was aligned using the MUSCLE algorithm (Edgar 2004), and variable and parsimony informative characters were calculated in MEGA 11 (Tamura et al. 2021); the DNA substitution model used in the phylogenetic analyses was selected following the Akaike Information Criterion (AIC) in MODELTEST 2.1.7 (Darriba et al. 2012).

A Bayesian inference analysis (BI) was performed in MrBayes 3.2.6 (Ronquist and Huelsenbeck 2003; Ronquist et al. 2012) of the concatenated matrix of ITS and 28S regions, which consisted of 1408 positions (703 of ITS and 705 of LSU), with 532 variable sites (37.8%) and 340 parsimony informative sites. (24.1%). The following parameters were set: substitution model GTR+I+G for both markers, two independent runs of 10 million generations, sampling every 1000 generations with one cold chain and three hot chains and the remaining parameters used as default. The substitution rates, character state frequency, gamma shape and proportion of invariable sites were unlinked for both partitions.

Additionally, a Maximum Likelihood (ML) analysis was carried out using the GTR+I+G substitution model and bootstrap (BS) based on 100 replicates using MEGA 11 (Tamura et al. 2021). The trees produced through the BI and ML analyses were visualized and edited with FigTree v.1.4.3 (Rambaut 2016).

Results

Phylogenetic analyses

For 28S, the blastn analysis of the collected specimens showed high levels of similarity (over 93%) with accessions of several genera within Geoglossales as well as with uncultured fungi from environmental DNA sequencing. The specimen JF-208-ITCV showed a maximum score with *Trichoglossum rasum* (GB: KY457227) (100% query cover, 98.69% identity), and the specimen JF-526-ITCV with *Trichoglossum hirsutum* (GB: KC222146) (100% query cover and 95.65% identity). For ITS, the sequence retrieved for the specimen JF-208-ITS was 384 bp in length, spanning the 18S gene (SSU) only (partial), so it could not be used for the phylogenetic analysis; however, the blastn analysis showed that the most similar sequences belong to the family Geoglossaceae: *Gluginoglossum* sp. (GB: OM672838), and two specimens of *Trichoglossum*

sp. (OM474029, OM672708), all with 78% of query cover and 78.86% of identity. For the specimen JF-526-ITCV the sequence was 528 bp and contained ITS1, 5.8S and ITS2; the most similar sequences in the blastn analysis were several specimens of *Trichoglossum* sp. from New Zealand, showing a query cover of 100% and identity over 99.24% (OM987287, OL653059, MH578528, OL653016, HQ222864); the most similar sequence of an identified specimen at the specific level was from *T. hirsutum*, also from New Zealand (query cover 99%, identity 98.67%).

The majority rule consensus tree produced by the BI analysis (Fig. 2) shows a moderately well supported clade (PP = 0.96) confirmed by all specimens of Geoglossomycetes, except

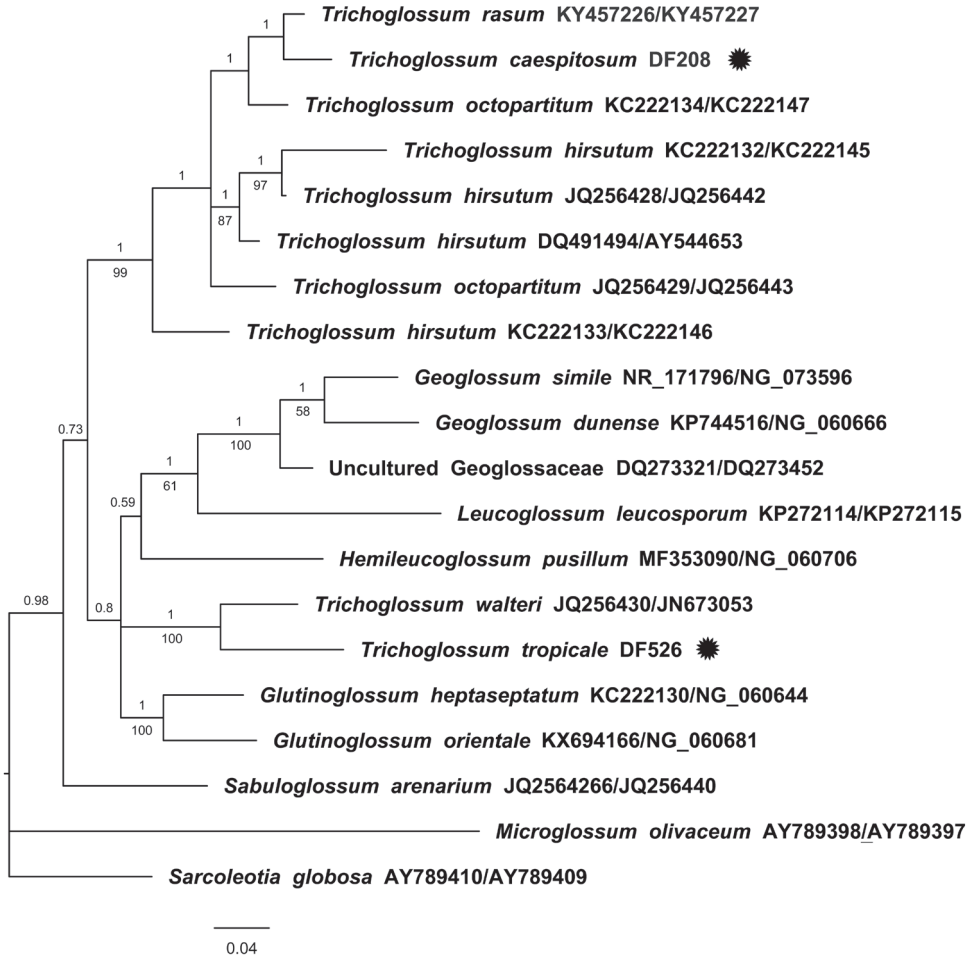

Figure 2. Majority rule consensus tree produced by a Bayesian Inference analysis of the concatenated matrix of nuc rDNA ITS1-5.8S-ITS2 and 28S (LSU) showing the phylogenetic position of *Trichoglossum caespitosum* (JF-208-ITCV) and *T. tropicale* (JF-525-ITCV) (marked with stars) within the Geoglossomycetes. GenBank accession numbers are indicated (ITS/28S). The posterior probabilities are shown above the branches, and bootstrap values (above 50) from a Maximum Likelihood analysis, below.

for *Sarcoleotia globosa*, which is collapsed at the base of the tree, together with *Microglossum olivaceum* (Leotiomycetes). Within the clade of Geoglossomycetes, *Sabuloglossum arenarium* is sister to the rest of the species (with a low posterior probability of 0.73), and two clades are identified, one formed by species of *Glutinoglossum*, *Hemileucoglossum*, *Leucoglossum*, *Geoglossum*, an uncultured Geoglossaceae, and the specimen JF-526-ITCV sister to *Trichoglossum walteri*, with a high support (PP = 1, BS = 100). The second clade is well supported (PP = 1, BS = 99), and it is composed exclusively with the rest of the species of *Trichoglossum* in which we find the specimen JF-208-ITCV, which is sister to *T. rasum* with a high posterior probability (PP = 1). Our phylogenetic analysis of *T. hirsutum* specimens suggests that the species is polyphyletic in its current circumscription. The topology of the ML tree (not shown) shows some incongruences with the BI majority rule tree, such as the position of *Hemileucoglossum pusillum* and of the specimen JF-208-ITCV, which is here sister to the clade of *T. hirsutum*-*T. octopartitum*-*T. rasum* but with low support (BS = 68). The remaining relationships were congruent with those obtained with the Bayesian Inference analysis.

Taxonomy

Trichoglossum caespitosum **de la Fuente, J. García & Raymundo, sp. nov.**
MycoBank No: 843008
Figs 3A–E, 5A–D

Holotype. Mexico. Quintana Roo: Othón P. Blanco Municipality, Chetumal, alt. 8 m, 18°31'N, 88°18'W, 01 December 2015, de la Fuente JF-208-ITCV; Isotype UADY 04867. GenBank: OM727118.

Diagnosis. *Trichoglossum caespitosum* is characterized by the unique combination of characters: Caespitose habit, paraphyses with rugose and coiled tips, and the ascospores of 119–127 × 5–7 µm with 9–11 septa.

Etymology. Named *caespitosum* in reference to the caespitose habit.

Description. ***Ascomata*** black, 18–30 × 4–10 mm, clavate to spathulate, stipitate, erect, caespitose, with compressed ascogenous portion of 3–7 mm long, 0.5–1 mm thick, glossoid, ellipsoidal, flattened, sometimes curved, black, hirsute with brownish to black setae projecting from the hymenium; ***stipe*** 1–33 mm long, up to 6 mm thick, cylindrical, solid, black to dark brown, hirsute.

Setae 250–300 × 5–9 µm, septate, smooth, straight, dark brown to black. ***Paraphyses*** filamentous, septate, with rugose, with wide, coiled to clavate terminal cells of 16–28 × 3–8 µm. ***Asci*** 183–221 × 16–20 µm, cylindrical to clavate, rounded at apex, short-pedicellate at the base, hyaline, thin walled, octosporic, inamyloid. ***Ascospores*** 119–127 × 5–7 µm, filiform, mostly 9–11 septate, slightly curved, hyaline when young, brown to olivaceous when mature, narrowed and rounded at both ends, thin walled, smooth.

Distribution. Known from the Mexican state of Quintana Roo, growing on soil under *Manilkara zapota* in urban vegetation.

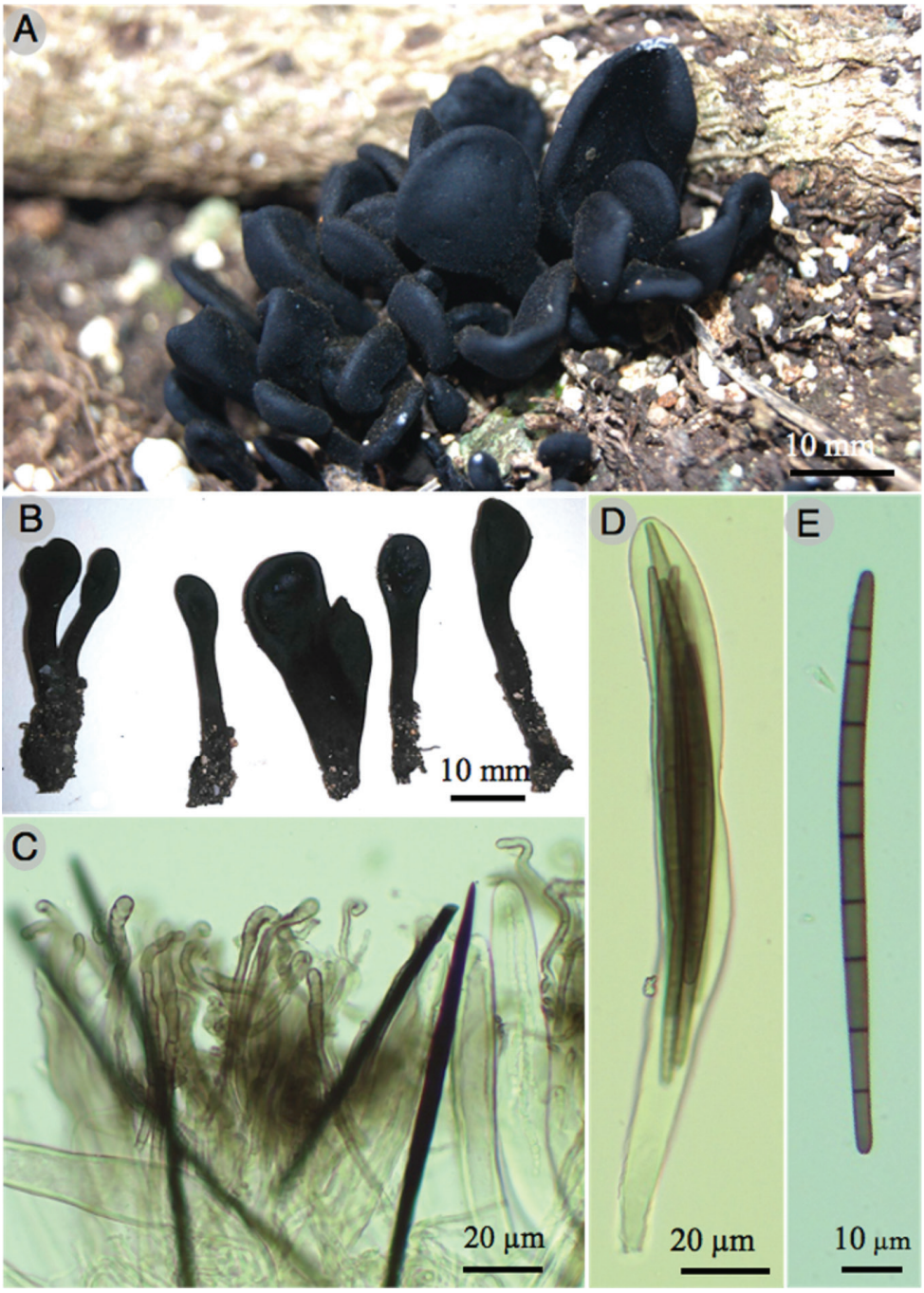

Figure 3. *Trichoglossum caespitosum* (Holotype) **A, B** ascomata **C** paraphyses, setae, and asci **D** detail of asci **E** ascospores. All microstructures are mounted in KOH.

Notes. This species differs from other species by the caespitose ascomata, paraphyses with rugose and coiled tips, and the ascospores of 119–127 × 5–7 µm with 9–11 septa. *Trichoglossum rasum* Pat. is morphologically similar by the octosporic asci, clavate spathulate ascoma with dark brown hues, and the tropical distribution but it differs in the bigger ascomata (10–60 mm), smaller setae (200–250 × 5–12 µm), larger ascospores (100–140 × 5–8 µm) with 3–7 septa (Mains 1954). *Trichoglossum octopartitum* Mains can also be found in the Yucatan peninsula biotic province and shows similar ascoma and ascospore size; nevertheless, the ascomata is never caespitose ascomata and shows 7-septate ascospores (Mains 1954; Ekanayaka et al. 2017). *Trichoglossum confusum* E.J. Durand has also similar ascoma size but differs in the smaller ascospores (57–75 × 5–7 µm) with 3–7 septa (Mains 1954).

Trichoglossum tropicale **de la Fuente, Sánchez-Flores & Raymundo, sp. nov.**
MycoBank No: 843009
Figs 4A–F, 5E–H.

Holotype. Mexico. Quintana Roo: Othón P. Blanco Municipality, Pulticub town, alt. 6 m, 19°04'N, 87°33'W, 04 February 2021, de la Fuente JF-526-ITCV, Isotype ENCB 140350. GenBank: OM727119.

Diagnosis. *Trichoglossum tropicale* is characterized by the combination of characteristics: capitate ascomata, straight paraphyses with bulbose tips, and the ascospores of 122–132 × 5–5.5 µm with 10–12 septa.

Etymology. Named *tropicale* in reference to the tropical occurrence.

Description. ***Ascomata*** black, 15–30 × 2–4 mm, clavate to capitate, stipitate, erect, solitary to gregarious with compressed ascogenous portion of 2–4 mm long, 1–2 mm thick, glossoid, ellipsoidal, flattened, sometimes curved, black, without visible setae. ***Stipe*** 10–20 mm long, up to 1 mm thick, cylindrical, solid, black to dark brown, hirsute.

Setae 98–200 × 5.5–6 µm, septate, smooth, straight, dark brown to black. ***Paraphyses*** filamentous, septate, with capitate to bulbous terminal cells of 8–46 × 6–10 µm. ***Asci*** 155–180 × 16–18 µm, cylindrical to clavate, rounded at apex, short-pedicellate at base, hyaline, thin walled, octosporic, inamyloid. ***Ascospores*** 122–132 × 5–5.5 µm, filiform, mostly 10–12 septate, slightly curved, hyaline when young, brown to olivaceous when mature, narrowed and rounded at both ends, thin walled, smooth.

Distribution. Known from the Mexican state of Quintana Roo, growing scattered on soil under *Birsonyma crassifolia*.

Notes. This new species differs from other *Trichoglossum* species by the combination of characteristics: ascomata with inconspicuous setae (98–200 × 5.5–6 µm), straight paraphyses with bulbose tips, and the ascospores of 122–132 × 5–5.5 µm with 10–12 septa. *Trichoglossum tropicale* is phylogenetically close to *T. walteri* but that species has ascospores of 60–125 × 5–6 µm with 7 septa and paraphyses curved to circinate (Mains 1954). A similar species is *T. hirsutum* due to the capitate ascomata, setae size (up to 225 µm long); differs in the thicker setae and larger ascospores

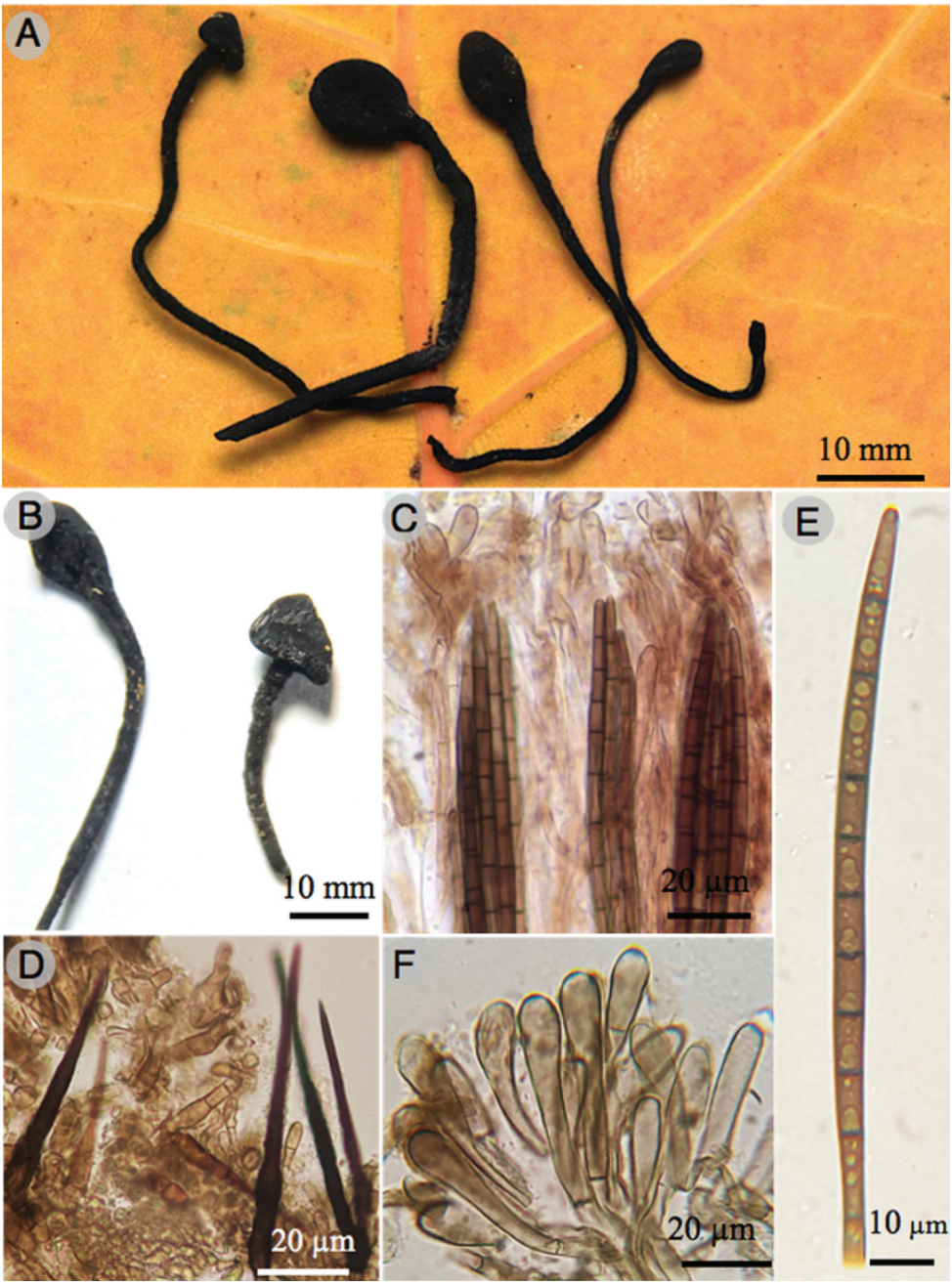

Figure 4. *Trichoglossum tropicale* (Holotype) **A, B** ascomata **C** asci **D** detail of setae **E** ascospore **F** detail of paraphyses. All microstructures are mounted in KOH.

(90–150 × 5–7 µm) with 15 septa (Beug et al. 2014). *Trichoglossum velutipes* has similar ascospore septation, but it has four-spored asci and bigger ascospores (110–145 × 6–7 µm) with 7–11 septa (Ekanayaka et al. 2017). *Trichoglossum variabile* has

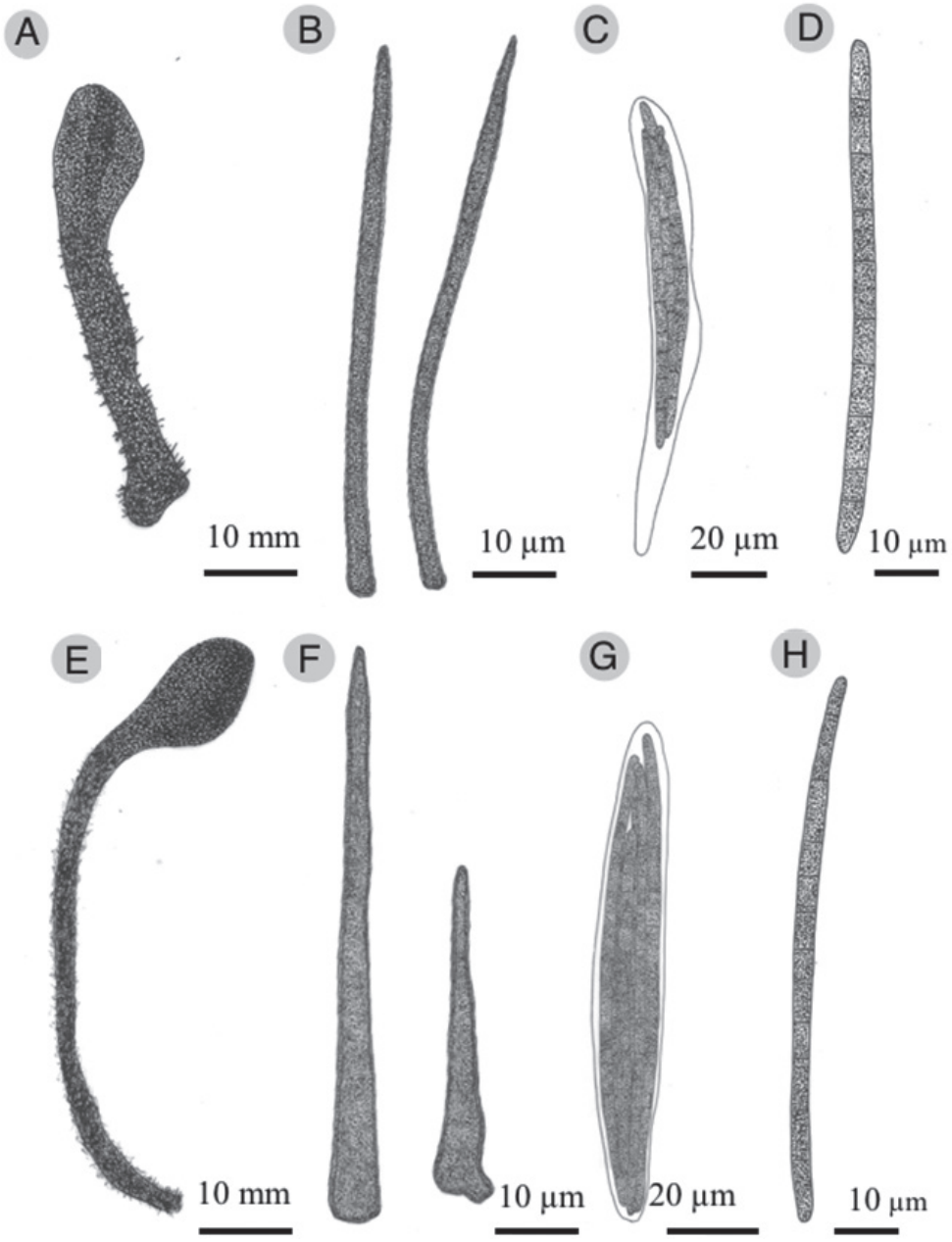

Figure 5. New *Trichoglossum* from Mexico. *Trichoglossum caespitosum* **A** ascomata **B** setae **C** ascus **D** ascospore. *Trichoglossum tropicale* **E** ascomata **F** setae **G** ascus **H** ascospore.

similar number of septa, but differs in the presence of four-spored asci, smaller setae (69–183 × 7.6–12 µm), and bigger ascospores (80–150 × 6 µm) with 9–14 septa (Mains 1954; Beug et al. 2014).

Table 1. Comparison of the species of *Tricholglossum* from America (according [1]Mains 1954; [2]Chacón and Guzmán 1983; [3]Ramírez-López and Villegas-Ríos 2007, and [4]this work).

Species	Asci (L = length × W = width)	Ascospores (L = length × W = width)
T. caespitosum[4]	184–220 × 16–20 µm, octosporic	120–128 × 5–7 µm, 9–11 septate
T. confusum[1]	150–200 × 12–16 µm, octosporic	45–75 × 5–6 µm, 7 septate
T. farlowii[1]	150–180 × 15–20 µm, octosporic	57–75 × 5–7 µm, 3–5 septate
T. hirsutum[1]	180–275 × 18–25 µm, octosporic	80–170 × 5–7 µm, 15 septate
T. hirsutum* var. *hirsutum[1,2]	180–250 × 14–16 (21.5) µm, octosporic	(80) 110–140 (170) × 5–7 µm, mostly 15 septate
T. hirsutum* var. *longisporum[1]	225–275 × 20–22 µm, octosporic	(120) 133–180 (195) × 6–7 µm, 15 septate
T. hirsutum* var. *irregulare[1]	No data	(90) 100–150 (165) × 5–7 µm, 15 septate, rarely 16–17
T. hirsutum* var. *heterosporum[1,3]	175–200 × 17–20 µm, octosporic	(95) 120–150 (160) × 5–6 (7) µm, less than 15 septate
T. hirsutum* var. *multiseptatum[1]	210–225 × 20–25 µm, octosporic	(145) 160–195 (210) × 6 µm, 12–22 septate
T. octopartitum[1]	175–200 × 18–20 µm, octosporic	(80) 100–120 (150) × 4–5.5 µm, 7–9 septate
T. rasum[1]	200–225 × 16–24 µm, octosporic	(50) 100–140 (175) × 5–8 µm, 3–9 septate
T. tetrasporum[1]	175–200 × 20–25 µm, tetrasporic	(110) 125–145 (150) × 6–7 µm, 0–17 septate
T. tropicale[4]	155–180 × 16–18 µm, octosporic	122–132 × 5–5.5 µm, 10–12 septate
T. variabile[1]	150–200 × 18–20 µm, octosporic	(80-) 110–130 (-150) × 4.5–6 µm, 4–16 septate
T. velutipes[1]	180–200 × 16–20 µm, tetrasporic	(90) 110–145 (160) × 6–7 µm, 7–13 septate
T. walteri[1]	165–200 × 15–18 µm, octosporic	(60) 72–100 (125) × 5–6 µm, 7 septate

Discussion

The results of the phylogenetic analyses are concordant with those of Hustad et al. (2013), recovering the Geoglossomycetes clade (except for *Sarcoleotia globosa*, collapsed at the base), as well as the *Geoglossum*, *Glutinoglossum*, and *Trichoglossum* clades. The inclusion of *Trichoglossum walteri* and *T. tropicale* in this clade make the genus non-monophyletic. Both species, *T. walteri* and *T. tropicale*, form a small clade close to *Glutinoglossum*, nevertheless both species have setae, an absent feature within *Glutinoglosssum*. Based on morphology and phylogenetic data (data set nuc rDNA), we describe and propose *Trichoglossum caespitosum* and *T. tropicale* as new species that inhabit tropical vegetations and associate with *Manilkara zapota* and *Birsonyma crassifolia* respectively in the Yucatán Peninsula.

Trichoglossum caespitosum is very close morphologically and phylogenetically to *T. rasum* (KY457226; KY457227), but differs because of its ascospores of 100–140 × 5–8 µm, 3–9 septa, bulbous and curved tips paraphyses; this species was described from New Caledonia (Patouillard 1909) and later it was cited from Bermuda, Cuba, Panama (Mains 1954) and India (Prabhugaonkar and Pratibha 2017). *Trichoglossum octopartitum* is phylogenetically related but differs mainly in the non-caespitose ascomata and the 7-septate ascospores (Mains 1954). According to our phylogenetic study, *T. caespitosum* is related to *T. hirsutum*. This species has been recorded in America, Asia and Europe; nevertheless, this could be a species complex or polyphyletic group

and needs further detailed study (Hustad et al. 2013). The main differences between *T. caespitosum* and *T. hirsutum* are the caespitose ascomata of the new species and the number of septa per ascospore. Whereas the ascospores of *T. caespitosum* show 9–11 septa, the ascospores of *T. hirsutum* generally show 15 septa; ascospores with fewer than 15 septa are rare according to Mains (1954). *Trichoglossum tropicale* is phylogenetically close to *T. walteri* (JQ256443) from North Carolina but differs in that it has spores with a size of 90–100 × 4–5.5 µm and paraphyses curved to circinate, besides, the type specimen of *T. walteri* is from Australia, but it was cited from Brazil, Jamaica, and the United States of America (Durand 1908; Mains 1954).

According to the blastn analysis of the ITS region, several sequences from New Zealand are close to the one obtained from *T. tropicale*. Nevertheless, those species are not described yet. Ekanayaka et al. (2017) gave a morphological description of a specimen from China that they referred to as *T. cf. octopartitum*. ITS sequences provided by Hustad et al. (2013) revealed that the species is also located in North America (being Belize the type locality) and Europe as well. Microscopical differences of the American species of *Trichoglossum* are presented in Table 1.

Acknowledgements

The first author thanks Karina Can, León Ibarra, Silvia Bautista and César Ramiro Martínez-González and Alfonso Daniel Gay-González for field and technical support. García-Jiménez thanks CONACYT, PRODEP, Tecnológico Nacional de México, Instituto Tecnológico de Ciudad Victoria, and the Estonian Science Foundation grant (PRG632) for financial support. Raymundo and Valenzuela thank the Instituto Politécnico Nacional with the project (SIP): 20220030 and 20221348. Also, we thank the reviewers and editors for their kind observations on the manuscript.

References

Beug MW, Bessette AE, Bessette AR (2014) Ascomycetes fungi from North America. University of Texas Press, Austin, 502 pp. https://doi.org/10.7560/754522

Chacón S, Guzmán G (1983) Ascomycetes poco conocidos de México. Boletín de la Sociedad Mexicana de Micología 18: 183–218.

Chakraborty N, Tarafder E, Paul A, Paloi A, Acharya K (2022) *Trichoglossum benghalense* (Geoglossales, Ascomycota) from India: New to science. Phytotaxa 536(1): 72–82. https://doi.org/10.11646/phytotaxa.536.1.4

Cubeta MA, Echandi E, Abernethy T, Vilgalys R (1991) Characterization of anastomosis groups of binucleate *Rhizoctonia* species using restriction analysis of an amplified ribosomal RNA gene. Phytopathology 81(11): 1395–1400. https://doi.org/10.1094/Phyto-81–1395

Darriba D, Taboada GL, Doallo R, Posada D (2012) jModelTest 2: More models, new heuristics and parallel computing. Nature Methods 9(8): 772. https://doi.org/10.1038/nmeth.2109

Dasgupta D, Baishkhiyar A, Chakraborty N (2022) A world review on the genus *Trichoglossum* (Geoglossales, Ascomycota). Kavaka 58(1): 33–39. https://doi.org/10.36460/Kavaka/58/1/2022/33–39

Díaz-Barriga H (1988) Primer registro de *Trichoglossum velutipes* (Geoglossaceae, Ascomycetes) Para México. Acta Botánica Mexicana 2(2): 1–4. https://doi.org/10.21829/abm2.1988.561

Durand EJ (1908) The Geoglosaceae of North America. Ann Myc 6: 387–477.

Edgar RC (2004) MUSCLE: Multiple sequence alignment with high accuracy and high throughput. Nucleic Acids Research 32(5): 1792–1797. https://doi.org/10.1093/nar/gkh340

Ekanayaka AH, Hyde KD, Gareth-Jones EB, Zhao Q, Elgorban AM, Bahkali AH (2017) A new species of *Trichoglossum* (Geoglossales, Ascomycota) from Thailand. Phytotaxa 316(2): 161–170. https://doi.org/10.11646/phytotaxa.316.2.5

Hall TA (1999) BioEdit: A user-friendly biological sequence alignment editor and analysis program for Windows 95/98/NT. Nucleic Acids Symposium Series 41: 95–98.

Hustad VP, Miller AN, Dentinger BTM, Cannon PF (2013) Generic circumscriptions in Geoglossomycetes. Persoonia 31(1): 101–111. https://doi.org/10.3767/003158513X671235

Lee SH, Ko PY, Koh KB, Jun YW, Kim YJ, Jung YH, Yoon WJ, Oh DJ (2021) A new species of *Trichoglossum* (Geoglossales, Ascomycota) from South Korea. Phytotaxa 527(2): 117–124. https://doi.org/10.11646/phytotaxa.527.2.4

Mains EB (1954) North American species of *Geoglossum* and *Trichoglossum*. Mycologia 46(5): 586–631. https://doi.org/10.1080/00275514.1954.12024398

Patouillard N (1909) Champignons de la Nouvelle Calédonie. Bull. Soc. Myc. France 25: 129–134.

Põldmaa K, Bills G, Lewis DP, Tamm H (2019) Taxonomy of the *Sphaerostilbella broomeana*-group (Hypocreales, Ascomycota). Mycological Progress 18(1–2): 77–89. https://doi.org/10.1007/s11557-018-01468-w

Prabhugaonkar A, Pratibha J (2017) New record of *Trichoglossum rasum* from Asia Mycosphere 8(4): 583–591. https://doi.org/10.5943/mycosphere/8/4/7

Rambaut A (2016) FigTree v1.4.3. Institute of Evolutionary Biology, University of Edimburgh, Edimburgh. http://tree.bio.ed.ac.uk/software/figtree/

Ramírez-López I, Villegas-Ríos M (2007) El conocimiento taxonómico de Geoglossaceae sensu lato (Fungi: Ascomycetes) en México con énfasis en la zona centro y sur. Revista Mexicana de Micología 25: 41–49.

Raymundo T, Soto-Agudelo R, Bautista-Hernández S, Morales-Campos AR, Valenzuela R (2016) Catálogo de los ascomicetos del bosque mesófilo de montaña de Tlanchinol, Hidalgo. Boletin de la Sociedad Micologica de Madrid 40: 83–108.

Rinaldi AC, Comandini O, Kuyper TW (2008) Ectomycorrhizal fungal diversity: Separating the wheat from the chaff. Fungal Diversity 33: 1–45.

Rodríguez-Alcántar O, Herrera-Fonseca MJ, Sáldivar-Sánchez AE, Figueroa-García D (2021) Registros nuevos de macromicetos para Jalisco, México. e-CUCBA 8: 10–20. https://doi.org/10.32870/e-cucba.v0i15.175

Ronquist F, Huelsenbeck JP (2003) MrBayes 3: Bayesian phylogenetic inference under mixed models. Bioinformatics 19(12): 1572–1574. https://doi.org/10.1093/bioinformatics/btg180

Ronquist F, Teslenko M, van der Mark P, Ayres DL, Darling A, Höhna S, Larget B, Liu L, Suchard MA, Huelsenbeck JP (2012) MrBayes 3.2: Efficient Bayesian phylogenetic inference and model choice across a large model space. Systematic Biology 61(3): 539–542. https://doi.org/10.1093/sysbio/sys029

Schoch CL, Wang Z, Townsend JP, Spatafora JW (2009) Geoglossomycetes cl. nov., Geoglossales ord. nov., and taxa above class rank in the Ascomycota tree of life. Persoonia 22(1): 129–138. https://doi.org/10.3767/003158509X461486

Tamura K, Stecher G, Kumar S (2021) MEGA11: Molecular evolutionary genetics analysis version 11. Molecular Biology and Evolution 38(7): 3022–3027. https://doi.org/10.1093/molbev/msab120

Tedersoo L, May TW, Smith ME (2010) Ectomycorrhizal lifestyle in fungi: Global diversity, distribution, and evolution of phylogenetic lineages. Mycorrhiza 20(4): 217–263. https://doi.org/10.1007/s00572-009-0274-x

Valenzuela R, Raymundo T, Reyes P, Guzmán-Guillermo J, Acosta S, Ramírez-Martínez C, Luna-Vega I (2021) Ascomycetes from the relic forest of *Oreomunnea mexicana*, Oaxaca Mexico. Phyotaxa 528(1): 19–44. https://doi.org/10.11646/phytotaxa.528.1.3

Vilgalys R, Hester M (1990) Rapid genetic identification and mapping of enzymatically amplified ribosomal DNA from several *Cryptococcus* species. Journal of Bacteriology 172(8): 4238–4246. https://doi.org/10.1128/jb.172.8.4238-4246.1990

Wang Z, Nilsson RH, Lopez-Giraldez F, Zhuang W, Dai Y, Johnston PR, Townsend JP (2011) Testing soil fungal diversity with earth tongues: Phylogenetic test of SATé alignments for environmental ITS data. PLoS ONE 6(4): e19039. https://doi.org/10.1371/journal.pone.0019039

White TJ, Bruns TD, Lee S, Taylor JW (1990) Amplification and direct sequencing of fungal ribosomal RNA genes for phylogenies. In: Innis MA, Gelfand DH, Sninsky JJ, White TJ (Eds) PCR Protocols: a guide to methods and applications. Academic Press, San Diego, 135–322. https://doi.org/10.1016/B978-0-12-372180-8.50042-1

MycoKeys 92: 109–130 (2022)
doi: 10.3897/mycokeys.92.86160
https://mycokeys.pensoft.net

RESEARCH ARTICLE

A peer-reviewed open-access journal
MycoKeys
Launched to accelerate biodiversity research

Multigene phylogeny and morphology reveal *Ophiocordyceps hydrangea* sp. nov. and *Ophiocordyceps bidoupensis* sp. nov. (Ophiocordycipitaceae)

Weiqiu Zou[1,2*], Dexiang Tang[1,2*], Zhihong Xu[1], Ou Huang[1,2], Yuanbing Wang[1], Ngoc-Lan Tran[3], Hong Yu[1]

1 *Yunnan Herbal Laboratory, College of Ecology and Environmental Sciences, Yunnan University, Kunming 650504, Yunnan, China* **2** *School of Life Science, Yunnan University, Kunming 650504, Yunnan, China* **3** *Institute of Regional Research and Development, Ministry of Science and Technology, Hanoi, Vietnam*

Corresponding author: Hong Yu (hongyu@ynu.edu.cn, herbfish@163.com)

Academic editor: Cecile Gueidan | Received 5 May 2022 | Accepted 10 August 2022 | Published 30 August 2022

Citation: Zou W, Tang D, Xu Z, Huang O, Wang Y, Tran N-L, Yu H (2022) Multigene phylogeny and morphology reveal *Ophiocordyceps hydrangea* sp. nov. and *Ophiocordyceps bidoupensis* sp. nov. (Ophiocordycipitaceae). MycoKeys 92: 109–130. https://doi.org/10.3897/mycokeys.92.86160

Abstract

Ophiocordyceps species have a wide range of insect hosts, from solitary beetle larva to social insects. However, among the species of *Ophiocordyceps*, only a few attack cicada nymphs. These species are mainly clustered in the *Ophiocordyceps sobolifera* clade in *Ophiocordyceps*. A new entomopathogenic fungus parasitic on cicada nymphs, and another fungus parasitic on the larva of Coleoptera, are described in this study. The two new species viz. *Ophiocordyceps hydrangea* and *Ophiocordyceps bidoupensis* were introduced based on morphology and multigene phylogenetic evidence. The phylogenetic framework of *Ophiocordyceps* was reconstructed using a multigene (nr*SSU*, nr*LSU*, *tef-1α*, *rpb1*, and *rpb2*) dataset. The phylogenetic analyses results showed that *O. hydrangea* and *O. bidoupensis* were statistically well-supported in the *O. sobolifera* clade, forming two separate subclades from other species of *Ophiocordyceps*. The distinctiveness of these two new species was strongly supported by both molecular phylogeny and morphology.

Keywords

2 new taxa, entomopathogenic fungi, morphology, phylogenetic analyses

* Those authors contributed equally to this work.

Introduction

Ophiocordyceps G.H. Sung, J.M. Sung, Hywel-Jones & Spatafora is the largest genus in the Ophiocordycipitaceae, comprising approximately 290 species. It was originally established by Petch, with *Ophiocordyceps blattae* Petch as the type species (Petch 1931). According to the arrangement of the perithecia, the size of asci, ascospores, and secondary ascospores, *Ophiocordyceps* was transferred to *Cordyceps* sensu lato by Kobayasi, as a subgenus of *Cordyceps* s.l. (Kobayasi 1941, 1982). Sung et al. (2007) used five to seven loci combined molecular datasets to revise the *Cordyceps* and the Clavicipitaceae. The species of *Cordyceps* and Clavicipitaceae were divided into three families (Cordycipitaceae, Ophiocordycipitaceae, Clavicipitaceae sense stricto) and four genera (*Cordyceps* sense stricto, *Ophiocordyceps*, *Elaphocordyceps*, and *Metacordyceps*). The research results of Sung et al. (2007) are currently the most widely accepted phylogenetic classification of *Cordyceps* s.l. In 2015, *Ophiocordyceps* was divided into *O. ravenelii* clade, *O. unilateralis* clade, *O. sobolifera* clade, and *O. sphecocephala* clade by Sanjuan et al. With the continuous revision of *Ophiocordyceps*, it has now been divided into four clades, including the *Hirsutella* clade, *O. sobolifera* clade, *O. sphecocephala* clade, and *O. ravenelii* clade (Mains 1958; Sung et al. 2007; Quandt et al. 2014; Sanjuan et al 2015; Simmons et al. 2015; Wang et al. 2018). Many phylogenetic classifications for entomopathogenic fungi have been revised in recent studies (Wang et al. 2018; Fan et al. 2021; Wang et al. 2021a, 2021b).

There are fewer species in the *O. sobolifera* clade than in the *Hirsutella* clade and the *O. sphecocephala* clade. The *O. sobolifera* clade is statistically well-supported in most studies and 11 species have been described in the Index Fungorum (Kobayasi and Shimizu 1963; Hywel-Jones 1995b; Sung et al. 2007, 2011; Luangsa-ard et al. 2008; Hyde et al. 2017; Crous et al. 2018, 2019; Lao et al. 2021; Wang et al. 2021a). Asexual morphs of *Ophiocordyceps* were reported as *Hirsutella* Pat., *Paraisaria* Samson & B.L. Brady, *Sorosporella* Sorokin, *Hymenostilbe* Petch and *Syngliocladium* Petch, etc. (Sung et al. 2007; Quandt et al. 2014). In most species of *Ophiocordyceps*, their dominant asexual morphs were *Hirsutella*, the conidiogenous cells basally swollen that taper to a narrow neck, producing a mucilaginous cluster of one or several conidia (Simmons et al. 2015; Wang et al. 2018).

Ophiocordyceps species have a wide range of insect hosts, from solitary beetle larvae to social insects. More than 10 insect orders were attacked, including Hemiptera, Coleoptera, Lepidoptera, Blattaria, Dermaptera, Diptera, Hymenoptera, Isoptera, Megaloptera, and Mantodea (Araújo et al. 2015; Araújo and Hughes 2016, 2019). Entomopathogenic fungi whose hosts are cicada nymphs have attractive stromata. The most typical representative of this group was *Cordyceps cicadae* (Miquel) Massee (Massee 1895) in Cordycipitaceae, with the stroma like a flower (Sung et al. 2007). However, for species of *Ophiocordyceps*, with cicada nymph hosts including *O. khonkaenensis* Tasanathai, Thanakitpipattana & Luangsa-ard (Crous et al. 2019), *O. sobolifera* (Hill ex Watson) G.H. Sung, J.M. Sung,

Hywel-Jones & Spatafora (Kobayasi and Shimizu 1963; Sung et al. 2007), and *O. longissima* (Kobayasi) G.H. Sung, J.M. Sung, Hywel-Jones & Spatafora (Kobayasi and Shimizu 1963; Sung et al. 2007, 2011) in *O. sobolifera* clade, their stromata were typically bright-colored and cylindrical. The hosts of the entomopathogenic fungi within the *O. sobolifera* clade were divided into two categories. One group with Hemiptera hosts was represented by *O. sobolifera.* These fungi had a hard texture stroma, which was cylindrical, and deep-colored, and had swollen fertile parts (Kobayasi and Shimizu 1963; Sung et al. 2011; Crous et al. 2019). Another group had Coleoptera hosts that were characterized by hard texture stromata, being cylindrical, bright-colored, and with a sterile apices cone at the top of the stroma (Hywel-Jones 1995b; Luangsa-ard et al. 2008; Crous et al. 2018; Lao et al. 2021; Wang et al. 2021a).

Cordyceps s.l. is globally distributed with the highest species diversity recorded in subtropical and tropical regions (Nguyen and Vo 2005; Ban et al. 2015; Doan et al. 2017; Luangsa-ard et al. 2018), especially in East and Southeast Asia (Sung et al. 2007; Fan et al. 2021; Wang et al. 2021a). To date, more than 800 species of *Cordyceps* and *Ophiocordyceps* have been named worldwide, and there are at least 200 species in China (Index Fungorum 2022). Yunnan Province, located in southwest China, has unique geographical and ecological features. Many species of *Ophiocordyceps* were reported from Yunnan, including *O. alboperitheciata* H. Yu, Q. Fan & Y.B. Wang (Fan et al. 2021), *O. furcatosubulata* H. Yu, Y. Wang & Y.B. Wang (Wang et al. 2021a), *O. highlandensis* Zhu L. Yang & J. Qin (Yang et al. 2015), *O. lanpingensis* H. Yu & Z.H. Chen (Chen et al. 2013), *O. laojunshanensis* J.Y. Chen, Y.Q. Cao & D.R. Yang (Chen et al. 2011), *O. liangshanensis* (M. Zang, D.Q. Liu & R.Y. Hu) H. Yu, Y. Wang, Y.D. Dai, Zhu L. Yang & Y.B. Wang (Wang et al. 2021b), and *O. pingbianensis* H. Yu, S.Q. Chen & Y.B. Wang (Chen et al. 2021). The unique geographical conditions of Yunnan have resulted in high *Cordyceps* s.l. species diversity. There is also a high species diversity of *Cordyceps* s.l. in Southeast Asia, where more than 500 species of entomopathogenic fungi have been reported. Approximately 400 species of entomopathogenic fungi are distributed in Thailand (Sung et al. 2007; Luangsa-ard et al. 2011, 2018; Ban et al. 2015; Tasanathai et al. 2019; Xiao et al. 2019). Vietnam is second to Thailand, in the number of entomopathogenic fungi species, with more than 100 species having been reported such as *Moelleriella pumatensis* T.T. Nguyen & N.L. Tran (Mongkolsamrit et al. 2011), *O. furcatosubulata* H. Yu, Y. Wang & Y.B. Wang (Wang et al. 2021a), and *O. puluongensis* H. Yu, Z.H. Xu, N.L. Tran & Y.B. Wang (Xu et al. 2022). These findings suggested that Vietnam should be abundant in species diversity of *Cordyceps* s.l. (Mongkolsamrit et al. 2011; Doan et al. 2017; Luyen et al. 2017).

Several studies have evaluated the taxonomy and biology of entomopathogenic fungi, especially species found in China and Southeast Asia. In this study, one unknown species of *Ophiocordyeps* attacking a cicada nymph was collected from Yunnan Province, Jinghong City, Nabanhe National Nature Reserve, in China. Another

Table 1. Specimen information and GenBank accession numbers of the sequences used in this study.

Species	Host	Isolate no./ specimen no.	GenBank accession no.				
			*nrS*SU	nr*LSU*	*tef-1α*	*rpb1*	*rpb2*
Hirsutella citriformis	Cixiidae (Hemiptera)	ARSEF 1446	KM652065	KM652106	KM651990	KM652031	–
Hirsutella fusiformis	*Brachyderes incanus* (Curculionidae, Coleoptera)	ARSEF 5474	KM652067	KM652110	KM651993	KM652033	–
Hirsutella gigantea	Pamphiliidae (Hymenoptera)	ARSEF 30	–	JX566977	JX566980	KM652034	–
Hirsutella guyana	*Empoasca kraemeri* (Cicadellidae, Hemiptera)	ARSEF 878	KM652068	KM652111	KM651994	KM652035	–
Hirsutella illustris	*Eriosoma lanigerum* (Aphididae, Hemiptera)	ARSEF 5539	KM652069	KM652112	KM651996	KM652037	–
Hirsutella kirchneri	*Abacarus hystrix* (Eriophyidae, Acari)	ARSEF 5551	KM652070	KM652113	KM651997	–	–
Hirsutella lecaniicola	*Parthenolecanium corni* (Coccidae, Hemiptera)	ARSEF 8888	KM652071	KM652114	KM651998	KM652038	–
Hirsutella liboensis	Larva of Cossidae (Lepidoptera)	ARSEF 9603	KM652072	KM652115	KY415588	KY945367	–
Hirsutella necatrix	Acari	ARSEF 5549	KM652073	KM652116	KM651999	KM652039	–
Hirsutella nodulosa	*Dioryctria zimmermani* (Pyralidae, Lepidoptera)	ARSEF 5473	KM652074	KM652117	KM652000	KM652040	–
Hirsutella radiata	Diptera	ARSEF 1369	KM652076	KM652119	KM652002	KM652042	–
Hirsutella rhossiliensis	*Mesocriconema xenoplax* (Criconematidae, Tylenchida)	ARSEF 3747	KM652080	KM652123	KM652006	KM652045	–
Hirsutella strigosa	*Nephotettix virescens* (Cicadellidae, Hemiptera)	ARSEF 2197	KM652085	KM652129	KM652012	KM652050	–
Hirsutella subulata	Microlepidoptae (Lepidoptera)	ARSEF 2227	KM652086	KM652130	KM652013	KM652051	–
Hirsutella thompsonii var. *synnematosa*	*Aceria sheldoni* (Eriophyidae, Acari)	ARSEF 2459	KM652099	KM652147	KM652027	KM652061	–
Hirsutella thompsonii var. *thompsonii*	*Phyllocoptruta oleivora* (Eriophyidae, Acari)	ARSEF 137	KM652087	KM652131	KM652014	KM652052	–
Hirsutella thompsonii var. *vinacea*	*Acalitus vaccinii* (Eriophyidae, Acari)	ARSEF 254	KM652101	KM652149	KM652028	KM652062	–
Ophiocordyceps acicularis	Larva of Coleoptera	OSC 110987	EF468950	EF468805	EF468744	EF468852	–
Ophiocordyceps acicularis	Larva of Coleoptera	OSC 110988	EF468951	EF468804	EF468745	EF468853	–
Ophiocordyceps agriotidis	Larva of Coleoptera	ARSEF 5692	DQ522540	DQ518754	DQ522322	DQ522368	DQ522418
Ophiocordyceps annulata	Larva of Coleoptera	CEM 303	KJ878915	KJ878881	KJ878962	KJ878995	–
*Ophiocordyceps aphodi*i	Larva of Scarabaeidae (Coleoptera)	ARSEF 5498	DQ522541	DQ518755	DQ522323	–	DQ522419
Ophiocordyceps appendiculata	Larva of Coleoptera	NBRC 106960	JN941728	JN941413	AB968577	JN992462	AB968539
Ophiocordyceps arborescens	Larva of *Pueraria lobata* (Lepidoptera)	NBRC 105891	AB968386	AB968414	AB968572	–	AB968534
Ophiocordyceps bidoupensis	**Larva of Elateridae (Coleoptera)**	**YFCC 8793**	**OM304638**	–	**OK556894**	**OK556898**	**OK556900**
Ophiocordyceps bidoupensis	**Larva of Elateridae (Coleoptera)**	**YHH 20036**	**OK571396**	–	**OK556893**	**OK556897**	**OK556899**
Ophiocordyceps brunneanigra	Cicadellidae (Hemiptera)	TBRC 8093	–	MF614654	MF614638	MF614668	MF614681
Ophiocordyceps brunneaperitheciata	Larva of Lepidoptera	TBRC 8100	–	MF614658	MF614643	–	MF614685
Ophiocordyceps brunneipunctata	Larva of Elateridae (Coleoptera)	OSC 128576	DQ522542	DQ518756	DQ522324	DQ522369	DQ522420
Ophiocordyceps citrina	Hemiptera	TNS F18537	–	KJ878903	KJ878983	–	KJ878954
Ophiocordyceps cochlidiicola	Cochlididae pupa (Lepidoptera)	HMAS 199612	KJ878917	KJ878884	KJ878965	KJ878998	–
Ophiocordyceps cossidarum	Larva of Cossidae (Lepidoptera)	MFLU 17-0752	MF398186	MF398187	MF928403	MF928404	–
Ophiocordyceps crinalis	Larva of Lepidoptera	GDGM 17327	KF226253	KF226254	KF226256	KF226255	–
Ophiocordyceps evansii	*Pachycondyla harpax* adult ant (Hymenoptera)	HUA 186159	KC610796	KC610770	KC610736	KP212916	–
Ophiocordyceps formicarum	Formicidae (Hymenoptera)	TNS F18565	KJ878921	KJ878888	KJ878968	KJ879002	KJ878946

Species	Host	Isolate no./ specimen no.	GenBank accession no.				
			*nrS*SU	nr*LSU*	*tef-1α*	*rpb1*	*rpb2*
Ophiocordyceps forquignonii	Adult fly (Diptera)	OSC 151902	KJ878912	KJ878876	–	KJ878991	KJ878945
Ophiocordyceps furcatosubulata	Larva of Elateridae (Coleoptera)	YFCC 904	MT774216	MT774223	MT774244	MT774230	MT774237
Ophiocordyceps furcatosubulata	Larva of Elateridae (Coleoptera)	YHH 17005	MT774217	MT774224	MT774245	MT774231	MT774238
Ophiocordyceps geometridicola	Larva of Geometridae (Lepidoptera)	TBRC 8095	–	MF614648	MF614632	MF614663	MF614679
Ophiocordyceps houaynhangensis	Larva of Coleoptera	TBRC 8428	–	MH092902	MH092894	–	–
Ophiocordyceps hydrangea	**Nymph of cicada (Hemiptera)**	**YFCC 8832**	**OM304636**	**OM304640**	**OM831277**	**OM831280**	**OM831283**
Ophiocordyceps hydrangea	**Nymph of cicada (Hemiptera)**	**YFCC 8833**	**OM304637**	**OM304641**	**OM831278**	**OM831281**	**OM831284**
Ophiocordyceps hydrangea	**Nymph of cicada (Hemiptera)**	**YFCC 8834**	**OM304635**	**OM304639**	**OM831276**	**OM831279**	**OM831282**
Ophiocordyceps karstii	*Hepialus jianchuanensis* (Lepidoptera)	MFLU:15-3884	KU854952	–	KU854945	KU854943	–
Ophiocordyceps kimflemingiae	*Camponotus castaneus/ americanus* (Hymenoptera)	SC09B	KX713631	KX713620	KX713698	KX713724	–
Ophiocordyceps kniphofioides	*Cephalotes atratus* adult ant (Hymenoptera)	HUA 186148	KC610790	KF658679	KC610739	KF658667	KC610717
Ophiocordyceps konnoana	Larva of Coleoptera	EFCC 7315	EF468959	–	EF468753	EF468861	EF468916
Ophiocordyceps langbianensis	Larva of Coleoptera	DL0017	MT928355	MT928306	–	–	–
Ophiocordyceps lanpingensis	Larva of Hepialidae (Lepidoptera)	YHOS0705	KC417458	KC417460	KC417462	KC417464	KC456333
Ophiocordyceps longissima	Cicada nymph (Cicadidae, Hemiptera)	NBRC 106965	AB968392	AB968420	AB968584	–	AB968546
Ophiocordyceps longissima	Hemiptera; cicada (nymph)	EFCC 6814	–	EF468817	EF468757	EF468865	–
Ophiocordyceps macroacicularis	Larva of Cossidae (Lepidoptera)	NBRC 100685	AB968388	AB968416	AB968574	–	AB968536
Ophiocordyceps multiperitheciata	Lepidoptera larva	BCC 69008	–	MF614657	MF614641	–	MF614682
Ophiocordyceps myrmicarum	Hymenoptera (Formicidae)	HIRS 45	KJ680150	JX566965	JX566973	KJ680151	–
Ophiocordyceps nigrella	Larva of Lepidoptera	EFCC 9247	EF468963	EF468818	EF468758	EF468866	EF468920
Ophiocordyceps pruinosa	Hemiptera	NHJ 12994	EU369106	EU369041	EU369024	EU369063	EU369084
Ophiocordyceps pseudoacicularis	Larva of Lepidoptera	TBRC 8102	–	MF614646	MF614630	MF614661	MF614677
Ophiocordyceps pulvinata	*Camponotus* adult ant (Hymenoptera)	TNS-F 30044	GU904208	AB721305	GU904209	GU904210	–
Ophiocordyceps ramosissimum	*Phassus nodus* larva (Lepidoptera)	GZUHHN8	KJ028012	–	KJ028014	KJ028017	–
Ophiocordyceps ravenelii	Beetle larva (Coleoptera)	OSC 110995	DQ522550	DQ518764	DQ522334	DQ522379	DQ522430
Ophiocordyceps robertsii	Larva of Hepialidae (Lepidoptera)	KEW 27083	–	EF468826	EF468766	–	–
Ophiocordyceps rubiginosiperitheciata	Larva of Coleoptera	NBRC 106966	JN941704	JN941437	AB968582	JN992438	AB968544
Ophiocordyceps satoi	*Polyrhachis lamellidens* (Hymenoptera)	J19	KX713650	KX713601	KX713684	KX713710	–
Ophiocordyceps sinensis	Larva of Hepialidae (Lepidoptera)	EFCC 7287	EF468971	EF468827	EF468767	EF468874	EF468924
Ophiocordyceps sinensis	Larva of Hepialidae (Lepidoptera)	YHH 1805	MK984568	MK984580	MK984572	MK984587	MK984576
Ophiocordyceps sobolifera	Cicada nymph (Cicadidae, Hemiptera)	TNS F18521	KJ878933	KJ878898	KJ878979	KJ879013	–
Ophiocordyceps sobolifera	Hemiptera (cicada nymph)	NBRC 106967	AB968395	AB968422	AB968590	–	–
Ophiocordyceps spataforae	Hemiptera adult	NHJ 12525	EF469125	EF469078	EF469063	EF469092	EF469111
Ophiocordyceps sphecocephala	Hymenoptera adult wasp	NBRC 101753	JN941695	JN941446	AB968592	JN992429	AB968553
Ophiocordyceps stylophora	Larva of Elateridae (Coleoptera)	OSC 110999	EF468982	EF468837	EF468777	EF468882	EF468931
Ophiocordyceps thanathonensis	Hymenotera adult ant	MFLU 16-2910	MF882926	MF850377	MF872614	MF872616	–

Species	Host	Isolate no./ specimen no.	GenBank accession no.				
			nrSSU	*nrLSU*	*tef-1α*	*rpb1*	*rpb2*
Ophiocordyceps tiputinii	Larva of Megaloptera	QCNE 186287	KC610792	KC610773	KC610745	KF658671	–
Ophiocordyceps tricentri	Adult of Cercopoidea (Hemiptera)	NBRC 106968	AB968393	AB968423	AB968593	–	AB968554
Ophiocordyceps unilateralis s. str.	Camponotus sericeiventris (Hymenoptera)	VIC 44303	KX713628	KX713626	KX713675	KX713730	–
Ophiocordyceps unituberculata	Larva of Lepidoptera	YFCC HU1301	KY923214	KY923212	KY923216	KY923218	KY923220
Ophiocordyceps xuefengensis	Larva of *Phassus nodus* (Lepidoptera)	GZUH2012HN14	KC631789	–	KC631793	KC631798	–
Ophiocordyceps yakusimensis	Cicada nymph (Cicadidae, Hemiptera)	HMAS 199604	KJ878938	KJ878902	–	KJ879018	KJ878953
Paraisaria amazonica	Adult of Acrididae (Orthoptera)	HUA 186143	KJ917562	KJ917571	KM411989	KP212902	KM411982
Paraisaria coenomyiae	*Coenomyia* sp. (Coenomyiidae, Diptera)	NBRC 106964	AB968385	AB968413	AB968571	–	AB968533
Paraisaria gracilis	Larva of Lepidoptera	EFCC 8572	EF468956	EF468811	EF468751	EF468859	EF468912
Paraisaria heteropoda	Cicada nymph (Hemiptera)	NBRC 100644	JN941718	JN941423	AB968596	JN992452	AB968557
Tolypocladium inflatum	Coleoptera (larva)	OSC 71235	EF469124	EF469077	EF469061	EF469090	EF469108
Tolypocladium ophioglossoides	Fungi (*Elaphomyces* sp.)	CBS 100239	KJ878910	KJ878874	KJ878958	KJ878990	KJ878944

unknown species of *Ophiocordyeps* attacking larvae of Elateridae was collected from Lintong Province, Bidoup Nuiba National Park, in Vietnam. The phylogeny and morphology of these two fungi were determined, and their systematic position was established in Ophiocordycipitaceae. The phylogenetic analyses results showed that the two new species belonged to *Ophiocordyceps*, and were named *Ophiocordyceps hydrangea* and *Ophiocordyceps bidoupensis* based on well-supported morphology and molecular data.

Materials and methods

Sample collection and isolation

The specimens were collected from China and Vietnam, and the collection site information was noted, including altitude, longitude, latitude, and habitat type. Samples were placed in sterilized tubes or plastic bags and boxes, returned to the laboratory, and stored at 4 °C. The specimens were photographed using a Canon 750 D camera (Canon Inc., Tokyo, Japan). The size was measured, and characteristics were recorded including length of the stroma, single or multiple, length and width of stipe clavate and fertile parts, shape, texture, and color. To obtain axenic cultures, the segments were removed from insect bodies, and these segments were placed onto Potato Dextrose Agar (PDA) consisting of peptone and yeast powder (potato 100 g/500 mL, dextrose 10 g/500 mL, agar 10 g/500 mL, yeast powder 5 g/500 mL, peptone 2.5 g/500 mL) plates. The plates were placed in a culture room at 25 °C until isolated into pure cultures. The cultures were saved on a PDA slant (to grow slowly), and stored at 4 °C. All specimens were deposited in the Yunnan Herbal Herbarium (YHH) of Yunnan University. The extypes of the two species were deposited in the Yunnan Fungal Culture Collection (YFCC) of Yunnan University.

Morphological observations

To describe the sexual morphs of the two species, frozen sections or hand sections of the fruiting structures of the stroma were immersed in water and then dyed with lactophenol cotton blue solution for morphological observation and photomicrography (Wang et al. 2021a). For observations on asexual morphs, new colonies were established from old cultures and placed on new PDA plates. The plates were cultured in an incubator for 6 or 12 weeks at 25 °C, and then asexual morphs were observed and recorded (shape, texture, and color of the colonies). Microscope slide cultures were made using the methods of Wang et al. (2020). The morphological observations and measurements were made using Olympus CX40 and BX53 microscopes.

DNA extraction, PCR, and sequencing

Five-centimeter segments from the stroma of fresh specimens and the cultures were used for DNA extraction to ensure the cultures and specimens were the same. Total DNA was extracted using cetyltrimethyl ammonium bromide (CTAB) according to the procedure described by Liu et al. (2001). The DNA was used for PCR amplification. The primer pair, NS4 (5'-CTTCCGTCAATTCCTTTAAG-3') and NS1 (5'-GTAGTCATATGCTTGTCTC-3') was used to amplify nr*SSU* (the nuclear ribosomal small subunit) (White et al. 1990). The primer pair, LR5 (5'-ATCCTGAGGGAAACTTC-3') and LR0R (5'-GTACCCGCTGAACTTAAGC-3') was used to amplify nr*LSU* (the nuclear ribosomal large subunit) (Vilgalys and Hester 1990; Rehner and Samuels 1994). The primer pair, 983F (5'-GCYCCYGGHCAYCGTGAYTTYAT-3') and 2218R (5'-ATGACACCRACRGCRACRGTYTG-3') was used to amplify *tef-1α* (the translation elongation factor 1α) (Rehner and Buckley 2005). The primer pair, CRPB1A (5'-CAYCCWGGYTTYATCAAGAA-3') and RPB1C (5'-CCNGCDATNTCRTTRTCCATRTA-3') were used to amplify *rpb1* (the largest subunit of RNA polymerase II) (Castlebury et al. 2004; Bischoff et al. 2006). The primer pair, fRPB2-5F (5'-GAYGAYMGWGATCAYTTYGG-3') and fRPB2-7cR (5'-CCCATRGCTTGYTTRCCCAT-3') was used to amplify *rpb2* (the second largest subunit of RNA polymerase II) (Liu et al. 1999). The polymerase chain reaction (PCR) for amplification of the five genes and their sequencing were described by Wang et al. (2015).

Phylogenetic analyses

Sequences of the five genes (nr*SSU*, nr*LSU*, *tef-1α*, *rpb1*, and *rpb2*) were downloaded from GenBank, and combined with the newly generated sequences in this study. The taxa information of the species and GenBank accession numbers of the five genes are listed in Table1. Sequences of the five genes were aligned using the Clustal X (v.2.0) and MEGA6 (v.6.0) (Larkin et al. 2007; Tamura et al. 2013). Ambiguously aligned sites were eliminated, and the gaps were treated as missing data. The aligned sequences of the five genes (nr*SSU*, nr*LSU*, *tef-1α*, *rpb1*, and *rpb2*) were concatenated into a single

combined dataset using MEGA6 (v.6.0.). Conflicts between the five genes were tested using PAUP* (v.4.0b10) (Swofford 2002). The results of the phylogenetic signals in the five genes were not in conflict. The concatenated dataset containing all five genes consisted of 11 data partitions, including one each for nr*SSU* and nr*LSU*, and three for each of the three codon positions of *tef-1α*, *rpb1*, and *rpb2*. Phylogenetic analyses based on the five genes were made using BI and ML methods (Ronquist and Huelsenbeck 2003; Stamatakis et al. 2008). We used the optimal model GTR+I with 1,000 rapid bootstrap replicates on the five genes for ML analyses (Stamatakis 2006). We conducted BI analyses using a GTR+G+I model determined by jModelTest (v.2.1.4), conducted on MrBayes (v.3.1.2) for 5 million generations (Darriba et al. 2012). The phylogenetic tree constructed was viewed and edited using FigTree (v.1.4.2) and Adobe Illustrator CS6.

Results

Phylogenetic analyses

A total of 83 samples were used for the phylogenetic analyses. Five gene sequences of the two new species collected were used to reconstruct the phylogenetic framework of *Ophiocordyceps*. Two taxa of *Tolypocladium* were designated as the outgroup, and these were, respectively, *Tolypocladium ophioglossoides* CBS 100239 and *Tolypocladium inflatum* OSC 71235. The alignment lengths of the 83 samples were composed of 4,486 bp sequence data, 971 bp of nr*SSU*, 921 bp of nr*LSU*, 943 bp of *tef-1α*, 726 bp of *rpb1*, and 925 of *rpb2*. The phylogenetic tree showed that these were identical in overall topologies to previous studies. Four clades (*Hirsutella* clade, *O. sobolifera* clade, *O. sphecocephala* clade, and *O. ravenelii* clade) of *Ophiocordyceps* were well-supported by ML bootstrap proportions and BI posterior probabilities (Fig. 1). The two new species in the *O. sobolifera* clade, *O. hydrangea* and *O. bidoupensis*, formed two separate subclades. Three samples of *O. hydrangea* (BP = 98%, PP = 1) formed a separate subclade with *O. longissima* and *O. yakusimensis*, while *O. bidoupensis* (BP = 83%, PP = 0.99) formed a separate subclade with *O. houaynhangensis*.

Taxonomy

Ophiocordyceps hydrangea **H. Yu, W.Q. Zou & D.X. Tang, sp. nov.**
MycoBank No: 843203
Fig. 2

Etymology. Hydrangea, referred to the top of the stroma similar to hydrangea.

Holotype. China, Yunnan Province, Jinghong City, Nabanhe National Nature Reserve, 22°8'21.32"N, 100°42'18.35"E, alt. 612 m, on cicada nymphs (Cicadidae, Hemiptera). The material was found in the soil of an evergreen broad-leaved forest, 18 August 2020, H. Yu (YHH 20081, holotype; YFCC 8834, ex-holotype culture).

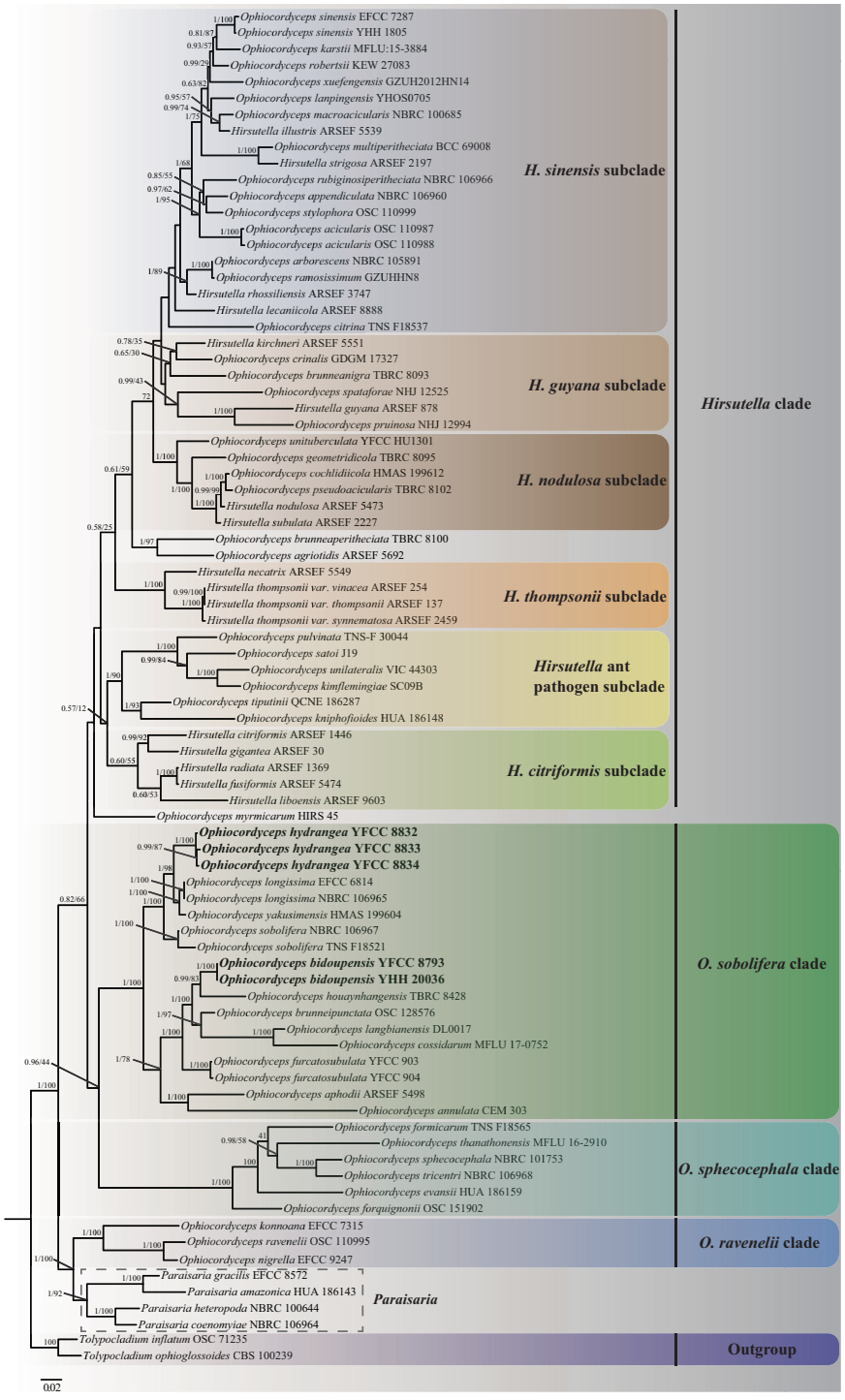

Figure 1. Phylogenetic relationships of *Ophiocordyceps hydrangea* and related species from the five genes dataset (nr*LSU*, nr*SSU*, *tef-1α*, *rpb1*, and *rpb2*) based on ML and BI analyses. Statistical support values of BI posterior probabilities and ML bootstrap proportions (0.5/≥50%) are shown at the nodes.

Sexual morph. The stroma was grown from the head of the host cicada nymph, solitary, the top of the stroma similar to hydrangea, pale pink, 1.6–6.4 cm long. Sexual morph was not observed.

Asexual morph. The colony grew slowly on PDA medium. Cultured at 25 °C for about 12 weeks, the diameter of the colony was 25–28 mm, pale pink, the edge white, hard texture. The back of the colony was white to brown. Surface hyphae rough,

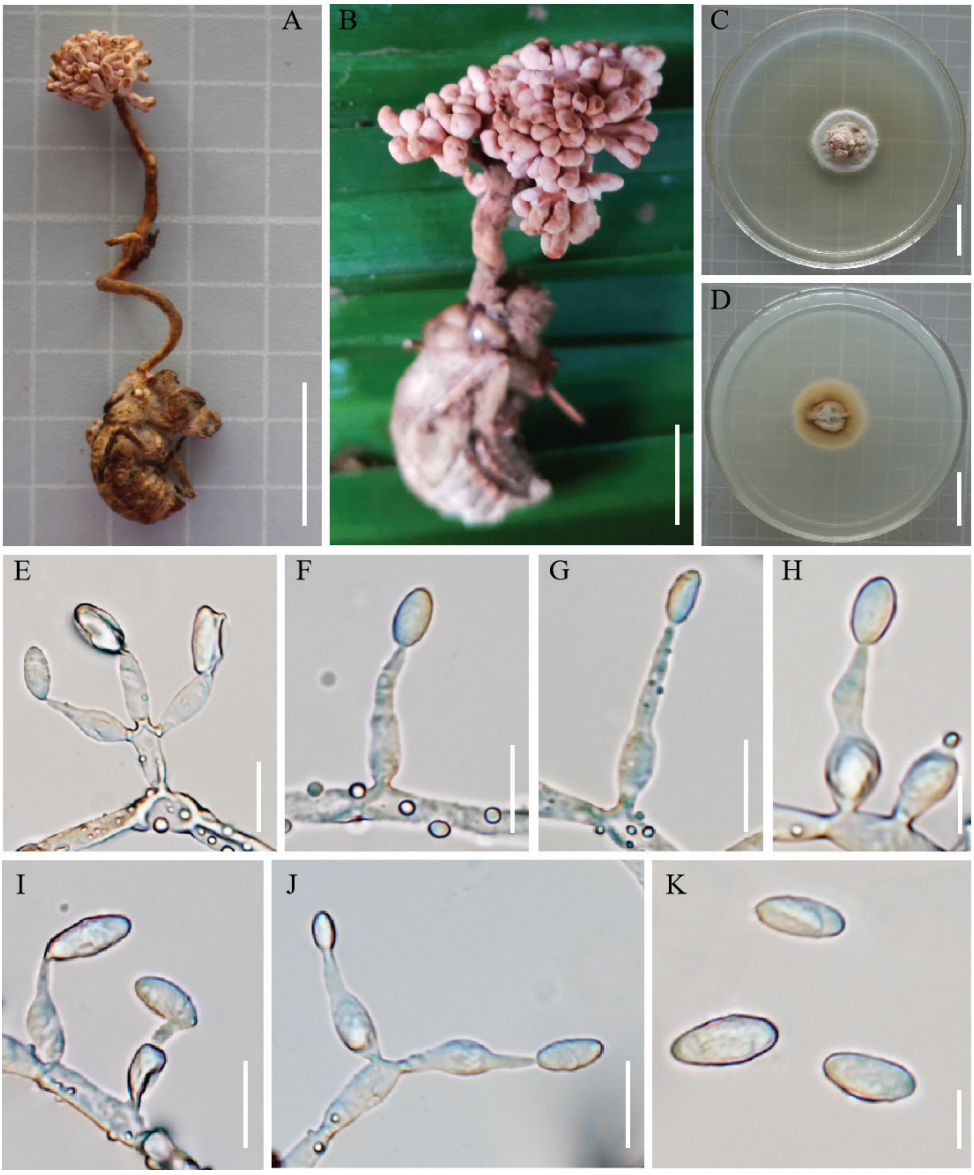

Figure 2. *Ophiocordyceps hydrangea* **A, B** fungus on a cicada nymph **C, D** colony on PDA medium **E** conidiophores, conidiogenous cells and conidia **F–J** conidiogenous cells and conidia **K** conidia. Scale bars: 1 cm (**A, B**); 2 cm (**C, D**); 10 μm (**E, F, G, I, J**); 5 μm (**H, K**).

hyaline, septate. Conidiophores were cylindrical. Conidiogenous cells were solitary or whorled, ampuliform, smooth-walled, forming on conidiophores or colonies, hyaline, with swollen base, and slender top, 10.6–17.6 μm long, 2.9–4.3 μm wide at the swollen base, and 1.1–2.2 μm wide at the slender top. Conidia hyaline, ovoid or long oval, solitary, 6.8–10.1 × 3.3–4.5 μm.

Host. Cicada nymph (Cicadidae, Hemiptera).

Habitat. In the soil of an evergreen broad-leaved forest.

Distribution. China.

Other material examined. China, Yunnan Province, Jinghong City, Nabanhe National Nature Reserve, 22°8'21.32"N, 100°42'18.35"E, alt. 612 m, on cicada nymphs (Cicadidae, Hemiptera) was found in the soil an evergreen broad-leaved forest, 18 August 2020, H. Yu (YFCC 8832, YFCC 8833).

Notes. Phylogenetic analyses showed that *O. hydrangea* clustered with *O. sobolifera*, *O. longissima*, and *O. yakusimensis* of the *O. sobolifera* clade (Fig. 1). Their hosts were cicada nymphs compared to other species of the *O. sobolifera* clade (Table 2). *Ophiocordyceps hydrangea* was well supported by BI and ML results, forming a separate subclade with *O. sobolifera*, *O. longissima*, and *O. yakusimensis*. The macro-morphology of *O. hydrangea* was clearly different from *O. sobolifera*, *O. longissima*, *O. khonkaenensis*, and *O. yakusimensis*. The stroma of *O. hydrangea* grew from the head of the host cicada nymph, solitary, and the top of the stroma was like a pale pink hydrangea.

Ophiocordyceps bidoupensis **H. Yu, W.Q. Zou & D.X. Tang, sp. nov.**

MycoBank No: 843204

Fig. 3

Etymology. Bidoupensis, referred to the type species collected from Bidoup Nuiba National Park.

Holotype. Vietnam, Lintong Province, Bidoup Nuiba National Park, 12°8'9.30"N, 108°31'51.38"E, alt. 1678 m, on larva of Elateridae (Coleoptera) buried in soil, emerging from the leaf litter on the forest floor, 16 October 2017, H. Yu (YHH 20036, holotype; YFCC 8793, ex-holotype culture).

Sexual morph. The stroma grew from the head of the host, solitary, solid, cylindrical, 11.8–22.5 cm long, yellow. Stipe clavate, yellow, curved, 10.7–21.2 cm long, 0.7–0.9 mm wide. Fertile parts cylindrical, yellow, slightly curved, 2.9–11.3 mm long, 0.9–1.6 mm wide. Sterile apices cone, yellow, 2.1–7.2 mm long, 0.2–0.7 mm wide. Perithecia immersed, pyriform to lanceolate, brown-yellow, 213.4–405.9 × 74.8–192.4 μm. Asci hyaline, slender, 116.1–192.7 × 4.8–7.5 μm. Asci cap prominent, capitate, 4.7–6.1 × 3.3–5.4 μm. Ascospores hyaline, filiform, multi-septate.

Asexual morph. The colony grew slowly on PDA medium. Cultured at 25 °C for about 6 weeks, the diameter of the colony was 38–45 mm, white, aerial mycelium on the surface, slightly convex. The back of the colony was grayish-white, dark brown in the middle. Surface smooth of hyphae, hyaline, septate. Conidiogenous cells cone, hyaline, septate, smooth-walled, forming on hyphae, with a hypertrophic base,

tapering abruptly to a thin neck, 13.80–46.4 × 0.42–5.13 µm. Conidia hyaline, oval or briolette, smooth-walled, 2.24–3.61 × 1.49–2.70 µm.

Host. Larva of Elateridae (Coleoptera).

Habitat. The hosts were buried in soil, and the stroma were found in the leaf litter on the forest floor.

Distribution. Vietnam.

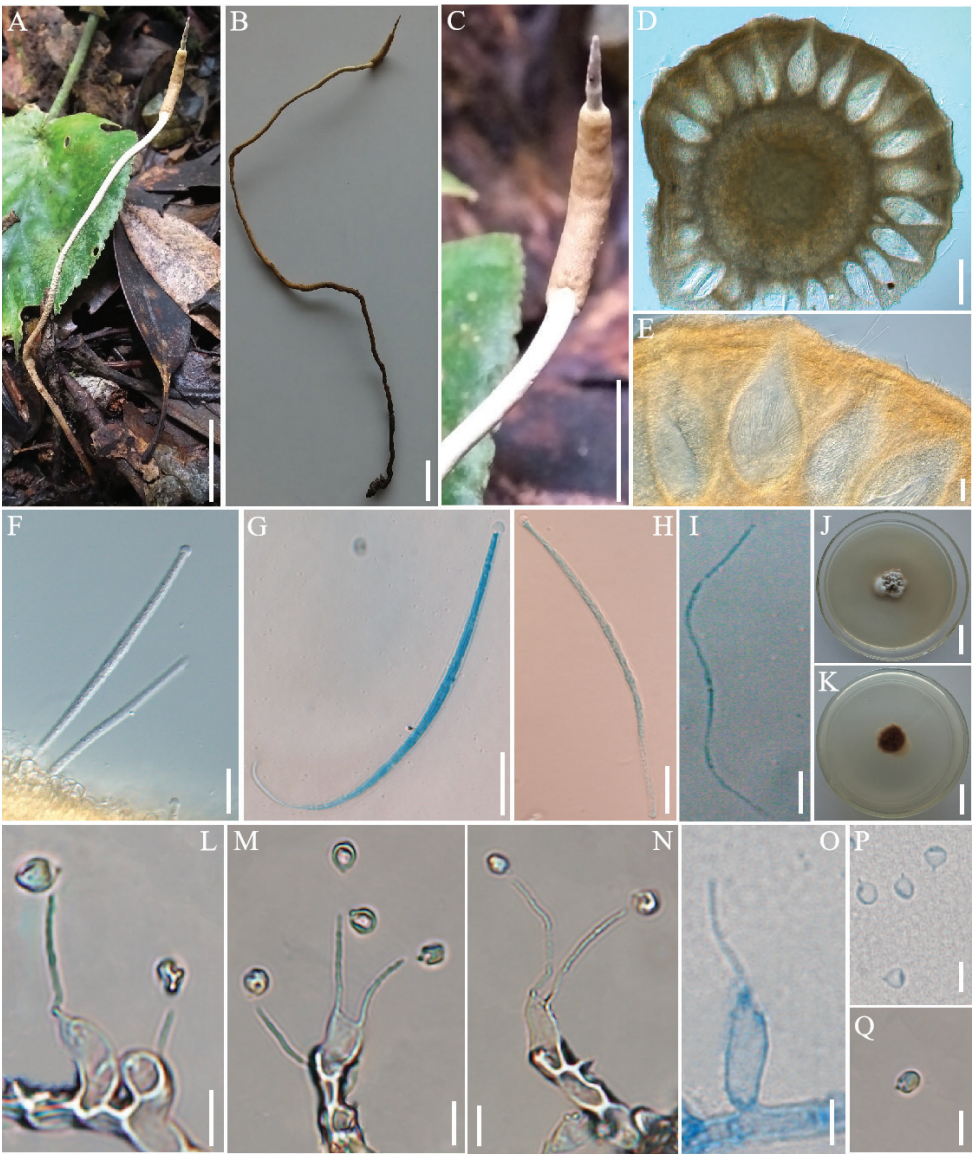

Figure 3. *Ophiocordyceps bidoupensis* **A–C** fungus on an Elateridae larva **D, E** cross-section of the ascoma showing the perithecial arrangement **F–H** asci **I** ascospores **J, K** colony on PDA medium **L–N** conidiogenous cells and conidia **O** conidiogenous cells **P, Q** conidia. Scale bars: 1 cm (**A–C**); 200 µm (**D**); 20 µm (**E–H**); 10 µm (**I**); 2 cm (**J, K**); 5 µm (**L–Q**).

Notes. Phylogenetic analyses showed that *O. bidoupensis* was clustered with *O. houaynhangensis*, *O. brunneipunctata*, *O. langbianensis*, *O. cossidarum*, and *O. furcatosubulata* of the *O. sobolifera* clade (Fig. 1). Their hosts were larvae of Elateridae compared to cicada nymph hosts of the other species of the *O. sobolifera* clade (Table 2). *Ophiocordyceos bidoupensis* was well-supported by bootstrap support and posterior probabilities, and formed a separate subclade with *O. houaynhangensis*, *O. brunneipunctata*, *O. langbianensis*, and *O. cossidarum*. The morphology of *O. bidoupensis* was clearly different in shape and size from other species of *O. sobolifera* clade (Table 2). The stroma of *O. bidoupensis* grew solitary from the head of the host; sterile apices of the stroma were different from the other species.

Discussion

Ophiocordyceps is the largest genus in the Ophiocordycipitaceae, with a wide range of hosts and various species. At present, more than 290 species of *Ophiocordyceps* have been reported (Index Fungorum 2022). However, only 11 species are described in the *O. sobolifera* clade and their hosts are mainly Coleoptera larvae and cicada nymphs (Hemiptera) (Table 2). We describe the new species *O. hydrangea* attacking cicada nymphs and the new species *O. bidoupensis* attacking Coleoptera larvae. Most species have diverse macro-morphological or micro-morphological characteristics due to the same entomopathogenic fungi having a different host, or different species of entomopathogenic fungi having the same host (Sung et al. 2007, 2011; Araújo et al. 2015; Araújo and Hughes 2016; Shrestha et al. 2016; Luangsa-ard et al. 2018; Crous et al. 2019; Fan et al. 2021; Wang et al. 2021a). Hemiptera hosts are widely present among the species of *Ophiocordyceps*, including species of the *Hirsutella* clade, *O. sobolifera* clade, *O. sphecocephala* clade, and *O. ravenelii* clade.

The entomopathogenic fungi whose host is Hemiptera have diverse morphological characteristics. For example, *O. nutans* (Patouillard) G.H. Sung, J.M. Sung, Hywel-Jones & Spatafora (Sung et al. 2007), its hosts were stink bugs (Hemiptera), stromata solitary or multiple, fertile parts was red (Hywel-Jones 1995a; Luangsa-ard et al. 2008), stromata of *O. brunneinigra* (Hemipteran host) were flexuous, arising from between the head and the thorax of the host (Luangsa-ard et al. 2018), stromata of *O. spataforae* Tasanathai, Thanakipipattana, Khonsanit & Luangsa-ard were cylindrical, cream to pale brown (Luangsa-ard et al. 2018). However, from previously reported Hemipteran hosts, only a few hosts of the *O. sobolifera* clade were cicada nymphs in *Ophiocordyceps* (Kobayasi and Shimizu 1963; Sung et al. 2011; Crous et al. 2019). In this study, the host of *O. hydrangea* was a cicada nymph. More interestingly, the *O. hydrangea* was significantly more beautiful than other species; the stroma grew from the head of the host cicada nymph, and the top of the stroma like a hydrangea (Sung et al 2007, 2011; Crous et al. 2019). Coleoptera hosts were common in species of *Ophiocordyceps*. More than 20 species of *Ophiocordyceps* were parasitic on Coleoptera larvae (Shrestha et al. 2016). These species included *O. acicularis* (Ravenel) Petch (Petch 1933), *O. annulata* (Kobayasi & Shimizu) Spatafora, Kepler & C.A. Quandt (Kobayasi and Shimizu 1982; Spatafora et al. 2015), *O. aphodii*

Table 2. Morphological comparisons of two new species and related species.

Species	Host	stromata	Perithecia	Asci	Ascospores	Conidiogenous cells	Conidia	References
O. bidoupensis	**Larva of Elateridae (Coleoptera)**	**Solitary, solid, cylindrical, yellow, 11.8–22.5 cm long.**	**Immersed, pyriform to lanceolate, brown-yellow, 213.4–405.9 × 74.8–192.4 µm.**	**Hyaline, slender, 116.1–192.7 × 4.8–7.5 µm.**	**Hyaline, filiform, multi-septate.**	**Cone, hyaline, septate, smooth-walled, forming on hyphae, with a hypertrophic base, tapering abruptly into a thin neck, smooth-walled, 13.8–46.4 × 0.42–5.13 µm.**	**Oval or briolette, hyaline, smooth-walled, 2.24–3.61 × 1.49–2.70 µm.**	**This study**
O. brunneipunctata	Larva of Elateridae (Coleoptera)	Solitary, rarely up to 3, simple, 25–90 mm high.	Immersed, perithecioid, brown, ovate to pyriform, brown-walled, 270–335 × 110–160 µm.	Hyaline, cylindric, capitate, 8-spored, 280–295 × 6–7 µm.	Hyaline, filiform, multiseptate breaking into 64 part spores, 4–6 × 1–1.5 µm.	Monophialidic, rarely polyphialidic, hyaline, smooth, 5.5–7.5 × 2.5–3.0 µm at the base, up to 15 × 0.5 µm above.	Hyaline, aseptate, smooth, spherical 1.5–2.5 µm diam., enveloped by a mucous sheath.	Hywel-Jones 1995b; Luangsa-ard et al. 2008
O. cossidarum	Larva of Cossidae (Lepidoptera)	Solitary, simple, 40–70 mm high.	Immersed, red, ovate to phialide, red-walled, 355–454 × 136–171 µm.	Hyaline, cylindrical, 8-spored with a thickened apex, 174–221 × 5.7–7 µm.	Hyaline, fifiliform, multiseptate,131–153 × 1.8–2.2 µm, breaking into 32 part-spores.	–	–	Hyde et al. 2017
O. furcatosubulata	Larva of Elateridae (Coleoptera)	Single, solid, yellow to brown, 40–80 mm long, 1.5–2.2 mm wide.	Immersed, long ovoid or pyriform, 289.6–405.8 × 87.0–159.2 µm.	Hyaline, cylindrical, 138.8–202.5 × 4.3–6.0 µm.	Hyaline, filiform, multi-septate, finally breaking into secondary ascospores, 3.7–5.3 × 1.3–2.0 µm.	Polyphialidic, forming on conidiophores or side branches, hyaline, with a slender or subulate base, tapering gradually, smooth-walled or verruculose, 3.5–15.8 × 0.9–1.7 µm.	Solitary, aseptate, smooth-walled, broadly ellipsoid or ellipsoid, 1.5–2.5 × 1.2–1.9 µm.	Wang et al. 2021a
O. houaynhangensis	Larva of Coleoptera	Solitary, cylindrical, cream, up to 11 cm long and 1.5–2.5 mm in width.	Completely immersed, obclavate, 300–450 × 80–170 µm.	Cylindrical, 100–250 × 4–7.5 µm.	Hyaline, cylindrical, breaking into 32 small truncate part-spores, 4–7 × 1–2 µm.	Monophialidic, phialides flasked-shaped with long necks, up to 30 µm long and 2–4 µm in breadth; phialide necks up to 18 µm long and 0.5 µm in breadth.	Hyaline, smooth, spherical, 2–3 µm.	Crous et al. 2018
O. langbianensis	Larva of Coleoptera	Solitary, rarely branched, 40–100 mm long.	Immersed, ovate or pyriform, 260–400 × 100–190 µm.	Cylindrical, with thickened cap, 200–250 × 5.0–6.0 µm.	Fliform, multiseptate, articulated in long-chain afer discharging, sometimes breaking into 1-celled part spores, 5–7.5 × 1.3–2 µm.	Divergent.	Chains, elliptical.	Lao et al. 2021
O. sobolifera	Cicada nymph (Cicadidae, Hemiptera)	Commonly single, rarely fasciculated by twos or threes, arising from head among polster, clavate or cylindric 2–8 cm long, 2–6 mm thick, become hollow after maturity.	Rectangularly immersed, ampullaceous 500–600 × 220–260 µm, with somewhat long neck, ostiola somewhat prominent, walls hyaline 8–16 µm thick.	Cylindric, 400–470 × 5.6–6.3 µm.	Finally breaking into secondary ascospores, truncate at both ends, 6–12 × 1.0–1.3 µm.	–	Terminal or lateral, ellpsoid or fusiformed, hyaline, 6.5–10.5 × 2.5–4.0 µm.	Kobayasi and Shimizu 1963
O. yakusimensis	Cicada nymph (Cicadidae, Hemiptera)	Very long attaining 14 cm, arising from the apical part between eyes.	Wholly embeddèd, narrow ovoid or almost naviculate, 740–800 × 170–230 µm, without protruding ostiola, neck almost destitute, wall 21–23 µm thick, composed of very thin cells.	270–310 × 5 µm.	Finally breaking into secondary ascospores, long cylindrical, somewhat attenuated on both sides, terminally truncate, 10–15 × 1 µm.	–	–	Kobayasi and Shimizu 1963

Species	Host	stromata	Perithecia	Asci	Ascospores	Conidiogenous cells	Conidia	References
O. longissima	Cicada nymph (Cicadidae, Homoptera)	5–20 cm long, some times much longer.	Ovoid to long ovoid, with a short neck, 440–590 × 130–300 µm.	190–350 × 5–6 µm.	–	–	–	Sung et al. 2011
O. khonkaenensis	Cicada nymph (Hemiptera)	Variable in number, solitary to three, 20–30 mm long and 2–3 mm in breath.	Immersed, flask shaped, 590–700 × 200–300 µm.	Cylindrical, 237.5–337.5 × 5–6 µm.	Filiform, 300–360 × 1–1.5 µm readily breaking into 32 part-spores, 7–13 × 1–1.5 µm.	Phialidic, hirsutella-like, 5.5–11 × 2–3 µm.	Hyaline, fusiform, smoothwalled, 3–5.5 × 1–3 µm.	Crous et al. 2019
O. hydrangea	**Cicada nymph (Cicadidae, Hemiptera)**	**Solitary, the top of the stroma similar to hydrangea, pale pink,1.6–6.4 cm long.**	–	–	–	**Solitary or whorled, ampuliform, smooth-walled, forming on conidiophores or colonies, hyaline, with swollen base, and slender top, 10.6–17.6 µm long, 2.9–4.3 µm wide at the swollen base, and 1.1–2.2 µm wide at the slender top.**	**Hyaline, ovoid or long oval, solitary, 6.8–10.1 × 3.3–4.5 µm.**	**This study**

(Mathieson) G.H. Sung, J.M. Sung, Hywel-Jones & Spatafora (Mathieson 1949; Sung et al. 2007), *O. brunneipunctata* (Hywel-Jones) G.H. Sung, J.M. Sung, Hywel-Jones & Spatafora (Hywel-Jones 1995b; Sung et al. 2007; Luangsa-ard et al. 2008), *O. furcatosubulata* H. Yu, Y. Wang & Y.B. Wang (Wang et al. 2021a), *O. houaynhangensis* Keochanpheng, Thanakitp., Mongkols. & Luangsa-ard (Crous et al. 2018), *O. langbianensis* T.D. Lao, T.A.H. Le & N.B. Truong (Lao et al. 2021), *O. melolonthae* (Tulasne & C. Tulasne) G.H. Sung, J.M. Sung, Hywel-Jones & Spatafora (Sung et al. 2007), and *O. ravenelii* (Berkeley & M.A. Curtis) G.H. Sung, J.M. Sung, Hywel-Jones & Spatafora (Sung et al. 2007). Most species with Coleopteran host occur in soil and have solid, cylindrical, and yellow stromata. This is consistent with the results of this study.

Phylogenetic analyses based on the data from five genes showed that our phylogenetic framework of *Ophiocordyceps* was consistent with previous studies (Sung et al. 2007, 2011; Quandt et al. 2014; Simmons et al. 2015; Crous et al. 2018, 2019; Wang et al. 2018, 2021a; Lao et al. 2021). The genus of *Ophiocordyceps* consists of four clades, including the *Hirsutella* clade, *O. sobolifera* clade, *O. sphecocephala* clade, and *O. ravenelii* clade. Phylogenetic analyses showed that *O. hydrangea* clustered with *O. sobolifera*, *O. longissima*, and *O. yakusimensis* in the *O. sobolifera* clade, and *O. bidoupensis* clustered with *O. houaynhangensis*, *O. brunneipunctata*, *O. langbianensis*, *O. cossidarum*, and *O. furcatosubulata* in the same clade. Species within the *O. sobolifera* clade had different hosts, and morphological characteristics. These two new species clustered in two separate subclades within the *O. sobolifera* clade. The hosts of one subclade were cicada nymphs with stromata cylindrical or sarciniform, bright-colored, conidia were macro (Kobayasi and Shimizu 1963; Crous et al. 2019), and the hosts of another subclade were Coleoptera, with stromata cylindrical, conidia small, and a sterile apex on top of the stroma (Hywel-Jones 1995b; Luangsa-ard et al. 2008; Crous et al. 2018; Lao et al. 2021; Wang et al. 2021a). Therefore, the species of the *O. sobolifera* clade could be divided into two separate subclades when more materials were collected.

The species of *O. sobolifera* clade had diverse morphological characteristics (Table 2). The entomopathogenic fungi with cicada nymph hosts shared similar characteristics, stromata solitary or multiple, cylindrical, and bright-colored. However, they also differed in morphology. For example, *O. sobolifera* lacked a protruding ostiole with immersed perithecia (Kobayasi and Shimizu 1963), and this seems to be contrary to *O. yakusimensis* (Kobayasi and Shimizu 1963). Stromata of *O. longissima* were longer than other species, and had a short neck in perithecia (Sung et al. 2011). Compared to the ovoid perithecia of *O. longissima* and *O. yakusimensis*, *O. khonkaenensis* was flask-shaped (Crous et al. 2019). The top of the stroma of *O. hydrangea* was similar to hydrangea, the size and shape of conidiogenous cells and conidia were different from *O. khonkaenensis* (Table 2). The entomopathogenic fungi using Coleoptera hosts shared similar characteristics, such as stromata solitary, cylindrical, sterile apices on top, bright-colored. However, they had different shape and size of perithecia, asci, ascospores, conidiogenous cells, and conidia. The perithecia of *O. bidoupensis* was pyriform to lanceolate and brown-yellow. It was similar to *O. brunneipunctata*, *O. furcatosubulata*, and *O. langbianensis*, and only *O. houaynhangensis* was clavate

(Hywel-Jones 1995b; Luangsa-ard et al. 2008; Crous et al. 2018; Lao et al. 2021; Wang et al. 2021a). Conidiogenous cells of *O. bidoupensis* were cone-shaped, forming on hyphae, with a hypertrophic base, tapering abruptly into a thin neck, smooth-walled, with a smaller thin neck (0.42 μm wide) than *O. brunneipunctata* (0.5 μm), *O. furcatosubulata* (0.9 μm), and *O. houaynhangensis* (0.5 μm).

Due to the unique geographical locations and climate conditions in China and Vietnam, these areas contain a rich species diversity of *Cordyceps* s.l. However, our survey of *Cordyceps* s.l. in China and Vietnam only represented a small portion of the total. More samples of *Cordyceps* s.l. will continue to be collected in China and Southeast Asia in order to uncover additional undescribed taxa, and revise species with the incorrect classification position of this group.

Acknowledgements

This work was funded by the National Natural Science Foundation of China (31870017, 32060007).

References

Araújo JPM, Evans HC, Geiser DM, Mackay WP, Hughes DP (2015) Unravelling the diversity behind the *Ophiocordyceps unilateralis* (Ophiocordycipitaceae) complex: Three new species of zombie-ant fungi from the Brazilian Amazon. Phytotaxa 220(3): 224–238. https://doi.org/10.11646/phytotaxa.220.3.2

Araújo JPM, Hughes DP (2016) Diversity of Entomopathogenic Fungi: Which Groups Conquered the Insect Body? Advances in Genetics 94: 1–39. https://doi.org/10.1016/bs.adgen.2016.01.001

Araújo JPM, Hughes DP (2019) Zombie-Ant Fungi Emerged from Non-manipulating, Beetle-Infecting Ancestors. Current Biology 29(21): 1–4. https://doi.org/10.1016/j.cub.2019.09.004

Ban S, Sakane T, Nakagiri A (2015) Three new species of *Ophiocordyceps* and overview of anamorph types in the genus and the family Ophiocordyceptaceae. Mycological Progress 14(1): e1017. https://doi.org/10.1007/s11557-014-1017-8

Bischoff JF, Rehner SA, Humber RA (2006) *Metarhizium frigidum* sp. nov.: A Cryptic Species of *M. anisopliae* and a Member of the *M. flavoviride* Complex. Mycologia 98(5): 737–745. https://doi.org/10.1080/15572536.2006.11832645

Castlebury LA, Rossman AY, Sung GH, Hyten AS, Spatafora JW (2004) Multigene phylogeny reveals new lineage for *Stachybotrys chartarum*, the indoor air fungus. Mycological Research 108(8): 864–872. https://doi.org/10.1017/S0953756204000607

Chen JY, Cao YQ, Yang DR, Li MH (2011) A new species of *Ophiocordyceps* (Clavicipitaceae, Ascomycota) from southwestern China. Mycotaxon 115(1): 1–4. https://doi.org/10.5248/115.1

Chen SQ, Wang YB, Zhu KF, Yu H (2021) Mitogenomics, Phylogeny and Morphology Reveal *Ophiocordyceps pingbianensis* sp. nov., an Entomopathogenic Fungus from China. Life (Chicago, Ill.) 11(7): e686. [16 pp] https://doi.org/10.3390/life11070686

Chen ZH, Dai YD, Yu H, Yang K, Yang ZL, Yuan F, Zeng WB (2013) Systematic analyses of *Ophiocordyceps lanpingensis* sp. nov. a new species of *Ophiocordyceps* in China. Microbiological Research 168(8): 525–532. https://doi.org/10.1016/j.micres.2013.02.010

Crous PW, Luangsa-ard JJ, Wingfield MJ, Carnegie AJ, Hernández-Restrepo M, Lombard L, Roux J, Barreto RW, Baseia IG, Cano-Lira JF, Martín MP, Morozova OV, Stchigel AM, Summerell BA, Brandrud TE, Dima B, García D, Giraldo A, Guarro J, Gusmão LFP, Khamsuntorn P, Noordeloos ME, Nuankaew S, Pinruan U, Rodríguez-Andrade E, Souza-Motta CM, Thangavel R, van Iperen AL, Abreu VP, Accioly T, Alves JL, Andrade JP, Bahram M, Baral HO, Barbier E, Barnes CW, Bendiksen E, Bernard E, Bezerra JDP, Bezerra JL, Bizio E, Blair JE, Bulyonkova TM, Cabral TS, Caiafa MV, Cantillo T, Colmán AA, Conceição LB, Cruz S, Cunha AOB, Darveaux BA, da Silva AL, da Silva GA, da Silva GM, da Silva RMF, de Oliveira RJV, Oliveira RL, De Souza JT, Dueñas M, Evans HC, Epifani F, Felipe MTC, Fernández-López J, Ferreira BW, Figueiredo CN, Filippova NV, Flores JA, Gené J, Ghorbani G, Gibertoni TB, Glushakova AM, Healy R, Huhndorf SM, Iturrieta-González I, Javan-Nikkhah M, Juciano RF, Jurjević Ž, Kachalkin AV, Keochanpheng K, Krisai-Greilhuber I, Li YC, Lima AA, Machado AR, Madrid H, Magalhães OMC, Marbach PAS, Melanda GCS, Miller AN, Mongkolsamrit S, Nascimento RP, Oliveira TGL, Ordoñez ME, Orzes R, Palma MA, Pearce CJ, Pereira OL, Perrone G, Peterson SW, Pham THG, Piontelli E, Pordel A, Quijada L, Raja HA, Rosas de Paz E, Ryvarden L, Saitta A, Salcedo SS, Sandoval-Denis M, Santos TAB, Seifert KA, Silva BDB, Smith ME, Soares AM, Sommai S, Sousa JO, Suetrong S, Susca A, Tedersoo L, Telleria MT, Thanakitpipattana D, Valenzuela-Lopez N, Visagie CM, Zapata M, Groenewald JZ (2018) Fungal Planet description sheets: 785–867. Persoonia 41(1): 238–417. https://doi.org/10.3767/persoonia.2018.41.12

Crous PW, Wingfield MJ, Lombard L, Roets F, Swart WJ, Alvarado P, Carnegie AJ, Moreno G, Luangsa-ard J, Thangavel R, Alexandrova AV, Baseia IG, Bellanger JM, Bessette AE, Bessette AR, De la Peña-Lastra S, García D, Gené J, Pham THG, Heykoop M, Malysheva E, Malysheva V, Martín MP, Morozova OV, Noisripoom W, Overton BE, Rea AE, Sewall BJ, Smith ME, Smyth CW, Tasanathai K, Visagie CM, Adamčík S, Alves A, Andrade JP, Aninat MJ, Araújo RVB, Bordallo JJ, Boufleur T, Baroncelli R, Barreto RW, Bolin J, Cabero J, Caboň M, Cafà G, Caffot MLH, Cai L, Carlavilla JR, Chávez R, de Castro RRL, Delgat L, Deschuyteneer D, Dios MM, Domínguez LS, Evans HC, Eyssartier G, Ferreira BW, Figueiredo CN, Liu F, Fournier J, Galli-Terasawa LV, Gil-Durán C, Glienke C, Gonçalves MFM, Gryta H, Guarro J, Himaman W, Hywel-Jones N, Iturrieta-González I, Ivanushkina NE, Jargeat P, Khalid AN, Khan J, Kiran M, Kiss L, Kochkina GA, Kolařík M, Kubátová A, Lodge DJ, Loizides M, Luque D, Manjón JL, Marbach PAS, Massola Jr NS, Mata M, Miller AN, Mongkolsamrit S, Moreau PA, Morte A, Mujic A, Navarro-Ródenas A, Németh MZ, Nóbrega TF, Nováková A, Olariaga I, Ozerskaya SM, Palma MA, Petters-Vandresen DAL, Piontelli E, Popov ES, Rodríguez A, Requejo Ó, Rodrigues ACM, Rong IH, Roux J, Seifert KA, Silva BDB, Sklenář F, Smith JA, Sousa JO, Souza HG, De Souza JT, Švec K, Tanchaud P, Tanney JB, Terasawa F, Thanakitpipattana D, Torres-Garcia D, Vaca I, Vaghefi N, van Iperen AL, Vasilenko OV, Verbeken A, Yilmaz N, Zamora JC,

Zapata M, Jurjević Ž, Groenewald JZ (2019) Fungal Planet description sheets: 951–1041. Persoonia 43(1): 223–425. https://doi.org/10.3767/persoonia.2019.43.06

Darriba D, Taboada GL, Doallo R, Posada D (2012) jModelTest 2: More models, new heuristics and parallel computing. Nature Methods 9(8): 772–772. https://doi.org/10.1038/nmeth.2109

Doan UV, Rojas BM, Kirby R (2017) Unintentional ingestion of *Cordyceps* fungus-infected cicada nymphs causing ibotenic acid poisoning in Southern Vietnam. Clinical Toxicology 1–4(8): 893–896. https://doi.org/10.1080/15563650.2017.1319066

Fan Q, Wang YB, Zhang GD, Tang DX, Yu H (2021) Multigene Phylogeny and Morphology of *Ophiocordyceps alboperitheciata* sp. nov., A New Entomopathogenic Fungus Attacking Lepidopteran Larva from Yunnan, China. Mycobiology 49(2): 133–141. https://doi.org/10.1080/12298093.2021.1903130

Hyde KD, Norphanphoun C, Abreu VP, Bazzicalupo A, Thilini Chethana KW, Clericuzio M, Dayarathne MC, Dissanayake AJ, Ekanayaka AH, He MQ, Hongsanan S, Huang SK, Jayasiri SC, Jayawardena RS, Karunarathna A, Konta S, Kušan I, Lee H, Li JF, Lin CG, Liu NG, Lu YZ, Luo ZL, Manawasinghe IS, Mapook A, Perera RH, Phookamsak R, Phukhamsakda C, Siedlecki I, Soares AM, Tennakoon DS, Tian Q, Tibpromma S, Wanasinghe DN, Xiao YP, Yang J, Zeng XY, Abdel-Aziz FA, Li WJ, Senanayake IC, Shang QJ, Daranagama DA, de Silva NI, Thambugala KM, Abdel-Wahab MA, Bahkali AH, Berbee ML, Boonmee S, Bhat DJ, Bulgakov TS, Buyck B, Camporesi E, Castañeda-Ruiz RF, Chomnunti P, Doilom M, Dovana F, Gibertoni TB, Jadan M, Jeewon R, Jones EBG, Kang JC, Karunarathna SC, Lim YW, Liu JK, Liu ZY, Plautz Jr HL, Lumyong S, Maharachchikumbura SSN, Matočec N, McKenzie EHC, Mešić A, Miller D, Pawłowska J, Pereira OL, Promputtha I, Romero AI, Ryvarden L, Su HY, Suetrong S, Tkalčec Z, Vizzini A, Wen TC, Wisitrassameewong K, Wrzosek M, Xu JC, Zhao Q, Zhao RL, Mortimer PE (2017) Fungal diversity notes 603–708: Taxonomic and phylogenetic notes on genera and species. Fungal Diversity 87(1): 1–235. https://doi.org/10.1007/s13225-017-0391-3

Hywel-Jones NL (1995a) *Cordyceps nutans* and its anamorph, a pathogen of Hemipteran bugs in Thailand. Mycological Research 99(6): 724–726. https://doi.org/10.1016/S0953-7562(09)80536-4

Hywel-Jones NL (1995b) *Cordyceps brunneapunctata* sp. nov. infecting beetle larvae in Thailand. Mycological Research 99(10): 1195–1198. https://doi.org/10.1016/S0953-7562(09)80277-3

Index Fungorum (2022) Index Fungorum. http://www.indexfungorum.org/names/Names.asp [Accessed on 26.04.2022]

Kobayasi Y (1941) The genus *Cordyceps* and its allies. Science Reports of the Tokyo Bunrika Daigaku. Section B 5: 53–260.

Kobayasi Y (1982) Keys to the taxa of the genera *Cordyceps* and *Torrubiella*. Nippon Kingakkai Kaiho 23: 329–364.

Kobayasi Y, Shimizu D (1963) Monographic studies of *Cordyceps* 2. Group parasitic on Cicadae. Bulletin of the National Science Museum, Tokyo 6: 286–314.

Kobayasi Y, Shimizu D (1982) *Cordyceps* species from Japan. 4. Bulletin of the National Science Museum, Tokyo 8(3): 79–91.

Lao TD, Le TAH, Truong NB (2021) Morphological and genetic characteristics of the novel entomopathogenic fungus *Ophiocordyceps langbianensis* (Ophiocordycipitaceae, Hypocreales)

from Lang Biang Biosphere Reserve, Vietnam. Scientific Reports 11(1): e1412. https://doi.org/10.1038/s41598-020-78265-7

Larkin MA, Blackshields G, Brown NP, Chenna R, McGettigan PA, McWilliam H, Valentin F, Wallace IM, Wilm A, Lopez R, Thompson JD, Gibson TJ, Higgins DG (2007) Clustal W and Clustal X version 2.0. Bioinformatics (Oxford, England) 23(21): 2947–2948. https://doi.org/10.1093/bioinformatics/btm404

Liu YJ, Whelen S, Hall BD (1999) Phylogenetic relationships among ascomycetes: Evidence from an RNA polymerse II subunit. Molecular Biology and Evolution 1799(12): 1799–1808. https://doi.org/10.1093/oxfordjournals.molbev.a026092

Liu ZY, Liang ZQ, Whalley AJS, Yao YJ, Liu AY (2001) *Cordyceps brittlebankisoides*, a new pathogen of grubs and its anamorph, *Metarhizium anisopliae* var. *majus*. Journal of Invertebrate Pathology 78(3): 178–182. https://doi.org/10.1006/jipa.2001.5039

Luangsa-ard JJ, Ridkaew R, Tasanathai K, Thanakitpipattana D, Hywel-Jones N (2011) *Ophiocordyceps halabalaensis*: A new species of *Ophiocordyceps* pathogenic to *Camponotus gigas* in Hala Bala Wildlife Sanctuary, Southern Thailand. Fungal Biology 115(7): 608–614. https://doi.org/10.1016/j.funbio.2011.03.002

Luangsa-ard JJ, Tasanathai K, Mongkolsamrit S, Hywel-Jones N (2008) Atlas of Invertebrate-Pathogenic Fungi of Thailand (Volume 2). National Center for Genetic Engineering and Biotechnology 2: 75.

Luangsa-ard JJ, Tasanathai K, Thanakitpipattana D, Khonsanit A, Stadler M (2018) Novel and interesting *Ophiocordyceps* spp. (Ophiocordycipitaceae, Hypocreales) with superficial perithecia from Thailand. Studies in Mycology 89(1): 125–142. https://doi.org/10.1016/j.simyco.2018.02.001

Luyen VT, Hanh TV, Luan TH, Thao NTB, Hiep DM, Nguyen TB, Thuan LD (2017) Discorvery of entomopathogenic fungi *Cordyceps takaomontana* at Langbian mountain, Lam Dong, Vietnam. Journal of Science Ho Chi Minh City Open University 1(13). https://doi.org/10.15625/2525-2518/55/1A/12378

Mains EB (1958) North American entomogenous species of *Cordyceps*. Mycologia 50(2): 169–222. https://doi.org/10.1080/00275514.1958.12024722

Massee G (1895) A revision of the genus *Cordyceps*. Annals of Botany 9(1): 1–44. https://doi.org/10.1093/oxfordjournals.aob.a090724

Mathieson J (1949) *Cordyceps aphodii*, a new species, on pasture cockchafer grubs. Transactions of the British Mycological Society 32(2): 113–136. https://doi.org/10.1016/S0007-1536(49)80001-5

Mongkolsamrit S, Nguyen TT, Tran NL, Luangsa-ard JJ (2011) *Moelleriella pumatensis*, a new entomogenous species from Vietnam. Mycotaxon 117(1): 45–51. https://doi.org/10.5248/117.45

Nguyen TL, Vo TBC (2005) Efficacy of some new isolates of *Metharhizium anisopliae* and *Beauveria bassiana* against rice earheadbug, *Leptocorisa acuta*. Omonrice 13: 69–75.

Petch T (1931) Notes on entomogenous fungi. Transactions of the British Mycological Society 16(1): 55–75. https://doi.org/10.1016/S0007-1536(31)80006-3

Petch T (1933) Notes on entomogenous fungi. Transactions of the British Mycological Society 18(1): 48–75. https://doi.org/10.1016/S0007-1536(33)80026-X

Quandt CA, Kepler RM, Gams W, Araújo JPM, Ban S, Evans HC, Hughes D, Humber R, Hywel-Jones N, Li ZZ, Luangsa-ard JJ, Rehner SA, Sanjuan T, Sato H, Shrestha B, Sung GH, Yao YJ, Zare R, Spatafora JW (2014) Phylogenetic-based nomenclatural proposals for Ophiocordycipitaceae (Hypocreales) with new combinations in *Tolypocladium*. IMA Fungus 5(1): 121–134. https://doi.org/10.5598/imafungus.2014.05.01.12

Rehner SA, Buckley E (2005) A *Beauveria* phylogeny inferred from nuclear ITS and EF1-α sequences: Evidence for cryptic diversification and links to *Cordyceps* teleomorphs. Mycologia 97(1): 84–98. https://doi.org/10.3852/mycologia.97.1.84

Rehner SA, Samuels GJ (1994) Taxonomy and phylogeny of *Gliocladium* analysed from nuclear large subunit ribosomal DNA sequences. Mycological Research 98(6): 625–634. https://doi.org/10.1016/S0953-7562(09)80409-7

Ronquist F, Huelsenbeck JP (2003) MrBayes 3: Bayesian phylogenetic inference under mixed models. Bioinformatics (Oxford, England) 19(12): 1572–1574. https://doi.org/10.1093/bioinformatics/btg180

Sanjuan TI, Franco-Molano AE, Kepler RM, Spatafora JW, Tabima J, Vasco-Palacios AM, Restrepo S (2015) Five new species of entomopathogenic fungi from the Amazon and evolution of neotropical *Ophiocordyceps*. Fungal Biology 119(10): 901–916. https://doi.org/10.1016/j.funbio.2015.06.010

Shrestha B, Tanaka E, Hyun MW, Han JG, Kim CS, Jo JW, Han SK, Oh J, Sung GH (2016) Coleopteran and lepidopteran hosts of the entomopathogenic genus *Cordyceps* sensu lato. Journal of Mycology 2016: 1–14. https://doi.org/10.1155/2016/7648219

Simmons DR, Kepler RM, Rehner SA, Groden E (2015) Phylogeny of *Hirsutella* species (Ophiocordycipitaceae) from the USA: Remedying the paucity of *Hirsutella* sequence data. IMA Fungus 6(2): 345–356. https://doi.org/10.5598/imafungus.2015.06.02.06

Spatafora JW, Quandt CA, Kepler RM, Sung GH, Shrestha B, Hywel-Jones NL, Luangsa-ard JJ (2015) New 1F1N Species Combinations in Ophiocordycipitaceae (Hypocreales). IMA Fungus 6(2): 357–362. https://doi.org/10.5598/imafungus.2015.06.02.07

Stamatakis A (2006) RAxML-VI-HPC: Maximum likelihood-based phylogenetic analyses with thousands of taxa and mixed models. Bioinformatics (Oxford, England) 22(21): 2688–2690. https://doi.org/10.1093/bioinformatics/btl446

Stamatakis A, Hoover P, Rougemont J (2008) A rapid bootstrap algorithm for the raxml web servers. Systematic Biology 57(5): 758–771. https://doi.org/10.1080/10635150802429642

Sung GH, Hywel-Jones NL, Sung JM, Luangsa-ard JJ, Shrestha B, Spatafora JW (2007) Phylogenetic classification of *Cordyceps* and the clavicipitaceous fungi. Studies in Mycology 57: 5–59. https://doi.org/10.3114/sim.2007.57.01

Sung GH, Shrestha B, Han SK, Sung JM (2011) Growth and Cultural Characteristics of *Ophiocordyceps longissima* Collected in Korea. Mycobiology 39(2): 85–91. https://doi.org/10.4489/MYCO.2011.39.2.085

Swofford DL (2002) PAUP*. phylogenetic analysis using parsimony (*and other methods). version 4.0b10. Sunderland, MA, Sinauer. https://doi.org/10.1111/j.0014-3820.2002.tb00191.x

Tamura K, Stecher G, Peterson D, Filipski A, Kumar S (2013) MEGA6: Molecular Evolutionary Genetics Analysis version 6.0. Molecular Biology and Evolution 30(12): 2725–2729. https://doi.org/10.1093/molbev/mst197

Tasanathai K, Noisripoom W, Chaitika T, Khonsanit A, Hasin S, Luangsa-ard J (2019) Phylogenetic and morphological classification of *Ophiocordyceps* species on termites from Thailand. MycoKeys 56: 101–129. https://doi.org/10.3897/mycokeys.56.37636

Vilgalys R, Hester M (1990) Rapid genetic identification and mapping of enzymatically amplified ribosomal DNA from several *Cryptococcus* species. Journal of Bacteriology 172(8): 4238–4246. https://doi.org/10.1128/jb.172.8.4238-4246.1990

Wang Y, Dai YD, Yang ZL, Guo R, Yu H (2021b) Morphological and Molecular Phylogenetic Data of the Chinese Medicinal Fungus *Cordyceps liangshanensis* Reveal Its New Systematic Position in the Family Ophiocordycipitaceae. Mycobiology 49(9): 1–11. https://doi.org/10.1080/12298093.2021.1923388

Wang Y, Wu HJ, Tran NL, Zhang GD, Souvanhnachit S, Wang YB, Yu H (2021a) *Ophiocordyceps furcatosubulata*, a new entomopathogenic fungus parasitizing beetle larvae (coleoptera: Elateridae). Phytotaxa 482(3): 268–278. https://doi.org/10.11646/phytotaxa.482.3.5

Wang YB, Nguyen TT, Dai YD, Yu H, Zeng WB, Wu CK (2018) Molecular phylogeny and morphology of *Ophiocordyceps unituberculata* sp. nov. (Ophiocordycipitaceae), a pathogen of caterpillars (Noctuidae, Lepidoptera) from Yunnan, China. Mycological Progress 17(6): 745–753. https://doi.org/10.1007/s11557-017-1370-5

Wang YB, Wang Y, Fan Q, Duan DE, Zhang GD, Dai RQ, Dai YD, Zeng WB, Chen ZH, Li DD, Tang DX, Xu ZH, Sun T, Nguyen TT, Tran NL, Dao VM, Zhang CM, Huang LD, Liu YJ, Zhang XM, Yang DR, Sanjuan T, Liu XZ, Yang ZL, Yu H (2020) Multigene phylogeny of the family Cordycipitaceae (Hypocreales): New taxa and the new systematic position of the Chinese cordycipitoid fungus *Paecilomyces hepiali*. Fungal Diversity 103(1): 1–46. https://doi.org/10.1007/s13225-020-00457-3

Wang YB, Yu H, Dai YD, Chen ZH, Zeng WB, Yuan F, Liang ZQ (2015) *Polycephalomyces yunnanensis* (Hypocreales), a new species of *Polycephalomyces* parasitizing *Ophiocordyceps nutans* and stink bugs (hemipteran adults). Phytotaxa 208: 34–44. https://doi.org/10.11646/phytotaxa.208.1.3

White TJ, Bruns TD, Lee SB, Taylor JW (1990) Amplification and direct sequencing of fungal ribosomal RNA genes for phylogenetics. PCR Protocols: A Guide to Methods and Application, Academic Press, New York, 315–322. https://doi.org/10.1016/B978-0-12-372180-8.50042-1

Xiao YP, Hongsanan S, Hyde KD, Brooks S, Xie N, Long FY, Wen TC (2019) Two new entomopathogenic species of *Ophiocordyceps* in Thailand. MycoKeys 47: 53–74. https://doi.org/10.3897/mycokeys.47.29898

Xu ZL, Tran NL, Wang Y, Zhang GD, Dao VM, Nguyen TT, Wang YB, Yu H (2022) Phylogeny and morphology of *Ophiocordyceps puluongensis* sp. nov. (Ophiocordycipitaceae, Hypocreales), a new fungal pathogen on termites from Vietnam. Journal of Invertebrate Pathology 192: 107771. https://doi.org/10.1016/j.jip.2022.107771

Yang ZL, Qin J, Xia C, Hu Q, Li QQ (2015) *Ophiocordyceps highlandensis*, a new entomopathogenic fungus from Yunnan, China. Phytotaxa 204(4): 287–295. https://doi.org/10.11646/phytotaxa.204.4.5

MycoKeys 92: 131–160 (2022)
doi: 10.3897/mycokeys.92.89960
https://mycokeys.pensoft.net

RESEARCH ARTICLE

A peer-reviewed open-access journal
MycoKeys
Launched to accelerate biodiversity research

New species of *Sticta* (lichenised Ascomycota, lobarioid Peltigeraceae) from Bolivia suggest a high level of endemism in the Central Andes

Emilia Anna Ossowska[1], Bibiana Moncada[2,3,4], Martin Kukwa[1], Adam Flakus[5], Pamela Rodriguez-Flakus[5], Sandra Olszewska[6], Robert Lücking[3,4]

1 *Department of Plant Taxonomy and Nature Conservation, Faculty of Biology, University of Gdańsk, Wita Stwosza 59, PL-80-308 Gdańsk, Poland* **2** *Licenciatura en Biología, Universidad Distrital Francisco José de Caldas, Cra. 4 No. 26D-54, Torre de Laboratorios, Herbario, Bogotá D.C., Colombia* **3** *Research Associate, Science & Education, The Field Museum, 1400 South Lake Shore, Chicago, IL 60605, USA* **4** *Botanischer Garten, Freie Universität Berlin, Königin-Luise-Straße 6–8, 14195 Berlin, Germany* **5** *W. Szafer Institute of Botany, Polish Academy of Sciences, Lubicz 46, PL-31-512 Kraków, Poland* **6** *10th High School in Gdynia, Władysława IV, PL-81-384 Gdynia, Poland*

Corresponding author: Emilia Ossowska (emilia.ossowska@ug.edu.pl)

Academic editor: Ester Gaya | Received 5 July 2022 | Accepted 11 August 2022 | Published 13 September 2022

Citation: Ossowska EA, Moncada B, Kukwa M, Flakus A, Rodriguez-Flakus P, Olszewska S, Lücking R (2022) New species of *Sticta* (lichenised Ascomycota, lobarioid Peltigeraceae) from Bolivia suggest a high level of endemism in the Central Andes. MycoKeys 92: 131–160. https://doi.org/10.3897/mycokeys.92.89960

Abstract

Six species of *Sticta* are described as new to science on the basis of material from Bolivia and supported by phylogenetic analysis of the fungal ITS barcoding marker. The species were resolved in all three of the clades (I, II, III) widespread and common in the Neotropics, as defined in an earlier study on the genus. Comparison with material from neighbouring countries (i.e. Colombia, Ecuador, Peru) suggests that these new species may be potentially endemic to the Bolivian Yungas ecoregion. For each species, a detailed morphological and anatomical description is given. *Sticta amboroensis* Ossowska, Kukwa, B. Moncada & Lücking is a medium-sized green-algal species with laminal to submarginal apothecia with hirsute margins and with light to dark brown lower tomentum. *Sticta aymara* Ossowska, Kukwa, B. Moncada, Flakus, Rodriguez-Flakus & Lücking is a comparatively small cyanobacterial taxon with *Nostoc* as photobiont, laminal, richly branched, aggregate isidia and a golden to chocolate-brown lower tomentum. The medium-sized, cyanobacterial *S. bicellulata* Ossowska, Kukwa, B. Moncada & Lücking has cyanobacterial photobiont, bicellular ascospores, apothecia with white to golden-brown hairs on the margins, K+ violet apothecial margin (ring around disc) and epihymenium and a white to dark brown lower tomentum. In contrast, the green-algal species, *S. carrascoensis* Ossowska, Kukwa, B. Moncada & Lücking is characterised by its large size, apothecia with dark brown hairs on the margins and a yellow medulla. The

cyanobacterial *S. catharinae* Ossowska, B. Moncada, Kukwa, Flakus, Rodriguez-Flakus & Lücking forms stipitate thalli with *Nostoc* as photobiont, abundant, laminal to submarginal apothecia and a golden-brown lower tomentum. Finally, the cyanobacterial *S. pseudoimpressula* Ossowska, Kukwa, B. Moncada & Lücking produces laminal apothecia with an orange-yellow line of pruina along the margins which reacts K+ carmine-red. In addition to the six new Bolivian taxa, the cyanobacterial *S. narinioana* B. Moncada, Ossowska & Lücking is described as new from Colombia and it represents the closely-related sister species of the Bolivian *S. aymara*; it differs from the latter largely in the marginal instead of laminal isidia.

Keywords
lichens, *Lobarioideae*, molecular barcoding, pigments

Introduction

Bolivia is one of two landlocked countries in South America, besides Paraguay, being located almost in the centre of the continent. Situated in the Neotropics, it encompasses a diversity of ecosystems, with twelve ecoregions and twenty-three sub-regions (Ibisch and Mérida 2004; Moraes and Sarmiento 2019). This ecogeographical diversity is the reason why Bolivia harbours one of the highest biodiversity levels in the world (Feuerer et al. 1998; Josse et al. 2003). About 15000 vascular plant species have been documented, over 2000 of which are endemic (Jørgensen et al. 2014; Meneses et al. 2015). An exceptionally high diversity is also observed in lichens and lichenicolous fungi (e.g. Flakus and Lücking 2008; Kukwa and Flakus 2009; Flakus et al. 2011, 2012, 2013, 2016, 2019; Oset and Kukwa 2012; Guzow-Krzemińska et al. 2019). Yet, the number of species reported from Bolivia is about 70% lower than the estimated number (Lücking et al. 2009; Rodriguez de Flakus et al. 2016).

Amongst lichenised fungi, *Sticta* (Schreb.) Ach. is one of the genera for which the diversity in Bolivia is certainly underestimated. Published records are based almost exclusively on classical taxonomy and use outdated concepts of largely widely-distributed taxa and only two recent papers dealing with Bolivian species have employed a phylogenetic approach (Moncada et al. 2014a; Ossowska 2021). Integrative taxonomy, based on molecular data and morphological and anatomical information, have substantially refined taxon concepts in this genus, revealing taxa with similar morphology and anatomy, so-called 'morphodemes', to represent multiple species (e.g. Moncada 2012; Moncada et al. 2013a, b, 2020, 2021a, b, c; Widhelm et al. 2018; Mercado-Díaz et al. 2020). For example, several previously unrecognised species have recently been described in the *S. weigelii* (Ach.) Vain. morphodeme – i.e. cyanobacterial forms with marginal isidia, such as *S. andina* B. Moncada, Lücking & Sérus. and *S. scabrosa* B. Moncada, Merc.-Díaz & Bungartz, which are even more abundant than *S. weigelii* s.str. (Moncada et al. 2021a).

Modern approaches have also contributed to the discovery or revised definition of endemic taxa in different regions; for example, *S. aongstroemii* Dal Forno, B. Moncada & Lücking, endemic to south-eastern Brazil, *S. borinquensis* Merc.-Díaz & Lücking,

endemic to Puerto Rico and *S. damicornis* (Sw.) Ach., a Caribbean endemic (Dal Forno et al. 2018; Moncada et al. 2018; Mercado-Díaz et al. 2020). Consequently, the number of formally described *Sticta* species is less than half the global estimate suggested by Moncada et al. (2013b, 2021a, b, c) and many new species may still remain unrecognised, especially in tropical ecosystems in South America and elsewhere, including Bolivia.

Here, we present the findings of a molecular revision of material of *Sticta* collected in Bolivia, integrating morphological and anatomical data, which resulted in the discovery of six new species, formally described in this study and an additional species from Colombia, closely related to one of the new Bolivian taxa. Their characteristics are elaborated in detail and a discussion on the potentially endemic occurrence of the new Bolivian species in the Yungas ecoregion of Bolivia is discussed.

Materials and methods

Taxon sampling

Sticta specimens were collected between 2010 and 2014 during fieldwork in the Yungas and Tucumano-Boliviano region. The collected material is deposited in KRAM, LPB and UGDA for the Bolivian specimens and in B and UDBC for the Colombian specimens. Morphology and anatomy were examined in Gdańsk and in Berlin, using Nikon SMZ800N and LEICA Zoom 2000 dissecting microscopes and ZEISS Axioskop compound microscopes, following the examination of characters as proposed by Moncada (2012) and Moncada et al. (2014a) and focusing on potentially diagnostic features at species level. Furthermore, we examined selected specimens from hitherto unpublished material collected in Colombia or other regions that turned out to be phylogenetically related to the Bolivian material. Spot reactions were performed with K (potassium hydroxide solution), C (sodium hypochlorite solution), Pd (paraphenylenediamine) and KC (K followed by C on the same thallus fragments) and secondary compounds were further analysed using thin-layer chromatography (TLC) in solvents A and C (Orange et al. 2001).

DNA extraction, PCR amplification and sequencing

A total of 11 new specimens of *Sticta* from Bolivia and three from Colombia were used for the molecular study. Additionally, 194 ITS rDNA *Sticta* sequences were downloaded from GenBank, representing the monophyletic assembly of clades I, II and III as defined by Widhelm et al. (2018), using *S. macrothallina* as outgroup; the downloaded sequences were complemented by some previously unpublished sequences from Colombian material (Suppl. material 1: Table S1). For new DNA extractions from Bolivian material, two separate thallus fragments were taken from each specimen to allow cross-check of the results and account for potential sample contamination.

Total genomic DNA was extracted using the Sherlock AX Plant kit (A&A Biotechnology, Poland) and the Plant & Fungi DNA Purification Kit (Eurx, Poland), following the manufacturers' protocol. Fungal ITS rDNA was amplified using the primers ITS1F and ITS4A (White et al. 1990; Gardes and Bruns 1993). The same primers were used for sequencing. PCR was carried out in a volume of 25 µl using 12.5 µl of Start-Warm HS-PCR Mix Polymerase (A&A Biotechnology, Poland), 1.0 µl of 10 µM of each primer, 1.0 µl of dimethyl sulphoxide (DMSO), 3.0 µl of template DNA (~ 10–100 ng) and water. The following PCR cycling parameters were applied: an initial denaturation at 94 °C for 3 min and 33 cycles of: 94 °C for 30 sec; annealing at 52 °C for 45 sec; extension at 72 °C for 1 min and final extension at 72 °C for 10 min. The PCR products were purified using PCR Clean Up System (Promega, US) and Clean-Up (A&A Biotechnology, Poland). The cleaned DNA was sequenced using Macrogen sequencing service (http://www.macrogen.com).

Sequence alignment and phylogenetic analysis

The obtained sequences were aligned with available sequences of the genus *Sticta* (Suppl. material 1: Table S1; Suppl. material 2: File S1), using a previous master alignment (Moncada et al. 2020). The new sequences were joined to the existing alignment using MAFFT 7.164 with the "--add" option (Katoh and Frith 2012; Katoh and Standley 2013), with subsequent manual inspection in BIOEDIT 7.0.9 (Hall 2011). Phylogenetic analysis was performed using Maximum Likelihood in RAxML 8.2.0 (Stamatakis 2014) on the CIPRES Science Gateway (Miller et al. 2010), with non-parametric bootstrapping using 400 pseudoreplicates (based on an automated saturation criterion) under the GTRGAMMA model. Trees were visualised in FigTree 1.4.2 (Drummond and Rambaut 2007). After initial analysis of the full taxon set containing 1,049 terminals, the alignment was reduced to fully-identified taxa with valid names (except for one case where Bolivian samples were most closely related to a hitherto unnamed taxon from Colombia), with 3–5(–10) selected accessions per species, for a total of 211 terminals and the phylogenetic analysis was repeated using the above approach.

Results and discussion

In the global phylogeny (Fig. 1; Suppl. material 3: Fig. S1), specimens from Bolivia formed five distinct lineages, suggesting six previously undescribed taxa, two of these representing closely-related sister taxa. The new species were recovered in all three clades (I, II, III) recognised by Widhelm et al. (2018) as common and widespread in the Neotropics: three in clade I (*fuliginosa* clade), one in clade II (*tomentosa* clade) and two in clade III (*weigelii* clade). With the use of the ITS barcoding marker only, the latter clade was not resolved as monophyletic, but formed a paraphyletic grade relative to clade II (Fig. 1; Suppl. material 3: Fig. S1). The first taxon, here named *Sticta aymara* and nested within the *S. cometia* clade, was recovered as sister to an

undescribed species from Colombia, which is also described below as *S. narinioana*. Two other novel taxa, *S. bicellulata* and *S. pseudoimpressula*, fell within the *S. sylvatica* clade, closely related to *S. peltigerella* (Nyl.) Trevis. and *S. sylvatica* (Huds) Ach. In both of these taxa, *S. bicellulata* and *S. pseudoimpressula*, the apothecial margins (ring around disc) and epihymenium react with K, although the reactions differ in colour: it is violet in *S. bicellulata* and carmine-red in *S. pseudoimpressula*. This observation is noteworthy as it confirms the uniqueness of *Sticta* in Bolivia since, in most so far known taxa of the genus, the reaction with K is restricted to the medulla and membrane of the cyphellae. Further two new species, *S. amboroensis* and *S. carrascoensis*, were recovered close to *S. weigelii* and *S. andina*, respectively, but these placements were not supported in the backbone, so their exact phylogenetic relationships remain unresolved. Finally, *S. catharinae* was recovered as a novel taxon sister to the recently-described *S. fuliginoides* Magain & Sérus. (Fig. 1; Suppl. material 3: Fig. S1).

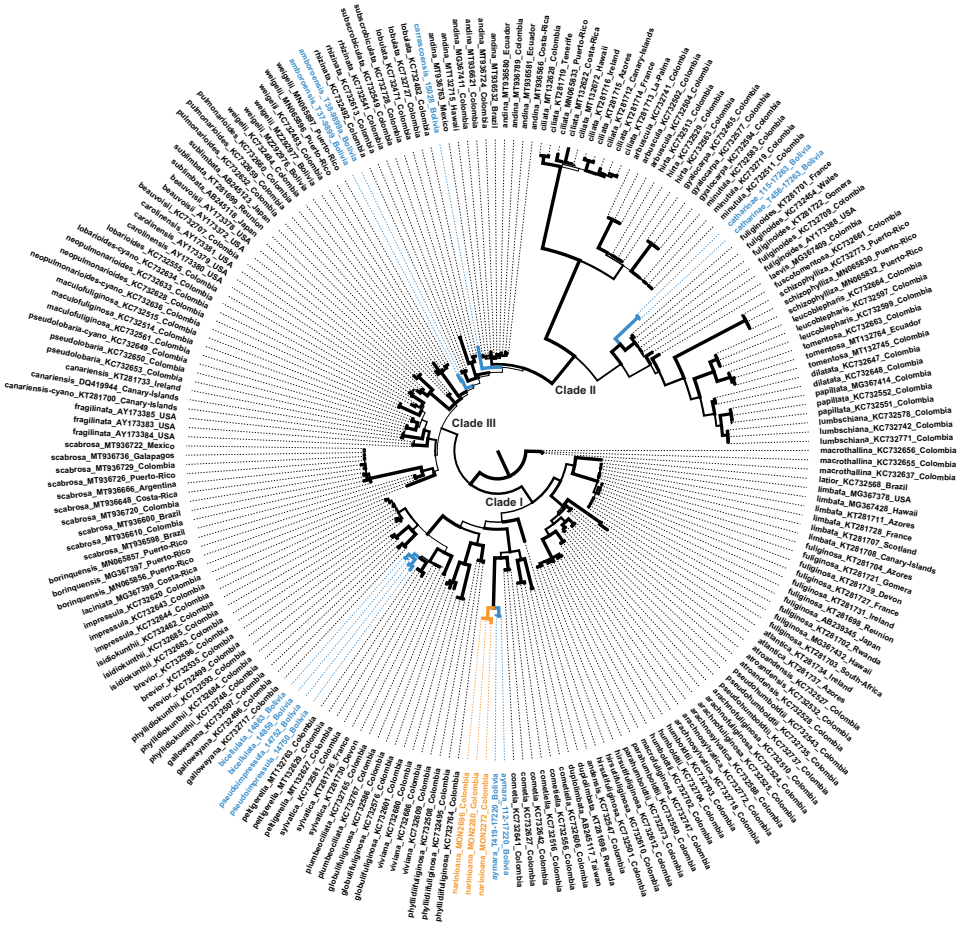

Figure 1. Best-scoring Maximum Likelihood tree of the *Sticta* clades I–III containing the new species from Bolivia (blue) and Colombia (orange), based on the fungal ITS barcoding marker. Supported clades are thickened. For a complete tree with individual support values, see Suppl. material 3: Fig. S1.

Analysis of morphological and anatomical features of these specimens and comparison with phylogenetically related and similar species supported their interpretation as new to science. These new species are characterised by various key features, described and discussed in detail along with overall morphological and anatomical characteristics in the 'Taxonomy' section below. At present, all species described below are known from only one site in Bolivia (although some are known from two collections); hence, it is difficult to estimate their frequency in this country. Nevertheless, it is reasonable to describe such species from single sites from such poorly studied countries, firstly due to the difficulty of exploring some areas of Bolivia and therefore the impossibility of splitting samples and secondly, because of the need for lichen conservation efforts in this country.

So far, the number of *Sticta* species known from Bolivia has not been critically assessed, most listings dating from the 19th and early 20th century (Nylander 1859, 1861; Rusby 1896; Herzog 1922, 1923). As a result, the recently assembled checklist (Rodriguez-Flakus et al. 2016) enumerates only 11 species, namely *S. damicornis* (Sw.) Ach., *S. dilatata* (Nyl.) Vain., *S. fuliginosa* (Dicks.) Ach., *S. isidiokunthii* B. Moncada & Lücking, *S. kunthii* Hook., *S. laciniata* (Sw.) Ach., *S. macrophylla* Bory ex Delise, *S. sinuosa* Pers., *S. tomentosa* (Sw.) Ach., *S. umbilicariiformis* Hochst. ex Flot. (Nylander 1861) and *S. weigelii*. Of these, the names *S. damicornis*, a Caribbean endemic, the paleotropical *S. macrophylla* and the African *S. umbilicariiformis* are certainly misapplications.

Recent research on *Sticta* (Moncada 2012; Moncada and Lücking 2012; Moncada et al. 2013a, b, 2014a, b, 2020, 2021a, b) has contributed to a much better understanding of the diversity of the genus and also facilitated further studies on this genus. As a consequence, *Sticta* has been more thoroughly assessed in other lichenologically poorly studied regions of the world (e.g. Simon et al. 2018; Widhelm et al. 2018; Mercado-Díaz et al. 2020; Moncada et al. 2020). In this respect, Bolivia remained as a 'white spot' on the map. The results presented here add to some previous works (Moncada et al. 2014a; Ossowska 2021) and substantially increase our knowledge of *Sticta* in Bolivia, cataloguing the true diversity of this genus in the country using more accurate delimitation of species supported by phylogenetic analyses. Yet unpublished data from our group, including a large number of still unnamed clades that require thorough revision including phenotype characters, suggest that the number of taxa present in Bolivia may be comparable to the diversity now known from Colombia (more than 200 species) (Moncada 2012; Moncada et al. 2013a, b, 2014a, b, 2020, 2021a).

Considering that the globally available sequence data of *Sticta* originate from nearly 30 different countries, it is notable that sequenced specimens from Bolivia mostly represent novel lineages, which suggests that these taxa may be endemic to the Yungas ecoregion in Bolivia. However, further studies in nearby regions are required to test this hypothesis. Endemic species of *Sticta* have been reported by other authors from various regions (e.g. Tønsberg and Goward 2001; Lendemer and Goffinet 2015; Dal Forno et al. 2018; Moncada et al. 2018, 2020; Widhelm et al. 2018). In Madagascar and the Mascarenes, for instance, where the genus has been very well sampled, 89% of the known species are endemic (Simon et al. 2018). A similarly high proportion has been reported from Puerto Rico, although Mercado-Díaz et al. (2020) noted that this number may be overestimated due to a lack of comparative data from neighbouring islands.

The degree of endemism of *Sticta* in Hawaii is estimated at 69% (Moncada et al. 2020). While the large number of endemic taxa on the islands is related to their geographical isolation (Nash 2008), a high proportion of endemic lichens is also observed, for example, in isolated tropical mountains or in fog-induced lichen zones in coastal deserts, like Namibia (Aptroot 2008; Aptroot and Schumm 2011; Sparrius et al. 2017).

The putative endemism of the species described here is also supported by the fact that the specimens were collected from different sites located within the Yungas ecoregion on the north-eastern slopes of the Andes. This is an area situated at 1000–4200 m altitude and extends over 55,556 km. It is mainly covered by evergreen humid forest and includes several protected areas, such as Madidi and Cotapata National Parks (Ibisch and Mérida 2004; Moraes and Sarmiento 2019). Yungas is a species-rich area and has been considered a centre of endemism in Bolivia for different groups of organisms, such as algae, bryophytes and orchids (e.g. Kessler 1999; Ibisch and Mérida 2004; Moraes and Sarmiento 2019; Kolanowska et al. 2021; Kosecka et al. 2021).

A large number of putatively endemic taxa within *Sticta*, not only in Bolivia, but also in other regions, may account for the discrepancy between the described and expected number of species in this genus, with 200 species known vs. 500 predicted (Moncada et al. 2013a, b, 2021b; Mercado-Díaz et al. 2020). Our results from Bolivia increase the global number of *Sticta* by another six new species, thus slowly chipping away at this knowledge gap.

Taxonomy

New species from Bolivia

Sticta amboroensis **Ossowska, Kukwa, B. Moncada & Lücking, sp. nov.**
MycoBank No: MB845385
Fig. 2

Diagnosis. Differing from *S. subscrobiculata* in the larger thalli with abundant marginal cilia and marginal and laminal apothecia with veined lower surface and the thickness of the upper cortex with 60–80 µm.

Type. Bolivia. Dept. Santa Cruz; Prov. Florida, Parque Nacional Amboró, above la Yunga Village, senda los Helechos, near view point, 18°02'50"S, 63°54'50"W, elev. 2330 m, Yungas cloud forest with abundant tree ferns, corticolous, 08 June 2011, M. Kukwa 9899 (holotype UGDA, isotype LPB).

Description. Primary photobiont a green alga. Stipe absent. Thallus irregular, up to 25 cm diam., moderately branched, with 3–5 branches per 5 cm radius, branching polytomous; lobes ligulate to laciniate, imbricate to adjacent, involute, with their apices rounded to obtuse and involute and their margins entire to sinuous, not thickened; lobe internodes (3–)7–10(–20) mm long, (4–)8–7(–18) mm broad; thallus coriaceous. Upper surface plane to rugose-pitted towards the centre, beige-brown with darker apices in the herbarium, shiny, with the brown marginal line; surface glabrous, without papillae, without pruina, but with irregular to indistinct, cream maculae, present in older parts of

lobes; marginal cilia abundant, simple to fasciculated, light to dark brown, rarely white, up to 0.5 mm long. Apothecia abundant, principally submarginal to laminal, sparse to aggregated, subpedicellate, without pronounced invagination on lower side, up to 3 mm diam.; disc light brown to brown (mature) and yellow (young), shiny to matt; margin entire to crenate, hirsute, with brown hairs, abundant in young apothecia, sparse in old ones. Vegetative propagules absent. Lower surface with somewhat elevated, diffuse ridges, cream to brown towards the centre; primary tomentum dense, sparse towards the margin, thick but thinner towards the margin, spongy to fasciculate, soft, light brown to dark brown; secondary tomentum absent. Rhizines scarce, brown to white, up to 8 mm long. Cyphellae 1–20 per cm^2 towards the thallus centre and 21–40 per cm^2 towards the margin, scattered, rounded to irregular, urceolate with wide pore, erumpent to prominent, remaining below the level of the primary tomentum, with the margin raised and involute, cream-coloured, with tomentum; pore 0.5–1.5 mm diam.; basal membrane pruinose in appearance, white to cream, K+ pale yellow, C–, KC–, Pd–. Medulla lax to compact, white, K–, C–, KC–, Pd–. No substances detected by TLC.

Upper cortex paraplectenchymatous, 60–80 µm thick, consisting of 6–7 cell layers with cells 6–16 µm diam. (with smaller cells in outside parts of the cortex), their walls 3–5 µm thick and their lumina rounded to isodiametric, 4–15 µm diam. Photobiont layer 35–50 µm thick, its cells 5–8 µm diam. Medulla 150–220 µm thick, its hyphae 4–5 µm broad, without crystals. Lower cortex paraplectenchymatous, 30–45 µm thick, with 3–4 cell layers; cells 6–17 µm diam., their walls 2–7 µm thick. Hairs of lower primary tomentum up to 1 mm long, in fascicles of 12–20, hyphae unbranched, 5–6 µm wide with rugose walls, forming a brush-like head with free apices. Cyphella cavity up to 300 µm deep; compacted cells of basal membrane rarely with one papillae. Apothecia biatorine, up to 700 µm high, without distinct stipe; excipulum 125–175 µm broad, laterally with projecting hairs, 50 µm long, simple or in groups. Hymenium 100–110 µm high, K+ yellow; epihymenium up to 20 µm high, yellow-brown, K+ yellow intensifying, with gelatinous upper layer, ca. 5 µm high. Asci 6–8-spored, ascospores fusiform, 1–3-septate, 27–42 × 6–10 µm.

Habitat and distribution. *Sticta amboroensis* is known only from one locality in Parque Nacional Amboró in Department Santa Cruz, where it grows on tree bark at altitude 2330 m.

Etymology. The name refers the Parque Nacional Amboró, where the species was found.

Additional material examined. Bolivia. Dept. Santa Cruz; Prov. Florida, Parque Nacional Amboró, above la Yunga Village, senda los Helechos, near view point, 18°02'50"S, 63°54'50"W, elev. 2330 m, Yungas cloud forest with abundant tree ferns, 08 June 2011, M. Kukwa 9899a (LPB, UGDA).

Notes. *Sticta amboroensis* forms an isolated lineage not far from other green algal species, such as *S. pulmonarioides* B. Moncada & Coca and *S. subscrobiculata* (Nyl.) Gyeln. These species are characterised by a similar morphology, but clearly distinguished phylogenetically. In *S. subscrobiculata*, the lobes are sparsely branched and pleurotomous and the marginal cilia are sparse to absent, although a cilia-like extension of the lower

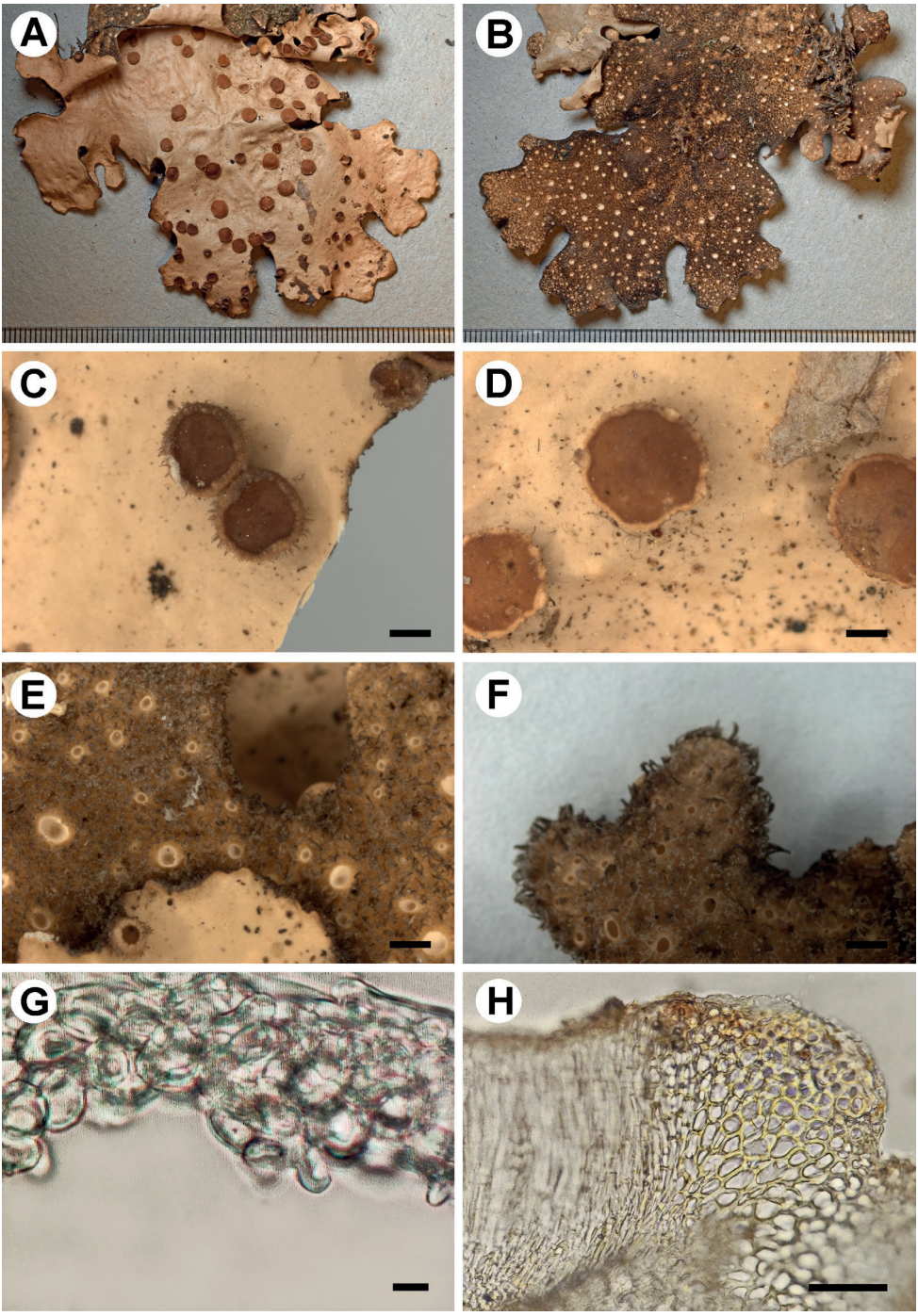

Figure 2. Morphology of *Sticta amboroensis* (holotype) **A** upper surface **B** lower surface **C–D** apothecia with hirsute margins **E** lower tomentum with cyphellae **F** marginal cilia **G** cyphella membrane **H** excipulum in section. Scale bars: 1 mm (**A–F**); 5 µm (**G**); 50 µm (**H**).

tomentum is usually visible (Moncada 2012). In the case of *S. pulmonarioides*, thallus is smaller, up to 15 cm in diam., with sparse, mainly submarginal apothecia. In addition, the lower tomentum is sparse over the entire lower surface (Moncada et al. 2013a).

***Sticta aymara* Ossowska, Kukwa, B. Moncada, Flakus, Rodriguez-Flakus & Lücking, sp. nov.**

MycoBank No: MB845386

Fig. 3

Diagnosis. Differing from *S. narinioana* in the presence of laminal isidia and in the absence of apothecia, as well as the less densely arranged cyphellae.

Type. Bolivia. Dept. La Paz; Prov. Nor Yungas, Parque Nacional y Área Natural de Manejo Integrado Cotapata, near Urpuma colony, 16°13'20"S, 67°52'34"W, elev. 1989 m, Yungas montane forest, 30 June 2010, A. Flakus 17220 & P. Rodriguez-Flakus (holotype KRAM, isotype LPB).

Description. Primary photobiont cyanobacterial (*Nostoc*). Stipe absent. Thallus orbicular to irregular, up to 5 cm diam., sparsely branched, with 0–2 branches per 5 cm radius, branching pleurotomous; lobes suborbicular to flabellate, interspaced to adjacent, plane to undulate, with their apices rounded and revolute and their margins entire to sinuous, not thickened; lobe internodes (1–)2–4(–7) mm long, (3–)5–6(–10) mm broad; thallus subcoriaceous. Upper surface smooth to pitted or rugose towards the centre, brownish-yellow with darker apices in the herbarium, shiny; surface glabrous, without papillae and pruina, but with irregular, scattered, yellow maculae; marginal cilia absent. Apothecia absent. Vegetative propagules present, abundant, in the form of isidia, predominantly laminal, aggregate, richly branched from the beginning, isidial branches cylindrical to coralloid, vertical, up to 0.6 mm long and 0.05 mm broad, darker than the thallus, grey, shiny; in cross-section, round or rarely slightly flattened. Lower surface with somewhat elevated, diffuse ridges, yellow to brown towards the centre; primary tomentum dense to the margin, thick but thinner towards the margin, spongy to fasciculate, soft, golden to chocolate; secondary tomentum present, arachnoid. Rhizines absent. Cyphellae sparse, 1–10 per cm^2 towards the thallus centre and 1–20 per cm^2 towards the margin, scattered, angular to irregular, urceolate with wide pore, prominent, remaining below the level of the primary tomentum, with the margin raised and involute, cream-coloured, with or without tomentum; pore 0.25–0.75 mm diam.; basal membrane ± smooth, white, K–, C–, KC–, Pd–. Medulla compact, cream, K–, C–, KC–, Pd–. No substances detected by TLC.

Upper cortex paraplectenchymatous, 15–40 µm thick, consisting of 2–3 cell layers with cells 7–18 µm diam. (with smaller cells in outside parts of the cortex), their walls 0.6–2 µm thick and their lumina rounded to isodiametric, 6–17 µm diam. Photobiont layer 25–70 µm thick, its cells 4–20 µm diam. Medulla 30–70 µm thick, its hyphae 2.5–6 µm broad, without crystals. Lower cortex paraplectenchymatous, 30–50 µm thick, with 3 cell layers; cells 6–20 µm diam., their walls 2–4 µm thick. Hairs of lower primary tomentum 150–400 µm long, in fascicles of more than 20, hyphae simple,

septate with interlocked apices. Cyphella cavity up to 130 µm deep; cells of basal membrane without papillae or with single papillae. Apothecia not observed.

Habitat and distribution. *Sticta aymara* is known only from the type locality in the Department La Paz, at an altitude of 1989 m.

Etymology. The name refers the Aymara people in the Andes and Altiplano regions of South America who coined the term Yungas.

Notes. Although this new taxon is known from a single collection only, we decided to describe it formally, as the material is well-developed and phylogenetically distinctive, shown by two sequences generated from different pieces of the specimen. *Sticta aymara* forms a sister clade with the also newly-described *S. narinioana* from Colombia (see below). Both taxa produce isidia, but in *S. narinioana*, they are concentrated along the thallus margins and horizontally orientated, while in *S. aymara*, they are laminal and upright. Moreover, sparse, submarginal apothecia, absent in *S. aymara*, were observed in *S. narinioana*. Cilia are absent in both taxa, but in *S. narinioana*, the white tomentum projects beyond the edge of the lobes and resembles cilia. The two species also differ in the abundance of cyphellae, which are more densely arranged in *S. narinioana*.

The presence of isidia is also characteristic for *S. isidiokunthii* B. Moncada & Lücking and *S. weigelii*, amongst other similar species (Moncada 2012). However, isidia in these species are mainly marginal and differ in colour. In *S. aymara* the isidia are grey, in *S. isidiokunthii*, greenish-brown to brown and in *S. weigelii*, blackish-brown. Moreover, the latter taxa are characterised by thalli larger than *S. aymara*, up to 10–15 cm in diam. Differences were also observed in the structure and colour of the lower surface. In *S. isidiokunthii*, it is uneven, beige to dark brown, while in *S. weigelii*, it is smooth to undulate, beige to red-brown (Moncada 2012; Moncada and Lücking 2012; Ossowska 2021). Additionally, *S. isidiokunthii* also produces laminal apothecia (Moncada and Lücking 2012). The medulla of both *S. isidiokunthii* and *S. weigelii* reacts with K, while in *S. aymara*, it is K negative.

The small size of the thalli, the presence of isidia and the absence of apothecia is also characteristic of *S. viviana* A. Suárez & Lücking. However, this taxon has a dark brown, scrobiculate to faveolate upper surface with cream-coloured maculae. Furthermore, the lower part is rugose to undulating, rather than ridged-veined as in *S. aymara*. The medulla of *S. viviana* is K+ orange-yellow and the cyphellae are K+ yellow. The latter species is known from Colombia and Costa Rica (Moncada 2012; Suárez and Lücking 2013; Moncada et al., unpub.). *Sticta aymara* and *S. viviana* are phylogenetically only distantly related (Fig. 1; Suppl. material 3: Fig. S1).

Sticta bicellulata **Ossowska, Kukwa, B. Moncada & Lücking, sp. nov.**
MycoBank No: MB845387
Fig. 4

Diagnosis. Differing from *S. pseudoimpressula* in the predominantly bicellular spores and the absence of secondary tomentum and the K+ violet (instead of carmine-red) reaction of the apothecial atraquinone.

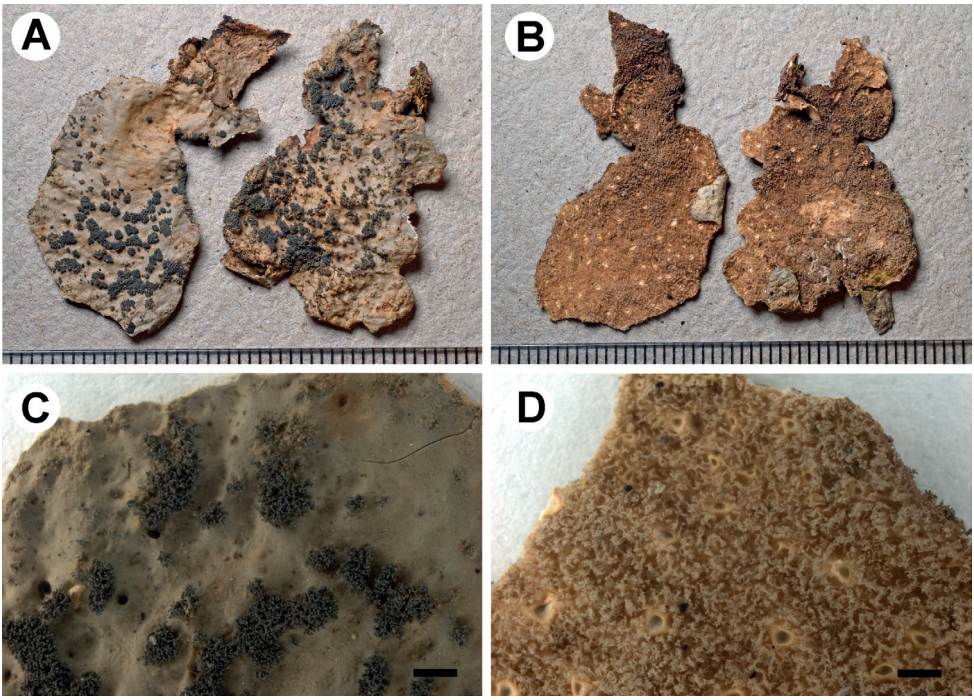

Figure 3. Morphology of *Sticta aymara* (holotype) **A** upper surface with isidia **B** lower surface showing shallow ridges (visible on right-hand lobe after removal of tomentum) **C** laminal and branched isidia **D** tomentum and cyphellae. Scale bars: 1 mm.

Type. Bolivia. Dept. La Paz; Prov. Franz Tamayo, Parque Nacional y Área Natural de Manejo Integrado Madidi, near Keara Bajo, 14°41'59"S, 69°04'34"W, elev. 3290 m, open area with shrubs and scattered trees, Ceja de Monte Inferior (Altimontano), on shrubs, 17 Nov 2014, M. Kukwa 14859 (holotype UGDA, isotype LPB).

Description. Primary photobiont cyanobacterial (*Nostoc*). Stipe absent. Thallus irregular to suborbicular, up to 10 cm diam., moderately branched, with 3–5 branches per 5 cm radius, branching polytomous; lobes laciniate to flabellate, adjacent, involute to weakly canaliculate, with obtuse to truncate, plane to revolute apices and their margins entire, slightly thickened; lobe internodes (3–)6–8(–20) mm long, (4–)7–10(–13) mm broad; thallus coriaceous. Upper surface pitted to shallowly scrobiculate to rugose, light brown with darker apices in the herbarium, shiny, with the marginal line in the same colour; surface glabrous, without papillae and pruina, without maculae; marginal cilia present, about 0.5 mm, abundant to scarce, white to golden brown, agglutinated. Apothecia scarce, laminal, dispersed, subpedicellate, with pronounced invagination on lower side, up to 2.5 mm diam.; disc orange-brown (in young apothecia) to brown or greenish (in older apothecia) due to the presence of pruina, along the margin with an orange pigment; margin hirsute, with white to golden brown hairs. Vegetative propagules absent. Lower surface uneven, beige to light brown; primary tomentum dense to the margin, thick, but thinner towards the margin, spongy, soft, white to dark brown often with brown tips; secondary tomentum

absent. Rhizines absent. Cyphellae 1–10 per cm^2 towards the thallus centre and 21–40 per cm^2 towards the margin, abundant, scattered, rounded to irregular, urceolate with wide pore, prominent, remaining below the level of the primary tomentum, with the margin raised and involute, white to brown coloured, without or with tomentum at the base; pore (0.25–)0.5–1(–1.5) mm diam.; basal membrane pruinose in the appearance, white, K– to K+ yellow, C–, KC–, Pd–. Medulla compact, white with yellow spots, K+ pale yellow, C–, KC–, Pd–. Apothecial margin (ring around disc) and epihymenium K+ violet. No substances detected by TLC in the thallus, unidentified anthraquinone in the apothecia.

Upper cortex paraplectenchymatous, 35–50 µm thick, consisting of 3–4 layers of cells 5–16 µm diam. (with smaller cells in outside parts of the cortex), their walls 1.5–3.5 µm thick and their lumina rounded to isodiametric, 4–15 µm diam. Photobiont layer 40–80 µm thick, its cells 5–10 µm diam. Medulla 35–50 µm thick, its hyphae 5 µm broad, without crystals. Lower cortex paraplectenchymatous, 25–35 µm thick, with 2–3 cell layers; cells 7–13 µm diam., their walls 2.5–5 µm thick. Hairs of lower primary tomentum 100–250 µm long, in fascicles of more than 20 when mature, simple to rarely branched hyphae, 5–6 µm broad, septate with free apices. Cyphella cavity up to 100 µm deep; cells of basal membrane loosely packed consisting of cells, without papillae or very rarely, with one papillae. Apothecia biatorine, up to 100–250 µm high, without a peduncle; excipulum 80–100 µm broad, laterally with projecting hairs, hairs simple, up to 110 µm long or in groups up to 300 µm long, hairs 4–6 µm broad, thick-walled, septate. Hymenium 100–112 µm high; epihymenium 12.5–20 µm high, orange-brown, with orange granules crystals, with thin gelatinous upper layer. Asci 6–8-spored, ascospores broadly fusiform, 1(–3)-septate, 30–41 × 9–12 µm.

Habitat and distribution. The species is known from the Parque Nacional y Área Natural de Manejo Integrado Madidi, a protected area in the Department La Paz. It was found epiphytic at an elevation of 3290 m.

Etymology. The epithet refers to the predominance of bicellular spores.

Additional material examined. Bolivia. Dept. La Paz; Prov. Franz Tamayo, Parque Nacional y Área Natural de Manejo Integrado Madidi, near Keara Bajo, 14°41'59"S, 69°04'34"W, elev. 3290 m, open area with shrubs and scattered trees, Ceja de Monte Inferior (Altimontano), on shrubs, 17 Nov 2014, M. Kukwa 14863 (LPB, UGDA).

Notes. *Sticta bicellulata* is similar to *S. pseudoimpressula* (another species described below), but the main discriminating character in *S. bicellulata* is the septation of the ascospores, which are predominantly bicellular (only very few are 3-septate whereas in *S. pseudoimpressula*, only young ascospores are bicellular. Both taxa have irregular to suborbicular thalli, with laciniate to flabellate lobes, but the lobe apices in *S. bicellulata* are obtuse to truncate vs. orbicular in *S. pseudoimpressula*. Furthermore, *S. bicellulata* has a paler upper surface than *S. pseudoimpressula*. In both species, marginal cilia are present, but in *S. bicellulata*, they are agglutinated, white to golden brown vs. fasciculated, light brown to golden brown in *S. pseudoimpressula*. Apothecia in *S. bicellulata* are sparse in contrast to the abundant apothecia in *S. pseudoimpressula*. They also differ in the colour of the disc, which in both species is covered by a pruina. The margin and epihymenium react with K in both taxa, but in *S. bicellulata* the reaction is K+ violet and in *S. pseudoimpressula* K+ carmine-red, suggesting the presence of different

anthraquinones. The lower surface in both species is uneven, but in *S. bicellulata*, the tomentum is thick, becoming thinner towards the margin and a secondary tomentum is absent. Conversely, in *S. pseudoimpressula*, the primary tomentum is consistently thick and long, with a secondary tomentum present and with rhizines. The cyphellae in these two taxa are similar in shape, but in *S. bicellulata*, their margins are raised and involuted.

Remarkably, the taxa form a sister group relationship, denoting the presence of apothecial anthraquinones as a synapormorphy, although apparently, the two species diverged to the point that the anthraquinones are of a different nature, as indicated by their different K+ reaction. This character appears to be rare in *Sticta*, but may also have been overlooked, as it is only obvious in a close-up of the apothecium.

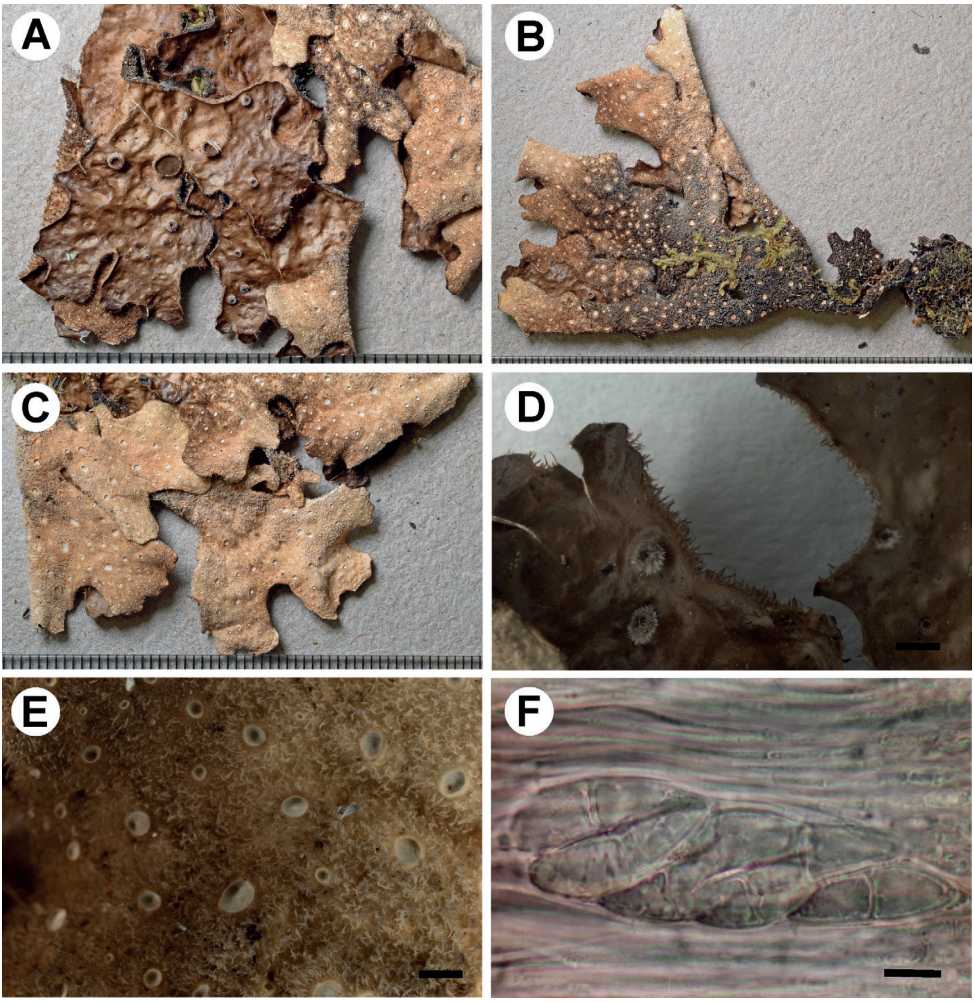

Figure 4. Morphology of *Sticta bicellulata* (holotype) **A** enlarged part of thallus showing pitted to rugose upper surface and laminal apothecia **B** lower surface **C** enlarged part of lower surface of the thallus **D** apothecia with hirsute margins and cilia at the lobe margins **E** tomentum and cyphellae **F** ascus with 1-septate ascospores. Scale bars: 1 mm (**A–E**); 10 µm (**F**).

The clade formed by *Sticta bicellulata* and *S. pseudoimpressula* is closely related to *S. sylvatica* and *S. peltigerella* (Fig. 1; Suppl. material 3: Fig. S1). The latter two produce numerous isidia distributed over the entire surface of the thalli (Moncada 2012). *Sticta sylvatica* is widespread, occurring in Europe, North and South America (Hodkinson et al. 2014), whereas *S. peltigerella* appears to be a Colombian endemic (Moncada 2012).

***Sticta carrascoensis* Ossowska, Kukwa, B. Moncada & Lücking, sp. nov.**
MycoBank No: MB845388
Fig. 5

Diagnosis. Differing from *S. andina* in the green algal photobiont, the absence of vegetative propagules and the yellow medulla.

Type. Bolivia. Dept. Cochabamba; Prov. Carrasco, Parque Nacional Carrasco, Meruvia close to Monte Punku, 17°35'06"S, 65°14'54"W, elev. 3283 m, *Podocarpus-Polylepis* forest, Ceja de Monte Inferior (Altimontano), corticolous, 26 Nov 2014, M. Kukwa 15028 (holotype UGDA, isotype LPB).

Description. Primary photobiont a green alga. Stipe absent. Thallus irregular to suborbicular, up to 30 cm diam., moderately branched, with 3–5 branches per 5 cm radius, branching pleurotomus; lobes laciniate to flabellate, interspaced to adjacent, involute, with their apices rounded and plane to involute and their margins entire, not thickened; lobe internodes (3–)6–9(–10) mm long, (3–)9–10(–12) mm broad; thallus coriaceous. Upper surface shallowly scrobiculate to rugose, yellow-brown to light brown, with darker apices in the herbarium, shiny; surface glabrous, without papillae, pruina and weakly maculate; marginal cilia present, brown, about 0.2 mm long, fasciculate. Apothecia abundant, marginal to laminal, dispersed to arranged, sometimes imbricate, subpedicellate, with pronounced invagination on lower side, up to 4 mm diam.; disc orange-brown (young apothecia) to red-brown (older apothecia), very shiny when young; margin crenate, hirsute, with dark brown hairs. Vegetative propagules absent. Lower surface somewhat ridged, yellow to dark brown towards the centre; primary tomentum dense to the margin, thick, thinner towards the margin, spongy, soft, pale to dark brown; secondary tomentum very scarce, up to 25 µm. Rhizines present, about 2 mm, brown with paler tips, fibrillose. Cyphellae 1–10 per cm^2 towards the thallus centre and 21–40 per cm^2 towards the margin, scattered, round to irregular, urceolate with wide pore, erumpent to prominent, remaining below the level of the primary tomentum, with the margin raised and involute, brown-coloured, without tomentum or with in the lower part; pore (0.2–)0.3–0.5(–0.6) mm diam.; basal membrane pruinose in the appearance, white to yellow, K– to K+ yellow, C–, KC–, Pd–. Medulla compact, pale yellow to yellow, K+ lemon-yellow, C–, KC–, Pd–. No substances detected by TLC.

Upper cortex paraplectenchymatous, external part orange-brown, 40–60 µm thick, consisting of 6–7 cell layers with cells 5–10 µm diam. (with smaller cells in outside parts of the cortex), their walls 2–3 µm thick and their lumina rounded to isodiametric, 3–10 µm diam., up to 12 µm broad. Photobiont layer 25–35 µm thick, its cells 4–6 µm diam. Medulla 120–150 µm thick, its hyphae 1.5–4.5 µm broad,

without or with yellow crystals. Lower cortex paraplectenchymatous, 25–30 µm thick, with 3 cell layers; cells 6–16 µm diam., their walls 1–3 µm thick. Hairs of lower primary tomentum up to 1 mm long, in fascicles up to 12, forming intricate mass in the dense part of tomentum, hyphae unbranched, 5–7 µm broad, septate with free apices. Cyphella cavity up to 250 µm deep; loosely packed cells of basal membrane sometimes with one papilla. Apothecia biatorine, up to 1 mm high, without or very short stipe, about 300 µm long; excipulum up to 100 µm broad, laterally with projecting hairs, simple or in groups, hyphae rarely branched, up to 180 µm long. Hymenium up to 100 µm high; epihymenium up to 25 µm high, pale brown, without gelatinous upper layer. Asci 6–8-spored, ascospores fusiform, 1–3-septate, 26–33 × 7–9 µm.

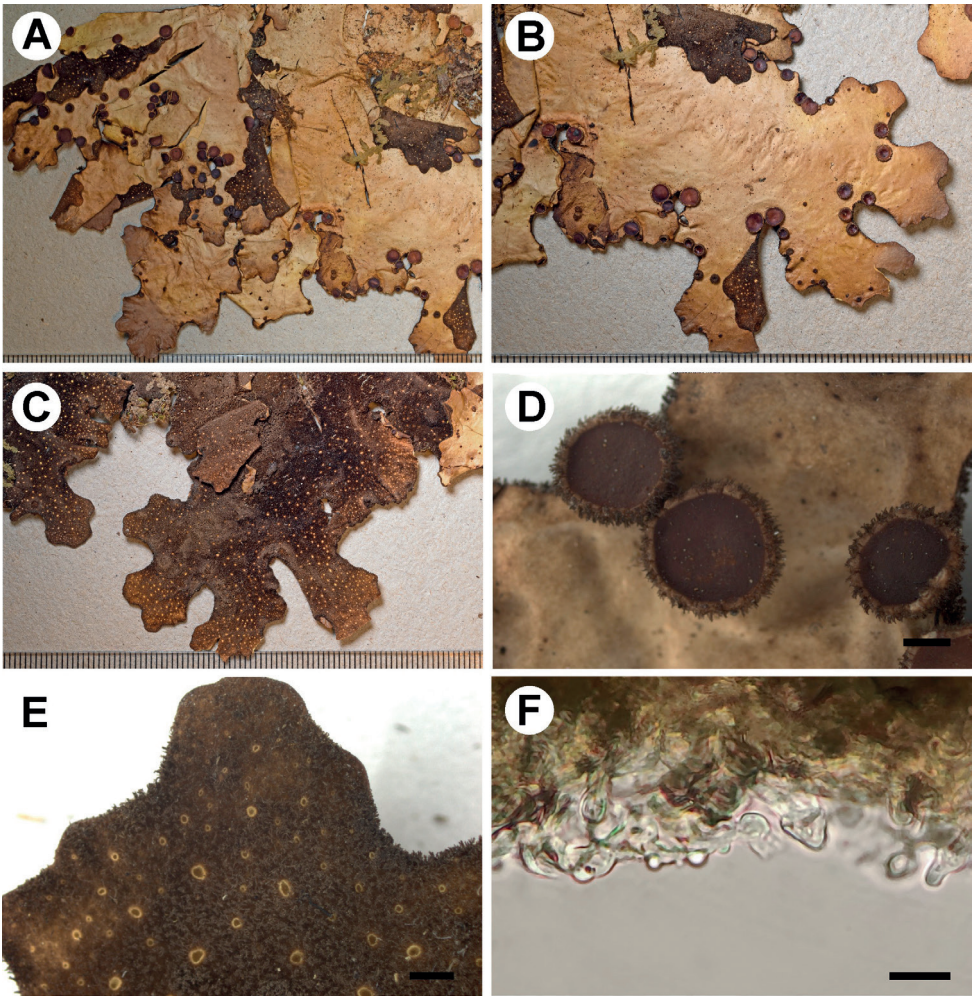

Figure 5. Morphology of *Sticta carrascoensis* (holotype) **A, B** upper surface with marginal and laminal apothecia **C** lower surface **D** apothecia with hirsute margins **E** tomentum, cyphellae and cilia at the lobe margin **F** basal membrane of cyphella with papillae. Scale bars: 1 mm (**A–E**); 10 µm (**F**).

Habitat and distribution. *Sticta carrascoensis* was collected at a single locality in the Parque Nacional Carrasco in the Department Cochabamba, at an altitude of 3283 m. The specimen grew on the bark of a tree in *Podocarpus-Polylepis* forest.

Etymology. The name refers the type locality.

Notes. *Sticta carrascoensis* is phylogenetically close to *S. andina*, although this relationship is not supported (Fig. 1; Suppl. material 3: Fig. S1). The latter differs by its cyanobacterial photobiont and the formation of isidia and/or phyllidia, not observed in *S. carrascoensis*. The thalli in *S. andina* are smaller (up to 15 cm in diam.), the margins of the lobes are sparsely covered by cilia and the medulla is white to cream, sometimes with yellowish patches and reacts K+ yellow (Moncada et al. 2021a). In *S. carrascoensis*, the medulla is distinctly yellow and reacts K+ lemon-yellow. *Sticta andina* is widespread in South America and, so far, has been confirmed from numerous localities from Brazil, Colombia and Ecuador and also from Costa Rica, Mexico and in Hawaii (Moncada et al. 2014a, b, 2020; Widhelm et al. 2018). Thus far, only one collection of *S. carrascoensis* is known, but it is well-developed and phylogenetically unique, with no close supported relative.

***Sticta catharinae* Ossowska, B. Moncada, Kukwa, Flakus, Rodriguez-Flakus & Lücking, sp. nov.**

MycoBank No: MB845389

Fig. 6

Diagnosis. Differing from other *Sticta* species in having a stipe, up to 1 cm long, a palmate thallus with abundant, submarginal to laminal apothecia, with the primary tomentum absent in the marginal parts of the thallus and a secondary tomentum present.

Type. Bolivia. Dept. La Paz; Prov. Nur Yungas, Parque Nacional y Área Natural de Manejo Integrado Cotapata, near Urpuma colony, 16°13'20"S, 67°52'34"W, elev. 1989 m, Yungas montane forest, 30 June 2010, A. Flakus 17263 & P. Rodriguez-Flakus (holotype KRAM, isotype LPB).

Description. Primary photobiont cyanobacterial (*Nostoc*). Stipe present, up to 1 cm long. Thallus palmate, up to 10 cm diam., moderately branched, with 3–5 branches per 5 cm radius, branching anisotomous to pleurotomous; lobes suborbicular to flabellate, interspaced to adjacent, involute, with their apices rounded and plane and their margins entire to sinuous, not thickened; lobe internodes (4–)6–15(–20) mm long, (6–)10–10(–20) mm broad; thallus coriaceous. Upper surface smooth to shallowly rugose in some parts, brown-grey, darker in the margins, shiny; surface glabrous, without papillae and pruina, without maculae; marginal cilia abundant, agglutinated to fasciculated, dark brown with pale tips, up to 0.5 mm long. Apothecia abundant, principally submarginal to laminal, dispersed, subpedicellate, sessile, up to 1.5 mm diam.; disc reddish-brown, shiny (in young apothecia) to matt (in older); margin entire to weakly crenate, excipulum hairs few to dense. Vegetative propagules absent. Lower surface folded to distinctly ridged and forming a reticulate pattern especially towards the margins, yellowish-brown to brown towards the centre; primary tomentum scarce, absent in the marginal part of the thallus, fasciculate, soft, golden brown; secondary

tomentum present, arachnoid, up to 25 µm. Rhizines absent. Cyphellae 1–20 per cm^2 towards the thallus centre and 21–40 per cm^2 towards the margin, scattered, irregular to elongate or rounded, urceolate with narrow to wide pore, prominent, on the same level as the primary tomentum or below, with the margin raised and involute to raised and involute-circinate, brown coloured, with or without tomentum; pore (0.25–)0.5–1(–2) mm diam.; basal membrane smooth, white, K+ yellowish, C–, KC–, Pd–. Medulla loose, white, K± yellowish, C–, KC–, Pd–. No substances detected by TLC.

Upper cortex paraplectenchymatous, 20–50 µm thick, differentiated into two cellular layers, the upper layer consisting of 1–2 layers of cells, with cells 5–6 µm diam., their walls 1–2 µm thick and their lumina rounded to isodiametric, 4–6 µm diam.; the lower layer of cortex 2–3 layers of cells, with cells 8–15 µm diam., their walls 1–2.5 µm thick and their lumina rounded to isodiametric, 3–5 µm diam. Photobiont layer 20–60 µm thick, its cells 6–12 µm diam. Medulla 100–220 µm thick, its hyphae 3–5.5 µm broad, without crystals. Lower cortex paraplectenchymatous, 20–50 µm thick, with 2–4 cell layers; cells 8–17 µm diam., their walls 2–4 µm thick. Hairs of lower primary tomentum up to 220 µm long and 3–5 µm broad, in groups to rarely simple, in fascicles up to 15, hyphae unbranched, septate, with free apices forming a brush-like head. Cyphella cavity up to 120 µm deep; membrane of cells densely packed, cells of basal membrane with 2–4 papillae. Apothecia biatorine, ca. 500 µm high, without distinct stipe; excipulum up to 120 µm broad, without or with projecting hairs, simple to fasciculate. Hymenium 100–120 µm high, hyaline, but K+ yellow; epihymenium ca. 10 µm high, orange-brown, K+ orange intensifying, without gelatinous upper layer. Asci 6–8-spored, ascospores fusiform, 2–4-septate, 31–37 × 8–9 µm.

Habitat and distribution. *Sticta catharinae* is known only from the type locality in Yungas forest in the Department La Paz.

Etymology. The new species is named to honour our late friend and teacher, Polish botanist Dr Katarzyna Żółkoś, for her contributions to the conservation of nature.

Notes. *Sticta catharinae* is the only species amongst those newly described here that is characterised by the presence of a stipe supporting the thallus. Morphologically, this taxon is similar to *S.* aff. *caliginosa* D. J. Galloway and the cyanomorph of *S. neopulmonarioides* B. Moncada & Coca, which share the stipe and the palmate thallus. However, in *S.* aff. *caliginosa* and *S. neopulmonarioides*, no apothecia are known, whereas vegetative propagules in the form of isidia or phyllidia and lobules are present (Galloway 1997; Moncada 2012; Moncada et al. 2013a). In addition, these taxa differ in the shape of the lobes and the presence of marginal cilia. In *S.* aff. *caliginosa*, the lobes are ligulate to flabellate, with their apices rounded to obtuse and with cilia being sparse to absent (Moncada 2012). In contrast, *S. neopulmonarioides* has flabellate lobes with irregular apices, without cilia (Moncada et al. 2013a). *Sticta neopulmonarioides* is widely distributed in Colombia, while *S.* aff. *caliginosa* is a rare taxon in that country (Moncada 2012; Moncada et al. 2013a, 2014b).

The new species is closely related to *S. fuliginoides* (Fig. 1; Suppl. material 3: Fig. S1), a morphologically disparate taxon with broad lobes producing laminal isidia (Magain and Sérusiaux 2015). It is also phylogenetically quite distinctive from the latter, with a total of 16 substitutions and nine indels in the ITS (Suppl. material 2: File S1), warranting its formal description, based on a single collection only.

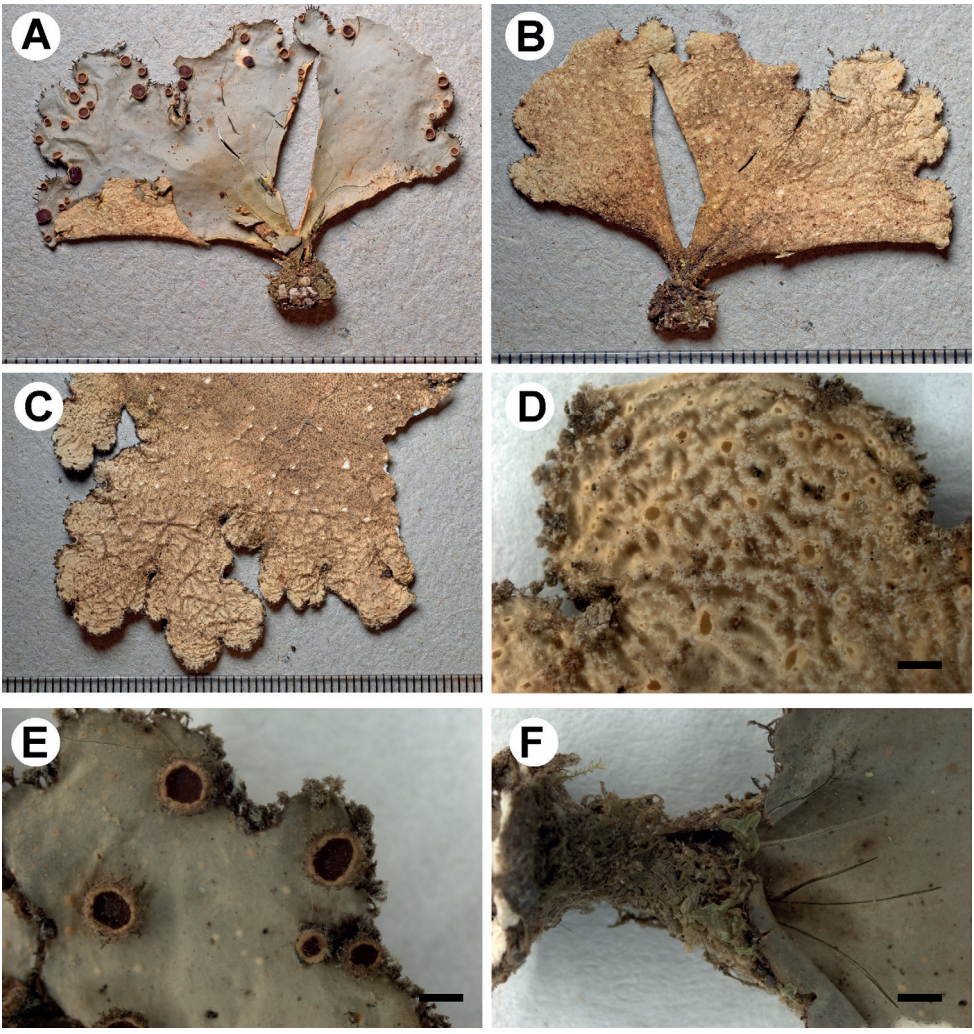

Figure 6. Morphology of *Sticta catharinae* (holotype) **A** upper surface with submarginal to laminal apothecia **B** lower surface **C** lower surface showing venation **D** enlarged part of the lower surface with tomentum and cyphellae **E** apothecia with margin tomentum and hairs and lobe margin with cilia **F** stipe. Scale bars: 1 mm.

Sticta pseudoimpressula **Ossowska, Kukwa, B. Moncada & Lücking, sp. nov.**
MycoBank No: MB845390
Fig. 7

Diagnosis. Differing from *S. impressula* in the presence of imbricately arranged and grouped apothecia with orange-yellow pruina along the margin of the disc, reacting K+ carmine-red and in the presence of a secondary tomentum.

Type. Bolivia. Dept. La Paz; Prov. Franz Tamayo, Área Natural de Manejo Integrado Nacional Apolobamba, near Río Pelechuco, below Pelechuco close to new road

to Apolo, 14°46'39"S, 69°00'35"W, elev. 2250 m, lower montane Yungas cloud forest, corticolous, 16 Nov 2014, M. Kukwa 14750 (holotype UGDA, isotype LPB).

Description. Primary photobiont cyanobacterial (*Nostoc*). Stipe absent. Thallus irregular to suborbicular, up to 10 cm diam., moderately branched, with 3–5 branches per 5 cm radius, branching polytomous; lobes laciniate to flabellate, adjacent, plane, with their apices orbicular and revolute to involute and their margins entire to crenate, not thickened; lobe internodes (4–)7–10(–15) mm long, (4–)7–9(–15) mm broad; thallus coriaceous. Upper surface pitted to scrobiculate to rugose towards the centre, yellowish-brown with darker apices in the herbarium, with marginal line in the same colour, shiny; surface glabrous, without papillae and pruina, without maculae; marginal cilia present, abundant, fasciculate, light brown to dark brown, about 0.5 mm. Apothecia abundant, laminal, dispersed, often imbricately arranged and grouped, subpedicellated, with pronounced invagination on lower side, up to 3.5 mm diam.; disc red-brown to brown, sometimes greenish-yellow due to the presence of pruina, shiny; margin entire to crenate and hirsute, with white hairs and orange-yellow pruina. Vegetative propagules absent. Lower surface uneven, beige to dark brown towards the centre; primary tomentum dense to the margin, thick (long), spongy, soft, grey-brown to black with paler tips; secondary tomentum present, but sparse, pubescent, up to 30 µm long. Rhizines sparse, black, up to 0.5 mm. Cyphellae 1–20 per cm^2 towards the thallus centre and 41–60 per cm^2 towards the margin, scattered, irregular, cupuliform to urceolate with wide pore, prominent, below the level of the primary tomentum, with the margin erect, cream to brown coloured, without or with tomentum in the lower half; pore (0.5–)0.6–1.3(–2.5) mm diam.; basal membrane pruinose in the appearance, white to pale beige in older part of thallus; K– to K+ pale yellow, C–, KC–, Pd–. Medulla compact, beige-white, K+ yellow, C–, KC–, Pd–. Apothecia margin (ring around disc) and epihymenium K+ carmine-red. No substances detected by TLC, unidentified anthraquinone in apothecia.

Upper cortex paraplectenchymatous, 20–40 µm thick, consisting of 2–3 cell layers with cells 6–22 µm diam. (with smaller cells in outside parts of the cortex), their walls 1–2 µm thick and their lumina rounded to isodiametric, 5–21 µm diam. Photobiont layer 60–110 µm thick, its cells 7–18 µm diam. Medulla 30–100 µm thick, its hyphae 3–5 µm broad, without crystals. Lower cortex paraplectenchymatous, 25–40 µm thick, with 3–4 cell layers; cells 8–18 µm diam., their walls 2–4 µm thick. Hairs of lower primary tomentum up to 1000 µm long, in fascicles of more than 20, hyphae unbranched to rarely branched, septate with flexuous apices. Cyphella cavity 100–125 µm deep; cells of basal membrane loosely packed consisting of cells without papillae or very rarely one. Apothecia biatorine, up to 700 µm high, without distinct stipe; excipulum up to 125 µm broad, laterally with projecting hairs, in groups to rarely simple, up to 0.5 mm, 5–6 µm broad. Hymenium 80–110 µm high; epihymenium 20 µm high, orange, with pigment granules on the top, without gelatinous upper layer. Asci 6–8-spored, ascospores fusiform, 1–3-septate, 28–35 × 8.5–10 µm.

Habitat and distribution. *Sticta pseudoimpressula* is an epiphytic species, found in Bolivia at one locality at an altitude of 2250 m in a lower montane Yungas forest in the Department La Paz.

Etymology. The name refers to the similarity in morphology to *Sticta impressula*.

Additional material examined. Bolivia. Dept. La Paz; Prov. Franz Tamayo, Área Natural de Manejo Integrado Nacional Apolobamba, near Río Pelechuco, below Pelechuco close to new road to Apolo, 14°46'39"S, 69°00'35"W, elev. 2250 m, lower montane Yungas cloud forest, corticolous, 16 Nov 2014, M. Kukwa 14752 (LPB, UGDA).

Notes. *Sticta pseudoimpressula* is similar to *S. impressula* (Nyl.) Zahlbr. Both species have a pitted to scrobiculate or rugose upper surface with abundant, laminal apothecia and the lobe margins with abundant, light brown cilia. The tomentum is dense to the margin in the latter (Moncada 2012). However, the two species are not closely related phylogenetically (Fig. 1; Suppl. material 3: Fig. S1): *Sticta impressula* is clustered in

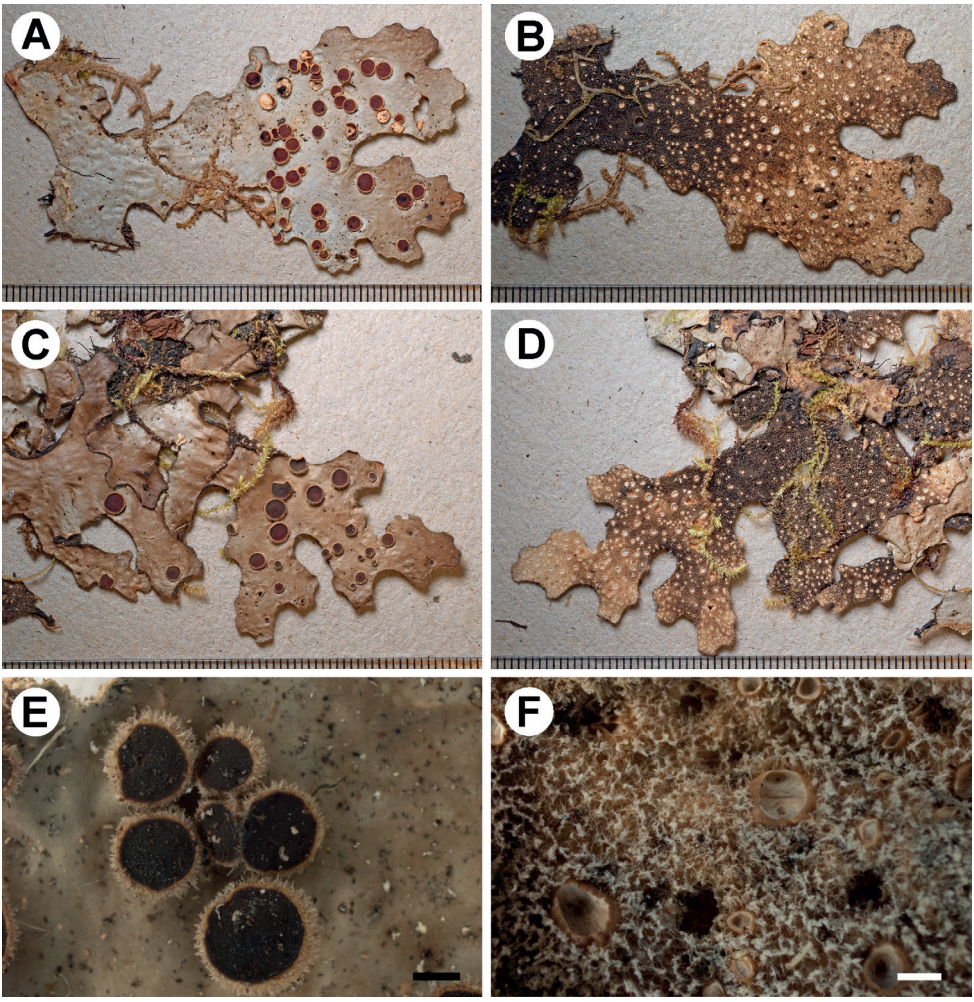

Figure 7. Morphology of *Sticta pseudoimpressula* (holotype) **A, C** upper surface with laminal apothecia **B, D** lower surface **E** group of imbricately arranged apothecia with hirsute margins **F** tomentum and cyphellae. Scale bars: 1 mm.

a neighbouring clade with *S. brevior* B. Moncada & Lücking and *S. isidiokunthii*. In contrast, *S. pseudoimpressula* shares a common ancestor with *S. bicellulata*, *S. peltigerella* and *S. sylvatica*. The differences between *S. pseudoimpressula* and *S. bicellulata* are discussed under the latter.

The morphological features that distinguish *S. pseudoimpressula* from *S. impressula* are the moderately-branched thalli and the laciniate to flabellate lobes. The apothecia in *S. pseudoimpressula* are often imbricately arranged and grouped and produced orange-yellow pruina along the disc margins and reacts K+ carmine-red. A secondary tomentum is present in *S. pseudoimpressula*, but absent in *S. impressula*. In addition, the cyphellae in *S. impressula* are rounded to angular and urceolate with a wide pore, erumpent to suprasessile and the margins raised to involute. The latter taxon is widely distributed in Colombia, where it grows at elevations between 1500 and 3800 m (Moncada 2012; Moncada et al. 2014b).

At first sight, *S. pseudoimpressula* can also be confused with *S. brevior*, but that taxon has smaller thalli with abundant apothecia, tomentose margins and the lower surface is undulating, creamy white to light brown (Moncada 2012; Moncada et al. 2013b). *Sticta brevior* is known from Colombia (Moncada et al. 2013b, 2014b).

New species from Colombia

***Sticta narinioana* B. Moncada, Ossowska & Lücking, sp. nov.**
MycoBank No: MB845384
Fig. 8

Diagnosis. Differing from *S. aymara* in the predominantly marginal and horizontally projecting isidia, the slightly projecting lower tomentum, giving the impression of marginal cilia, the absence of a secondary tomentum and the more densely arranged cyphellae.

Type. Colombia. Dept. Nariño; Laguna de la Cocha, Reserva el Encanto Andino, sendero al páramo, 01°04'12.3"N, 77°07'38.1"W, elev. 2810 m, andine forest, epiphytic on tree trunk, 24 Oct 2013, B. Moncada & R. Lücking 7614 (holotype UDBC, isotype B).

Description. Primary photobiont cyanobacterial (*Nostoc*). Stipe absent. Thallus orbicular to irregular, up to 5 cm diam., moderately branched, with 2–5 branches per 5 cm radius, branching pleurotomous; lobes suborbicular to flabellate, interspaced to adjacent, plane to undulate, with their apices rounded to somewhat truncate and revolute and their margins entire to sinuous, not thickened; lobe internodes (3–)5–10 mm long, (3–)5–8(–10) mm broad; thallus subcoriaceous. Upper surface smooth to uneven-rugose towards the centre, greyish-brown when fresh, light to medium yellowish-brown with darker apices in the herbarium, somewhat shiny; surface glabrous, without papillae, pruina or maculae; true marginal cilia absent, but lower tomentum partly projecting beyond the margins and resembling cilia. Apothecia rare to moderately abundant, submarginal, dispersed, subpedicellate, with invagination on

lower side, up to 2 mm diam.; disc orange-brown, somewhat shiny; margin densely hirsute, with white hairs. Vegetative propagules present, abundant, in the form of isidia, predominantly marginal, becoming branched and somewhat coralloid, terminally cylindrical, but with the base flattened, more or less obliquely orientated, up to 0.1 mm long and 0.03 mm broad, dark brown and darker than the thallus, shiny. Lower surface somewhat uneven, beige, somewhat darker towards the centre; primary tomentum dense and comparatively thick to the margin, fasciculate, soft, whitish to cream-coloured or pale brownish; secondary tomentum absent, except for the lower sides of the apothecia. Rhizines absent. Cyphellae frequent, 10–20 per cm^2 towards the thallus centre and 20–50 per cm^2 towards the margin, dense, rounded to somewhat irregular, urceolate with wide pore, erumpent, remaining below the level of the primary tomentum, with the margin raised and involute, whitish to cream-coloured, with or without tomentum; pore 0.3–1.5 mm diam.; basal membrane ± smooth, white, K–, C–, KC–, Pd–. Medulla compact, cream, K–, C–, KC–, Pd–. No substances detected by TLC.

Upper cortex paraplectenchymatous, 20–40 µm thick, consisting of 2–4 layers of cells 8–15 µm diam. with thin, hyaline walls and one layer of smaller cells with thicker, yellowish-brown walls. Photobiont layer 20–30 µm thick, its cells 5–10 µm diam. Medulla 50–100 µm thick, its hyphae 2.5–5 µm broad, without crystals. Lower cortex paraplectenchymatous, 15–30 µm thick, consisting of 2–3 cell layers; cells 5–10 µm diam., their walls 1–2 µm thick, but lowermost walls much thicker. Hairs of lower primary tomentum 100–200 µm long, in fascicles of 5–20, hyphae simple, septate with partly intertwined apices. Cyphella cavity up to 150 µm deep; cells of basal membrane without papillae or with one papillae. Apothecia biatorine, up to 500 µm high, without distinct stipe; excipulum up to 100 µm broad, laterally with projecting hairs in groups, up to 0.5 mm long and 4–5 µm broad. Hypothecium 60–80 µm high, light yellowish-green. Hymenium 80–110 µm high; epihymenium 15–20 µm high, orange, with pigment granules, without gelatinous upper layer. Asci 8-spored, ascospores fusiform, 1-septate, 35–40 × 7–8 µm.

Habitat and distribution. *Sticta narinioana* is known as epiphyte from two localities of well-preserved (sub-)andine forest in southern Colombia.

Etymology. The epithet honours Antonio Amador José Nariño (y Álvarez del Casal) (1765–1823), one of the critical architects of the independence of Colombia and after whom the Department of Nariño was named.

Additional material examined. Colombia. Dept. Nariño; Laguna de la Cocha, Reserva el Encanto Andino, sendero al páramo, 01°04'12.3"N, 77°07'38.1"W, 2810 m elev., andine forest, epiphytic on tree trunk, 24 October 2013, B. Moncada & R. Lücking 7525 (B, UDBC). Boyacá: Garagoa, Vereda Ciénaga, Valvanera, Reserva Privada El Secreto; 12 June 2014, D. Simijaca et al. 2044 (B, UDBC).

Notes. *Sticta narinioana* is closely related to the Bolivian *S. aymara* described above. Both taxa are cyanobacterial, isidiate species, but *S. aymara* has largely laminal isidia and the lower tomentum is not projecting to resemble cilia. Additionally, the cyphellae are less densely arranged and smaller.

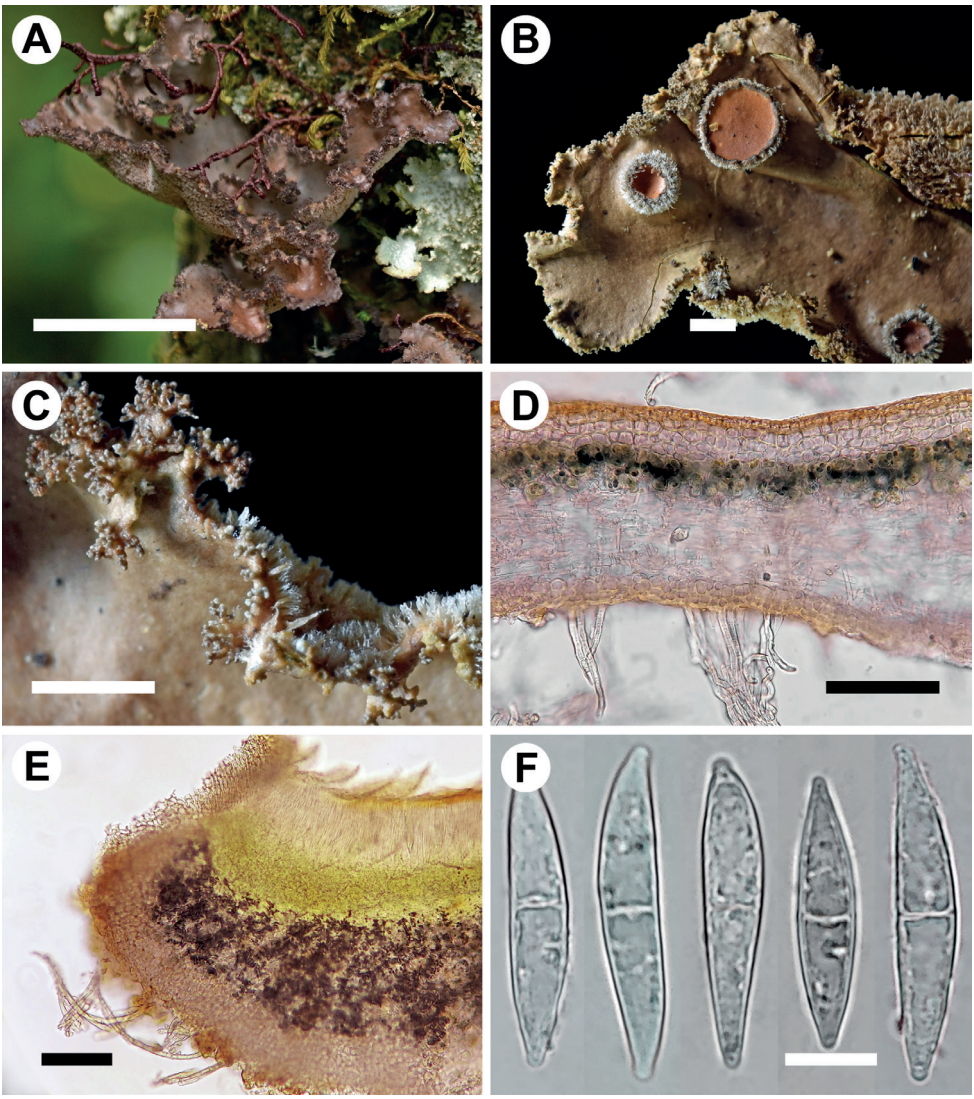

Figure 8. Morphology and anatomy of *Sticta narinioana* (**A** Moncada & Lücking 7525 **B–F** Simijaca et al. 2044) **A** thallus in situ **B** lobe tip with apothecia **C** lobe margin with isidia **D** section through thallus **E** section through apothecium **F** ascospores. Scale bars: 10 mm (**A**); 1 mm (**B, C**); 50 µm (**D**); 100 µm (**E**); 10 µm (**F**).

Acknowledgements

We are grateful to the members of Herbario Nacional de Bolivia, Instituto of Herbario Nacional de Bolivia, Instituto de Ecología, Universidad Mayor de San Andrés, La Paz, for the generous cooperation. Pierine España helped with the generation of some of the anatomical photographs. This research received support from the SYNTHESYS Project (DE-TAF-8180) http://www.synthesys.info/ which is financed by European Communi-

ty Research Infrastructure Action under the FP7 "Capacities" Programme and University of Gdansk, granted to EO. Lichen samples were collected in Bolivia with the permission of Ministerio de Media Ambiente y Agua and in cooperation with Herbario Nacional de Bolivia (LPB), who in turn made specimens available to the Herbarium of University of Gdańsk and W. Szafer Institute of Botany, Polish Academy of Sciences in Kraków.

References

Aptroot A (2008) *Sticta alpinotropica*, a new saxicolous lichen species from the alpine zone of Mt Wilhelm, Papua New Guinea. Lichenologist 40(05): 419–422. https://doi.org/10.1017/S0024282908007834

Aptroot A, Schumm F (2011) Fruticose Roccellaceae, an anatomical-microscopical atlas and guide with a worldwide key and further notes on some crustose Roccellaceae or similar lichens. Books on Demand, Norderstedt, 374 pp.

Dal Forno M, Moncada B, Lücking R (2018) *Sticta aongstroemii*, a newly recognized species in the *S. damicornis* morphodeme (Lobariaceae) potentially endemic to the Atlantic Forest in Brazil. Lichenologist 50(6): 691–696. https://doi.org/10.1017/S0024282918000403

Drummond AJ, Rambaut A (2007) BEAST: Bayesian evolutionary analysis by sampling trees. BMC Evolutionary Biology 7(1): e214. https://doi.org/10.1186/1471-2148-7-214

Feuerer T, Ahti T, Vitikainen O (1998) Lichenological investigations in Bolivia. In: Marcelli MP, Seaward MRD (Eds) Lichenology in Latin America: History, current knowledge and applications. CETESB – Companhia de Tecnologia de Saneamento Ambiental – Estado de Sao Paulo, Sao Paulo, Brazil, 71–86.

Flakus A, Lücking R (2008) New species and additional records of foliicolous lichenized fungi from Bolivia. Lichenologist 40(5): 423–436. https://doi.org/10.1017/S0024282908007378

Flakus A, Oset M, Jabłońska A, Rodriguez Saavedra P, Kukwa M (2011) Contribution to the knowledge of the lichen biota of Bolivia. 3. Polish Botanical Journal 56: 159–183. https://doi.org/10.2478/pbj-2014-0020

Flakus A, Etayo J, Schiefelbein U, Ahti T, Jabłońska A, Oset M, Bach K, Rodriguez Flakus P, Kukwa M (2012) Contribution to the knowledge of the lichen biota of Bolivia. 4. Polish Botanical Journal 53: 427–461.

Flakus A, Sipman HJM, Bach K, Rodriguez Flakus P, Knudsen K, Ahti T, Schiefelbein U, Palice Z, Jabłońska A, Oset M, Meneses RIQ, Kukwa M (2013) Contribution to the knowledge of the lichen biota of Bolivia. 5. Polish Botanical Journal 58(2): 697–733. https://doi.org/10.2478/pbj-2013-0073

Flakus A, Oset M, Rykaczewski M, Schiefelbein U, Kukwa M (2016) Contribution to the knowledge of the lichen biota of Bolivia. 8. Polish Botanical Journal 61(1): 107–126. https://doi.org/10.1515/pbj-2016-0009

Flakus A, Etayo J, Miądlikowska J, Lutzoni F, Kukwa M, Matura N, Rodriguez-Flakus P (2019) Biodiversity assessment of ascomycetes inhabiting *Lobariella* lichens in Andean cloud forests led to one new family, three new genera and 13 new species of lichenicolous fungi. Plant and Fungal Systematics 64(2): 283–344. https://doi.org/10.2478/pfs-2019-0022

Galloway DJ (1997) Studies on the lichen genus *Sticta* (Schreber) Ach. IV. New Zealand species. Lichenologist 29(2): 105–168. https://doi.org/10.1006/lich.1996.0066

Gardes M, Bruns TD (1993) ITS primers with enhanced specificity for basidiomycetes-application to the identification of mycorrhizae and rust. Molecular Ecology 2(2): 113–118. https://doi.org/10.1111/j.1365-294X.1993.tb00005.x

Guzow-Krzemińska B, Flakus A, Kosecka M, Jabłońska A, Rodriguez-Flakus P, Kukwa M (2019) New species and records of lichens from Bolivia. Phytotaxa 397(4): 257–279. https://doi.org/10.11646/phytotaxa.397.4.1

Hall T (2011) BioEdit: An important software for molecular biology. GERF Bulletin of Biosciences 2: 60–61.

Herzog T (1922) Beitrag zur Flechtenflora von Bolivia. Hedwigia 63: 263–268.

Herzog T (1923) Die Pflanzenwelt der bolivianischen Anden und ihres östlichen Vorlandes. In: Engler A, Drude O (Eds) Die Vegetation der Erde, volume XV. Leipzig, 258 pp.

Hodkinson BP, Lendemer JC, McDonald T, Harris RC (2014) The status of *Sticta sylvatica*, an 'Exceedingly Rare' lichen species, in Eastern North America. Evansia 31(1): 17–24. https://doi.org/10.1639/079.031.0103

Ibisch PL, Mérida G (2004) Biodiversity: the richness of Bolivia. State of knowledge and conservation. Ministry of Sustainable Development, Editorial FAN, 638 pp.

Jørgensen PM, Nee MH, Beck SG (2014) Catálogo de las Plantas Vasculares de Bolivia. Monographs in Systematic Botany (MSB) Vol. 127, 1741 pp.

Josse C, Navarro G, Comer P, Evans R, Faber-Langendoen D, Fellows M, Kittel G, Menard S, Pyne M, Reid M, Schulz K, Snow K, Teague J (2003) Ecological Systems of Latin America and the Caribbean: A Working Classification of Terrestrial Systems. Nature-Serve, Arlington, 47 pp.

Katoh K, Frith MC (2012) Adding unaligned sequences into an existing alignment using MAFFT and LAST. Bioinformatics 28(23): 3144–3146. https://doi.org/10.1093/bioinformatics/bts578

Katoh K, Standley DM (2013) MAFFT multiple sequence alignment software version 7: Improvements in performance and usability. Molecular Biology and Evolution 30(4): 772–780. https://doi.org/10.1093/molbev/mst010

Kessler M (1999) Plant species richness and endemism during natural landslide succession in a perhumid montane forest in the Bolivian Andes. Ecotropica 5: 123–136.

Kolanowska M, Baranow P, Nowak S, Fuentes A (2021) Materials to the revision of the genus *Cranichis* (Orchidaceae) in Bolivia. PhytoKeys 186: 11–41. https://doi.org/10.3897/phytokeys.186.71499

Kosecka M, Guzow-Krzemińska B, Černajová I, Škaloud P, Jabłońska A, Kukwa M (2021) New lineages of photobionts in Bolivian lichens expand our knowledge on habitat preferences and distribution of *Asterochloris* algae. Scientific Reports 11(1): e8701. https://doi.org/10.1038/s41598-021-88110-0

Kukwa M, Flakus A (2009) *Lepraria glaucosorediata* sp. nov. (Stereocaulaceae, lichenized Ascomycota) and other interesting records of *Lepraria*. Mycotaxon 108(1): 353–364. https://doi.org/10.5248/108.353

Lendemer JC, Goffinet B (2015) *Sticta deyana*: A New Endemic Photomorphic Lichen from the Imperiled Mid-Atlantic Coastal Plain of Eastern North America. Systematic Botany 40(4): 933–941. https://doi.org/10.1600/036364415X689979

Lücking R, Rivas Plata E, Chaves JL, Umaña L, Sipman HJM (2009) How many tropical lichens are there really? Bibliotheca Lichenologica 100: 399–418.

Magain N, Sérusiaux E (2015) Dismantling the treasured flagship lichen *Sticta fuliginosa* (Peltigerales) into four species in Western Europe. Mycological Progress 14(10): e97. https://doi.org/10.1007/s11557-015-1109-0

Meneses RI, Beck S, García E, Mercado M, Araujo A, Serrano M (2015) Flora of Bolivia – where do we stand? Rodriguésia 66(4): 1025–1031. https://doi.org/10.1590/2175-7860201566406

Mercado-Díaz JA, Lücking R, Moncada B, Widhelm TJ, Lumbsch HT (2020) Elucidating species richness in lichen fungi: The genus *Sticta* (Ascomycota: Peltigeraceae) in Puerto Rico. Taxon 69(5): 851–891. https://doi.org/10.1002/tax.12320

Miller MA, Pfeiffer W, Schwartz T (2010) Creating the CIPRES Science Gateway for Inference of Large Phylogenetic Trees. Proceedings of the Gateway Computing Environments Workshop (GCE), 14 November, 2010, New Orleans, 8 pp. https://doi.org/10.1109/GCE.2010.5676129

Moncada B (2012) El género *Sticta* (Schreb.) Ach. en Colombia, Taxonomía, Ecogeografía e Importancia. Doctoral thesis, Universidad Nacional de Colombia, Bogotá.

Moncada B, Lücking R (2012) Ten new species of *Sticta* and counting: Colombia as a hot spot for unrecognized diversification in a conspicuous macrolichen genus. Phytotaxa 74(1): 1–29. https://doi.org/10.11646/phytotaxa.74.1.1

Moncada B, Coca LF, Lücking R (2013a) Neotropical members of *Sticta* (lichenized Ascomycota: Lobariaceae) forming photosymbiodemes, with the description of seven new species. The Bryologist 116(2): 169–200. https://doi.org/10.1639/0007-2745-116.2.169

Moncada B, Lücking R, Coca LF (2013b) Six new apotheciate species of *Sticta* (lichenized Ascomycota: Lobariaceae) from the Colombian Andes. Lichenologist 45(5): 635–656. https://doi.org/10.1017/S0024282913000376

Moncada B, Lücking R, Suárez A (2014a) Molecular phylogeny of the genus *Sticta* (lichenized Ascomycota: Lobariaceae) in Colombia. Fungal Diversity 64(1): 205–231. https://doi.org/10.1007/s13225-013-0230-0

Moncada B, Aguirre J, Lücking R (2014b) Ecogeografía del género *Sticta*. (Ascomycota liquenizados: Lobariaceae) en Colombia. Revista de Biología Tropical 62(1): 257–272. https://doi.org/10.15517/rbt.v62i1.3564

Moncada B, Mercado-Díaz JA, Lücking R (2018) The identity of *Sticta damicornis* (Ascomycota: Lobariaceae): a presumably widespread taxon is a Caribbean endemic. Lichenologist 50(5): 591–597. https://doi.org/10.1017/S0024282918000373

Moncada B, Lücking R, Lumbsch HT (2020) Rewriting the evolutionary history of the lichen genus *Sticta* (Ascomycota: Peltigeraceae subfam. Lobarioideae) in the Hawaiian islands. Plant and Fungal Systematics 65(1): 95–119. https://doi.org/10.35535/pfsyst-2020-0005

Moncada B, Mercado-Díaz JA, Smith CW, Bungartz F, Sérusiaux E, Lumbsch HT, Lücking R (2021a) Two new common, previously unrecognized species in the *Sticta weigelii* morphodeme (Ascomycota: Peltigeraceae). Willdenowia 51(1): 35–45. https://doi.org/10.3372/wi.51.51103

Moncada B, Smith CW, Lücking R (2021b) A taxonomic reassessment of the genus *Sticta* (lichenized Ascomycota: Peltigeraceae) in the Hawaiian archipelago. Lichenologist (London, England) 53(1): 117–133. https://doi.org/10.1017/S0024282920000353

Moncada B, Mercado-Díaz JA, Magain N, Hodkinson BP, Smith CW, Bungartz F, Pérez-Pérez RE, Gumboski E, Sérusiaux E, Lumbsch HT, Lücking R (2021c) Phylogenetic diversity of two geographically overlapping lichens: Isolation by distance, environment, or fragmentation? Journal of Biogeography 48(3): 676–689. https://doi.org/10.1111/jbi.14033

Moraes MR, Sarmiento J (2019) Biodiversity in Bolivia. In: Pullaiah T (Ed.) Biodiversity in Bolivia in: Global Biodiversity Volume 4: Selected Countries in the Americas and Australia. Apple Academic Press, 574 pp.

Nash TH (2008) Lichen Biology (2nd edn.). Cambridge University Press, Cambridge, 486 pp.

Nylander W (1859) Lichenes in regionibus exoticis quibusdam vigentes exponit synopticis enumerationibus. Annales des Sciences Naturelles, la botanique 11: 205–264.

Nylander W (1861) Additamentum ad lichenographiam Andium Boliviensium. Annales des Sciences Naturelles, la botanique 15: 365–382.

Orange A, James PW, White FJ (2001) Microchemical methods for the identification of lichens. British Lichen Society, London, 101 pp.

Oset M, Kukwa M (2012) Notes on *Stereocaulon* species from Bolivia. Mycotaxon 121(1): 447–453. https://doi.org/10.5248/121.447

Ossowska EA (2021) First records of *Sticta weigelii* s.str. from Bolivia confirmed by molecular data. Folia Cryptogamica Estonica 58: 65–72. https://doi.org/10.12697/fce.2021.58.09

Rodriguez-Flakus P, Kukwa M, Etayo J, Lücking R, Meneses RI, Rivas Plata E, Stanton D, Truong C, Vargas R, Flakus A (2016) Preliminary catalogue of lichens and lichenicolous fungi from Bolivia. http://bio.botany.pl/lichens-bolivia/en,strona,catalogue,5.html [Version 1.5. 31 December 2016]

Rusby HH (1896) An enumeration of the plant collected in Bolivia by Miguel Bang, with description of new genera and species. Part III. Memoirs of the Torrey Botanical Club 6(1): 1–130.

Simon A, Goffinet B, Magain N, Sérusiaux E (2018) High diversity, high insular endemism and recent origin in the lichen genus *Sticta* (lichenized Ascomycota, Peltigerales) in Madagascar and the Mascarenes. Molecular Phylogenetics and Evolution 122: 15–28. https://doi.org/10.1016/j.ympev.2018.01.012

Sparrius LB, Aptroot A, Sipman HJM, Pérez-Vargas I, Matos P, Gerlach A, Vervoort M (2017) Estimating the population size of the endemic lichens *Anzia centrifuga* (Parmeliaceae) and *Ramalina* species (Ramalinaceae) on Porto Santo (Madeira archipelago). The Bryologist 120(3): 293–301. https://doi.org/10.1639/0007-2745-120.3.293

Stamatakis A (2014) RAxML Version 8: A tool for Phylogenetic Analysis and Post-Analysis of Large Phylogenies. Bioinformatics 30(9): 1312–1313. https://doi.org/10.1093/bioinformatics/btu033

Suárez A, Lücking R (2013) *Sticta viviana* (lichenized Ascomycota: Peltigerales: Lobariaceae), a new species from Colombian paramos. Lichenologist 45(2): 153–157. https://doi.org/10.1017/S0024282912000680

Tønsberg T, Goward T (2001) *Sticta oroborealis* sp. nov. and other Pacific North American lichens forming dendriscocauloid cyanotypes. The Bryologist 104(1): 12–23. https://doi.org/10.1639/0007-2745(2001)104[0012:SOSNAO]2.0.CO;2

White TJ, Bruns T, Lee S, Taylor J (1990) Amplification and direct sequencing of fungal ribosomal RNA genes for phylogenetics. In: Innis MA, Gelfand DH, Sninsky JJ, White TJ (Eds) PCR Protocols: a Guide to Methods and Applications Academic Press. New York, 315–322. https://doi.org/10.1016/B978-0-12-372180-8.50042-1

Widhelm TJ, Bertoletti FR, Asztalos MJ, Mercado-Díaz JA, Huanga J-P, Moncada B, Lücking R, Magain N, Sérusiaux E, Goffinet B, Crouch N, Mason-Gamerb R, Lumbsch HT (2018) Oligocene origin and drivers of diversification in the genus *Sticta* (Lobariaceae, Ascomycota). Molecular Phylogenetics and Evolution 126: 58–73. https://doi.org/10.1016/j.ympev.2018.04.006

Supplementary material 1

Table S1

Authors: Emilia Anna Ossowska, Bibiana Moncada, Martin Kukwa, Adam Flakus, Pamela Rodriguez-Flakus, Sandra Olszewska, Robert Lücking

Data type: docx file

Explanation note: **Tables S1.** Specimens used in this study with the voucher information, references and GenBank accession numbers. Sequences generated during this study are in bold.

Link: https://doi.org/10.3897/mycokeys.92.89960.suppl1

Supplementary material 2

File S1

Authors: Emilia Anna Ossowska, Bibiana Moncada, Martin Kukwa, Adam Flakus, Pamela Rodriguez-Flakus, Sandra Olszewska, Robert Lücking

Data type: fas file

Explanation note: Final alignment of the ITS barcoding marker for the studied taxa and the reference sequences.

Link: https://doi.org/10.3897/mycokeys.92.89960.suppl2

Supplementary material 3

Figure S1

Authors: Emilia Anna Ossowska, Bibiana Moncada, Martin Kukwa, Adam Flakus, Pamela Rodriguez-Flakus, Sandra Olszewska, Robert Lücking

Data type: pdf file

Explanation note: **Figure S1.** Best-scoring Maximum Likelihood tree of the *Sticta* target clade containing the new species from Bolivia (blue) and Colombia (orange), based on the fungal ITS barcoding marker. Supported clades are thickened and individual support values are indicated.

Link: https://doi.org/10.3897/mycokeys.92.89960.suppl3

MycoKeys 92: 161–163 (2022)
doi: 10.3897/mycokeys.92.91389
https://mycokeys.pensoft.net

CORRIGENDA

A peer-reviewed open-access journal
MycoKeys
Launched to accelerate biodiversity research

Corrigenda for: "Two new species of *Craterellus* (Cantharellales, Hydnaceae) with veined hymenophore from north-eastern China" published in MycoKeys 91: 97–111, doi: 10.3897/mycokeys.91.84730

Gui-Ping Zhao[1], Jia-Jun Hu[1], Yong-Lan Tuo[1], Yu Li[1], Bo Zhang[1]

1 *Engineering Research Center of Edible and Medicinal Fungi, Ministry of Education, Jilin Agricultural University, Changchun, Jilin 130118, China*

Corresponding authors: Bo Zhang (zhangbofungi@126.com), Yu Li (yuli966@126.com)

Academic editor: Thorsten Lumbsch | Received 8 August 2022 | Accepted 8 August 2022 | Published 13 September 2022

Citation: Zhao G-P, Hu J-J, Tuo Y-L, Li Y, Zhang B (2022) Corrigenda for: "Two new species of *Craterellus* (Cantharellales, Hydnaceae) with veined hymenophore from north-eastern China" published in MycoKeys 91: 97–111, doi: 10.3897/mycokeys.91.84730. MycoKeys 92: 161–163. https://doi.org/10.3897/mycokeys.92.91389

It was because of our mistakes, we mixed the figures used in our manuscript, and after it was published, we attention that our figures were in the wrong place. Thus, we provide below the new figures with corrected information.

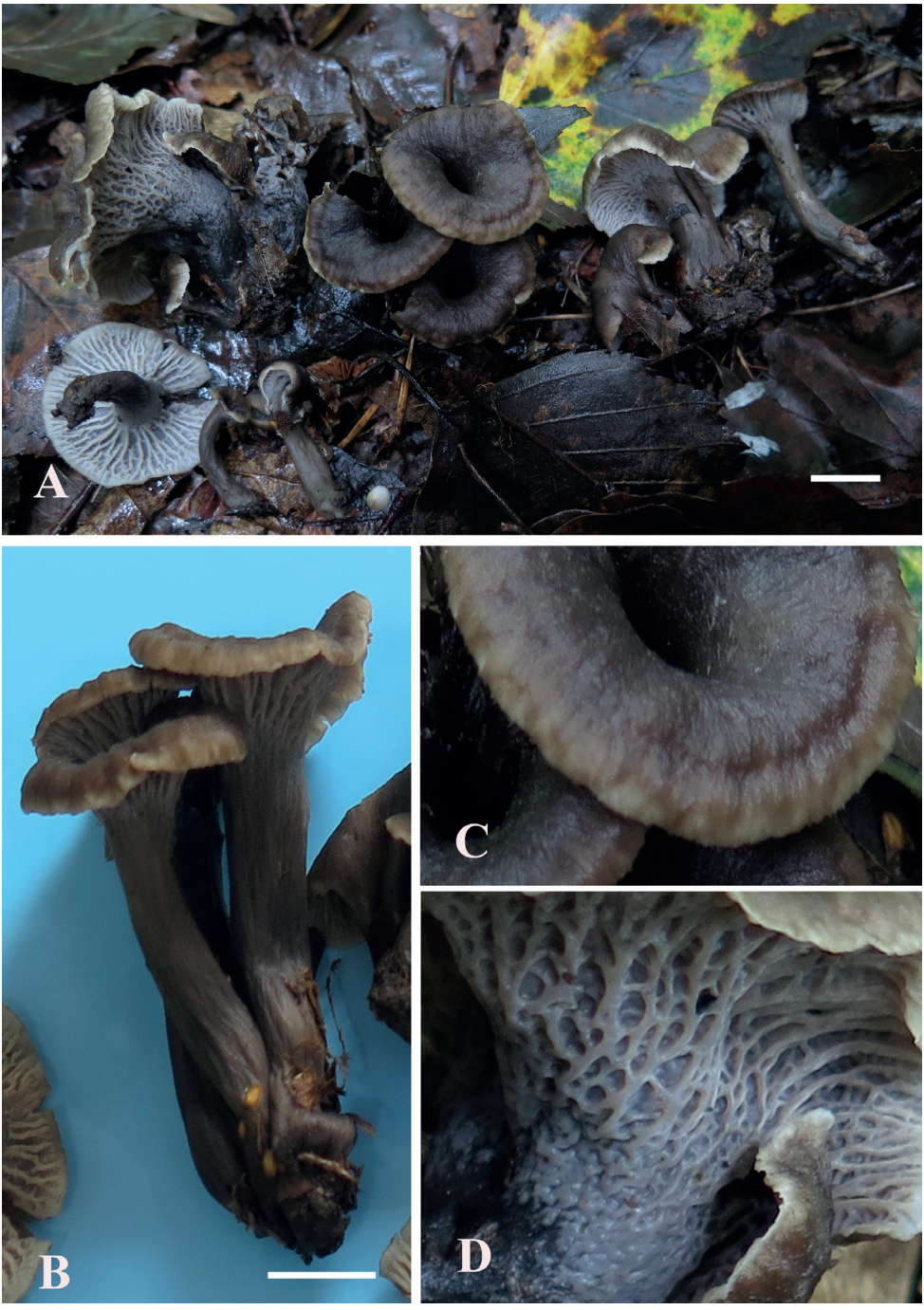

Figure 2. *Craterellus connatus* (HMJAU 60411, holotype) **A** fresh basidiocarps **B** connate stipes **C** margin of pileus **D** hymenophore. Scale bars: 1 cm (**A, B**).

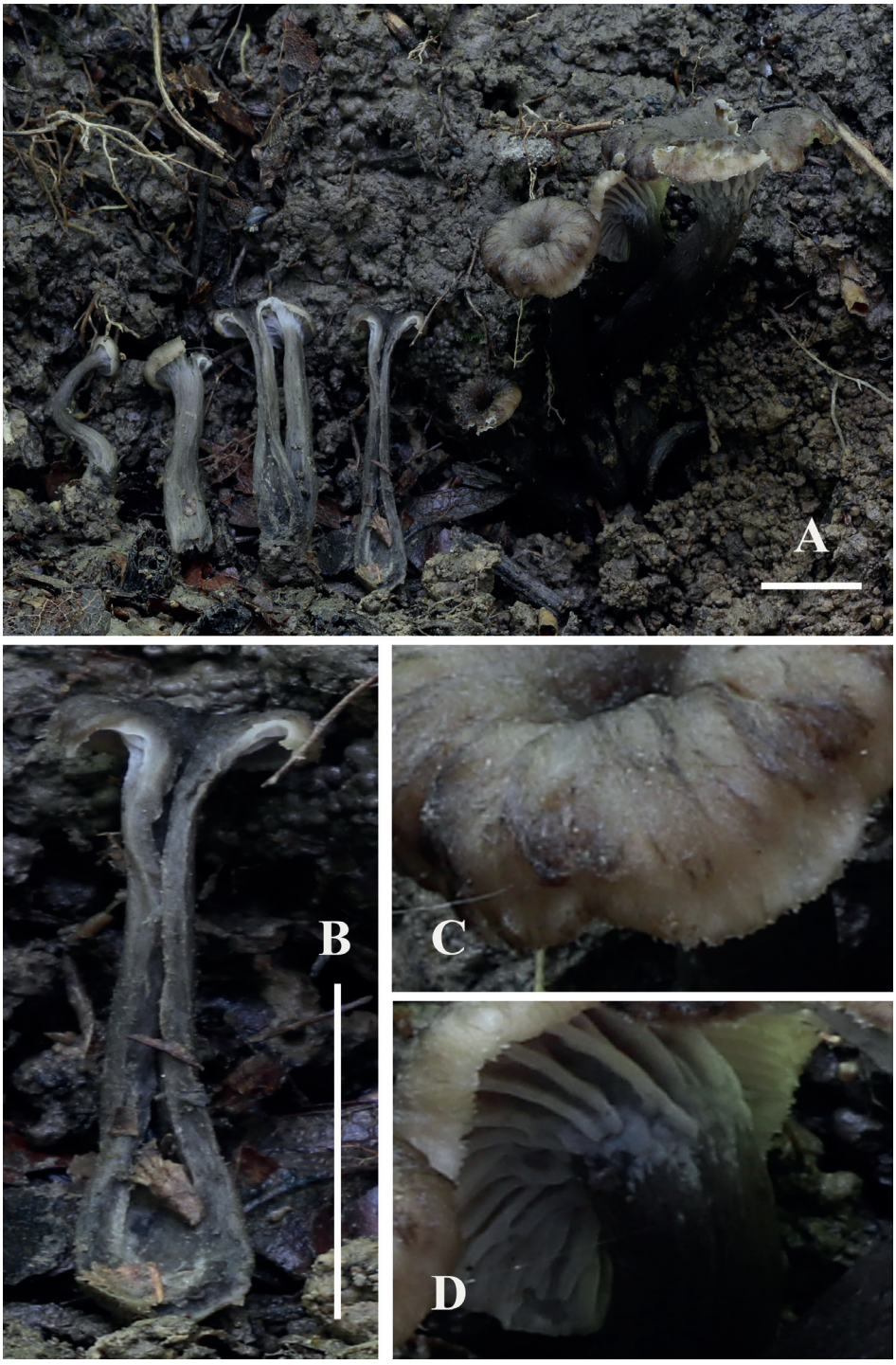

Figure 4. *Craterellus striatus* (HMJAU 60412, holotype) **A** fresh basidiocarps **B** stipe **C** pileus **D** hymenophore. Scale bars: 1 cm (**A, B**).

MycoKeys 92: 165–166 (2022)
doi: 10.3897/mycokeys.92.94104
https://mycokeys.pensoft.net

CORRIGENDA

A peer-reviewed open-access journal
MycoKeys
Launched to accelerate biodiversity research

Corrigendum: Pintos Á, Alvarado P (2022) New studies on *Apiospora* (Amphisphaeriales, Apiosporaceae): epitypification of *Sphaeria apiospora*, proposal of *Ap. marianiae* sp. nov. and description of the asexual morph of *Ap. sichuanensis*. MycoKeys 92: 63–78. https://doi.org/10.3897/mycokeys.92.87593

Ángel Pintos[1], Pablo Alvarado[2]

1 *Interdisciplinary Ecology Group, Universitat de les Illes Balears, Palma de Mallorca, Spain* **2** *ALVALAB, Oviedo, Spain*

Corresponding author: Pablo Alvarado (pablo.alvarado@gmail.com)

Academic editor: Thorsten Lumbsch | Received 26 August 2022 | Accepted 26 August 2022 | Published 13 September 2022

Citation: Pintos Á, Alvarado P (2022) Corrigendum: Pintos Á, Alvarado P (2022) New studies on *Apiospora* (Amphisphaeriales, Apiosporaceae): epitypification of *Sphaeria apiospora*, proposal of *Ap. marianiae* sp. nov. and description of the asexual morph of *Ap. sichuanensis*. MycoKeys 92: 63–78. https://doi.org/10.3897/mycokeys.92.87593. MycoKeys 92: 165–166. https://doi.org/10.3897/mycokeys.92.94104

In the published version of the article "New studies on *Apiospora* (Amphisphaeriales, Apiosporaceae): epitypification of *Sphaeria apiospora*, proposal of *Ap. marianiae* sp. nov. and description of the asexual morph of *Ap. sichuanensis*" by Pintos & Alvarado, MycoKeys 92: 63–78 (2022) the culture designated as holotype of *Apiospora marianiae* was not indicated as being preserved in a metabolically inactive state. As a consequence, the proposed new species name is invalid due to Art. 40.8 of the Shenzhen Code (Turland et al. 2018).

The species is validated herein:

Apiospora marianiae Pintos & P. Alvarado, sp. nov. MB 845455 For a detailed description see: Pintos & Alvarado, MycoKeys 92: 70 (2022). Holotype: CBS 148710 (preserved in a metabolically inactive state).

In addition, the epitypification of *Sphaeria apiospora* was published without an identifier and is therefore not Code compliant (Art. F.5.4, Shenzhen Code).

Here, we designate the epitype again:

Apiospora montagnei Sacc., Nuovo Giorn. Bot. Ital. 7: 306 (1875). Replaced synonym: *Sphaeria apiospora* Durieu & Mont., Exploration scientifique de l'Algérie 1(13): 482, tab. 25, fig. 1 (1849)

Supported lectotype: PC 0125160.

Epitype (designated here, MBT 10008889): Spain, Catalonia, Girona, L'Escala, 42°07'06.5"N 3°09'01.0"E, on dead culms of *Arundo micrantha*, 30 Nov. 2020, Marc Grañem, PC 0125164; exepitype CBS 148707.

Acknowledgements

Authors are grateful to Dr. Konstanze Bensch for warning them about the nomenclatural problems in Pintos & Alvarado, MycoKeys 92: 63–78 (2022), writing the text of the corrigenda, and obtaining the necessary MycoBank codes.

References

Turland NJ, Wiersema JH, Barrie FR, Greuter W, Hawksworth DL, Herendeen PS, Knapp S, Kusber W-H, Li D-Z, Marhold K, May TW, McNeill J, Monro AM, Prado J, Price MJ, Smith GF (2018) International Code of Nomenclature for algae, fungi, and plants (Shenzhen Code) adopted by the Nineteenth International Botanical Congress Shenzhen, China, July 2017. [Regnum Vegetabile no. 159.] Glashütten: Koeltz Botanical Books. https://doi.org/10.12705/Code.2018